A dissertation submitted in partial fulfillment of the requirements
for the degree of Doctor of Philosophy

Development of Cultivation Schema and Automated Gully Convey-Spacing System for Multilayer Plant Factory

February 2015

Alireza Ashtiani Araghi

Major of Biosystems Engineering
Department of Biosystems & Biomaterials Science and Engineering

SEOUL NATIONAL UNIVERSITY

Development of Cultivation Schema and Automated Gully Convey-Spacing System for Multilayer Plant Factory

지도교수 이 중 용

이 논문을 공학박사 학위논문으로 제출함.

2015년 2월

서울대학교 대학원

바이오시스템.소재학부 바이오시스템공학전공

Alireza Ashtiani Araghi

Alireza Ashtiani Araghi 의 공학박사 학위논문을 인준함.

2015년 2월

위 원 장 _____ (인)

부 위 원 장 Rhee, Joong Yong (인)

위 원 Son, Jung Tek (인)

위 원 Kim, Hak Jin (인)

위 원 Ryu, Yong Su (인)

Development of Cultivation Schema and Automated Gully Convey-Spacing System for Multilayer Plant Factory

Alireza Ashtiani Araghi

ABSTRACT

Cultivation of leafy vegetables with hydroponic gullies in multilayer plant factories is one of the initiatives used to increase the plant production in artificially controlled indoor environments. Multistage mobile or dynamic cultivation with variable row spacing between gullies, used in single-layer cultivation, is another option to increase the average crop density and more efficient utilization of available area. Employment of dynamic cultivation in multilayer growing units can further increase the plant production rate, if an appropriate cultivation plan is adopted and executed during the process. To this end, developing a model for i) evaluating the performance of multilayer dynamic cultivation plans and comparing their performances with alternative static option, and ii) finding the details of the procedure used for executing the evaluated cultivation plan is a major objective in the first part of this study. Indices such as plant production rate, turning point day, and total number of produced plants during a certain period of time were defined and used to measure the performance of cultivation plans. Using the Labview programming, the model is then converted into a simulation module with visual input-output panel which represents a cultivation schema after the end of each simulation. In this way, a cultivation schema includes the characteristics and performance of a cultivation plan as well as the procedure to execute it. The visual panel was used to obtain the cultivation schemas of all dynamic and static cultivation plans applicable for continuous crop production in total eight cultivation layers during a maximum 180-day period. Various input conditions such as dissimilar clustering conditions, zigzag and square planting arrangements, and two crop types (Romaine and Korean lettuce cultivars) with different canopy growth behaviors were used in different simulations. A combinational cultivation plan including a dynamic plan with 1-2-3 clustering optimized with one static-dynamic hybrid layer, and two independent static layers was selected as the best cultivation plan with highest plant production for zigzag planting of Romaine lettuce. The increase in total plant production by this plan was

found to be 7.5% (232 lettuce heads) higher than the alternative static plan, although the last crop output of this plan was supplied 10 days later than the static option. The best plan for cultivation of Korean lettuce in total eight cultivation layers was a dynamic plan with 3-5 clustering with one optimized hybrid static-dynamic layer. Comparing to static plan, the increase in total plant production by this plan was about 19% (512 lettuce heads) in 168 days. These results indicated that employment of multilayer dynamic cultivation for increasing the plant production is less beneficial for the crops with lower growth rate of canopy diameter, e.g., Romaine lettuce, while opposite of this is true about the crops with faster horizontal growth, e.g., Korean lettuce. Results of simulations revealed that the dynamic plans with inappropriate clustering conditions, excessive row spacing, and improper timing of growth stages would cause inefficiency in the utilization of crop growing area and has no preference over the less cumbersome and cheaper to implement static option. It was also found that multilayer dynamic cultivation is not an advantageous option for increasing the total plant production in short term (1-2 months) cultivation periods. Moreover, adopting a greater number of growth stages in executing a dynamic cultivation plan was not the determinant factor for enhancing the amount of plant production.

The purpose of the second part of this study is to design and develop an automated system with reduced manufacturing costs and new technical features for gully handling operation e.g., row spacing operation and controlled gully conveying, based on the procedure of executing the plans given by the cultivation schema. Obtaining a flexible and precise automated row spacing operation in different cultivation layers of the growing unit and providing bi-directional controlled conveying of gullies in vertical direction are the key objectives in this design. The developed automated gully convey-spacing system consists of three sub-systems including, i) a couple of 4-layer growing units equipped with gully load/unloading mechanisms, ii) an autonomous vehicle, and iii) the gully supplier. Different types of actuators, sensors, and a PLC extended with special modules as the controller unit of the system were employed. Since adjustment of row spacing values between the gullies in cultivation layers is the most critical functional objective of the automated system, the automated scheme of this operation was examined before using in the real operation through motion analysis of system virtual prototype by CAE simulation. No deviation from determined target row spacing values was observed at the end of simulations and thus, results of the motion analysis confirmed the effectiveness of the schemes proposed for row spacing operation in all defined spacing modes. Moreover,

results of the experiments conducted to evaluate the ability of system in executing automated row spacing operation indicated that the average error in positioning of the gullies was 5.4, 5 and 8.5 % in spacing modes 1, 2, and 3, respectively. Experiments for testing the system functionality and the control schemes developed for other automated operations of the system such as layer targeting, manipulators locking, and displacement of gullies between different cultivation layers were also conducted with successful results. Using the output data obtained from the simulation module-cultivation schema in part one, a case study was also carried out to analyze and estimate the performance and operation time of the system during an integrated automated operation for executing the optimal cultivation plan of the Korean lettuce in total eight cultivation layers. Results of time analysis of system operation in different working days showed that an estimated time of 9 hours of automated operation is required for handling 220 gullies in eight cultivation layers. This operation time can be considerably reduced if faster linear actuators with higher duty cycles, and higher speeds of vertical gully conveying are used in the current developed system. Lower initial costs and easier control of the system due to less number of motors and actuators for running the automated operation in all growing units caused by centralization of all power sources in a single autonomous vehicle, and the ability to create a wide range of accurate row spacing values at any cultivation layer of the growing unit, simply through tuning of related parameters in the control program are some of new features of the developed automated system.

Keywords: automation, hydroponic gully, multilayer growing unit, programmable logic controller, simulation module, static and dynamic cultivation

Student number: 2008-31118

List of Contents

List of Figures

List of Tables

Nomenclature

α_j	number of layers in jth group of incompletely loaded layers
β_j	difference between gully per layer in jth group of incompletely loaded layers and complete loaded layer
δ	row spacing between the gullies in a layer (used in virtual prototyping)
δ_f	row spacing in the layers of final cluster (cm)
δ_i	row spacing applied in the layers of cluster i (cm)
δ_i^*	optimal row spacing in the layers of cluster i (cm)
δ_S	row spacing in the layers of multilayer growing unit during static cultivation (cm)
ψ	displacement of loaded gullies inside the cultivation layer by a 4-step loading cycle (mm)
ε	target row spacing value in spacing mode 3 (mm)
A(n)	present analog to digital converted value in analog distance sensor
C_F	filter constant in filter processing of analog distance sensor
d_f	size of canopy diameter at the end of final growth stage/harvest time (cm)
d_i	maximum allowed diameter of plant canopy in the layers of cluster i (cm)
d_{th}	threshold canopy diameter for zero spacing in zigzag planting (cm)
e	maximum allowed back and forth stroke of the lower bar (cm)
F(n)	present filter output value in analog distance sensor
F(n-1)	previous filter output value in analog distance sensor
GS_i	growth stage i
h	downward travel distance of the gully carriers during a loading cycle (cm)
H_{pp}	horizontal distance between centers of two adjacent gullies (cm)
L	length of cultivation layer (cm)
m	index for final cluster or final growth stage in multilayer dynamic cultivation
n	number of incompletely loaded layers
N_{CB}	number of gullies per crop batch in dynamic cultivation

$N_{CB:i}$	number of gullies in the crop batch based on maximum gully maintaining capacity of certain cluster i
N_i	maximum number of gullies per layer of cluster i (fully loaded layer)
$N_{LC.5}$	number of 5-step loading cycles executed during gully loading operation in a cultivation layer
$N_{LC.6}$	number of 6-step loading cycles executed during gully loading operation in a cultivation layer
N_{LEDPS}	number of LED photo sensor signals counted by PLC in control program
N_{PSS}	number of proximity sensor signals counted by PLC in control program
N_S	number of gullies in fully loaded layers of MGU during static cultivation
P	number of plants per gully
PPR_D	plant production rate obtained by dynamic cultivation plan (plants/day)
PPR_S	plant production rate obtained by static cultivation plan (plants/day)
r_i	number of layers in cluster i
t	number of a day within one growth period
T	total length of plant growth period in MGU (days)
T_i	length of growth stage i (days)
T_{max}	length of longest growth stage (days)
u	horizontal distance between front edge of cultivation layer and right wall of a gully when gully is on the gully carriers
V_{pp}	distance between centers of adjacent plants grown on one gully (cm)
w	width of hydroponic gully (cm)
X(i)	diagonal distance between centers of two neighboring plants growing on adjacent gullies during growth stage i (cm)

Abbreviations

AV	Autonomous vehicle
A/D	Analog to digital
BDL	Bottom down left
BDR	Bottom down right
BUL	Bottom up left
BUR	Bottom up right
CAD	Computer aided design
CAE	Computer aided engineering
DFT	Deep flow technique
GC	Gully carrier
HMI	Human machine interface
IR	Infra red
LA	Linear actuator
LB	Lower bar
MGU	Multilayer growing unit
NFT	Nutrient film technique
PAI	Plant area index
PLC	Programmable logic controller
PPR	Plant production rate
SMPS	Switch mode power supply
TDL	Top down left
TDR	Top down right
TPD	Turning point day
TSZ	Temporary storage zone
TUL	Top up left
TUR	Top up right
UB	Upper bar
VI	Virtual instrument

1. INTRODUCTION

According to increasing rate of world population, evolving demands for high quality food products and, serious constraints in available production resources, more serious attentions have been paid to technical developments of indoor cultivation methods during the recent decade. Indoor plant cultivation in greenhouses within which a controlled environment and a well-organized structure for plant growing are provided, is a promising solution for increasing the total plant production throughout the year (Giacomelli et al., 2007). This advantageous feature is mainly because that using indoor growing systems such as those installed in greenhouses and enclosed plant factories (Takatsuji, 2008) enables the farmer to produce any desired crop all the year round regardless of existing outdoor climate conditions. In addition to extend the plant production period to a year-round scale, the possibility to obtain higher crop yields per unit floor area due to factors such as providing better growing, treatment and protection conditions for the crop, and more efficient utilization of area, is the other reason which would increase the total plant production if indoor growing systems are exploited. The increase in annual plant production per unit of floor area through employing indoor growing systems can specially be a substantial beneficial point in the countries with limited amount of arable lands or inadequate number of favorable days for outdoor farming due to existence of extremely hot or cold climates. Some features of indoor plant production whose application is not generally feasible in conventional open farming are explained in the following sub-sections.

1.1. Soilless culture and hydroponics

The feasibility of adopting a wide range of growing techniques and plant production systems is a positive feature in indoor cultivation. According to advantageous attributes of plant production by soilless culture (Hydroponics and Areoponics), a remarkable portion of the demands for high-value horticultural products is currently grown using soilless cultivation methods in controlled indoor environments. In general, crops grown this way are high value crops that have a high rate of economic return, thus ensuring that the deployed inputs-intensive system is profitable for the grower (Raviv and Lieth, 2008).Various methods are currently used

to implement the soilless culture in greenhouses and plant factories most common of which are sprinkler and drip irrigations, Nutrient Film Technique (NFT), Deep Flow Technique (DFT), Ebb/flow and finally, Aeroponics (Raviv and Lieth, 2008).

1.2. Automation

Indoor cultivation can provide much better conditions for employment of automation since their environment is much more controllable and observable than that in the open filed agriculture. Mechanization of indoor and outdoor agricultural operations has been effectively used by the farmers for many years; however, the concept and applications of agricultural automation and robotics is much wider than those tasks covered and handled by agricultural mechanization. The automated systems used in agriculture have capabilities beyond what are normally seen with a mechanized system, which leads to reduced level of human supervision in respective operations due to added quasi-anthropomorphic intelligence to mechanized processes or devices (Ting, 1997). According to Ting et al. (1996), employment of flexible automation systems in which programmability of computers and the versatility of hardware tools are integrated allows the system to perform various tasks mainly by the change of the software, is a useful option for indoor plant production. Automated “data acquisition”, “decision making” and, “executing of operation” are the fundamental actions found in the automated systems used in indoor cultivation, while the more generic terms sensor, controller and, actuator have been alternatively adopted by Schueller (2013) for above mentioned actions in agricultural automated systems.

Greenhouse interior space is a relatively easy environment for introduction of automated systems due to its structured nature and therefore, the development of such systems is easier and simpler in large greenhouses (Edan et al., 2009). Pekkeriet and Van Henten (2011) identified numerous incentives such as increasing size of production facilities, specialization of crop production, individualization of plant treatment, unavailability of skilled labor, product quality and escalating competition in product marketing as some of the driving forces to develop automated greenhouses. Different automated operations can be found in greenhouses some of which are

indoor climate control (temperature, humidity, lighting, etc), automatic seedling production, crop conveying and spacing, irrigation and spraying and, harvesting. However, the pinnacle of automation technology in indoor plant production is invention of fully automated plant factories as highly automated facilities, where vegetables can be produced with minimal human intervention in an environment free of disease, insects and the risk of mechanical damage (Grift et al., 2008). Serial automatic machines and environments for seeding, germination, seedling nursery, transplanting, crop moving and spacing, harvesting and packaging as well as intensive control of ambient conditions and lighting are commonly provided in such plant factories (RDA, 2005; Kim et al., 2013a,b).

1.3. Multilayer and multistage cultivation

Due to high investment expenses and intensive application of artificial control and more specialized equipments such as hydroponic and automation systems in indoor cultivation, the associated costs of plant production are drastically increased as well. To cover these additional costs, it is necessary to obtain the highest possible production rates through effective utilization of available resources. In this regard, more efficient use of crop growing space should be one of the primary goals in indoor growing systems, in which a limited amount of area is devoted to crop production.

A general solution to improve the area utilization and to increase the rate of plant production in indoor growing systems such as plant factories is to use the overhead space of crop growing area by adding extra cultivation layers in order to maintain a greater number of plants during the cultivation process. In a broad sense, a plant factory is defined as an indoor cultivation system in which plants are under continuous production control throughout the growth period until the harvest time, while a narrow definition in this case is a year-round plant cultivation system in a completely artificial environment (Murase, 2000). Kozai (2013a) estimated that an indoor closed plant production system with ten layers can attain up to a 96-fold increase in annual production capacity per land area, compared to similar sized open field farm.

Another solution for more effective utilization of crop growing area is to increase average plant density during the cultivation process through continuous application of multistage mobile cultivation. In this method, the duration of plant growth period (excluding the seedling stage spent in the nursery) is divided into several growth stages and location of plants in the unit and their spacing relative to neighboring plants are increased when a new growth stage begins. Controlled moving of the growing crop, variable plant spacing and phase dependent treatment of plants (Garcia Victoria et al., 2007) are the main features applied in such mobile cultivation. Due to dynamic utilization of crop growing area and mobility of plants in multistage cultivation, the shorter term “dynamic cultivation” has been adopted for “multistage mobile cultivation” in this study. The term “static” as used in some sources, e.g., Van ’t ooster et al., 2014, implies is an opposite cultivation method in which a fixed crop spacing with no displacement of plants during the growth period is observed. A recent application of cultivation in multilayer growing units is continuous production of leafy vegetables in movable hydroponic (NFT) gullies which can be implemented through either of static and dynamic cultivation methods. Compound application of multilayer and multistage dynamic cultivations can be a remarkable step for further increase of plant production rate in indoor growing system if appropriately executed.

1.4. Necessity of research

Employment of different kinds and sizes of multilayer growing units in plant factories is a popular option for producing high quality and healthy leafy vegetables through soilless cultivation methods. A large amount of research has been conducted to investigate the impacts of environment factors such as artificial lighting and nutrient solutions on the growth quality of the crops grown in multilayer plant factories. However, despite the high potential of multilayer cultivation for increasing the total production per unit floor area, limited attention has been paid to studies which concern the improvement of area utilization and plant production rate in multilayer growing units. Research topics such as effect of multistage cultivation and plant spacing on the production performance of multilayer growing units are some examples which can be included in such studies. In addition, with increasing the size

of commercial multilayer plant factories containing a greater number of larger multilayer growing units, more difficulties will be involved with proper implementation of crop handling operations, particularly if complex operation with frequent crop mobility are adopted. Automation and robotics may provide some effective solutions for such applications. However, number of automated systems designed and employed for crop handling operations, e.g., vertical and horizontal displacement of plants, adjusting the plant spacing, etc, in multilayer plant factories is low and limited to specific applications. Hence, development of more flexible automated systems with higher abilities and improved technical performance is necessary for multilayer cultivation methods.

1.5. Scope and objectives

The main theme of this study is associated with continuous production of leafy vegetables with movable hydroponic NFT gullies in multilayer growing units. Therefore, all methods and objectives defined in dual parts of this research are related to this type of plant production.

The first part of this study presented in chapter 3 is an attempt to investigate the effects of executing multistage dynamic cultivation on plant production performance in multilayer growing units. The major objectives defined in this part of the study can be summarized as follows:

1- Introducing the concept of static and dynamic cultivation methods in multilayer growing units and their executing approach

2- Developing a model and converting it into a simulation module with visual input-output panel for i) evaluating the performance of multilayer dynamic cultivation plans and comparing their performances with alternative static option, and ii) finding the executive results of evaluated cultivation plans and thus, establishing the procedure to execute them. The information indicated by the panel after the end of each simulation represents a cultivation schema.

3- Investigating and analysis of various factors affecting the performance of static and dynamic cultivation plans by means of simulation results

4- Selecting the best cultivation plans with highest plant production and thus, most efficient area utilization for growing different lettuce cultivars under certain growing conditions by means of simulation results

The second part of this study described in chapter 4 concentrates on inventing a practical automation solution in form of an automated gully convey-spacing system for implementing multilayer static and dynamic cultivation plans introduced in part one of this study. The main objectives of this part of the study are as follows:

1- Design and development of an automated gully convey-spacing system with several sub-systems such that, i) controlled vertical conveying of gullies between different working heights in the multilayer growing unit, and ii) creating any desired row spacing value between the gullies in different cultivation layers of the growing unit with high precision, are provided through a fully automated process

2- Development of appropriate automated schemes and respective control programs for different operations of the system and examining them through virtual prototyping and the experiments conducted with the real system

3- Investigating the best order of executing different operations, and analysis and estimation of system operation time during integrated automated operation

2. REVIEW OF THE LITERATURE

2.1. Background of plant factory

A first example known as the origin of a plant factory refers back to 1957 when Danish Christensen farm invented a system for mass production of cress sprouts. It was an automated plant production system staring the process from the seedling stage to final harvesting point. This system was equipped to separate seeding, germination and cultivation rooms as well as pesticide free chambers in which chemical free and clean sprout vegetables were carried through a flat conveyor system as the transportation facility. Supplementary lighting using high pressure sodium lamps were also provided due to very short sunlight duration of daytime in the north of Europe. This type of plant factories were gradually developed in the Netherlands and Belgium in 1960s (Takatsuji, 2008). In 1970, several plant growth systems consisting of systematically integrated growth chambers were used to demonstrate the significant improvement of plant growth by applying optimum growth conditions in terms of environmental factors. Those scientific achievements motivated the early development of a closed plant growing systems in plant factories that involve technologies such as process control for the plant growth environment, mechanization for material handling, system control for production, and computer applications (Murase, 2000). The advantages of such plant factories included production stabilization, higher production efficiency, and better quality management of products through a shortened growing period, better conditions, lower labor requirements, and easier application of industrial concepts (Takatsuji, 1987). During intermittent years in 1970s, American companies such as General Electric, General Mills, Phyto-Farm and General Foods developed a few types of fully controlled plant factories. However, their attempts discontinued due to lack of profitability for commercialization. First serious attempts to design a plant factory in Japan go back to 1974 by Hitachi company central research center which led to fully automated plant production facilities in 1983. Since 1980, large scale combined automated plant factories came into practice by several companies. In that time, cultivation systems moving in three dimensional space were in great interest and development of the pioneer type of these kinds of plant factories using supplementary lighting was seriously pursued (Takatsuji,

2008). The growing trend in development of new types of plant factories with fully artificial control was continued in the next decades as well, and many researchers concentrated on studying the effects of employing different methods and techniques of controlling the environment factors and energy, and also application of new technologies in such plant factories. In the East Asia, the extra interest in this research area has led to widespread utilization of small to medium scale multilayer plant factories with artificial lighting for research and commercial purposes (Kozai, 2013b).

2.2. Classification of plant factories

According to the second definition of plant factory presented in section 2.1, the term plant factory is mostly refers to multilayer closed cultivation systems utilizing artificial control and lighting such as color LEDs (Hashimoto, 2000). However, various types of plant factories and different methods to classify them have been introduced by the researchers of this field.

Recognition of plant factories based on the lighting source they use for crop production has been considered as a classification method in some literature. According to this classification, Takakura (1996) and Kim (2011) specified three types of plant factories including those with natural (solar radiation), supplemental (combination of solar and artificial) and full artificial lighting systems. In the second group, the plant cultivation depends on the sunlight as the main, and the artificial light as the auxiliary light sources. The term greenhouse-type plant factory has been used by Hashimoto (2000) to introduce the plant factories using both solar and artificial light, while the term closed fully controlled plant factory has been selected for the plant factories employing full artificial lighting. Referring to Kozai (2006) fully controlled plant factories with full artificial lighting are closed production systems because they releases negligible amount of pollutants during their operation and all their primary by-products such as returned nutrient solutions are recycled and used again. In some references, the plant factories using supplementary lighting have been considered in the category of the plant factories with natural lighting. Hence, only two types of plant factories including those with natural and artificial lighting have been introduced in such texts (Takatsuji, 2008; Kim et al., 2013a; Kim et al., 2013b).

Another criterion used for classification of plant factories is layout and configuration of the planting beds in the growing system. Based on this criterion, Kim (2011) enumerated three kinds of plant factories including “horizontal single-layer”, “vertical bed”, and “horizontal multilayer” types. A horizontal single-layer plant factory is a highly automated greenhouse-type plant factory which can utilize both natural and artificial lights for the crop production. It has a single horizontal planting bed extended on the surface of the indoor environment. Slow conveying systems with mechanical crop spacing devices are installed beneath the planting bed, which are used to move the crops horizontally from the starting point toward the harvesting point, while spacing values between the crop rows are also regulated as the plants grow larger. The low efficiency in space utilization is the main drawback of such horizontal plant factories (Kim, 2011). Figures 2-1 (a) and (b) display schematic layout and internal view of a horizontal single-layer or greenhouse-type plant factory.

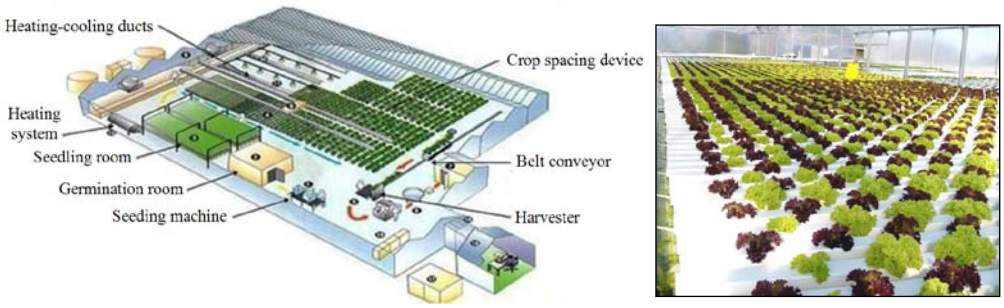

(a) (b)

Figure 2-1. (a) Schematic layout of a horizontal type single-layer automated plant factory, and (b) a view from internal space of crop production hall

In a vertical bed plant factory, the vertical space of the indoor environment has been used to obtain a more productive cultivation process through maintaining the growing plants on a circulating carousel moving up and down (Figure 2-2). An early design of this type of tower-like mobile plant production system was suggested by Ruthner (1966) and named as high-rise greenhouse. The efficiency of space utilization is higher than the horizontal single-layer type plant factory (Kim, 2011). The images in Figure 2-2 show several views from the structure and layout of a vertical bed plant factory developed by Korea rural development administration.

Figure 2-2. Structure and layout of a vertical bed plant factory developed by Korea rural development administration (RDA)

A horizontal multilayer plant factory (Figure 2-3) is a high density growing system, which consist of a number of growing units with multiple identical cultivation layers, vertically arranged and stacked on top of each other. Plant production by this type of plant factory (and also the vertical bed type), is a practical application of vertical farming which emphasizes to increase the crop production per unit of surface by employment of the vertical space instead of expansion of production area (Despommier, 2010). This type of plant factory is fully controlled, and the light used for crop growing inside its layers, is completely provided by artificial light sources such as special fluorescent lamps or LEDs in different colors. According to Kim (2011), this plant factory has the highest efficiency in space utilization among all described plant factories.

Figure 2-3. View of 15-layer growing units installed in a fully controlled horizontal multilayer plant factory

Although not considerably in operation, but some other configurations of planting beds with special designs have been introduced for increasing the efficiency of space utilization in plant factory environments. One commercial design is “Verticrop” mobile growing system with multilayer horizontal circulating plant beds which has been presented by Valcent Company, UK in 2009 (Figure 2-4 (a)). The growing plants are maintained in vertically hung trays which rotate on an overhead closed loop conveyor by electrical motor.

Another design is the idea of rotary gardens commercially presented by Omega Garden, Canada (Figures 2-4 (b) and (c)). This mobile growing system includes a number of rotary growth cylinders with artificial lighting source in the middle axis of each cylinder, which are all mounted on a vertical carousel. The growing crops are placed on the periphery of growth cylinder. Each cylinder rotates on its own axis, while also moves on the carousel track to reach the nutrient tray installed at the bottom of the system.

(a) (b) (c)

Figure 2-4. (a) Verticrop multilayer growing unit with horizontal crop circulation, (b) Omega Garden rotary growth cylinder, and (c) a number of rotary growth cylinders mounted a vertical carousel

2.3. Crop mobility and plant spacing operation

Despite the conventional outdoor farming in which the position of each growing plant is fixed in the field ground, moving the plants during their growth period is possible in indoor growing facilities such as greenhouses and plant factories. The movable units holding the growing plants can be items such as pots (for floriculture), hydroponic gullies (for leafy vegetables), and special trays and boxes. According to Van Henten (2006), optimal use of greenhouse space is a major reason to equip the greenhouse operations with automated mobile growing systems.

Different applications of crop mobility may be observed in indoor growing systems. Internal transport of growing crops in greenhouse-type plant factories for changing their current storage zone and release the space for new coming plants, and carrying the crops to special areas for operations such as spacing, spraying and harvesting is a common application of crop mobility. As related examples, Fang et al. (1990) and Annevelink (1992, 1999) discussed about the controlling such internal transport movements to obtain the most efficient time and space allocation plans in automated pot plant production. Commercial examples of such crop transportation systems are automatic transport vehicles, automatic wall-mounted transport carts, and autonomous rail-guided shuttles developed by Logiqs B.V. (The Netherlands). An autonomous rail-guided robot vehicle for transporting large size hydroponic gullies in a commercial greenhouse-type plant factory equipped with mobile gully system (Hortiplan, Belguim) is shown in Figure 2-5 (a). Employment of an autonomous rail-guided vehicle robot developed by LG CNS, Korea (2010) used for controlled displacement of hydroponic trays between different cultivation layers in a multilayer plant factory in Kyunggi-do institute of technology for agriculture is displayed in Figure 2-5 (b).

Controlled mobility of plants within large indoor growing facilities can also be provided using automatic transportation lines and tracks that consist of horizontal conveyors. The main purpose of such transportation lines (e.g., Kurata, 1984; MFAFF, 2003; Hayashi et. al 2011; Van ’t ooster et al. 2012) is to continuously move or circulate the crops toward the stationary points distributed in different locations of the indoor growing system in which specific crop treatment operations are executed.

(a) (b)

Figure 2-5. Autonomous rail-guided robot vehicles in (a) greenhouse-type plant factory with mobile gully system (Hortiplan, Belguim), and (b) multilayer plant factory (LG CNS, 2010)

Plant spacing operation refers to the activities through which the plants are placed at greater distances from each other to let the leaves and roots have sufficient space to grow and avoid interfere. In a multistage cultivation, the plant spacing operation would take place several times. A specific application of crop mobility in factory-like plant production systems is to implement plant spacing operation during multistage mobile crop cultivation by which a wider distance is applied between the growing plants through one of the common methods including: i) controlled spacing operation at stationary spacing machines located out of the main growing zone (Annevelink (1999), ii) direct re-distribution of plants in new growing zones, e.g., Space-o-Mat spacing system by Visser, The Netherlands, and iii) stepwise increase of plant spacing on the moving tracks (Mori, 1991; Horibe et al., 1993; Korea RDA 2005; Chang et al. 2005; Chang et al. 2006, Mobile Gully System (MGS) by Hortiplan, Belguim).

2.4. Mechanical designs and systems for variable plant spacing

During the last decades, some attempts have been made for design and development of the mechanical systems which manually or automatically adjust the plant spacing on the moving tracks for accomplishment of multistage mobile cultivation processes. An early attempt in this area was observed in the study of

Prince and Bartok (1978) in which a plant advancing-spacing device with a slip-joint spacing mechanism was used for multilayer cultivation of lettuce in a controlled environment.

Haub et al. (1982) proposed a design for gradual increase of the spacing between hydroponic gullies using a variable pitch screw (Figure 2-6). The gullies containing smaller plants were placed in parallel with each other at one side of the growing system. Tubular variable pitch screws with big helical grooves were employed to advance the gullies from the loading point toward the other end of the system with their slow rotation. The value of screw pitch was considerably greater at the unloading end of the system in order to make larger spacing values for the increased size of the mature plants. The disadvantage of this mechanism can be its limitation to create any desired row spacing values due to rigid design of the variable pitch screw. This system has been introduced as one of the mechanisms in use for application in plant factories with natural lighting by Kim et al. (2013b).

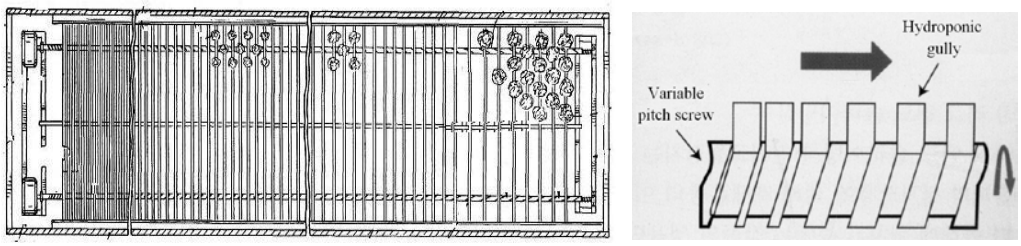

Figure 2-6. Gradual increase in the row spacing between hydroponic gullies in multistage crop cultivation by variable pitch screw

Drury (1984) invented a device for transporting and spacing the growing plants (Figure 2-7). Plants are positioned and transported in a hydroponic growing system by notched spacer bars riding on wheeled rails and interlocked with external ribs on elongated. The gullies are moved over a period of time in spaced parallel arrays through the length of the system. The apparatus permits easy and efficient movement of large arrays of plants by one worker or a motorized mover, while maintaining the gullies in precise spatial relationship to each other. This system had a simple design and easy to use, yet automatic aspects of spacing operation were relatively low. An upgraded and mechanized version of this design was also presented by Jansen (2004).

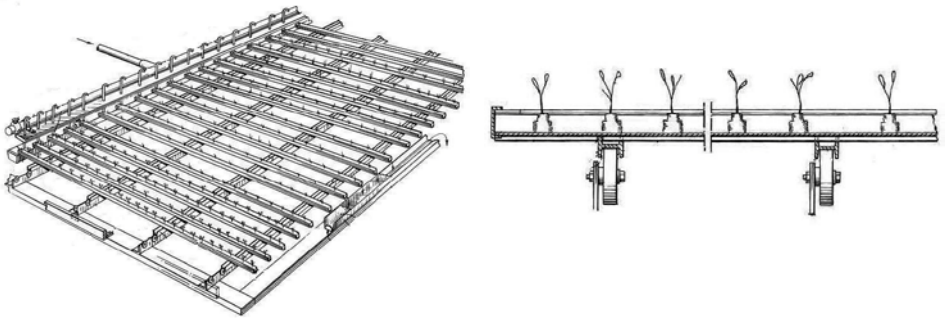

Figure 2-7. Schematic views from the mechanical system with wheeled rails and spacer bars for transporting and spacing of hydroponic gully (Drury, 1984)

Ikeda et al. (1986) proposed a system for the automated multistage cultivation of plants. This design included a plurality of guide rail pairs which supported conveyor driven jigs carrying individual plants thereon. As the plants were driven by the conveyors, the driving elements on successive conveyors were increasingly spaced to allow the increment of plant spacing. The guide rails were arranged in a radial array to allow for increasing side-wise plant clearance. Details of this design supporting the increase in plant spacing for eight growth stages can be observed in Figure 2-8.

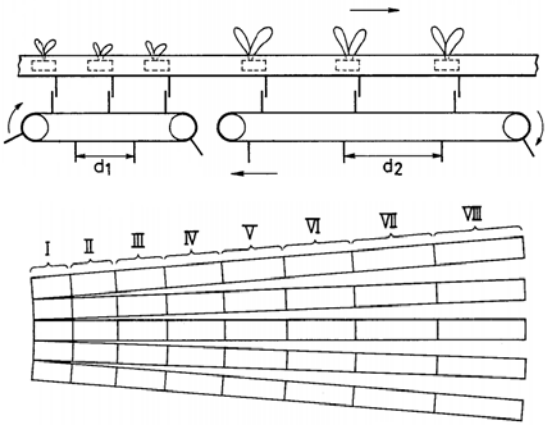

Figure 2-8. Schematic views of the automated spacing system for 8-stage plant cultivation process (Ikeda et al., 1986)

Roberts (1990) invented a method and apparatus for hydroponic gardening within which batch type individual cultivation units were produced. A new feature of this design was extending the benefits of variable spacing to the root zone of the plants. In all previous invented methods, the mechanical mechanism moved the plant units at gradually widening x-y spacing to provide appropriate space for leaves but not for the roots and thus, the roots might tend to dam the free flow of nutrient water. However, in this proposed system, plants were hydroponically grown in a cellular water table provided with divergent grow lines along which plants were moved in the plant holders. The grow lines are arranged to provide spacing between adjacent rows of plants as they mature. A variable pitch screw was used within each grow line to provide an increased spacing between adjacent plants as the plant growth stage proceeds further. Figure 2-9 shows more details of this mechanical plant spacing system.

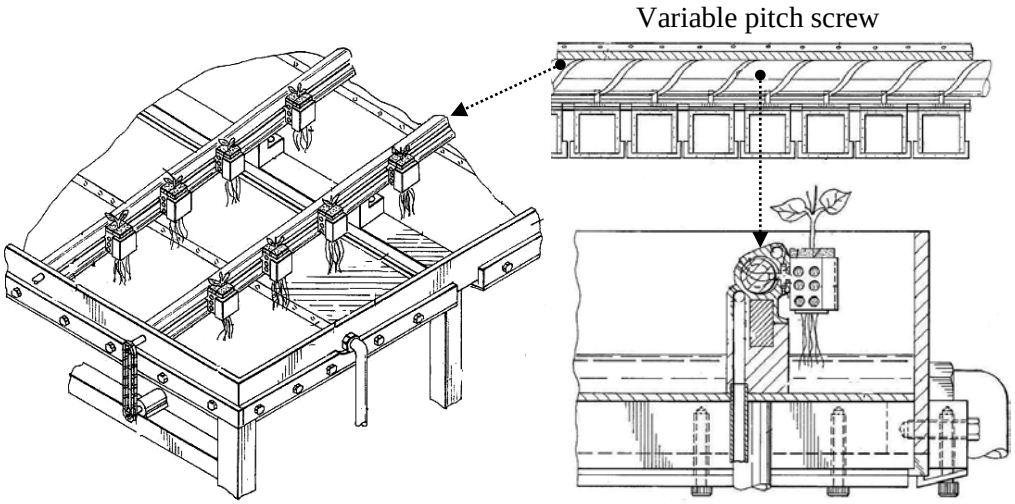

Figure 2-9. Schematic views of batch-type hydroponic growing system with automated plant spacing mechanism (Roberts, 1990)

Horibe et al. (1993) designed and successfully tested a mechanical mobile growing device which was able to increase the spacing between the plants in two dimensions. As a new point, using this device the spacing value between the planting rows and also between the plants growing on the same row was provided. The detailed calculation related to driving forces and design of mechanical components

have been presented in this study. Rasin (1998) from Swedeponic invented a device for moving the growing hydroponic gullies in a horizontal single-layer plant factory. Growing gullies had a gradual movement along a defined growth line where relative distance between growing gullies increased in a stepwise manner to create a larger space for the crops during their growth. Growth line was divided into different sections and a predetermined spacing value was assigned to each section. Moving the plants along the growth line was provided using a driving motor which supplied the power to longitudinal drawbars though a shaft and mechanical linkages. Several vertical fingers were attached to longitudinal drawbars. These fingers were engaged with the gullies and pulled them along the growth line toward the system outlet when the drawbar moved. Special flange coupling mechanisms were installed in the boundaries between different sections where the spacing values had to be changed. The two halves of each flange were individually attached to left and right drawbars, while it was also possible for the flanges to slide on the bolts arranged around flange plates. When the left drawbar is subject to a pulling force it moves leftward, while the right flange is still fixed and the bolts can slide through the flange holes. Once the bolts reach to the end of their sliding motion, heads of the bolts contact the right face of the right flange and right flange also moves leftward and a spacing value equal to the bolt stem clearance can be applied as the interval of the fingers and thus, to the gullies engaged to them. This happens with entering the gullies into the next spacing phase, an increment in spacing value could be made using these special flange coupling mechanisms. Figure 2-10 indicates a side view of this system with more details.

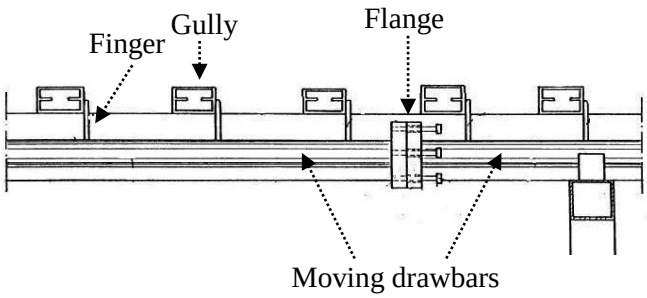

Figure 2-10. Schematic side view of mobile growing system with the ability of increasing the row spacing of gullies by bolt-flange mechanism (Rasin, 1998)

Employment of serially installed chain conveyors with different linear speeds was adopted by Chang et al. (2005) in development of an automated row spacing system for multistage mobile (dynamic) cultivation of hydroponic gullies in the plant factory environment. The main body of this growing system is a longitudinal platform (Figure 2-11) on which the hydroponic gullies are gradually moved and spaced by several chain conveyors from one side of the platform to its other end based on the growth stage and size of the growing plants.

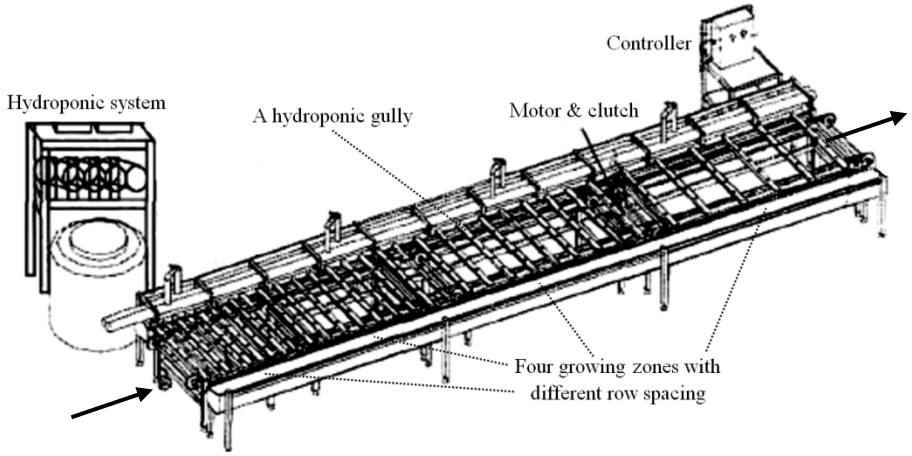

Figure 2-11. Schematic view from horizontal single-layer hydroponic growing system using chain drives for automated row spacing (Chang et al., 2005)

The platform of the system has been designed to provide four growing zones, in each of which a certain value of row spacing can be applied. One chain conveyor for moving the gullies was assigned to each growing zone, while one set of a special spacing mechanism displayed in Figure 2-12 (a) and (b), was also installed between two serial chain conveyors. This enables the system to make three row spacing operations during one growth period of the crop. The row spacing value between the hydroponic gullies can be increased when they enter a new growing zone according to the speed ratio between two sequential chain conveyors working in two adjacent growing zones. The difference in the linear speeds of the two chain conveyors is controlled by the mechanical spacing mechanism and leads to increased row spacing between the gullies when it passes the spacing zone (Figure 2-12 (b)). In the experiments done for evaluating the performance of the spacing mechanism, four row

spacing values including 100, 150, 200 and 250 mm were selected for application in four growing zones, while the linear speed for moving the gullies in growing zones one to four was 6.4, 9.6, 12.3, and 15.8 cm/s, respectively. According to Chang et al. (2005), by using these speed ratios between the chain conveyors of the growing zones, the average value of obtained row spacing for growth stages one to four by this system was 115.4, 155.4, 198.6, and 245.4 mm, respectively.

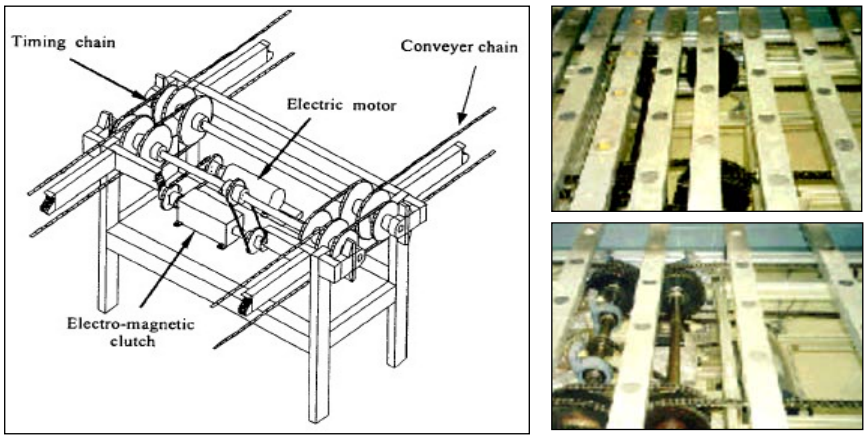

(a) (b)

Figure 2-12. (a) Mechanical spacing mechanism in automated row spacing system (Chang et al., 2005), and (b) increase in row spacing value by the spacing mechanism

A well-known example of the commercial products developed based on the design of chain conveyors with different linear speeds is the “Mobile Gully System” presented by Hortiplan (Belguim) in 2005 for the use in large greenhouse-type plant factories. This fully automated system enables the multistage mobile cultivation of leafy vegetables in seven meter long hydroponic gullies. Using a large size powerful chain drive system, the gullies are moved on their tracks from one side of the growing hall to its other end. According to the principles explained for chain conveyors with different linear speeds, this system is capable of increasing the row spacing of gullies as the crop develops and moves. As an integrated part of this automated plant factory system, autonomous rail-guided carrier robot vehicles are also used to carry and transport the hydroponic gullies to and from the crop growing line (see Figure 2-5 (a)).

In an another attempt to design automated mechanical row spacing systems for hydroponic gullies, Chang et al. (2006) developed and tested a vegetable row spacing system using an adjustable slider and lugs mechanism. In this automated spacing system, a platform similar to that developed in the design of Chang et al. (2005) was used. A pneumatic slider was employed to linearly move all hydroponic gullies together. A number of spacing lugs were installed in different intervals on a rotating bar installed beneath the gullies. Small rotation of this bar around its own axis could cause the lugs to contact the gullies. By operating the slider mechanism, gullies start to move forward slowly, while the spacing lugs have no contact with them. The desired row spacing could be created by preventing the gullies from further forward motion at determined points. The physical contact to prevent the gullies is provided by rotating the lugs bar and blocking the forward motion of gullies by the spacing lugs. Figure 2-13 shows the main growing platform and the spacing lugs bar of the described hydroponic mobile growing system.

Figure 2-13. Views from horizontal single-layer hydroponic growing system using slider-lug mechanism for automated row spacing (Chang et al., 2006)

The data acquired from the experiments conducted to evaluate the spacing ability of this system indicated a negligible amount of error in positioning of hydroponic gullies. According to gradual increase in the size of growing lettuce canopies in different growth stages, seven row spacing values including 6, 8, 10, 13, 16, 19, 22, 26, and 34 cm were selected as the desired row spacing values to be achieved. The measured row spacing corresponding to these seven values after the operation of system was 6.05, 7.93, 10.02, 13.07, 16.15, 19.07, 21.95, 26, and 34 cm, respectively.

However, since the fixed physical distance between the spacing lugs on the rotating bar is the factor which determines the row spacing value in this automated row spacing system, obtaining such precise row spacing values was expected. In other words, despite the high performance in obtaining the selected experimental row spacing values, this system is not able to create row spacing values other than the selected ones above, unless the positions of the spacing lugs on the bar are changed. This can be probably considered as a disadvantage of this row spacing system, because changing the fixed positions of lugs is not practically possible due to rigid design of the rotating bar.

Reviewing the systems and designs developed for plant spacing operation indicated that the multistage mobile cultivation with variable row spacing has been originally devised for application in single-layer growing systems. However, due to more efficient space utilization in multilayer cultivation employment of dynamic (multistage mobile) cultivation through application of variable plant spacing has been recently recommended for multilayer cultivation of leafy vegetables grown in movable hydroponic gullies. Kim (2011) and Kim et al., (2013a) introduced an automatic gully handling system for the use in a multilayer plant factory. The prototype of this hydroponic cultivation system including a number of 6-layer growing units with artificial lighting (Figure 2-14 (a)) was developed by Korea Rural Development Administration (RDA). In this system, a stepwise automated crop flow, moving from lower to upper layers of the multilayer unit was established (Figure 2-14 (b)). Due to the larger size of the more grown plants in the upper layers, the row spacing values applied in these layers were greater than the lower layers. The vertical conveyance of the gullies was provided at two ends of the multilayer units through employment of several screw lead-driven vertical lifts. Each lift could carry a single gully upward during its operation. Creating the row spacing in each layer was carried out through a reciprocating mechanical operation powered by the motors embedded inside the units. Figure 2-15 displays selected views from the automated gully operations implemented in this multilayer plant factory. No report or technical data has been released from the performance of this system and the effects of employing dynamic cultivation within its multilayer structure.

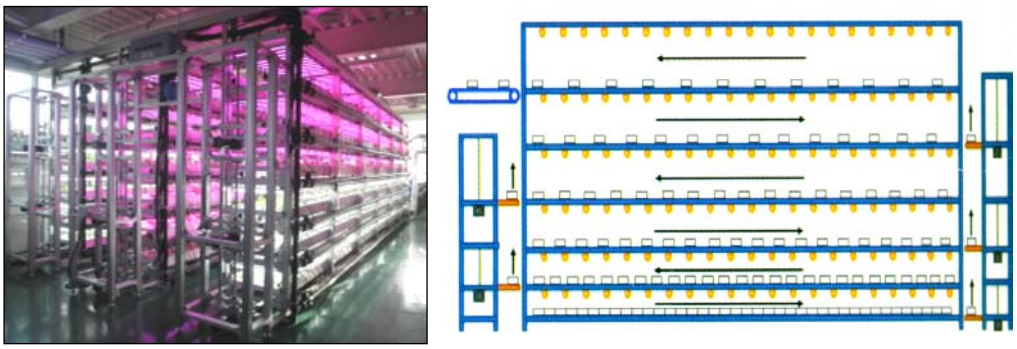

(a) (b)

Figure 2-14. (a) Multilayer growing units in RDA automated plant factory, and (b) direction of crop flow and variable row spacing in plant factory (Kim et al., 2013a)

Figure 2-15. Different views from automated gully operation and row spacing in multilayer plant factory developed by Korea RDA (2011)

2.5. Effect of multistage cultivation and plant spacing

Despite the development of various mechanical designs and systems for implementation of multistage cultivation and adjustment of plant spacing during the plant production process, investigating the effects and outcomes of employing multistage cultivation and application of variable plant spacing on the performance of the cultivation processes has been considered in a limited number of studies.

Prince et al. (1981) designed an experiment to determine the growth response of lettuce to periodic movements and increased spacing values. To conduct this experiment, they used the plant advancing-spacing device by Prince and Bartok (1978) in which the lettuce was hydroponically grown in individual special cups. A five step crop spacing plan was applied for a 34-day growth period according to the growth of plant canopy diameter. To determine the plant spacing in different stages, the value of plant canopy diameter was predicted as a function of growing time based on the following equation:

$$d_1 = d_2 . e^{\frac{-(t_2 - t_1)\ln 2}{3}} \qquad (2\text{-}1)$$

where d_1 and d_2 were diameters of plant canopy (mm) at certain times t_1 and t_2 (days). The final results obtained by the experiment with variable plant spacing showed improvements in total yield of crop, while existing of 15% void spaces in total available growing space was also reported. They emphasized that effective space utilization and variable plant spacing are important criteria for higher plant production.

Giacomelli (1987) introduced a hydroponic growing system with movable rows for continuous production of tomato in the greenhouse. He found that a 26% increase in yearly fruit production per unit floor area can be achieved if optimized row spacing and plant density are applied during three different growth stages with proper timing of successive crop planting.

Goto et al. (1994) conducted a study to investigate the effect of three different spacing options for hydroponic lettuce production. Two types of productivity including the productivity per gross growing area and the productivity per net growing area were discussed in relation to plant form, plant growth rate, and crop

quality. The net growing area covered by plants was estimated according to the projected plant area by image analysis techniques. Factor of growing area utilization was defined to compare the practical and ideal spacing management practices for individual days during the production period. The factor of space utilization could reach the value of one under the ideal spacing policy. Based on the conclusions of this study, the ideal plant spacing strategy is the one which allows each plant to attain the exact projected area if it grows in isolation.

Effects of variable plant spacing and its optimality in indoor cultivation of lettuce have been analyzed and discussed through mathematical modeling by Seginer and Ioslovich (1999). In this study, optimization of major design elements of an industrialized crop production system with emphasis on variable crop spacing and supplementary lighting has been considered. Finding the optimal plant spacing method and cultivation intensity was discussed under two economic constraints including quota-limited (marketing conditions) and area-limited (growing system conditions). In case of quota-limited operation in which marketing quota is the limiting factor, the objective of plant producer was to maximize the gain for every single plant he is permitted to supply to the market, while in an area-limited operation, available area was the limiting factor and grower aimed to maximize the gain per unit of the available area. Mathematical models were developed to describe the behavior of the system under two mentioned situations. In this way, two performance criteria were defined and formulated which expressed the production income per plant, and per unit area for cultivation under quota-limited and area-limited conditions, respectively. Using the optimization in the developed model, it was concluded that young and old plants can grow together in a single climatic compartment such as a plant factory if proper plant spacing values are applied between them. It was also concluded that plant spacing should always be scheduled to maintain a nearly constant canopy density during each stage of the cultivation process. More intensive crop cultivation (smaller plant spacing) asks for more energy consumption and carbon dioxide enrichment, which results in higher expenditures on per unit of production. Thus, using multistage cultivation with optimal plant spacing in each stage can partly prevent such extra expenditures. In a similar study, Iosolovich and Gutmann (2000) used a crop growth model to investigate the optimal control problem associated with plant factory operation. The defined goal was to find the optimal age-dependent

spacing between individual plants such that the profit is maximized. Analyses were carried out to find the best crop spacing based on optimal control theory regulations such as Pontrygin maximum principle. It was shown that the optimal spacing between the growing plants in a plant factory with free growing time is such that the crop density is constant.

Employing multistage cultivation of hydroponic lettuce with the automated row spacing system developed by Chang et al. (2005) resulted in greater number of produced plants and crop yield compared to a similar cultivation process with fixed row spacing. The total duration of both cultivations was 35 days. However, in the experimental 4-stage mobile cultivation with varying row spacing from 100 to 250 mm (see section 2.4), the duration of applied growth stages for first to fourth growth stages was 14, 7, 7 and 7days, respectively. Based on the numerical data obtained by this study, the average final weight of the lettuce produced by both methods was almost the same. However, a total number of 405 lettuce heads was produced in the growing system by the cultivation method which used the variable row spacing. This number was 308 lettuce heads in the same growing area and days when a fixed row spacing method was employed. This means that the using the multistage cultivation has led to more efficient utilization of available area and an approximate 31.5% increase in total plant production. As a commercial example of such growing systems, by applying multistage mobile cultivation and variable row spacing in continuous production of leafy vegetables, a 30-40% increase in the number of plants produced per square meter has been reported in commercial hydroponic production lines (Green Automation, Finland).

In a study by Kim et al. (2011) computer simulation was used for observing the output results of implementing different single-stage and multistage cultivation methods and evaluating their area utilization efficiency. In this study, a parameter so called “planted index area” (PAI) was defined and adopted for evaluation of efficiency of area utilization in cultivation with hydroponic gullies in a single-layer plant factory. The numerical value of PAI was calculated according to equation 2-2:

$$\mathrm{PAI} = \frac{A_H}{A_P} \qquad (2\text{-}2)$$

where A_H is the occupied area per plant at the harvest time, and A_P is average occupied area by a plant at the certain time t during the growth period. Higher values for PAI indicate a higher productivity of available area or more efficient area utilization. This index was used to compare the results of applying fixed and variable row spacing (single-stage and multistage cultivation methods) in terms of area efficiency. Moreover, two common planting arrangements including square and zigzag were applied in each method. Based on dimensional relations of the growing system and assuming a circular plant canopy, all four possible options including square planting with fixed and variable row spacing as well as zigzag planting with fixed and variable row spacing were mathematically modeled and used in simulation. Figure 2-16 displays the general configuration from three of these spacing options.

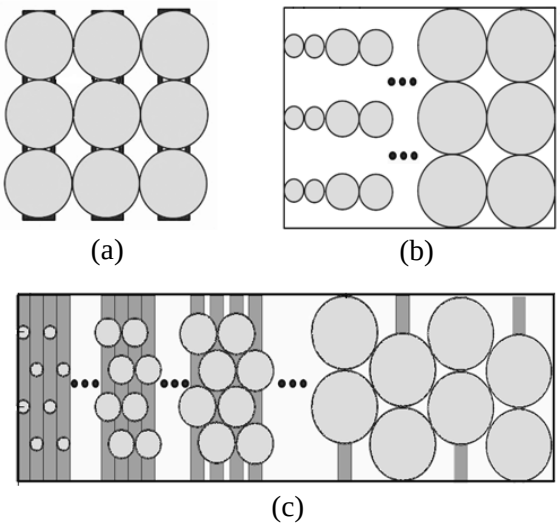

Figure 2-16. (a) Square planting with fixed row spacing, (b) square planting with variable row spacing, and (c) zigzag planting with variable spacing used in the simulation study of Kim et al., (2011)

The simulation encompassed a 30-day growth period during which the plant canopy radius was increased from 3 to 15 cm. Up to fifteen growth stages and four different types of growth curves including linear, sigmoid, exponential, and logarithmic were used for simulation. A summary of results has been presented in Table 2-1.

Table 2-1. Maximum planted area index (PAI) for producing 2000 to 2200 plants under different spacing methods, planting arrangements and growth models (Kim et al., 2011)

Growth model	Maximum planted area index (PAI)			
	Fixed row spacing		Variable row spacing	
	Square planting	Zigzag planting	Square planting	Zigzag planting
Linear	1	1.125	1.596	2.811
Sigmoid	1	1.125	1.575	2.707
Exponential	1	1.125	1.911	3.181
Logarithmic	1	1.125	1.222	2.251

As can be observed, in case of square planting with fixed row spacing, the PAI value is always equal to one which implies a poor efficiency compared to other situations. Results of simulations showed that zigzag planting with fixed row spacing has a better efficiency in area utilization the potential which is 1.125 times greater than its alternative square option at the same amount of area. The higher efficiency area utilization in zigzag planting was also observed in the cultivations with variable row spacing. Considering 2000 to 2200 plants within a single crop production period, the highest value of PAI among all possible options (3.181) was observed when exponential growth curve was employed for zigzag planting in variable row spacing. This finding confirmed the proposal of Marshal and Roberts (2000), who stated that increasing the number of simultaneously expanding leaves on a single stem, in which the area of each single leaf develops based on a sigmoid curve, causes an exponential growth in the total area of plant leaves. Numerical results were also analyzed based on the number of applied growth stages and dimensions of the system.

3. PART I- OBTAINING THE CULTIVATION SCHEMA FOR CONTINUOUS CROP PRODUCTION IN MULTILAYER GROWING UNITS

3.1. Introduction

Multilayer cultivation of plants in NFT gullies is generally possible through either single-stage static or multistage dynamic cultivation methods. The purpose of dynamic cultivation in multilayer plant factories is to further increase the plant production rate per unit floor area, as it is commonly obtained in single-layer growing systems. However, the increase in plant production by dynamic method can be obtained only if an appropriate cultivation plan is adopted and properly executed during the cultivation process. The detailed method for making and evaluating multilayer dynamic cultivation plans as well as finding the procedure to execute them, would be described in this chapter. Characteristics and performance of a certain cultivation plan and the procedure to implement it would be provided through a visual panel which represents a cultivation schema. The information provided by a cultivation schema can assist the grower to make decisions on selecting a certain cultivation plan and execute it in the most efficient way.

3.2. Materials and methods

3.2.1. Layout and methods of multilayer cultivation

General structure of a multilayer growing unit (MGU) consists of multiple identical cultivation layers, which are vertically arranged and stacked on top of each other. MGU provides the required area and growth facilities for hydroponic cultivation of leafy vegetables in NFT gullies in either of static or dynamic cultivation methods. In this study, both of these methods are employed to establish a continuous plant production process in the MGU.

3.2.1.1. Static cultivation

In multilayer static cultivation, entire layers of the MGU are loaded and filled with an equal number of gullies, all of which contain plants with the same planting date (Figure 3-1 (a)). To avoid any interference between the leaves of adjacent plants during the growth period, gullies are sufficiently spaced from each other from the day they enter the MGU and remain in the same place until the harvesting day. Thus, no displacement of gullies is needed during plant growing days and all plants are harvested together as one crop output at the end of the growth period. Thus, static cultivation can be known as the "single-stage stationary" cultivation approach. Overlapping between the plants growing on a single gully is prevented by choosing an adequately large distance between plant holder holes.

3.2.1.2. Dynamic cultivation

Employment of static cultivation increases the yield in unit floor area. However, a further increase in production amount of MGU can be achieved if proportional and time-variant utilization of available area is accomplished through dynamic cultivation. Dynamic cultivation is a multistage mobile cultivation. Figure 3-1 (b) shows the schematic configuration and details of dynamic cultivation in an r-layer growing unit, in which the plant growth in the MGU is completed during "m" growth stages.

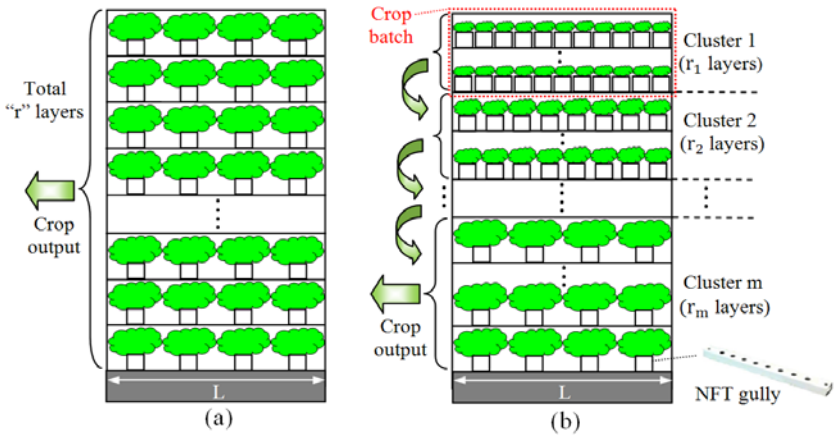

Figure 3-1. General configuration of an r-layer growing unit during static cultivation, and (b) dynamic cultivations

The initial step in implementation of multilayer dynamic cultivation is “clustering” of MGU layers, which is defined as dividing the MGU layers into several groups, each called a cluster, and assigning a certain number of layers to each of them. The area provided by each cluster is used to maintain plants with the same planting date and size. In this study, the term “crop batch” (CB) is used to nominate a given number of growing plants of the same age that are kept in one cluster and whose growth level lies within a common growth stage. Based on the above statements, it is concluded that, i) the number of created clusters, crop growth stages, and present CBs in the MGU are equal to each other, and ii) no cluster or layer contains plants belonging to different CBs. Stepwise reduction of plant density when progressing to higher growth stages is an essential objective in dynamic cultivation. To this end, the cultivation process is started from cluster 1 at the top of the MGU, where the gullies containing the youngest plants are densely loaded. Young plants of this CB stay in cluster 1 until the last day of the first growth stage. In this study, the measure to determine the length of a growth stage (in terms of days) is to prevent overlapped plant canopies during the days of that stage. Accordingly, the end of growth stage 1 is when the loaded CB in cluster 1 demands an additional area due to the onset of interference between its plant canopies. At this point, entire gullies in cluster 1 are moved and redistributed into the layers of larger cluster 2. This reduces the plant density in the CB for growth stage 2. This cycle is similarly applied in next growth stages until the fully grown CB is issued as a crop output from cluster “m”. In order to achieve a continuous plant production in the MGU, a younger CB with the same number of gullies is loaded into discharged layers of cluster 1 and follows the same steps applied to the previous CB. The arrows in Figure 3-1 (b) indicate stepwise displacement of serial growing CBs in the MGU. According to the above descriptions, it can be perceived that the number of layers in certain cluster i (r_i) must always be higher than its preceding cluster. In addition, because there are same number of gullies per CB in all clusters, the distance between consecutive gullies, henceforth called “row spacing”, is different in various clusters but equal within the layers of a common cluster.

Figures 3-2 (a) and (b) indicate top views from the entire length of a cultivation layer in certain cluster “i” for two planting patterns including square and zigzag plant arrangements, respectively. The patterns of these two planting arrangements are

plotted using the dashed lines. In both arrangements a constant value of row spacing (δ_i) is evenly applied between the gullies.

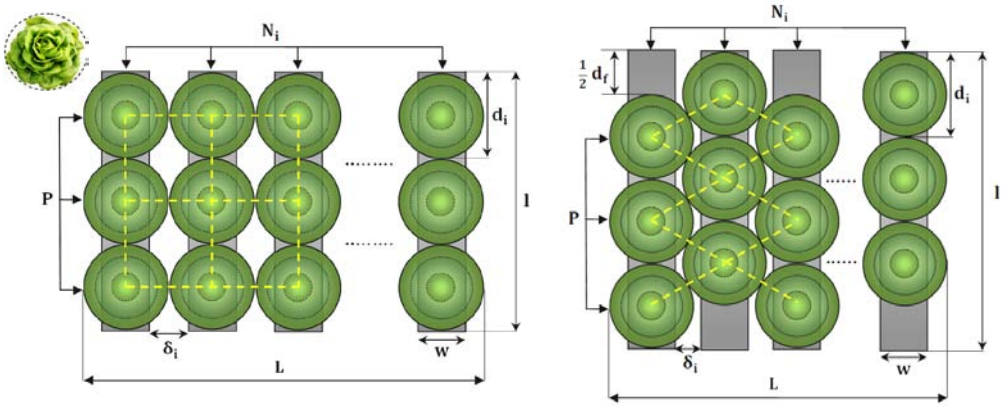

(a) (b)

Figure 3-2. Multistage increase of canopy diameter and arrangement of gullies in a cultivation layer under (a) square, and (b) zigzag planting arrangements

For simplicity in estimating the increase in canopy diameter, a circle is circumscribed about the projected area of plant growing canopy and the diameter of this circle is taken as an estimator of plant growth. The concentric circles shown for each plant denote the multistage increase in the plant canopy, in which the largest circle depicts the maximum canopy size allowed to be kept in the indicated layer.

In Figures 3-2 (a) and (b), parameters “w” and “l” are gully width and length, respectively and “P” is number of plants per gully. “N_i” is maximum number of gullies in a fully loaded layer of cluster “i” and “L” is the length of the cultivation layer along which the gullies are spread. The parameter “d_i” is maximum allowed canopy diameter in the layers of cluster “i” when row spacing δ_i is applied. Plants are allowed to stay in a certain layer of cluster “i” up to the day on which the canopy diameter reaches this threshold value. Thus, the value of d_i is a determinant factor in deciding the length of the growth stage “i”. Finally, ”d_f“ is size of canopy diameter at the end of final growth stage (growth stage m) or harvest time. The unit of all dimensions stated above is centimeters.

3.2.2. Dimensional relations in multistage dynamic cultivation with square and zigzag planting

Gradual growth of projected area of plant canopies and the multistage increase of row spacing between the gullies caused by that are separately demonstrated in Figures 3-3 (a) and (b) for square and zigzag planting arrangements, respectively. Assuming that the largest diameter of plant canopy available at the end of last stage (d_f) is not allowed to exceed the gully length, under equal conditions involving the same number of plants per gully and crop type, the length of employed gullies in zigzag planting must be longer than the gullies used in square planting. As indicated in Figure 3-2 (b), the value of this length difference should be at least $0.5d_f$. This means that in compare to square planting, a relatively larger area would be occupied by the gullies during zigzag planting when a same row spacing value is applied to both. However, due to later occurrence of canopy overlapping in zigzag planting, it is possible to keep smaller values of row spacing when equal canopy diameters are growing under both planting arrangements (Figure 3-3).

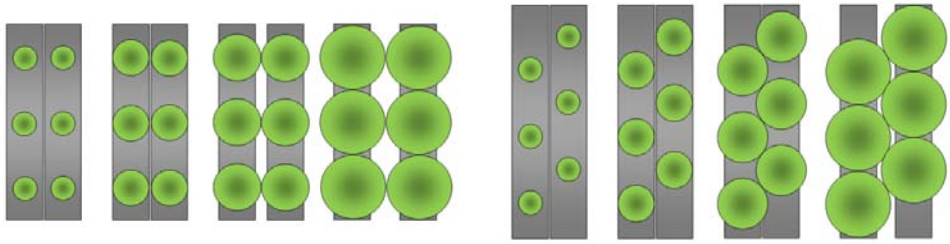

(a) (b)

Figure 3-3. General phases and situations in stepwise increase of row spacing value for (a) square, and (b) zigzag planting arrangements

In square planting two general phases including “zero” and “non-zero” can be distinguished in row spacing process (Figure 3-4 (a) and (b)) such that more than one growth stage can be included within each phase. As also shown in two left images of Figure 3-3 (a), keeping “zero row spacing” is possible during the days in which the size of canopy diameter is smaller than the gully width. In this case, the horizontal distance between the centers of two adjacent gullies (H_{pp}) would be equal to the gully width (Figure 3-4 (a)). Application of “non-zero row spacing” would be necessary

when the size of canopy diameter begins to exceed the gully width. In such a case, the row spacing value applied in each growth stage will be equal to the maximum allowed canopy diameter at the end of that growth stage (d_i) (Figure 3-4 (b)).

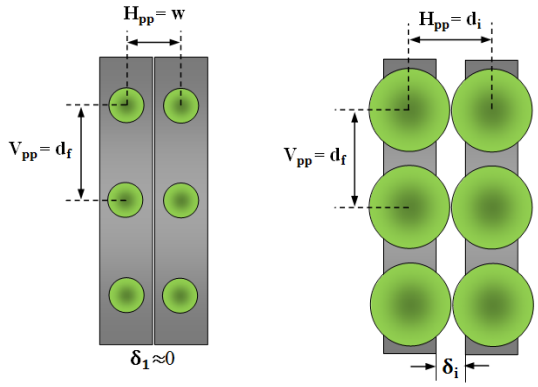

Figure 3-4. Dimensional relations in two general phases of row spacing in square planting

As shown in Figures 3-5 (a) to (c), the row spacing process in zigzag planting can be specified in three general phases. In both Figures 3-4 and 3-5, the parameter "V_{pp}" denotes the fixed distance between centers of adjacent plants growing on the same gully that should not be smaller than canopy diameter at the end of the final growth stage (d_f). Available duration of zero row spacing phase (the first phase) in zigzag planting (Figure 3-5 (a)) is longer than that in square planting. This is because in square planting, the overlapping between the plant canopies growing on adjacent gullies appears when the canopy diameters reach the size of gully width, while such first overlaps in zigzag planting would be visible when the canopy diameter is somewhat larger than the gully width. Based on this, shifting from zero row spacing to the next larger row spacing value can be partly prolonged in zigzag planting.

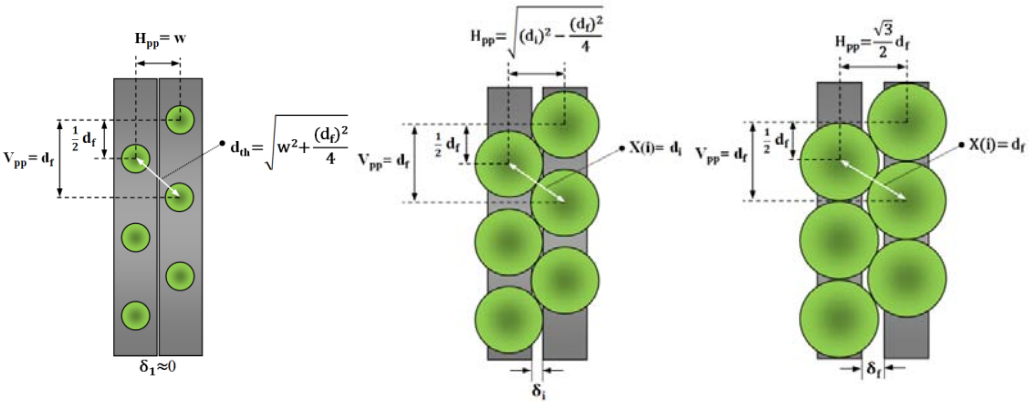

(a) (b) (c)

Figure 3-5. Dimensional relations in three general phases of row spacing in zigzag planting

Accordingly, the threshold canopy diameter in zigzag planting (d_{th}) is defined as the maximum canopy diameter until which no overlap between canopies occur and zero row spacing between gullies is kept. As illustrated in Figure 3-5 (a), this diameter is the diagonal distance between the centers of two neighboring plants growing on adjacent zero spaced gullies. According to this figure, the threshold canopy diameter in zigzag planting (d_{th}) can be calculated using Equation 3-1 whose parameters have been previously defined:

$$d_{th}=\sqrt{w^2+\frac{(d_f)^2}{4}} \qquad (3\text{-}1)$$

The second phase of row spacing process in zigzag planting arrangement is distinguished when canopy diameters exceed the d_{th} value, but still not large enough to cause overlaps between the plants growing on a common gully (Figure 3-5 (b)). In the growth stages whose ends lie within this phase, the horizontal distance between the centers of two adjacent gullies (H_{pp}) would directly depend on the value of d_i. As can be observed in Figure 3-5 (b), d_i represents the diagonal distance between the centers of two neighboring plants growing on adjacent gullies during the certain

growth stage i (X(i)). Equation 3-2 is used to calculate the value of H_{pp} in the growth stages of phase 2:

$$H_{pp}=\sqrt{(d_i)^2-\frac{(d_f)^2}{4}} \qquad (3\text{-}2)$$

The third phase of row spacing in zigzag planting (Figure 3-5 (c)) includes the final growth stage of plant growth period which is ended when the plant canopies get their largest size represented by the previously explained parameter d_f. By substituting d_f for d_i in Equation 3-2, the approximate value of $0.866d_f$ is found for the H_{pp} which should be appropriately applied in the final growth stage.

Determination of H_{pp} value in each of the five row spacing phases described for square and zigzag planting arrangements is a step to find other relevant dimensions and items of the growing unit. Considering a multistage dynamic cultivation in a MGU as that shown in Figure 3-1 (b), the optimal row spacing value in the layers of cluster "i" (δ_i^*) can be specified by Equation 3-3:

$$\delta_i^* = H_{pp}\text{-}w \qquad (3\text{-}3)$$

Although the values obtained from Equation 3-3 denote the optimal row spacing values calculated based on the size of plant canopy in different growth stages, the row spacing values applied in MGU layers are to some extent larger than their respective optimal values in most cases. This is because the row spacing applied in a cultivation layer is determined based on number of available gullies in that layer as well as the length of that cultivation layer (L). Referring back to the schematic MGU displayed in Figure 3-1(b), the cultivation layers shown in Figure 3-2 and considering a multilayer cluster such as "i" in the MGU, maximum number of gullies per layer of cluster i (N_i) under square and zigzag planting arrangements, are calculated using Equations 3-4 and 3-5, respectively.

$$N_i = \left\lfloor \frac{L}{H_{pp}} \right\rfloor \qquad (3\text{-}4)$$

$$N_i = \left\lfloor 1 + \frac{L - d_i}{H_{pp}} \right\rfloor \qquad (3\text{-}5)$$

Since the value related to number of gullies must be an integer, the values calculated in the right side of Equations 3-4 and 3-5 are rounded down to the nearest integer. The semi-bracket notation enclosing the right term of each equation represents the floor function which converts a real number to the largest previous integer. The N_i values calculated by Equations 3-4 and 3-5 would be again inserted in Equation 3-6 to find the row spacing applied in the layers of certain cluster i.

$$\delta_i = \frac{L - (N_i \times w)}{N_i} \qquad (3\text{-}6)$$

The values calculated by the Equation 3-6 are applied to entire gullies loaded in the layers of a common cluster at the beginning day of a growth stage and remain unchanged until the end of ongoing growth stage.

3.2.3. Time interval between crop outputs

It is obvious that the time interval between successive crop outputs in continuous static cultivation equals the length of plant growth period in the MGU (T days). On the other hand, continuous plant production by dynamic cultivation provides a steady stream of crop outputs such that the time interval between them is shorter than in the static cultivation when both cultivations are employed to grow the same type of crop in similar MGUs. Using the time diagram in Figure 3-6, it can be seen that the time interval between consecutive crop outputs in a continuous multilayer dynamic cultivation with multiple growth stages of different length is equal to the length of the longest growth stage (T_{max}). In this figure, the length of plant growth period (T) has

been divided into 3 growth stages with unequal number of days (here, $T_1 < T_2 < T_3$). Thus, growth stage 3 has the longest length among all growth stages ($T_3 = T_{max}$).

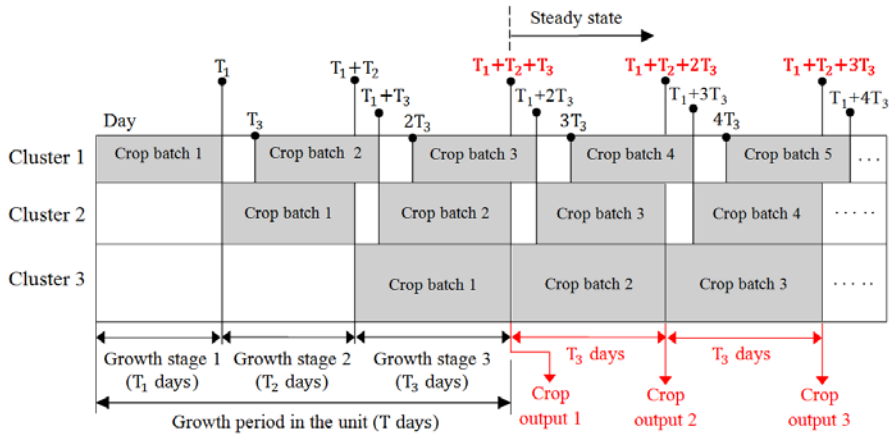

Figure 3-6. Time diagram of a dynamic cultivation process with unequal growth stages in a MGU

As demonstrated in Figure 3-6, CB1 remains in cluster 1 for T_1 days and is then moved to the larger cluster 2 to stay for T_2 days. Plants of CB1 are displaced to cluster 3 after T_1+T_2 days and are finally harvested at the end of day $T_1+T_2+T_3$ (crop output 1). The resulting time diagram reveals that if this multi-step procedure is applied to next CBs, time events such as "starting" or "final" days of a CB in different clusters (solid dots) and crop output days (shown in red) would regularly recur every T_3 days, which is the duration of the longest growth stage. Hence, T_{max} is the recurrence interval (return period) of similar time events in the cultivation process. Another point to note in Figure 3-6 is the necessity of maintaining certain time delays for loading successive CBs in clusters 1 and 2 to prevent concurrent retention of serial CBs in clusters 2 and 3. In this example, length of applied delays are T_3-T_1 and T_3-T_2 days in cluster 1 and 2, respectively. Application of such time delays is not required when a dynamic cultivation with same length growth stages is in progress. Table 3-1 represents the parametric displacement schedule of serial CBs in the MGU containing the days after which a CB must be moved from its current position, based on the time diagram of Figure 3-6.

Table 3-1. Parametric displacement schedule of serial crop batches in different clusters of the MGU shown in Figure 3-6

Cluster	Moving day to next cluster or harvester*					Recur. interval (days)
	CB1	CB2	CB3	CB4	CBi	
1	T_1	T_1+T_3	T_1+2T_3	T_1+3T_3	$T_1+(i-1)T_3$	T_3
2	T_1+T_2	$T_1+T_2+T_3$	$T_1+T_2+2T_3$	$T_1+T_2+3T_3$	$T_1+T_2+(i-1)T_3$	T_3
3	$T_1+T_2+T_3$	$T_1+T_2+2T_3$	$T_1+T_2+3T_3$	$T_1+T_2+4T_3$	$T_1+T_2+iT_3$	T_3

*In cluster 3

Reminding that employment of static and dynamic cultivations is possible in similar MGUs, Figure 3-7 contains a time diagram in which the crop outputs of two continuous static and dynamic cultivation processes, executed in similar MGUs, are simultaneously shown during a certain period of time. Plant growth period in the dynamic cultivation has been divided into “m” growth stages. Length of the final growth stage m (T_m), that is also the longest stage among all, is the interval of the crop outputs in the dynamic cultivation (D arrows), while the crop outputs of static cultivation (S arrows) are repeated every T days. As observed, due to shorter length of T_m, number of the outputs in the dynamic cultivation is comparatively higher within a certain period of time.

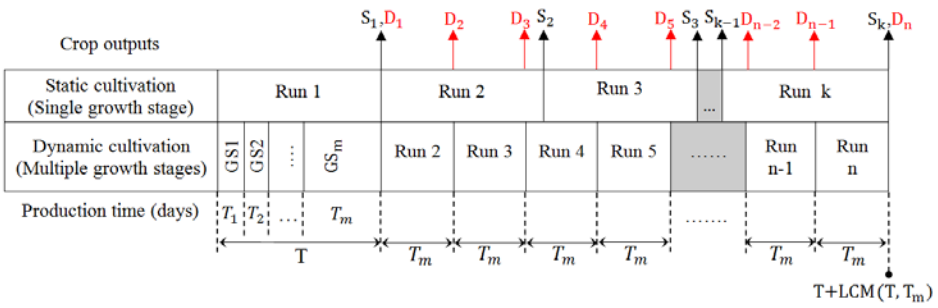

Figure 3-7. Comparison of crop output intervals in static and dynamic cultivations

The cultivation process in Figure 3-7 is shown until the day T+ LCM (T, T_m), where LCM stands for least common multiple. This day is the second joint crop output of static and dynamic cultivations during a continuous plant production process.

3.2.4. Plant production rate (PPR)

In this study, the term plant production rate (PPR) has been defined as the average number of produced plants per day during the time interval between two successive crop outputs. Although the daily production of plants is mostly feasible in large growing systems, the PPR defined in this study is an implicit index used to evaluate and compare the production capacities of different static and dynamic cultivation plans regardless of availability of the daily harvest. Considering that the total number of layers is the same in the MGUs shown in Figures 3-1 (a) and (b), the PPR values obtained by static and dynamic cultivations are calculated using Equations 3-7 and 3-8, respectively.

$$PPR_S = \frac{\sum_{i=1}^{m} r_i \times N_S \times P}{T} \qquad (3\text{-}7)$$

$$PPR_D = \frac{N_{CB} \times P}{T_{max}} \qquad (3\text{-}8)$$

where PPR_S and PPR_D are plant production rates (plants/day) obtained by static and dynamic cultivation plans, respectively. The first factor in the numerator of Equation 3-7 represents the total number of layers in the MGU, N_S is the number of gullies in fully loaded layers of the MGU during static cultivation, and N_{CB} is the number of gullies per CB in dynamic cultivation. Other terms have been explained previously. Note that the values in the numerators of Equations 3-7 and 3-8 will give the number of plants in crop outputs of static and dynamic cultivation plans. Likewise, T and T_{max} in the denominators of these equations represent the time intervals between crop outputs of static and dynamic cultivations, respectively. The existence of a smaller value in denominator of Equation 3-8 is a potential factor to increase the value of PPR_D relative to PPR_S; however, a lower calculated value in the numerator of Equation 3-7 would partially or, in some cases, totally neutralize this effect.

3.2.5. Turning point day (TPD)

Due to possibility of employing one static and multiple dynamic cultivation plans in a certain MGU, the grower should be able to evaluate all these applicable plans and select the one with the best production performance. The PPR resulting from a particular cultivation plan is a measure to express the production capacity of that plan. Based on this measure, any static or dynamic cultivation plan that is able to provide the highest PPR value in a certain MGU is nominated to be the optimal plan. In this study, however, the supplementary evaluation index "Turning point day" (TPD) is also defined for the dynamic plans that provide higher PPR values compared to their alternative static option ($PPR_D > PPR_S$).

TPD is specified as the common day in two continuous static and dynamic cultivations on which the accumulated number of plants produced by both is the same. Similar MGUs, and same starting date and crop type are assumed in both cases. Figure 3-8 displays serial crop outputs (solid dots) of two static and dynamic cultivation processes in terms of accumulated number of produced plants (Y axis) versus plant production days (X axis). Slopes of relevant trend-lines of static and dynamic crop outputs are PPR_S and PPR_D, respectively. Referring to Figure 3-8, the intersection of these two trend-lines, i.e., the point where the higher position of the static trend-line relative to the dynamic trend-line is reversed, is the TPD point.

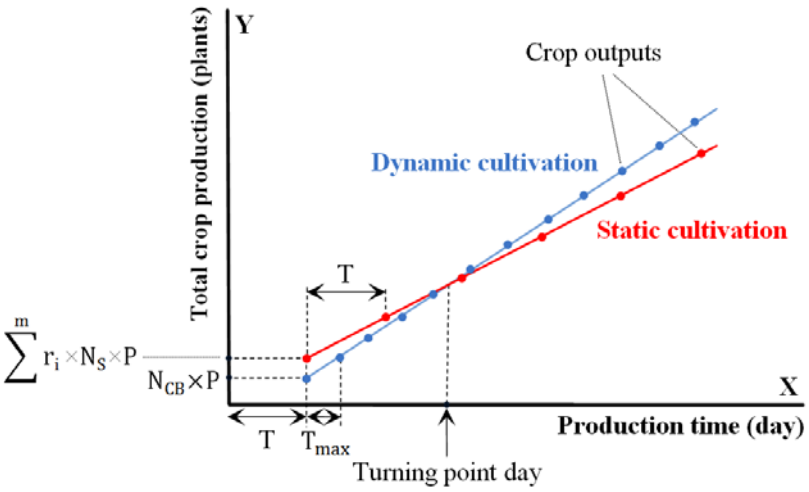

Figure 3-8. Trend-lines of crop outputs for static and dynamic cultivations, and concept of turning point day

Since crop output days of static and dynamic cultivations are discrete events and are repeated according to the fixed time intervals T and T_{max}, TPD may not always coincide with a crop output day. Therefore, TPD is used as a theoretical criterion to estimate the time required for a dynamic cultivation plan to overtake its alternative static plan in plant production. A smaller TPD is an advantage for a dynamic cultivation plan. According to Figure 3-8, the basic (non-simplified) Equations in 3-9 and 3-10 can be used to calculate accumulated number of produced plants in different crop output days of static and dynamic cultivations, respectively.

$$\begin{cases} Y = PPR_S.(X - T) + (\sum_{i=1}^{m} r_i . N_S . P); \\ X=kT, \quad (k=1,2,3,\ldots) \end{cases} \qquad (3\text{-}9)$$

$$\begin{cases} Y = PPR_D.(X - T) + (N_{CB}.P); \\ X=T+kT_{max}, \quad (k=0,1,2,\ldots) \end{cases} \qquad (3\text{-}10)$$

The k values in discrete domains of (3-9) and (3-10) represent the number of each crop output. The k value 1 implies the first crop output in the static cultivation process, while the k value for the first crop output in dynamic cultivation process is 0.

3.2.6. Modeling and simulation of cultivation plans

Simulation can be used as an assisting tool to observe the results of multilayer cultivation implemented by different executive plans and more specifically, to select the plan with best performance for plant production. In this way, the steps involved in development of a model to provide the required data for evaluation and implementation of different executive plans for multilayer cultivation and convert it into a computer simulation module with visual panel are explained in the following sections.

3.2.6.1. Modeling of cultivation plan

The proposed model in this study involves an algorithm by which the maximum obtainable PPR by a dynamic cultivation plan with “m” growth stages, the PPR of its alternative static plan, TPD, and executive results of static and dynamic plans are acquired for different crops and MGU conditions. Figure 3-9 shows inputs, outputs and general steps of the model in a simplified view, while the details of model algorithm used for programming the simulation module are illustrated in Figure 3-10. As can be perceived from the figures, the proposed model enables the user to have simultaneous evaluation of static and dynamic cultivation plans.

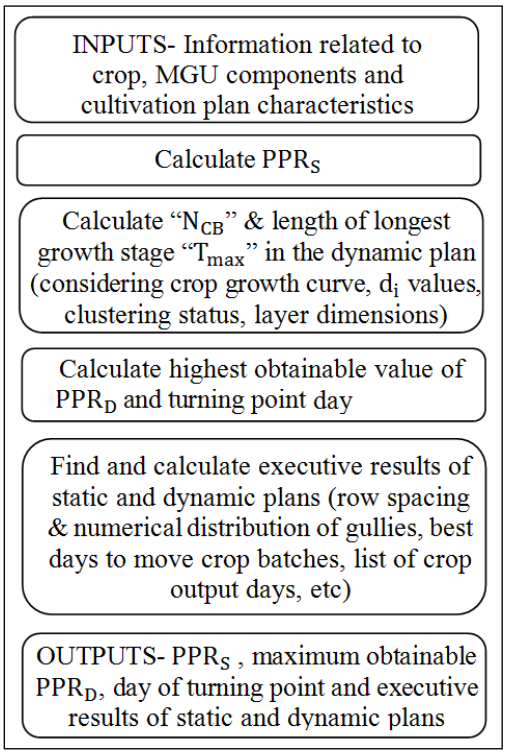

Figure 3-9. Inputs, outputs and general steps of the model

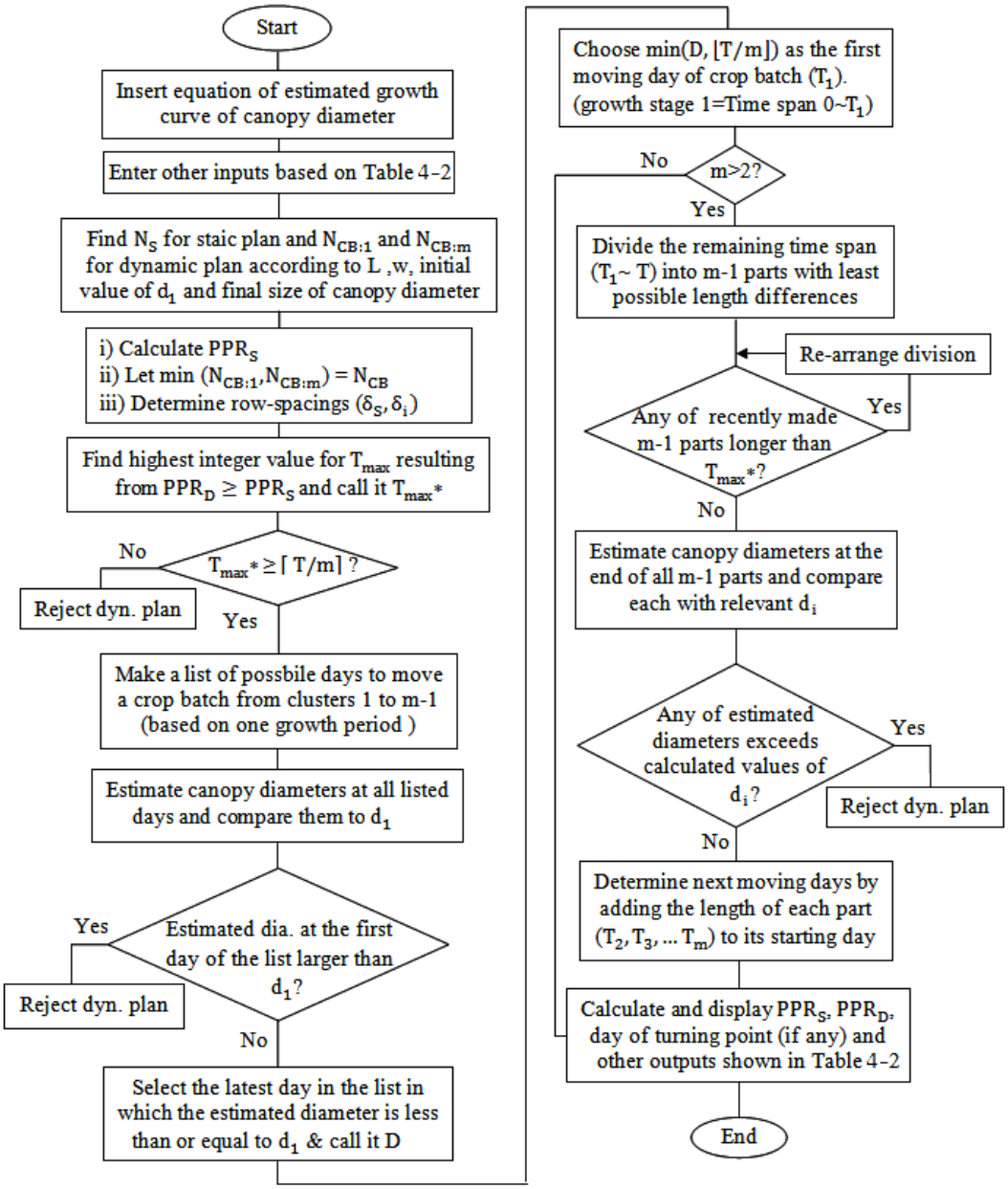

Figure 3-10. Model algorithm used for programming of simulation module

A complete list of model inputs, outputs and their units is presented in Table 3-2. Since simulation of dynamic cultivation and its alternative static option are involved in the same model structure, the relevance of inputs and outputs to static or dynamic options has been indicated using the letters S and D, respectively. Model outputs can be classified into two major groups including those based on which a decision on employing a certain executive plan is made (PPR_S, maximum obtainable PPR_D and TPD) and, the executive results of each cultivation plan that can be used as a practical guide for proper implementation of the cultivation process. Lists of crop output days and accumulated plant production in crop output days are the executive results which can further help the grower in decision making. Estimating the size of canopy diameter on different days of the growth period is a key component in model operation. To estimate this value, the growth equation of canopy diameter has been specified as one of the model inputs. As an illustrative example about clustering status listed in model inputs, a 2-3-4 clustering implies that a total of nine cultivation layers have been divided into three clusters (m=3), where 2, 3, and 4 are the number of layers assigned to clusters 1, 2 and 3, respectively (r_1=2, r_2=3, r_3=4).

Table 3-2. List of model inputs and outputs and their relevance with static or dynamic cultivation plans

Input		Unit	Plan	Output	Unit	Plan
Growth equation of canopy diameter		-	S,D	Plant production rate of static plan (PPR_S)	plants/day	S
Length of plant growth period in the MGU (T)		day	S,D	Plant production rate of dynamic plan (PPR_D)	plants/day	D
Length of cultivation layer (L)		cm	S,D	Turning point day (TPD)	day	D
Width of gully (w)		cm	S,D	Row spacing in static cultivation (δ_S)	cm	S
Type of planting arrangement		-	S,D			
Initial value of max. allowed canopy diameter in the layers of cluster 1		cm	S,D	Row spacing in the layers of different clusters (δ_i)	cm	D
Length of gully (l)		cm	S,D	Length of longest growth stage (T_{max})[1]	day	D
Plants per gully (P)		plant	S,D	Moving days of a crop batch [2]	day	D
Estimated duration of continuous cultivation process		day	S,D	List of crop output days during the process	-	S,D
Clustering status	Number of growth stages/clusters (m)	-	D	List of accumulated plant production in crop outputs	plant	S,D
	Total number of layers (r)	-	S	Numerical distribution of gullies in different clusters	-	D
	Layers per cluster (r_i)	-	D	Other monitoring data	-	S,D

[1] Recurrence interval in dynamic cultivation; [2] Based on the length of one growth period

3.2.6.2. Description of the model

PPR_S, maximum obtainable PPR_D and TPD are model outputs on the basis of which the final plan for implementing continuous cultivation in MGU is selected by the user. In case of the static cultivation plan, Equation 3-7 automatically calculates the highest possible value of PPR_S according to definition of N_S. However, exploring for maximum available N_{CB} , i.e., number of gullies per CB in dynamic cultivation, and lowest possible value of T_{max} are the necessary steps to obtain the maximum value of PPR_D (see Equation 3-8). Determining the TPD would be feasible after PPR_S and maximum PPR_D values are finalized.

To start calculations, maximum possible number of gullies in each layer of first and final clusters must be estimated. According to the planting arrangement (square or zigzag) selected in the cultivation plan, one of the Equations 3-4 or 3-5 is employed for this purpose. Maximum allowed canopy diameters in the layers of cluster 1 (d_1) and final size of canopy diameter at the end of the growth period (d_f) are the determinant factors for using these equations. "d_f" is estimated by inserting the total length of plant growth period (T) into the growth equation of canopy diameter, whereas the initial value of d_1 is a user-defined input of the model. In the case that calculated value by Equation 3-4 (or 3-5) is made based on respective H_{pp} of d_f , the obtained results are also considered as the number of gullies in fully loaded layers of MGU during static cultivation (N_S), using which PPR_S can be calculated by Equation 3-7. Continuing the calculations, the values calculated by Equations 3-4 and 3-5, together with the information on clustering status (see Table 3-2) are used to determine the maximum possible value of N_{CB}. In the current model, the N_{CB} is determined based on the smaller value between $N_{CB:1}$ and $N_{CB:m}$, where $N_{CB:1}$ ($r_1 \times N_1$) and $N_{CB:m}$ ($r_m \times N_S$) are the number of gullies per CB based on maximum gully maintaining capacity of the first and last clusters, respectively. It is reminded that since either of static cultivation and final growth stage of dynamic cultivation deal with the final size of canopy diameter (d_f), N_S is also used in the calculation of $N_{CB:m}$. The determined N_{CB} is then inserted into Equation 3-8 whose denominator should be the lowest possible value of T_{max} if maximum PPR_D is to be achieved.

Lowest possible value of T_{max}, or shortest possible crop output interval creates the maximum PPR_D in the dynamic cultivation plan. "Timing of growth stages" involves finding the best possible length for each growth stage of the plan as a result of which the lowest possible value of T_{max} and best moving days of CBs during a growth period are also determined. Dividing the length of plant growth period (T days) into "m" time spans (number of growth stages) with equal or near-equal number of days is the general way to attain the lowest possible T_{max}. In this case, length of T_{max} is estimated through dividing the "T" by "m" and rounding up the obtained value to the nearest integer value ($\lceil T/m \rceil$). For example, the lowest possible T_{max} in a plan with a growth period length of 28 days and 3 growth stages is 10 days, which can be drawn from any of near-equal timing combinations of 9-9-10, 9-10-9, or 10-9-9 days. In cases that a combination of the same length growth stages forms the optimal timing, e.g., 9-9-9 days for T=27 days, the equal length of all growth stages is selected as the T_{max}. In the recent example, the appropriate days for moving a CB from clusters 1, 2 and 3 are the days 9, 18 and 27.

Although the equal or near-equal length of growth stages provides the lowest possible value of T_{max} in a dynamic plan, the feasibility of applying such timings must be examined and confirmed by the model through comparing the size of canopy diameter in the days determined by equal or near-equal growth stage timing with maximum allowed canopy diameters in different clusters (d_i, i=1,2,..,m). Details of the applied procedure for an m-stage dynamic cultivation plan can be observed in Figure 3-10. Performing this comparison in all clusters of the MGU will give determine the best moving days of a CB based on one growth period from which the lowest value of T_{max} is also found and subsequently inserted in Equation 3-8 to obtain the highest PPR_D of the dynamic cultivation plan. Displacement schedule of serial CBs in the MGU and list of crop output days in dynamic cultivation are executive results of the plan, which would be available after finding the best timing of growth stages.

Row spacing values applied in different clusters (δ_i) and numerical distribution of gullies in different layers of MGU clusters are the model outputs which are determined according to factors such as length of the cultivation layer (L), number of layers per cluster (r_i) and number of gullies in the crop batch (N_{CB}). Since N_{CB} is selected based on the gully maintaining capacity of either first or final cluster in the

MGU, a balanced gully distribution with equal number of gullies in all layers of a cluster may not be always obtained. In such cases, at least one layer of some clusters may contain less number of gullies and appear as an incompletely loaded layer. For example, loading a crop batch with 51 gullies in a cluster with 5 layers is possible through numerical gully distribution of 11-11-10-10-9 (N_i=11), where the layers containing 10 and 9 gullies are the incompletely loaded layers. Equation 3-11 represents a mathematical relation between N_{CB} and numerical distribution of gullies in the layers of a certain cluster, when incomplete layers of a cluster containing the same number of gullies are bundled in individual groups. This equation is used by the model to find all possible options of numerical distribution of gullies in different clusters of an MGU.

$$N_{CB}=\left(r_i-\sum_{j=1}^{n}\alpha_j\right)N_i+\sum_{j=1}^{n}[\alpha_j(N_i-\beta_j)] \qquad (3\text{-}11)$$

Assuming “n” different groups of incompletely loaded layers in a certain cluster, α_j indicates the number of incomplete layers with the same number of gullies bundled in group j and β_j is the difference between number of gullies in complete layer (N_i) and number of gullies in incompletely loaded layer of group j. Referring to the most recent numerical example stated above (N_{CB}=51, N_i=11, r_i=5), two groups of incompletely loaded layers (n=2) can be observed. The first group (j=1) has two incomplete layers ($\alpha_1=2$) each with 10 gullies which is one unit less than 11 loaded gullies in the complete layer (β_1=1). The second group (j=2) with only one cultivation layer ($\alpha_2=1$) maintains 9 gullies that is two units lower than the determined N_i (β_2=2).

3.2.6.3. Simulation module with visual panel for obtaining the cultivation schema

To provide a more convenient and easier way for using the described model, and allow the user to obtain the entire information, results and procedure of executing a certain cultivation plan in form of a cultivation schema, the developed algorithm (Figure 3-10) was converted a virtual instrument (VI) by Labview programming (National Instruments, TX, USA). The outcome of this conversion is a computer simulation module with an input-output visual panel. VI is the equivalent term for programs and subroutines written in Labview and consists of two interrelated parts including “block diagram” and “front panel”. Block diagram is the executive body of a VI in which the programming elements are incorporated. Appendices A.1 and A.2 display the block diagrams of the VIs developed for simulating the cultivation plans under square and zigzag planting arrangements. The front panel of a VI is a visual interface which enables the user to control and monitor the functioning of the block diagram. Figure 3-11 demonstrates an image from the developed visual panel of the simulation module used for evaluating the performance of different dynamic and static cultivation plans and observing their executive results, based on which the procedure to implement the plan is also determined. The general display of this panel after the end of each simulation, as it is also shown in Figure 3-11, represents a cultivation schema including the characteristics and performance of simulated cultivation plan as well as the procedure to execute it.

Referring to Figure 3-11, the user can insert and change the value of the parameters related to a cultivation plan through the numeric controls of “INPUT” sub-panel and observe the simulation outputs through different numeric indicators distributed on the visual panel. The input “growth equation of canopy diameter” is inserted into the simulation module via a text-based formula node embedded within an independent sub-VI in the block diagram (Figure 3-12). Clustering of the cultivation layers in dynamic cultivation plans is manipulated by entering desired number of layers into numeric controls assigned to each cluster placed in the upper part of the input sub-panel. As can be observed, the developed module can be used for simulating the dynamic cultivation plans with maximum three growth stages.

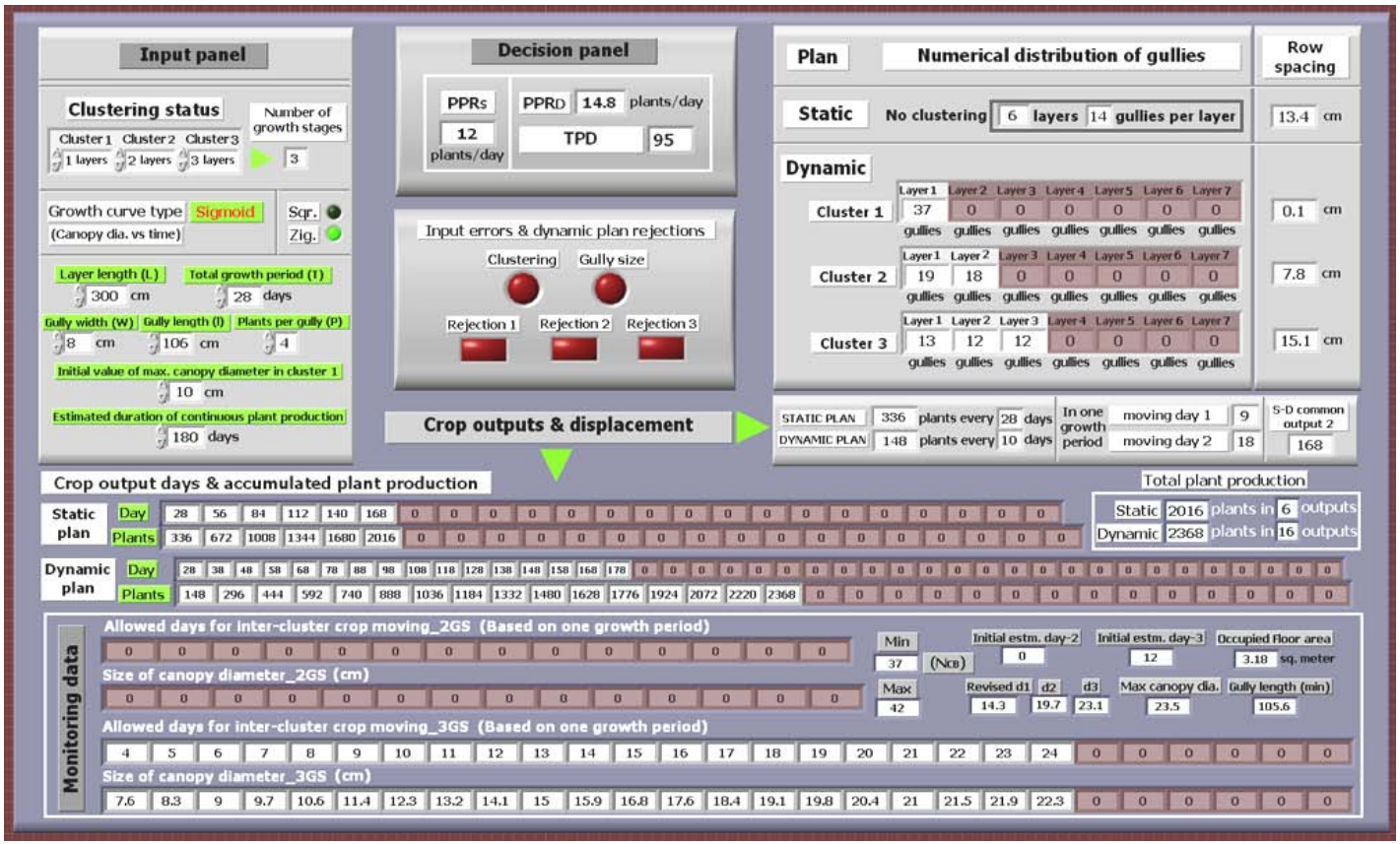

Figure 3-11. Visual simulation panel representing a cultivation schema

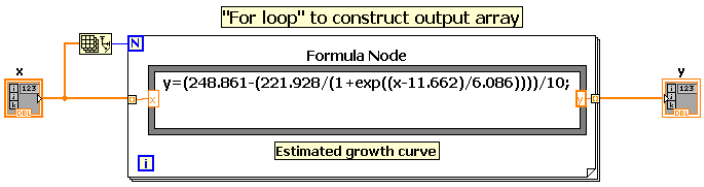

Figure 3-12. Sub-VI and formula node for growth equation of canopy diameter

The “DESICION” sub-panel contains the numeric indicators displaying calculated values of three outputs including PPR_S, maximum obtainable PPR_D, and TPD, which can be used to make a decision on proper cultivation plan. Numerical values of other outputs related to executive results of cultivation plans are displayed in other parts of the visual panel. For example, the outputs related to row spacing values and numerical distribution of gullies in both static and dynamic cultivation plans are presented in a sub-panel located in the right side of Figure 3-11. A couple of the twin horizontal lists containing crop output days and accumulated plant production of continuous static and dynamic cultivations within the estimated duration of the cultivation process, and the crop moving days are some other outputs shown in the visual panel.

The “MONITORING DATA” box located at the bottom part of the visual panel contains a number of data that are not included among the listed outputs of Table 3-2. However, they are directly used in the model operation and can also help the user to understand and interpret the simulation results in related cases. As an example, a list of the days, only in which the displacement of crop batch causes a higher value of PPR_D than PPR_S can be seen in this box. However, in some instances PPR_D can never be larger than PPR_S due to specific conditions of specified plans and as a result, rejection of simulated dynamic plan is informed to the user through the visual panel. Accordingly, the frame tagged as “INPUT ERRORS AND DYNAMIC PLAN REJECTIONS” contains five LEDs which will be on to notify the user in the situation of either a mistake in inserting input data or a case rejecting the usefulness of dynamic plan. For example, the “clustering error” LED would be turned on if the number of layers assigned to a cluster is equal to or higher than its next clusters. Table 3-3 indicates the full list of related errors and rejections announced by LEDs.

Table 3-3. Reasons of input errors and rejections of dynamic plan shown in the simulation panel

Error/rejection	Reason
Clustering	Number of layers assigned to a cluster is higher than its next clusters
Gully size	Product of final size of canopy diameter and number of plants per gully (P) exceeds the gully length (l)
Plan rejection 1	Impossible to provide a higher PPR_D than PPR_S due to insufficient value of N_{CB} even with lowest possible value of T_{max}
Plan rejection 2	PPR_S is larger than PPR_D because canopy diameter exceeds the d_1 value some days before the starting of allowed listed days for crop moving
Plan rejection 3*	PPR_S stands higher than PPR_D due to incompatibility between timing of grow stages 2 and 3 (caused by d_2) and maximum possible value of T_{max}

*In dynamic plans with 3 growth stages only

3.2.6.4. Evaluation and optimization of multilayer cultivation plans by simulation results

The developed simulation module can be used to observe the results of executing different static and dynamic cultivation plans with disparate input conditions such as dissimilar crop types and planting arrangements, different layer clustering conditions, various MGU and gully dimensions, and variable durations of continuous cultivation process.

Using the simulation results, the production performance of each cultivation plan can be evaluated and compared with other applicable plans. This helps the user to select the most appropriate applicable plan according to provided input conditions. Investigating the effects of changing the value of certain inputs on the performance (outputs) of a certain cultivation plan is another application of the developed simulation module with visual panel. Inefficient utilization of the area used for plant production may happen in some dynamic cultivation plans due to insufficient number of gullies in some clusters. Such inefficiency in form of area under-utilization can be

discovered by interpreting that part of the simulation results related to row spacing values. In such cases, optimizing the area utilization may lead to hybrid static-dynamic cultivation plans in which the amount of unused productive area is minimized.

To carry out above stated issues by the simulation module, the input data shown in Table 3-4 were used to observe the outputs of different static and dynamic plans employed for continuous plant production. Simulations were independently run for two lettuce cultivars including Romaine lettuce and Korean Cheong Chug Myeon lettuce, while both square and zigzag planting arrangements were applied to each cultivar.

Table 3-4. Input values used in simulation of different cultivation plans for two lettuce cultivars

Input	Value and unit
Length of cultivation layer (L)	200-400 cm
Width of gully (w)	8-10 cm
Length of gully (l)	95 & 106 cm
Initial value of d_1	Variable
Number of plants per gully (P)	4
Total length of plant growth period (T)	28 days
Estimated duration of cultivation process	180 days
Number of growth stages	2-3
Total number of layers	8
Layers per cluster (r_i)	1 to 7
Type of canopy growth equation	Sigmoid
Planting arrangement	Square-Zigzag

3.2.6.5. Estimating the growth equations of canopy diameter

As mentioned in previous sections, estimating the size of canopy diameter in different days of plant growth period is necessary for getting the output results of model and simulation. In order to achieve more reliable results from the model operation, practical attempts were made to obtain canopy diameter growth equations of two different crops including Romaine and Korean Cheong Chug Myeon lettuce cultivars. The growth curve related to each cultivar presents the size of canopy diameter (cm) versus the growing day of the plant. The required data for fitting the curves and finding the growth equations were acquired by daily measurement of canopy diameters during a 28-days cultivation period within two separate layers of a developed experimental 4-layer growing unit in Seoul national university. The size of canopy diameters was measured manually using a steel ruler according to the imaginary circles circumscribed about the projected area of growing canopies (Figure 3-13). However, for getting more precise and applicative outcomes in this field, employment of automated measurement and monitoring systems for growth of leafy vegetables such as that suggested by Yeh et al. (2014) may be more appropriate. Data collection was accomplished during one cultivation run for both lettuce cultivars from April 15 to May 13 2014. Total number of plants in the measuring samples related to Romaine and Korean cultivars was 34 and 15 plants, respectively. Using IBM SPSS Statistics 21 analysis software, curve estimation and regression fit for two acquired data sets were performed based on five basic mathematical model structures including linear, quadratic, cubic, power, exponential models as well as 4-parametric Boltzmann sigmoid model (Table 3-5). The most appropriate model for expressing the canopy growth equation was selected after investigating entire curve fitting results and adopted for the use in simulation panel. Figure 3-13 shows some views from the experimental cultivation runs.

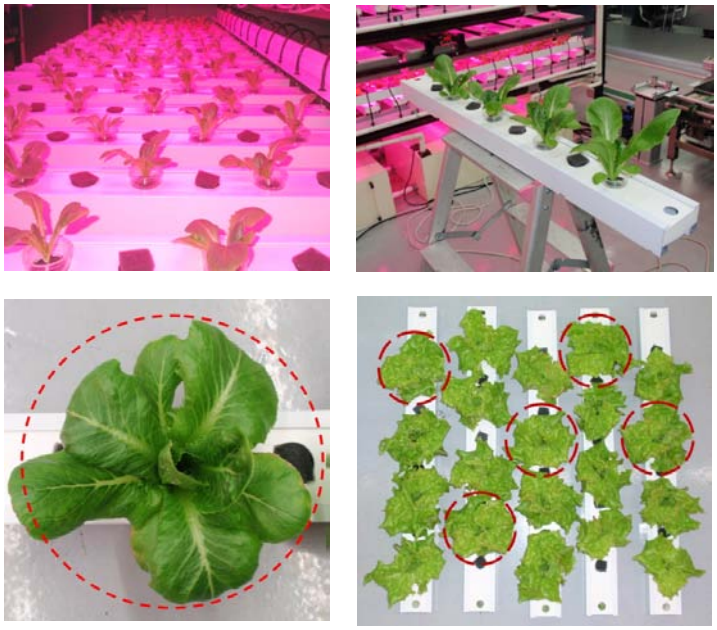

Figure 3-13. Different views from NFT cultivation of lettuce cultivars in experimental growing unit for estimating canopy growth equation

Table 3-5. Different model types of the fitted curves for obtaining growth equation of canopy diameter

Type	Model structure
Linear	$Y = b_1X + b_0$
Quadratic	$Y = b_2X^2 + b_1X + b_0$
Cubic	$Y = b_3X^3 + b_2X^2 + b_1X + b_0$
Power	$Y = b_0X^{b_1}$
Exponential	$Y = b_0\exp(b_1X)$
Sigmoid (Boltzmann)	$Y = b_2 + \frac{b_1 - b_2}{1+\exp\left(\frac{X-b_3}{b_4}\right)}$

3.3. Results and discussion

3.3.1. Selecting the best fitted curve for canopy diameter growth

Figure 3-14 (a) and (b) show the scatter plots of the measured canopy diameters for Romaine and Korean lettuce cultivars in which the horizontal and vertical axes represent the plant growing days and size of canopy diameter, respectively. Both plots are shown when smoothing of sampled data has been executed through removing the outlier data from the acquired data sets. Based on this, size of the sample used for final curve fitting was decreased to 28 and 12 plants for Romaine and Korean lettuce, respectively. As can be clearly observed, the measured data related to Korean lettuce exhibit a steeper growth trend in compare to the Romaine lettuce within the 28 days of the cultivation period. This might be mainly due to more tendency of the Romaine lettuce to vertical growth during the growing days while the horizontal spread of canopy leaves was more visible in case of the Korean lettuce. The stated difference in the canopy growth behavior of these two cultivars and the probable effect it may have on the simulation results was the main reason to select them for using in simulations.

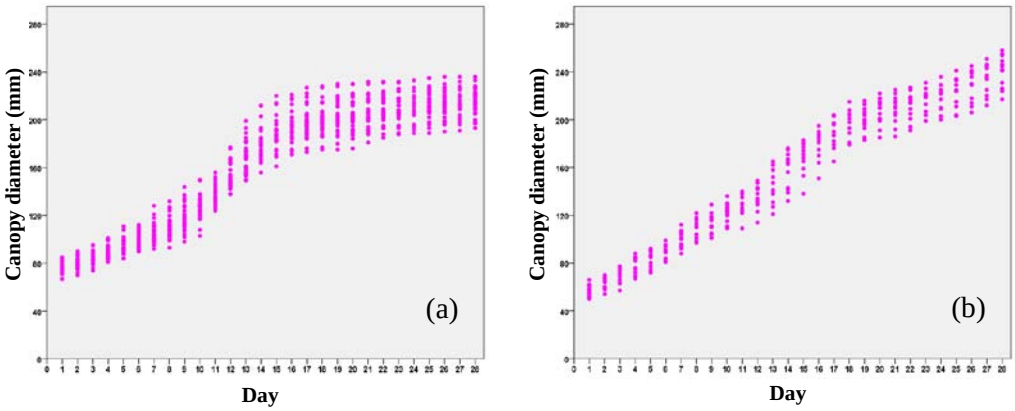

Figure 3-14. Scatter plots of the sampled data (canopy diameter vs. growing day) after data smoothing for (a) Romaine lettuce, and (b) Korean lettuce

Tables 3-6 contains the curve fitting results of the data set related to Romaine lettuce when five basic models including linear, quadratic, cubic, power and exponential are used for regression fitting. The results related to sigmoid model has been separately presented in Table 3-7. The items presented in these tables consist of a summary of each model including the coefficient of determination (R^2) and also, the parameter estimates of the models. Similarly, Tables 3-8 and 3-9 display the results of curve fitting and the information of the relevant regressions for the data set of the Korean lettuce. Accordingly, the resulted fitted curves obtained from the data presented in Tables 3-6 to 3-9 are drawn for all model types and are individually displayed for Romaine and Korean lettuce cultivars in Figures 3-15 and 3-16, respectively. Details on the regression analysis of these models have been presented in appendices B.1 and B.2.

Table 3-6. Model summary and parameter estimates in five basic models for Romaine lettuce

Model	Model summary				Parameter estimates			
	R^2	F	df_1	df_2	Constant (b_0)	b_1	b_2	b_3
Linear	0.882	5817.348	1	782	73.767	5.994		
Quadratic	0.924	4770.889	2	781	47.198	11.308	-0.183	
Cubic	0.941	4172.668	3	780	69.252	2.910	0.528	-0.016
Power	0.879	5660.589	1	782	55.645	0.412		
Exponential	0.863	4940.242	1	782	82.285	0.042		

Table 3-7. Parameter estimates in 4-parametric sigmoid (Boltzmann) model for Romaine lettuce (R^2 = 0.954)

Parameter	Estimate	Standard error	95% Confidence interval	
			Lower bound	Upper bound
b_1	77.011	1.583	73.903	80.118
b_2	212.538	0.829	210.910	214.165
b_3	11.157	0.111	10.939	11.375
b_4	2.815	0.102	2.615	3.014

Table 3-8. Model summary and parameter estimates in five basic models for Korean lettuce

Model	Model summary				Parameter estimates			
	R^2	F	df_1	df_2	Constant (b_0)	b_1	b_2	b_3
Linear	0.954	6951.765	1	334	52.557	7.147		
Quadratic	0.962	4222.191	2	333	39.477	9.763	-0.09	
Cubic	0.967	3201.405	3	332	52.517	4.797	0.33	-0.01
Power	0.928	4301.462	1	334	41.617	0.51		
Exponential	0.914	3560.554	1	334	67.442	0.052		

Table 3-9. Parameter estimates in 4-parametric sigmoid (Boltzmann) model for Korean lettuce (R^2 = 0.968)

Parameter	Estimate	Standard error	95% Confidence interval	
			Lower bound	Upper bound
b_1	26.933	8.133	10.934	42.932
b_2	248.861	4.317	240.368	257.354
b_3	11.662	0.389	10.898	12.427
b_4	6.086	0.453	5.196	6.976

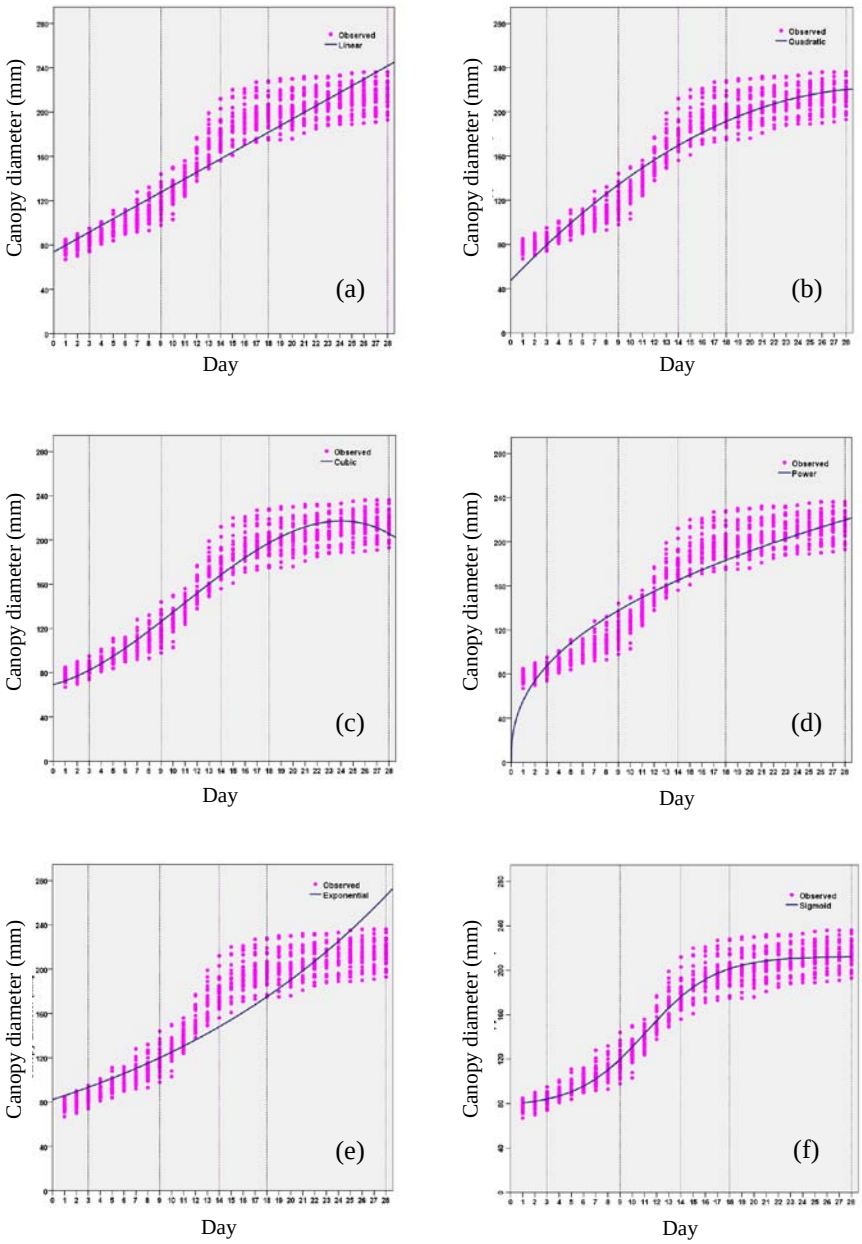

Figure 3-15. Final fitted curves for estimating the size of canopy diameter in different growing days for Romaine lettuce, (a) linear, (b) quadratic, (c) cubic, (d) power, (e) exponential, and (f) sigmoid

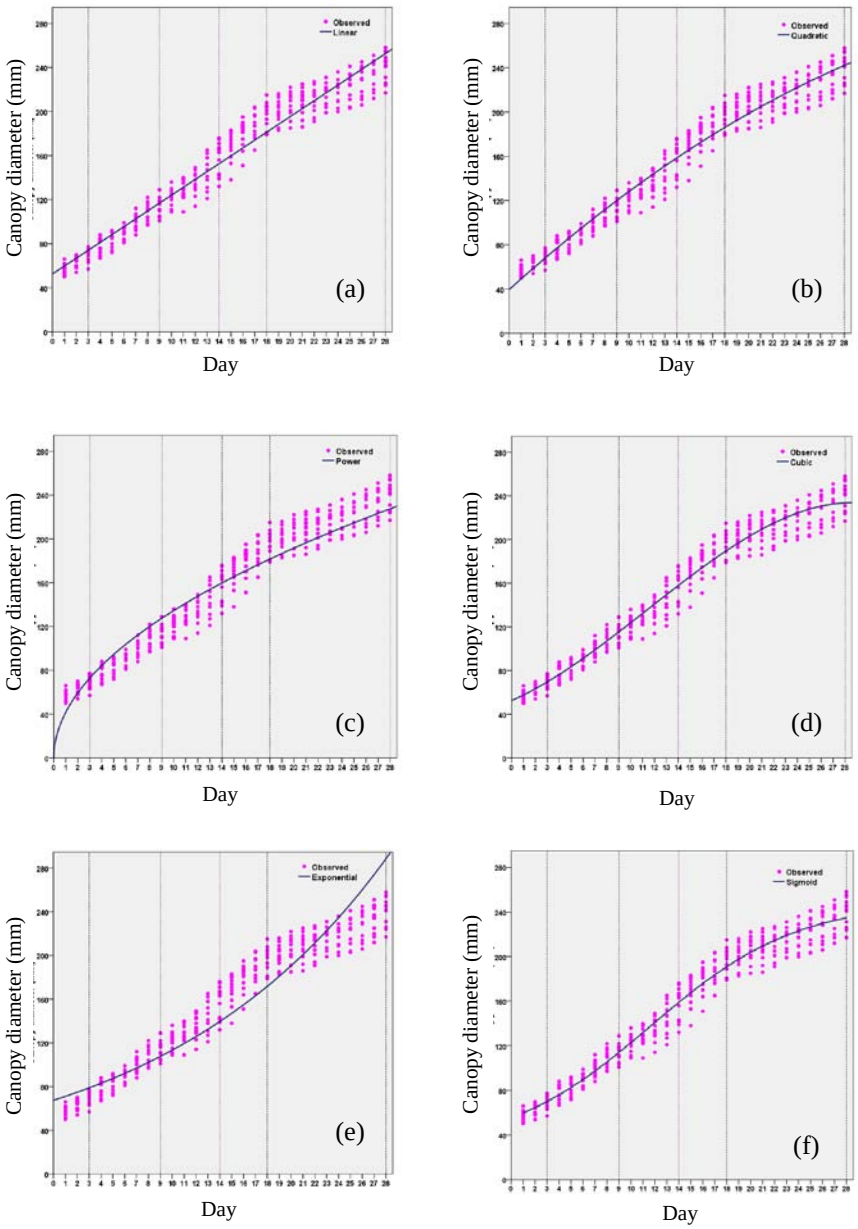

Figure 3-16. Final fitted curves for estimating the size of canopy diameter in different growing days for Korean lettuce, (a) linear, (b) quadratic, (c) cubic, (d) power, (e) exponential, and (f) sigmoid

In order to designate the best fitted curve among all available models for each cultivar and insert its relevant equation into the input of the simulation panel, R^2 value of each model, as well as the adaptability of fitted curves with the general trend of the sampled data sets were considered as determinant factors for the final selection.

According to calculated R^2 values shown in Tables 3-6 to 3-9, the R^2 values obtained in the models of Korean lettuce are generally larger than that of the Romaine lettuce which implies a relatively higher correlation between the dependent (canopy diameter) and independent (growing day) variables of Korean lettuce fitted curves. In both lettuce cultivars, slightly higher values of R^2 are observed in quadratic, cubic and sigmoid models compared to other three models which keeps them as final selection candidates. In case of the Romaine lettuce, despite the high R^2 value for the cubic model (0.941), the fitted curve displays an unusual sudden drop in the size of canopy diameter during the final growing days (Figure 3-15 (c)) which differs from the trend observed in the sampled data. Deviation from the observed trend of the sampled data can also be found in the quadratic fitted curve during the first and middle days of the growth period. Since the sigmoid curve has the highest available R^2 and it provides the closest trend prediction of canopy diameter size during most growing days, it was selected as the best fitted curve for estimating the canopy diameter in the Romaine lettuce. Similar analyses were carried out to select the best fitted curve for the Korean lettuce and sigmoid curve was found to be the most appropriate option after it was compared with cubic and quadratic models.

3.3.2. Effect of different clustering conditions on simulation results

Employment of different clustering conditions within a certain number of cultivation layers would cause dissimilar results in the simulation outputs. These results are also different with that obtained from the static cultivation plan implemented within the same number of layers. The data presented in Tables 3-10 to 3-13 are the classified results of simulating all five possible clustering options used for continuous plant production of Romaine and Korean lettuce cultivars under square and zigzag planting arrangements in a total of eight cultivation layers. Simulation result of the single applicable static plan is also shown in the first row of each table. In all simulations, initial values of the input d_1 have been selected such that the highest rate of plant production would be obtained. Width of gully and length of cultivation layers are 8 and 300 cm in, respectively. Other inputs are applied based on the information presented in Table 3-4.

As shown in column 3 of Table 3-10, employment of static cultivation for square planting of Romaine lettuce provides a PPR value higher than all those created by dynamic cultivation plans. Since in cases that calculated PPR_S is higher than a certain PPR_D no TPD is reported for that dynamic plan, the column 4 of Tables 3-10. As can be seen in columns 5 and 6 of this table, existence of extra imbalanced durations in growth stages of the dynamic plans, causing long crop output intervals, is a reason for low PPR_D values in all simulated dynamic plans.

In continuous production of Korean lettuce by square planting (Table 3-12), the PPR_D provided by 3-5 clustering (16 plants/day) is the only case standing higher than the PPR_S (13.7 plants/day). The determined lengths for first and second growth stages in this dynamic plan are 13 and 15 days, respectively. The resulting TPD for this dynamic plan is 91 days which is a reasonable time for plant production within the total cultivation period of 180 days. As can be observed from the three last columns of Table 3-12, the total number of produced plants by the dynamic cultivation plan with 3-5 clustering is 2640 plants supplied during 11 crop outputs in 178 days which is 336 plants higher than that produced by the static cultivation under the same input conditions. However, due to asynchronous timing of the crop outputs supplied by each of these two plans, the total duration of cultivation process is 10 days longer in

the dynamic plan. In other words, the expense for producing 336 more lettuce heads through employment of the dynamic plan with 3-5 clustering is extending the duration of the cultivation process for an extra 10 days.

Similar to the previous case, dynamic cultivation plan with 3-5 clustering is likewise the only dynamic plan which creates a higher PPR compared to the static plan in zigzag planting of the Romaine lettuce (Table 3-11). However, in this case, the difference between PPR_S and respective PPR_D of 3-5 dynamic plan is negligible (0.3 plants/day). This causes the TPD of the dynamic plan to occur 385 days after the start of the cultivation process. This late TPD makes the dynamic plan inefficient for utilizing in short and mid-term cultivation periods such as that applied in the current simulations (180 days). As shown in Table 3-11, total number of plants produced by the 8-layer static plan is 3072 plants in 168 days, while only 2880 plants in 164 days can be produced by its alternative dynamic plan with 3-5 clustering. This confirms that employment of dynamic plan with 3-5 clustering is an inappropriate option for this length of cultivation process although it provides a slightly higher PPR value compared to the static plan.

Investigating the simulation data in Table 3-13 related to zigzag planting of Korean lettuce shows that either of 2-6 and 3-5 clustering conditions can make PPR values higher than that generated by the static plan. Reasonable low TPDs calculated for these two dynamic cultivation plans makes them suitable for the use in short and mid-term cultivation processes. Here also, the 2-stage dynamic plan with 3-5 clustering seems to have the best executive plan among all six available options due to highest generated PPR_D (20 plants/day) and the earliest TPD it provides that is the day 70 after the start of cultivation process. The highest available performance including the production of 3080 lettuce heads in 168 days is a proof for this. Moreover, the dynamic plan with 3-5 clustering was the only case among all simulated plans in which equal number of days (14 days) were determined in its growth stages.

Table 3-10. Simulation results of static plan and all possible dynamic cultivation plans with different clustering conditions in total eight cultivation layers for Romaine lettuce-square planting

Clustering	Number of growth stages	PPR type & value (plants/day)	TPD	Combination of GS timing (days)	Crop output interval (days)	Final crop output day	Number of crop outputs[1]	Total plant production[1]
None	1	PPR_S 16	N/D[2]	28	28	168	6	2688
1-7	2	PPR_D 5.8	-	4-24	24	172	7	980
2-6	2	PPR_D 11.7	-	4-24	24	172	7	1960
3-5	2	PPR_D 14.7	-	9-19	19	180	9	2520
1-2-5	3	PPR_D 9.3	-	4-9-15	15	178	11	1540
1-3-4	3	PPR_D 11.7	-	4-12-12	12	172	13	1820

[1] Until the final crop output day; [2] Not defined

Table 3-11. Simulation results of static plan and all possible dynamic cultivation plans with different clustering conditions in total eight cultivation layers for Romaine lettuce-zigzag planting

Clustering	Number of growth stages	PPR type & value (plants/day)	TPD	Combination of GS timing (days)	Crop output interval (days)	Final crop output day	Number of crop outputs[1]	Total plant production[1]
None	1	PPR_S 18.3	N/D[2]	28	28	168	6	3072
1-7	2	PPR_D 8.2	-	10-18	18	172	9	1332
2-6	2	PPR_D 16.4	-	10-18	18	172	9	2664
3-5	2	PPR_D 18.8	385	11-17	17	164	9	2880
1-2-5	3	PPR_D 13.6	-	9-9-10	10	178	16	2176
1-3-4	3	PPR_D 14.8	-	9-9-10	10	178	16	2368

[1] Until the final crop output day; [2] Not defined

Table 3-12. Simulation results of static plan and all possible dynamic cultivation plans with different clustering conditions in total eight cultivation layers for Korean lettuce-square planting

Clustering	Number of growth stages	PPR type & value (plants/day)	TPD	Combination of GS timing (days)	Crop output interval (days)	Final crop output day	Number of crop outputs[1]	Total plant production[1]
None	1	PPR_S 13.7	N/D[2]	28	28	168	6	2304
1-7	2	PPR_D 6.3	-	5-23	23	166	7	1008
2-6	2	PPR_D 12.5	-	5-23	23	166	7	2016
3-5	2	PPR_D 16	91	13-15	15	178	11	2640
1-2-5	3	PPR_D 11.3	-	5-11-12	12	172	13	1768
1-3-4	3	PPR_D 12.3	-	5-11-12	12	178	13	1924

[1] Until the final crop output day; [2] Not defined

Table 3-13. Simulation results of static plan and all possible dynamic cultivation plans with different clustering conditions in total eight cultivation layers for Korean lettuce-zigzag planting

Clustering	Number of growth stages	PPR type & value (plants/day)	TPD	Combination of GS timing (days)	Crop output interval (days)	Final crop output day	Number of crop outputs[1]	Total plant production[1]
None	1	PPR_S 16	N/D[2]	28	28	168	6	2688
1-7	2	PPR_D 9.3	-	12-16	16	172	10	1480
2-6	2	PPR_D 18.5	89	12-16	16	172	10	2960
3-5	2	PPR_D 20	70	14-14	14	168	11	3080
1-2-5	3	PPR_D 14.8	-	9-9-10	10	178	16	2368
1-3-4	3	PPR_D 14.8	-	9-9-10	10	178	16	2368

[1] Until the final crop output day; [2] Not defined

The diagrams illustrated in Figures 3-17 and 3-18 are generated based on the data presented in Tables 3-10 to 3-13. The basic form of these diagrams has been earlier displayed in Figure 3-8. Each of the trend-lines drawn in a diagram represents a certain cultivation plan by which the accumulated number of produced plants on different crop output days is shown. It is reminded that the PPR of each cultivation plan is the slope of its respective trend-line. As stated in the legend of these diagrams, one of the trend-lines in each diagram represents the static cultivation plan, which has been shown in the first rows of Tables 3-10 to 3-13, while the other five trend-lines are related to the dynamic plans with different clustering conditions listed in the tables. As it is evident in all four diagrams, the vertical position of the beginning point in the trend-lines related to crop outputs of the static cultivation plan always stand higher than the starting points of all dynamic trend-lines. This is because of the larger number of plants produced by static cultivation in the first common crop output of all cultivation plans at day 28.

It can be clearly seen in Figure 3-17 (a) (square planting of Romaine lettuce) that the vertical position of the solid static trend-line is higher than all other trend-lines during all days of the production time. An increasing divergence between the static trend-line and the trend-lines of dynamic plans can also be observed in this diagram. Due to the lack of intersection between the static trend-line and other dynamic trend-lines no TPD is available. This is the same situation shown by Table 3-10 in which the PPR value (16 plants/day) and the number of plants per crop output (448 plants) were the highest in the static plan, and no TPD was reported for any of the dynamic plans. Similar conditions can be observed in Figure 3-17 (b) which demonstrates the crop outputs trend-lines of different applicable cultivation plans for zigzag planting of the Romaine lettuce. However, since in the recent case, the PPR value of the dynamic plan with 3-5 clustering (D 3-5) is slightly higher than the PPR_S, the static trend-line and the D 3-5 trend-lines are slowly converged to each other as the production time increases. However, the intersection of these two lines (TPD) can't be seen in this diagram since it happens in the day 385.

In the diagrams shown in Figures 3-17(a) and (b) the vertical position of the static trend-line was always higher than the dynamic trend-lines. In Figures 3-18 (a), this superiority of the static plan will no more exist after the day 91 of the cultivation process (TPD) in case of the dynamic plan with 3-5 clustering (D 3-5) whose PPR

value is considerably higher than the PPR_S. Excelling of the D 3-5 on static trend-line at the end of the cultivation process is numerically shown in the last column of Table 3-12, where the reported quantity for total plant production by D 3-5 cultivation plan (2640 plants) exceeds the 2304 plants produced by the static cultivation. Similar conditions can be observed in Figure 3-18 (b) between the static plan and either of D 2-6 and D 3-5 cultivation plans.

The results of simulating the cultivation plans related to a common lettuce cultivar reveal that the PPR values and total plant production obtained by zigzag planting are higher in compare to the square planting in both static and dynamic cultivation plans. This is mainly due to larger value of the maximum allowed canopy diameter in each cluster and more available time for maintaining the growing plants in each growth stage and hence, more balanced combination of growth stage timing in zigzag planting. Expressing in another way, more number of gullies per unit length of cultivation layer in zigzag planting is the relevant factor in less efficient area utilization in square planting arrangement.

The observations obtained from different simulations also showed that the response of Romaine lettuce cultivation to increasing its plant production by applying dynamic cultivation plans was not promising in neither of the two different planting arrangements. This might be related to lower growth rate of canopy diameter in the Romaine lettuce (Figure 3-14 (a)) compared to faster growth of canopy diameter in the Korean lettuce cultivar (Figure 3-14 (b)). This is because the demand for larger growing area and stepwise increase in the row spacing value occurs later in the crops with slow trend in canopy diameter growth and thus, employment of multistage dynamic cultivation for increasing the production rate is not always beneficial and successfully reacted.

Considerably higher and dominant production performance of the 2-stage dynamic cultivation plan with 3-5 clustering when 3-stage dynamic plans (D 1-2-5 and D 1-3-4) were also among the applicable options, demonstrates that cultivation through a higher number of growth stages is not always the determinant factor for enhancing the amount of plant production in multistage cultivation. This was similarly found in the study of Kim et al. (2011), in which more efficient area utilization was observed in some cases when multistage mobile cultivations with fewer growth stages were applied.

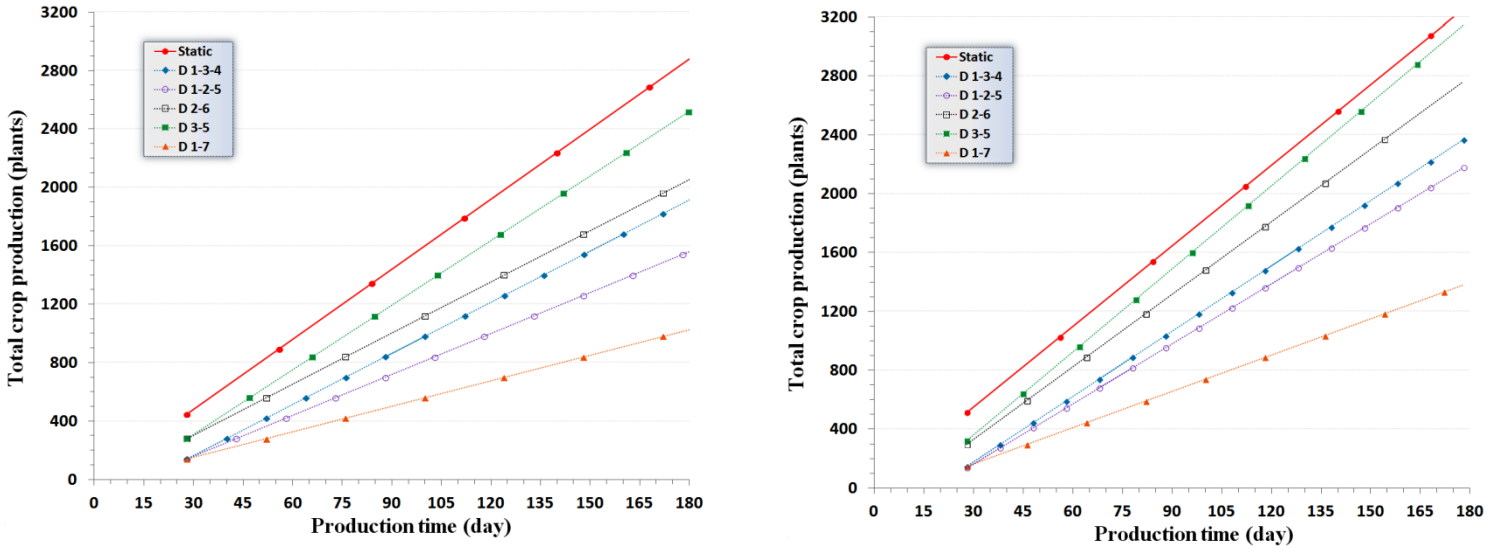

(a) (b)

Figure 3-17. Accumulated number of produced plants in different crop output days, and their relevant trend-lines under various clustering conditions in total 8 cultivation layers for Romaine lettuce: (a) square planting, (b) zigzag planting

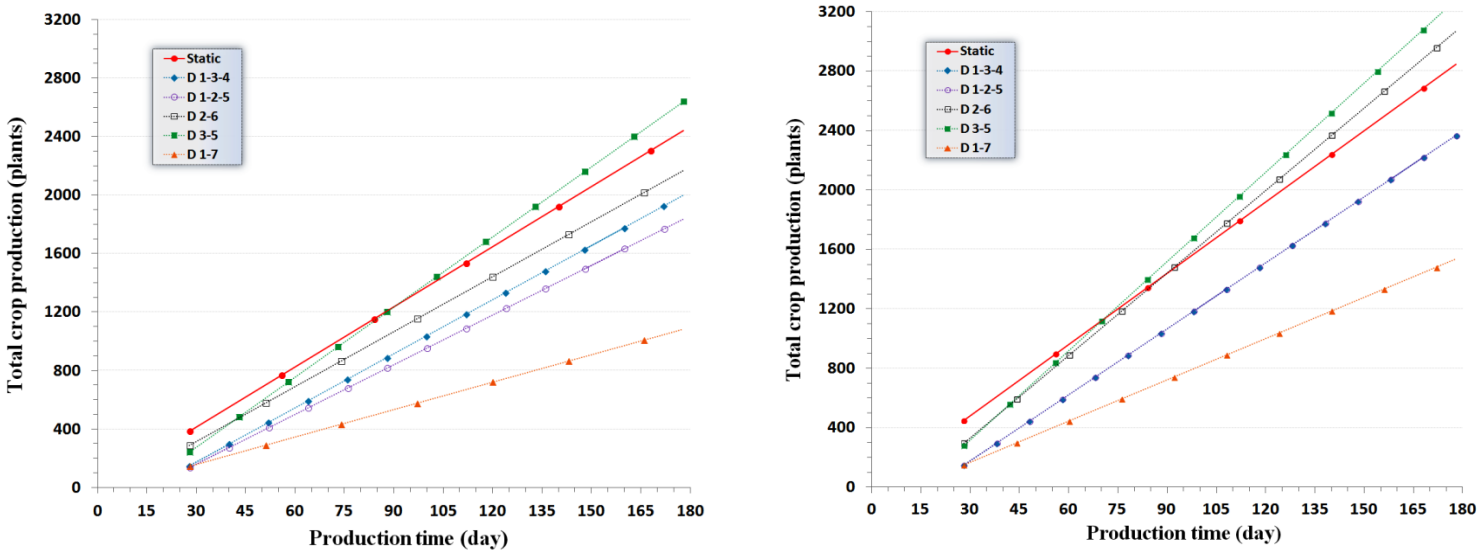

(a) (b)

Figure 3-18. Accumulated number of produced plants in different crop output days, and their relevant trend-lines under various clustering conditions in total 8 cultivation layers for Korean lettuce: (a) square planting, (b) zigzag planting

3.3.3. Effect of gully width and length of cultivation layer on simulation results

The effect of using different sizes of gully width (w) and cultivation layer length (L) on the production performance and area utilization of a cultivation plan was evaluated through two series of simulations. A certain range of gully width (8~10 cm) and layer length (200~400 cm) were inserted into respective inputs of the visual simulation panel during their related series of simulation. In both series of simulations, Korean lettuce and zigzag pattern were selected as the growing crop and planting arrangement and, 1-2-3 clustering was adopted to execute the dynamic cultivation in 6-layer MGU (see Figure 3-11).

3.3.3.1. Gully width

In the first series of simulations, conducted to examine the effect of gully width on simulation outputs, the length of cultivation layers was set to be 300 cm, while the width of gully was increased from 8 to 10 cm through 0.1 cm incremental steps. The initial value selected for d_1 was such that it could make the highest possible PPR_D in the process. Other related simulation inputs were same as in Table 3-4.

Figure 3-19 has been provided based on the outputs obtained from these series of simulations. In the top part of Figure 3-19, the effect of changing the gully width on PPR_D and TPD of the dynamic plan with 1-2-3 clustering has been numerically shown. The value observed for PPR_S was always 12 plants per day during all 21 simulations done for different gully widths which implies the unchanged number of gullies during the static cultivation even when wider gullies are used. However, in case of multistage dynamic cultivation, increasing the gully width from the minimum required 8 cm causes the PPR and total plant production of the dynamic plan to be gradually diminished. This is because in the current dynamic plan, the number of gullies per crop batch (N_{CB}) is selected based on the gully maintaining capacity of single-layered cluster 1. With increasing the gully width, this capacity and thus, the value of N_{CB} (replicated in 3 clusters) also decrease and some part of potential plant production would be then unavailable. According to the obtained results, the N_{CB}

number of gullies per crop batch (in each cluster) is 37 when a gully width of 8 to 8.1 cm is used, while this reduces to 30 gullies after a wider gully with 10 cm width is employed for the cultivation. This causes the PPR_D to be reduced in a stepwise manner, while an increasing trend can also be observed in the estimated TPDs which indicates more inefficiency of employing the dynamic plan against its alternative static option as the gully width increases. As can be observed, if gullies with a width of 9.7 cm or larger are used in this cultivation, the calculated values for both PPR_S and PPR_D would be 12 plants per day and no TPD would also be indicated in the simulation panel. Under such conditions the static plan would be able to supply 2016 plants after 168 days, while the dynamic plan can produce 1920 plants in 178 days. More comparisons also show that in a certain dynamic cultivation plan, employing the gullies with 2 cm larger width causes a remarkable drop (448 plants) in total number of produced plant during a 178 day cultivation period.

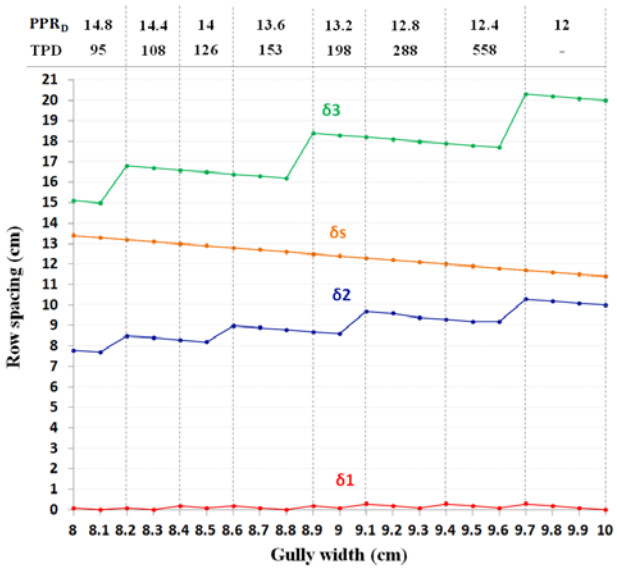

Figure 3-19. Effect of changing the gully width on PPR_D and TPD of the dynamic plan with 1-2-3 clustering (top), and on different row spacing values in static and dynamic plans (bottom)

The diagrams shown in the bottom part of Figure 3-19 illustrates the row spacing variations in MGU layers caused by changing the gully width in different simulation

runs. The three diagrams δ_1, δ_2 and, δ_3 are related to row spacing variations in the layers of clusters 1, 2 and 3 during the dynamic plan. The remaining diagram δ_s indicates the variations observed in the row spacing between the gullies in all MGU layers during the static cultivation. As can be seen, δ_s has a smooth linear declining trend as the size of gully width increases. In the static cultivation, the row spacing applied between two gullies is 13.4 cm when the gully width is 8 cm. With increasing the gully width to 10 cm, a similar 2 cm decrease in the row spacing between gullies is observed. This happens because the number of gullies per layer during the static cultivation (14 gullies per layer) does not change when the gully width increases. Thus, any increment in the size of gully width always reduces the distance between the gullies placed inside a layer. In case of dynamic cultivation, both decreasing and increasing trends are observed in row spacing values. The sharp increases in row spacing values occur when the number of gullies per crop batch (N_{CB}), and thus per layer, is reduced due to limited capacity of cluster 1 in maintaining the wider gullies.

3.3.3.2. Length of cultivation layers

The effect of using different layer lengths on several simulation outputs including the PPR, TPD and total plant production was examined through a series of simulations in which the length of cultivation layers was changed from 200 to 400 cm, while all other inputs were fixed. The width of gully was 8 cm in all simulation and other inputs were same as in the last section. As also shown in Figure 3-20 and Table 3-14, plant production in a MGU with longer cultivation layers would increase static and dynamic PPRs and cause a higher number of plants to be produced at the end of a certain cultivation period. Based on the diagrams displayed in Figure 3-20, the gradual increase in the values of PPR_S and PPR_D are stepwise and discrete. Therefore, each of these two diagrams is found in form of a number of parallel small segments such that the vertical position of each segment represents the related value of PPR_S or PPR_D. The longer length of the segments related to PPR_S diagram denotes that the response (change in PPR) of the static cultivation to layer length variation is relatively slower than that of the dynamic cultivation. Based on the data presented in

Table 3-14, the horizontal interval between two incremental steps in the PPR_S discrete diagram is nearly 20 cm, while this is about 7 cm for the dynamic cultivation.

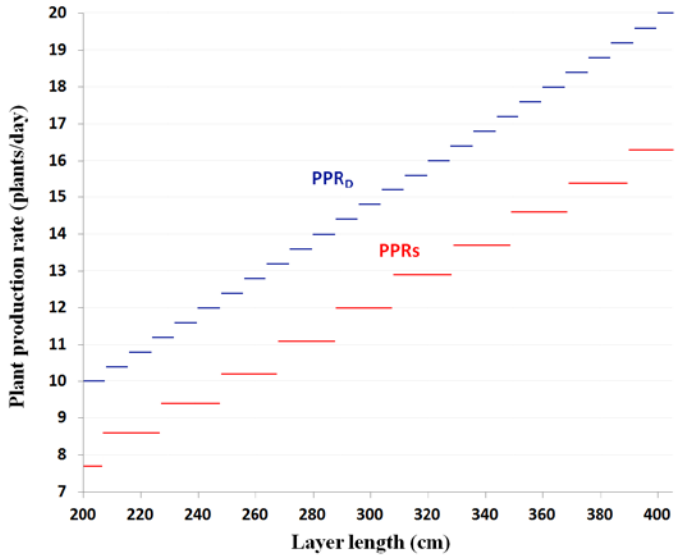

Figure 3-20. Stepwise variations in static and dynamic plant production rates due to different layer lengths

In Figure 3-20, the reasonable higher position of the segments belonging to the PPR_D diagram in compare to those of the PPR_S shows that employment of the dynamic cultivation is beneficial under all simulated conditions and TPDs can be estimated for related dynamic plans in all layer lengths.

Figure 3-21 displays the variation of estimated TPDs when different lengths of cultivation layers were examined in the simulation. Concurrent investigation of Figures 3-20 and 3-21 confirms that advantageous lower TPDs can be observed within those intervals in which larger vertical distances are found between the parallel segments of lower and upper diagrams. Additional data on total plant production and exact details of the data presented in Figures 3-20 and 3-21 are found in Table 3-14.

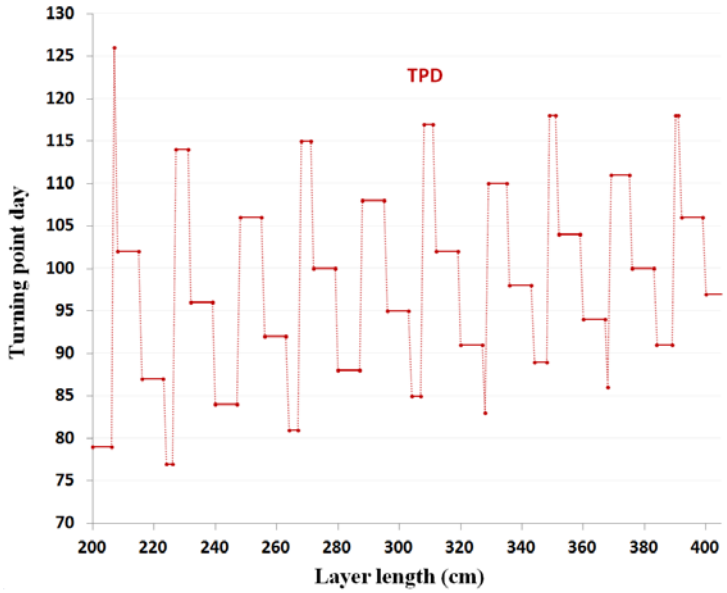

Figure 3-21. Variation of turning point day resulted by different layer lengths

Table 3-14. Numerical changes in different simulation outputs caused by variation of the layer length

Variation in layer length (cm)	PPR_S (plants/day)	PPR_D (plants/day)	TPD (day)	Total plant production by static plan[1]	Total plant production by dynamic plan[2]
200~206	7.7	10	79	1296	1600
207	8.6	10	126	1440	1600
208~215	8.6	10.4	102	1440	1664
216~223	8.6	10.8	87	1440	1728
224~226	8.6	11.2	77	1440	1792
227~231	9.4	11.2	114	1584	1792
232~239	9.4	11.6	96	1584	1856
240~247	9.4	12	84	1584	1920
248~255	10.3	12.4	106	1728	1984
256~263	10.3	12.8	92	1728	2048
264~267	10.3	13.2	81	1728	2112
268~271	11.1	13.2	115	1872	2112
272~279	11.1	13.6	100	1872	2176
280~287	11.1	14	88	1872	2240
288~295	12	14.4	108	2016	2304
296~303	12	14.8	95	2016	2368
304~307	12	15.2	85	2016	2432
308~311	12.9	15.2	117	2160	2432
312~319	12.9	15.6	102	2160	2496
320~327	12.9	16	91	2160	2560
328	12.9	16.4	83	2160	2624
329~335	13.7	16.4	110	2304	2624
336~343	13.7	16.8	98	2304	2688
344~348	13.7	17.2	89	2304	2752
349~351	14.6	17.2	118	2448	2752
352~359	14.6	17.6	104	2448	2816
360~367	14.6	18	94	2448	2880
368	14.6	18.4	86	2448	2944
369~375	15.4	18.4	111	2592	2944
376~383	15.4	18.8	100	2592	3008
384~389	15.4	19.2	91	2592	3072
390~391	16.3	19.2	118	2736	3072
392~399	16.3	19.6	106	2736	3136
400~407	16.3	20	97	2736	3200

[1] After 168 days; [2] After 178 days

3.3.4. Combination of dynamic and supplementary static plans

Total applicable options for multilayer plant production in eight cultivation layers are not limited to those static and dynamic plans listed in each of the Tables 3-10 to 3-13. Implementing combinational solutions such as simultaneous employment of individual static and dynamic plans to cover all available layers is another possible option which may, in some cases, improve the production performance and the efficiency of area utilization in a multilayer growing system. A list of such combinational plans for production of Romaine and Korean lettuce cultivars by zigzag planting in total eight cultivation layers is presented in Tables 3-15 and 3-16, respectively. Due to the results observed in Tables 3-10 to 3-13 indicating lower performance and inefficiency of square planting, adoption of this arrangement has been excluded from further simulations of this study and thus, not used in these series of simulations as well.

Each row of Tables 3-15 and 3-16 represents a certain combinational cultivation plan including a dynamic plan and its supplementary static plan such that the total number of cultivation layers supported by two plans together is eight. Columns 3 to 6 of the tables contain the simulation results related to dynamic parts of combinational plans, while total number of plants produced by dynamic, supplementary static and, combinational cultivation plans at the end of respective final crop output days are indicated in the last three columns. It is obvious that the total plant production by the combinational cultivation plan is the sum of dynamic and supplementary static plans as its constitutive components.

Table 3-15. Simulation results related to combination of dynamic plans and supplementary static plans for cultivation in total eight cultivation layers (Romaine lettuce-zigzag planting)

Clustering in dynamic plan	Suppl. static layers	PPR_D (plants/day)	Combination of GS timing (days)	Number of crop outputs (Dyn. plan)	Final crop output day (Dyn. plan)	Total plant production		
						Dynamic	Static*	Combinational
1-2	5	7.1	10-18	9	172	1152	1920	3072
1-3	4	8.2	10-18	9	172	1332	1536	2868
1-4	3	8.2	10-18	9	172	1332	1152	2484
1-5	2	8.2	10-18	9	172	1332	768	2100
1-6	1	8.2	10-18	9	172	1332	384	1716
2-3	3	12	12-16	10	172	1920	1152	3072
2-4	2	14.2	10-18	9	172	2304	768	3072
2-5	1	16.4	10-18	9	172	2664	384	3048
3-4	1	17.1	13-15	11	178	2816	384	3200
1-2-3	2	13.6	9-9-10	16	178	2176	768	2944
1-2-4	1	13.6	9-9-10	16	178	2176	384	2560

*Supplementary static plan (six crop outputs in 168 days)

Table 3-16. Simulation results related to combination of dynamic plans and supplementary static plans for cultivation in total eight cultivation layers (Korean lettuce-zigzag planting)

Clustering in dynamic plan	Suppl. static layers	PPR_D (plants/day)	Combination of GS timing (days)	Number of crop outputs (Dyn. plan)	Final crop output day (Dyn. plan)	Total plant production		
						Dynamic	Static*	Combinational
1-2	5	7.5	13-15	11	178	1232	1680	2912
1-3	4	9.3	12-16	10	172	1480	1344	2824
1-4	3	9.3	12-16	10	172	1480	1008	2488
1-5	2	9.3	12-16	10	172	1480	672	2152
1-6	1	9.3	12-16	10	172	1480	336	1816
2-3	3	12	14-14	11	168	1848	1008	2856
2-4	2	15	13-15	11	178	2464	672	3136
2-5	1	17.5	12-16	10	172	2800	336	3136
3-4	1	16	14-14	11	168	2464	336	2800
1-2-3	2	14.8	9-9-10	16	178	2368	672	3040
1-2-4	1	14.8	9-9-10	16	178	2368	336	2704

*Supplementary static plan (six crop outputs in 168 days)

3.3.5. Optimization of area utilization by hybrid static-dynamic layers

As stated in section 3.2.6.4, in most cases under-utilization of plant growing area and thus, some waste in area utilization exists in some cultivation layers of a MGU during the implementation of the dynamic cultivation plans described in this study. The reason for such inefficiency in area utilization is that the number of gullies per crop batch (N_{CB}) applied in the dynamic plan is selected based on the maximum gully maintaining capacity of either first or the final (here, third) cluster (see section 3.2.6.2). Therefore, a less than maximum possible number of gullies might be placed in the layers of two out of three clusters which would cause the potential plant production to be decreased at the end of a cultivation process.

The left picture in Figure 3-22 (a) demonstrate that part of the simulation panel that involves the outputs related to row spacing and numerical distribution of gullies when dynamic cultivation of Korean lettuce with 1-2-3 clustering and zigzag planting has been simulated. In this simulation, width of gullies and length of cultivation layers are 8 and 300 cm, respectively. The schematic layout shown in the right picture of Figure 3-22 (a) illustrates how to execute this dynamic plan in a 6-layer growing unit. Loading and unloading of gullies into and from the cultivation layers have been indicated using the arrows whose directions are toward and outward the growing unit, respectively. The downward arrows denote the displacement of gullies between the layers of different clusters and the digits in parentheses indicate the number of gullies entering each cultivation layer.

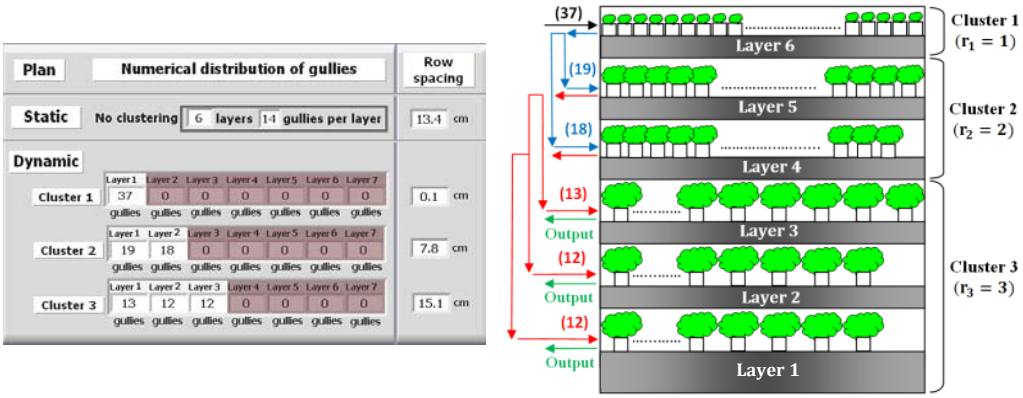

(a)

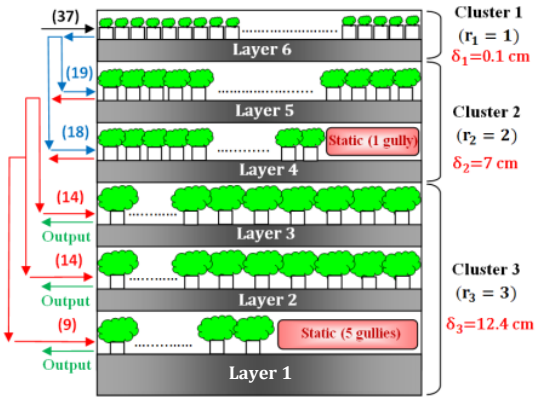

(b)

Figure 3-22. (a) Numerical distribution and row spacing of gullies in 3-stage dynamic cultivation plan with 1-2-3 clustering, and (b) optimizing the area utilization by hybrid static-dynamic cultivation layers

The existence of unused plant growing areas in the layers of clusters 2 (4,5) and 3 (1,2,3) was found and calculated by comparing the optimal row spacing values in the layers of these two clusters (Equation 3-3) and the applied row spacing values (Equation 3-6) indicated in the simulation panel. To release the unused areas in the layers of clusters 2 and 3, optimal row spacing values calculated for the layers of these clusters (7 and 12.4 cm) were replaced with the previous ones, as a result of which the numerical distribution of gullies was also modified in these two clusters

(Figure 3-22 (b)). Since the amount of the released area in each cluster was large enough to maintain some gullies containing fully grown lettuce heads, the total areas retrieved from cluster 2 and 3 were aggregated in layers 4 and 1, respectively, and individually exploited for maintaining 1 and 5 gullies during a static cultivation. As can be seen in Figure 3-22 (b), static and dynamic cultivation methods are both executed in layers 1 and 4 and thus, the term hybrid cultivation layer is used for such layers. Optimization of area utilization through employment of hybrid static-dynamic layers added an extra stream of static plant production (24 plants every 28 days) to the previous plant production by the dynamic plan (148 plants every 10 days).

Optimizing the area utilization through constructing hybrid static-dynamic layers was also applied to all dynamic cultivation plans executed for zigzag planting of Romaine and Korean lettuce cultivars (Tables 3-11, 3-13, 3-15 and 3-16). The number of plants added to the plant production of each of these dynamic plans after the optimization is presented in column 3 of Tables 3-17 and 3-18, which have been individually provided for zigzag planting of Romaine and Korean lettuce cultivars, respectively. Since the maximum duration of cultivation process has been 180 days in all simulations and thus, the final crop output day by static cultivation is 168, the added plants shown in these tables are gradually supplied in 28 day intervals within a 168 day period. The values presented in column 5 of Tables 3-17 and 3-18 are the maximum available plant production (after optimizing the area utilization) which can be achieved by continuous production of these lettuce cultivars within a maximum 6 month cultivation process in total eight layers. The last column shows the latest day a crop output is available by the applied respective cultivation plan.

Table 3-17. Comparison of plant production in total eight cultivation layers by different cultivation plans before and after space optimization in the dynamic part (Romaine lettuce-zigzag planting)

	Clustering	Plant production by dynamic plan	Added plants after optimization[1] (hybrid layers)	Plant production by supplementary static plan	Maximum available plant production	Final crop output day
	1-7	1332	1800	N/A[2]	3132	172
	2-6	2664	528	N/A	3192	172
	3-5	2880	96	N/A	2976	168
	1-2-5	2176	1128	N/A	3304	178
	1-3-4	2368	912	N/A	3280	178
Combinational plans	1-2	1152	48	1920	3120	172
	1-3	1332	264	1536	3132	172
	1-4	1332	648	1152	3132	172
	1-5	1332	1032	768	3132	172
	1-6	1332	1416	384	3132	172
	2-3	1920	48	1152	3120	172
	2-4	2304	96	768	3168	172
	2-5	2664	144	384	3192	172
	3-4	2816	48	384	3248	178
	1-2-3	2176	360	768	3304	178
	1-2-4	2176	744	384	3304	178

[1] In 168 days; [2] Not available

Table 3-18. Comparison of plant production in total 8 cultivation layers by different cultivation plans before and after space optimization in dynamic part (Korean lettuce-Zigzag planting)

	Clustering	Plant production by dynamic plan	Added plants after optimization[1] (hybrid layers)	Plant production by supplementary static plan	Maximum available plant production	Final crop output day
	1-7	1480	1464	N/A[2]	2944	172
	2-6	2960	240	N/A	3200	172
	3-5	3080	120	N/A	3200	168
	1-2-5	2368	816	N/A	3184	178
	1-3-4	2368	792	N/A	3160	178
Combinational plans	1-2	1232	24	1680	2936	178
	1-3	1480	120	1344	2944	172
	1-4	1480	456	1008	2944	172
	1-5	1480	792	672	2944	172
	1-6	1480	1128	336	2944	172
	2-3	1848	144	1008	3000	168
	2-4	2464	48	672	3184	178
	2-5	2800	24	336	3160	172
	3-4	2464	288	336	3088	168
	1-2-3	2368	144	672	3184	178
	1-2-4	2368	480	336	3184	178

[1] In 168 days; [2] Not available

3.3.6. Selecting the optimal cultivation plan for each lettuce cultivar based on the simulation results

As stated earlier, a major application of the simulation module and obtaining purpose of the cultivation schema is to find the cultivation plan with best production performance or most efficient area utilization, applicable for certain input conditions. Accordingly, Table 3-19 shows the selected cultivation plans with highest number of plant production for Romaine and Korean lettuce cultivars. The cultivation plans presented in this table has been selected from all available options including static and dynamic plans (Tables 3-11 and 3-13) and combinational plans (Tables 3-15 and 3-16) after that optimizing the area utilization with hybrid static-dynamic layers was accomplished (Tables 3-17 and 3-18). Note that the area utilization in a static cultivation plan is always in its highest degree and thus, no more optimization is available for this cultivation method.

Table 3-19. Cultivation plans with best production performance for two lettuce cultivars*

Lettuce cultivar	Max. plant production	Final crop output	Selected cultivation plan	Optimized by hybrid layers
Romaine	3304	178	1-2-3 dynamic+ 2-layer static	Yes
Korean	3200	168	3-5 dynamic	Yes

*Zigzag planting in 8 layers within maximum 180-day cultivation process

Based on Table 3-19, a combinational cultivation plan including a 1-2-3 dynamic plan optimized with a couple of hybrid static-dynamic layers in cluster 2 and 3, and two supplementary static layers is the optimal cultivation plan for zigzag planting of Romaine lettuce when a total of eight cultivation layers with 300 cm length, 8 cm width gullies (4 plants per gully) and finally, a maximum duration of 180 days are available for plant production. This combinational plan can supply 148 fully grown plants every 10 days through its dynamic cultivation, while 188 harvestable plants are provided every 28 days by the static part. The final crop output of this plan is a

dynamic crop output with 148 plants which occurs 178 days after the start of continuous cultivation process. As can be observed in columns 2 and 3 of Table 3-19, the ability of selected combinational plan is to produce a total number of the 3304 plants in 178 days, while according to the first row of Table 3-11, the easier to execute static plan can produce a maximum of 3072 plants during a shorter time period of 168 days under the same input conditions. The result of this comparison is another proof showing the general low response of Romaine lettuce to employment of dynamic cultivation method. Producing 232 more lettuce heads in expense of continuing the cultivation process for more 10 days as well as considering more labor needed for intermittent displacement of gullies between the layers in the dynamic part of the combinational plan, is a point which may affect the final decision of the grower on the employed plan after more assessments.

The optimal cultivation plan for Korean lettuce is a dynamic plan with 3-5 clustering optimized with one hybrid static-dynamic layers. Result of implementing this cultivation plan is supplying 280 and 20 plants through 14 and 28 day intervals by dynamic and static parts, respectively. This optimized dynamic plan can produce 512 more plants in compare to its alternative static plan during the same number of 168 days spent for static cultivation as well (see Table 3-13). This confirms the higher response of the fast canopy growing plants to employment of dynamic cultivation method.

3.3.7. Numerical distribution of gullies

Numerical distribution of gullies in a MGU and the applied row spacing values between the gullies in its different layers are the components of a cultivation schema which determine the steps of the procedure used to execute the cultivation plan. According to Equation 3-11 various options might be available for numerical distribution of gullies when a certain number of gullies (N_{CB}) in form of a crop batch are placed into the layers of a cluster. Table 3-20 displays all applicable options for distributing a crop batch with 37 gullies (148 plants) into a cluster when the number of layers in the cluster (r_i) varies from 1 to 6.

Table 3-20. Different options for numerical distribution of gullies and their related characteristics in the clusters with certain number of layers (N_{CB}=37 and L=300 cm)

r_i (layers)	Option	δ_i (cm)	N_i (gullies)	α_1	β_1	α_2	β_2	Displayed in panel	Numerical distribution of gullies					
									L1	L2	L3	L4	L5	L6
1	I	0.1	37	0	0	0	0	✓	37	-	-	-	-	-
2	I	7.8	19	1	1	0	0	✓	19	18	-	-	-	-
3	I	15.1	13	2	1	0	0	✓	13	12	12	-	-	-
	II	//	//	1	2	0	0		13	13	11	-	-	-
4	I	22	10	3	1	0	0	✓	10	9	9	9	-	-
	II	//	//	1	1	1	2		10	10	9	8	-	-
	III	//	//	1	3	0	0		10	10	10	7	-	-
5	I	29.5	8	3	1	0	0	✓	8	8	7	7	7	-
	II	//	//	1	1	1	2		8	8	8	7	6	-
	III	//	//	1	3	0	0		8	8	8	8	5	-
6	I	34.8	7	5	1	0	0	✓	7	6	6	6	6	6
	II	//	//	3	1	1	2		7	7	6	6	6	5
	III	//	//	1	1	2	2		7	7	7	6	5	5
	IV	//	//	2	1	1	3		7	7	7	6	6	4
	V	//	//	1	2	1	3		7	7	7	7	5	4
	VI	//	//	1	1	1	4		7	7	7	7	6	3
	VII	//	//	1	5	0	0		7	7	7	7	7	2

Indicated values for maximum number of gullies per layer of certain cluster i (N_i) and row spacing values (δ_i) are results of in cultivation layers with 300 cm length. Table 3-20 also contains the determined values of coefficient α_j and β_j (Equation 3-11) for each option. These values that are used by the simulation VI give an interpretation on numerical distribution of gullies in the layers of a cluster. For example, existence of only one pair of coefficient values (α_1=2, β_1=1) in a cluster with 3 cultivation layers means that, i) there is only one group of incompletely loaded layers in this cluster, ii) two out of three available layers are not completely loaded and, iii) each of these two incomplete layers contains one less gully compared to fully loaded layer which maintains 13 gullies. In cases that distribution of crop batch gullies is possible through more than one option, e.g., r_i=3 to 6, the most balanced numerical option with only one group of incomplete layers (j=1) and β_1 value of 1, is displayed in the simulation panel. Because of disparate number of loaded gullies in the layers of clusters 2 and 3, while the same value of row spacing is applied in all layers of these clusters, three incompletely loaded layers with one less contained gully seen in layers 1, 2 and 4. This is unavoidable because adding one or two extra gullies to fill these incomplete layers will make a crop batch whose number of gullies is beyond maximum maintaining capacity of layer 6. The simulation VI operating based on model algorithm searches among all possible numerical distributions in a cluster and selects and displays the most balanced option which has at most one group of incomplete layers and one gully less than N_i in its layers.

3.3.8. Schedule of crop displacement in dynamic plans

As an important component of a cultivation schema, one application of the simulation module is to assist the grower for creating the best time schedule for displacement of gullies containing the growing plants. The structure of such schedule would be made according to the timing of growth stages indicated in the visual simulation panel in form of best moving days 1 and 2 within one growth period. Table 3-21 shows a sample schedule which is used for executing a dynamic cultivation plan with 1-2-3 clustering within maximum 180 day continuous cultivation process. All sixteen serial crop batches growing under this simulated plan are displayed in the table, while the days indicated in the last row are the crop output days of the respective cultivation process. The recurrence interval in presented schedule is 9 days, which is due to resulted 9-9-10 combination of growth stage timing (T_1=9 days, T_2=9 days, T_3=10 days). Due to unequal number of days in different growth stages, one day delays would be created in refilling the layers of clusters 1 and 2. For example, although all gullies of crop batch 1 are moved to cluster 2 and 3 at the end of days 9 and 18, depleted layers of clusters 1 and 2 are refilled with crop batch 2 gullies at the end of days 10 and 19.

Table 3-21. Biannual schedule for displacement of gullies in serial crop batches during a 3-stage dynamic cultivation in a 6-layer growing unit

	Moving day to next cluster/harvester*															
Cluster Layers	CB 1	CB 2	CB 3	CB 4	CB 5	CB 6	CB 7	CB 8	CB 9	CB 10	CB 11	CB 12	CB 13	CB 14	CB 15	CB 16
Cluster 1 L 6	9	19	29	39	49	59	69	79	89	99	109	119	129	139	149	159
Cluster 2 L 4,5	18	28	38	48	58	68	78	88	98	108	118	128	138	148	158	168
Cluster 3 L1,2,3	28	38	48	58	68	78	88	98	108	118	128	138	148	158	168	178

*For the days indicated in the last row (cluster 3)

3.4. Conclusions

The following items are the major outcomes and findings of this part of the current study which was mainly concentrated on describing the static and dynamic cultivation methods in multilayer plant factories, and creating a model and its relevant simulation module used for obtaining the cultivation plan and procedure in form of a cultivation schema.

1- Employment of multilayer dynamic cultivation for continuous plant production can increase the average crop density during the cultivation process and improve the PPR, only if a plan with adequate number of plants per crop batch and appropriate timing of growth stages is adopted. Dynamic plans with inappropriate clustering conditions, excessive row spacing values, and improper timing of growth stages would cause inefficiency in the utilization of crop growing area. Application of such dynamic plans has no preference over the less cumbersome and cheaper to implement static option.

2- In cases that a dynamic cultivation plan provides a higher PPR value compared to its alternative static plan ($PPR_D > PPR_S$), employment of dynamic cultivation would only be worthwhile if the cultivation process is continued for a time duration sufficiently longer than the calculated TPD. According to this statement and the simulation results obtained in this study, the multilayer dynamic cultivation is not generally an advantageous solution for increasing the total plant production in short term (1-2 months) cultivation periods. Thus, static cultivation method is the recommended option for short term multilayer cultivation.

3- An appropriately selected dynamic cultivation plan has the capability to improve the efficiency of area utilization and total plant production within a certain cultivation period and to bring extra income for the grower, compared to its alternative static option. However, the associated costs and difficulties with implementing the dynamic cultivation method should always be taken into consideration. The additional costs caused by executing a dynamic plan are the expenses imposed by the labor or automated equipments required to displace the gullies between different cultivation layers during the plant growth period. The amount of these displacements and their respective costs can be remarkable if a great number of large size multilayer growing units are used in the plant factory.

4- In both Romaine and Korean lettuce cultivars, the value of PPR and total plant production obtained by zigzag planting are considerably higher in compare to those of square planting. The better performance by zigzag planting was observed in either of static and dynamic cultivation plans. In static cultivation of Romaine and Korean lettuce cultivars, replacing the planting arrangement from square to zigzag could result in 14.3 and 16.7% increase in total number of produced plants during a 168 day cultivation period, respectively. The amount of this increase was even more in dynamic cultivation plans. The superiority of zigzag planting in total plant production confirms its higher efficiency of area utilization.

5- The response of Romaine lettuce to increasing the plant production through dynamic cultivation was not promising in neither of square and zigzag planting arrangements, while opposite of this was observed in Korean lettuce cultivation. The lower growth rate of canopy diameter in the Romaine lettuce compared to the Korean lettuce with faster horizontal growth is the reason of this phenomenon. In other words, the demand for larger growing area and stepwise increase in row spacing occurs later in the crops with slower canopy growth and thus, employment of multistage dynamic cultivation with the aim of increasing plant production rate is not so beneficial for such crops.

6- Providing a higher PPR and producing a greater number of Korean lettuce heads by 2-stage dynamic cultivation plans with 2-6 and 3-5 clustering conditions, when other dynamic plans with three growth stages were also among the options, demonstrates that adopting a greater number of growth stages is not the determinant factor for enhancing the plant production in the dynamic cultivation.

7- Effect of changing the size of the gully width on the performance of static and dynamic plans was investigated by the simulation panel. No change was found in the value of PPR_S and total plant production by the static cultivation when wider gullies were used. However, increasing the width of gullies in the multilayer growing unit of this study, decreased the PPR_D and total number of plants supplied by the dynamic cultivation plan. Reduced number of produced plants resulted by 2 cm wider gullies was estimated to be 448 plants (18.9% decrease) during a 178 day cultivation period. Therefore, adopting the minimum sufficient gully width is recommended in the cultivation process.

8- Adding the length of cultivation layers increases the PPR in both static and dynamic cultivation processes. However, the increasing rate of PPR_S caused by longer cultivation layers was relatively slower than that of the PPR_D. Simulation results indicated that an increment in the PPR_D value occurs when 7 cm is added to the length of the cultivation layer, while an approximate 20 cm increase in the layer length is required to elevate the PPR_S.

9- Under-utilization and waste of plant growing area may probably be observed in some cultivation layers during the implementation of dynamic cultivation plans. In such a case, a less than maximum possible number of gullies are placed in those layers, which causes the potential plant production of the cultivation process to be decreased. This deficiency was removed by changing the applied row spacing values to optimal ones, and rearranging the numerical distribution of gullies in some layers. The total released area from these modifications was used to grow some more plants under the static cultivation. Based on this, some of the cultivation layers, so called “static-dynamic hybrid layers”, simultaneously contain the plants growing under static or dynamic cultivation. In this study, the technique of hybrid static-dynamic layers were successfully invented and used to optimize the area utilization and minimize the amount of unused productive area.

10- Considering a total of eight available cultivation layers and a maximum 6-month cultivation process, the combinational cultivation plan including i) a dynamic plan with 1-2-3 clustering optimized with static-dynamic hybrid layers, and ii) two independent supplementary static layers was selected as the optimal cultivation plan with highest plant production for zigzag planting of Romaine lettuce under the given simulating conditions. Comparing to the basic static cultivation plan, the increase in total plant production by this plan was about 7.5% (232 plants), while the last crop output of the selected plan was supplied 10 days later than the static option. According to this delay, and considering that the implementation of 3-stage dynamic cultivation included in the selected combinational plan imposes additional costs and difficulties to the grower, involving the economic and marketing features into the appraisals is necessary for the grower.

Adopting the same conditions as used for the Romaine lettuce, the optimal cultivation plan for growing the Korean lettuce was found to be a dynamic cultivation plan with 3-5 clustering, optimized with one static-dynamic hybrid

layer. Comparing to the basic static plan, the increase in total plant production by this plan was about 19% (512 plants) during the same number of days with the static plan (168 days). Thus, unlike the selected cultivation plan for the Romaine lettuce, the grower can be more confident about the benefits of the cultivation plan selected for the Korean lettuce. The considerable increase in plant production through using a pure dynamic plan with no supplementary static layer, confirms the higher response of fast canopy growing plants such as Korean lettuce to the dynamic cultivation method.

4. PART II- DEVELOPMENT OF AUTOMATED SYSTEM FOR MULTILAYER CULTIVATION WITH ADJUSTABLE GULLY ROW SPACING

4.1. Introduction

This part of the current study describes the structure, development stages, operation details and automated control schemes of a multi-component mechatronic system that would be used for automated implementation of the multilayer cultivation plans described in chapter 3. The developed system introduced in this chapter can be analogized to automated storage and retrieval systems used in industrial warehousing (Roodbergen and Vis, 2009) which has been customized to meet the specific requirements of multilayer cultivation of leafy vegetables in NFT gullies.

As shown in chapter 3, the visual simulation module is used to evaluate the production performance of different multilayer cultivation plans and determine their executive results by means of which a cultivation schema (plan and procedure) is obtained. As illustrated in Figure 4-1, when a certain cultivation plan is selected as the optimal option, the executive results of that plan obtained by the module guide the user to establish the procedure to execute the plan. Detailed steps of such procedure are then transmitted to the control unit of the automated gully convey-spacing system which conducts an automated implementation of the selected plan through sequenced operation of different working parts and mechanisms of the system.

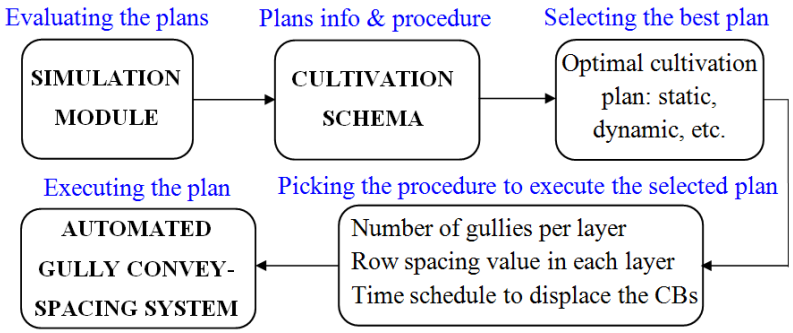

Figure 4-1. Relation between a cultivation schema and automated gully convey-spacing system

4.2. Materials and methods

4.2.1. Design criteria and assumptions

As a preliminary step prior to design and development of the automated convey-spacing system for multilayer plant factory, the assumptions and criteria listed below were made and adopted according to design objectives and conditions.

1- The automated system will exclusively support the hydroponic cultivation using nutrient film technique (NFT) in commercial available gullies.

2- Due to the existing constraint in the height and available area of the experimental site where the plant factory is established, only two multilayer growing units with limited number of four cultivation layers are developed.

3- In order to execute different multilayer static, dynamic cultivation plans, and also those with hybrid layers, the system must have the ability to adjust the row spacing between the growing gullies to any desired value in different layers of the growing unit. Controlled conveying of gullies along the vertical direction is another criterion which must be considered in the system design.

4- The automated system only deals with gully handling operations including controlled loading of gullies into the cultivation layers (row spacing operation) and its opposite action gully unloading, as well as stable conveying of gullies in horizontal and vertical directions.

5- The system and its whole operation must be fully automated. However, to reduce the production costs in the plant factory, economic considerations should be taken into account for developing a low expense and economically feasible product. To this end, using less number of cost effective motors, actuators, and sensors, as well as choosing an effective controller with reasonable price for covering the full scale automated operation should be adopted in designing the system.

6- The system is developed based on a modular design in which a composition of independent sub-systems with individual working units are designed and collaborate to implement the defined functions of the automated system.

7- Flexible operation for different conditions should be provided by means of the modification made in the software, i.e., automation schemes and control programs, and not through changing the hardware

4.2.2. Design, development and control of the system

4.2.2.1. Sub-systems, working units and mechanisms

In order to provide an automated execution of the cultivation plans indicated in chapter 3, the employed system must be able to provide bi-directional horizontal and vertical gully conveying and the ability of creating any desired row spacing value between the gullies in all MGU layers. To achieve these abilities, the automated gully conveying-spacing system developed in this study, consists of three sub-systems including i) two 4-layer growing units equipped with special gully load/unloading mechanisms, ii) an autonomous vehicle (AV), and iii) the gully supplier.

MGU with mechanical mechanisms

The 4-layer growing unit designed for automated convey-spacing system is not just a multilayer structure to maintain the growing plants and hold the growth facilities. The extra technical feature added to this MGU is its participation in loading/unloading the gullies into/from the cultivation layers using a number of multi-component mechanical mechanisms embedded in its frame, although the actuating power sources of these mechanisms are not installed in the MGU. It will be explained in section 4.2.3 that the row spacing operation, i.e., adjusting a desired distance between the gullies in a cultivation layer, is the direct result of controlled loading of the gullies. Figure 4-2 shows the installing position and details of a single set of this compound mechanical mechanism in the CAD model of MGU. As shown in this Figure, each set includes two horizontal sliding bars (one upper and one lower bar) and a couple of “roll-lift devices”. Employing two sets of this mechanism in the left and right of a layer is necessary for gully loading and unloading operation in one

cultivation layer. The red arrows in Figure 4-2 indicate that side of the MGU though which the gullies enter the layers.

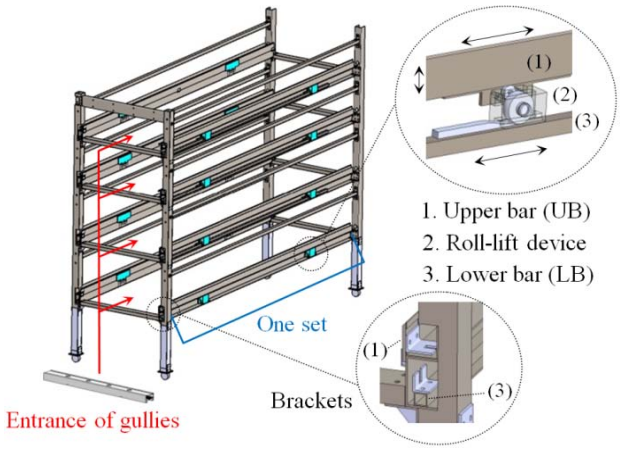

Figure 4-2. Frame of the 4-layer growing unit and details of the mechanical mechanism used for load/unloading of gullies

To move the sliding bars and actuate the mechanism for loading and unloading of gullies, special brackets have been installed in the front end of lower and upper bars (Figure 4-3) which will be locked into the hook-like connectors of AV's linear actuators rods during the operation.

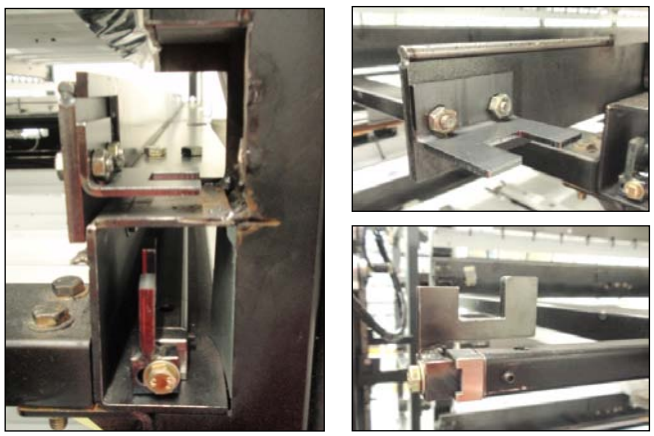

Figure 4-3. Brackets installed in the front end of lower and upper sliding bars

A roll-lift device and its details are shown in Figure 4-4 (a) to (d). The inner structure of this device consists of two small and large roll bearings mounted on an up-down moving block. All these components are assembled inside a fixed aluminum casing which will be installed on the body of MGU.

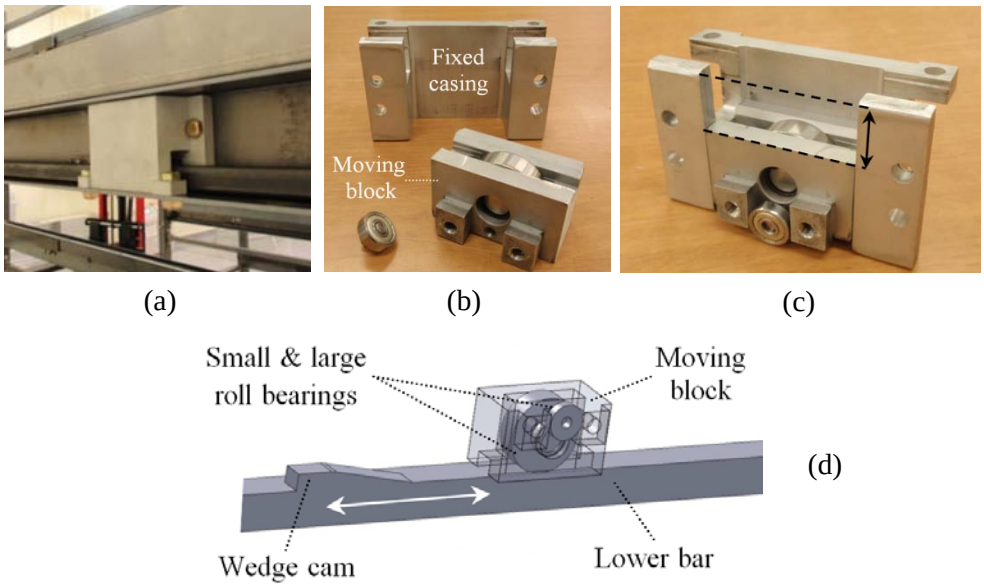

Figure 4-4. (a) Roll-lift device installed on MGU, (b) disassembled parts of roll-lift device, (c) working stroke of moving block, and (d) CAD models of roll-lift device, lower bar and the wedge cam

The upper bars of the compound mechanical mechanism are always placed on the small roll bearings of roll-lift devices. This causes an easier and smoother back and forth motion of the upper bars. The lifting action in the roll-lift device is activated when a lower bar is moved forward and the contact between the large roll bearing and the declined plane of a wedge cam, fixed on the top surface of the lower bar, occurs. Result of this interaction is a tiny upward motion of the moving block inside the fixed casing. This is because the rolling axis of the large roll bearing is fixed on the moving block and the only available direction for the block to move is upward. Since the small roll bearing is an attached part of the moving block, the created upward motion will cause the small bearing and the upper bar placed on it to be lifted as well. The

block moves down again when the lower bar and wedge cam move backward. The key role of lifting the upper bars in loading and unloading of the gullies would be explained later.

Autonomous vehicle (AV)

Autonomous vehicle (Figure 4-5) is the central power supplier for all automated operations in the system except of horizontal conveying of gullies on the ground level. Four working units including the locomotion, chain elevator, twin manipulator (×4) and vertical lift of manipulators (×2) have been developed and used in the final design of the AV. Since the automated convey-spacing of gullies in all MGUs is supported by a single AV, it is necessary to move the vehicle to the determined working positions in the front of each MGU. To this end, the locomotion unit provides a controlled linear motion for the AV.

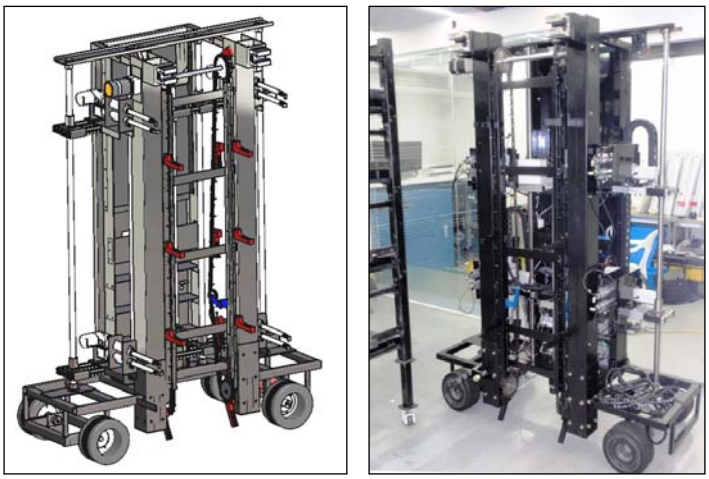

Figure 4-5. CAD model and developed prototype of the autonomous vehicle

Figure 4-6 (a) to (c) displays individual CAD models of remaining working units of the AV. Chain elevator consists of two parallel chain strands in form of closed loops, on each of which eight free to rotate L-shaped elements, called “gully carriers”, are attached in equally spaced intervals. The function of chain elevator is to provide a controlled continuous upward-downward gully conveying along the vertical direction.

A gully carrier is kept horizontal and non-rotating by leaning on a narrow metal wall (not shown here) installed behind it, when traveling in the vertical section of the chain loop. This section of the chain loop, along which the conveying of gullies occurs, is located in the front side of the AV.

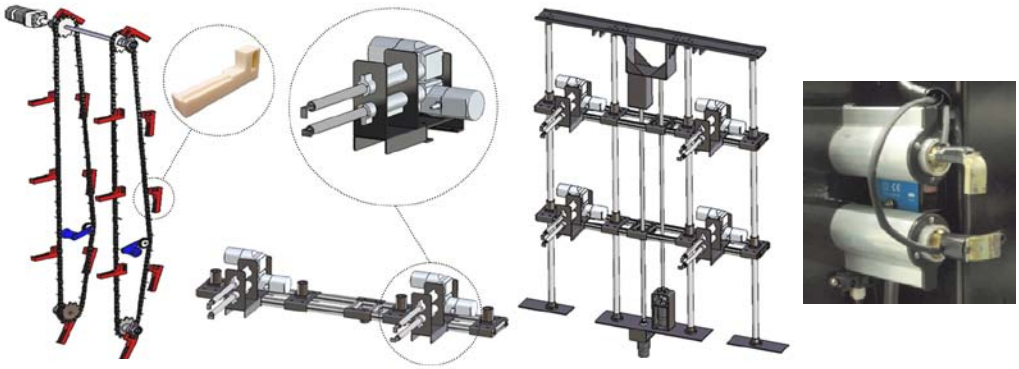

(a) (b) (c) (d)

Figure 4-6. (a) CAD model of chain elevator and gully carriers, (b) CAD models of twin manipulator and the common frame for two manipulators, (c) CAD model of manipulators vertical lifts, and (d) hook-like connectors in the tip of linear actuator rods of a twin manipulator

The twin manipulator (Figure 4-6 (b) top and 4-6 (d)) is composed of two linear actuators which push and pull the lower and upper bars embedded in the MGU. Moving the lower and upper bars by the actuators would be possible when hook-like connectors installed in the tip of linear actuators rods (Fig 4-6 (d)) and brackets of the bars (Figure 4-3) are interlocked. The details of manipulator locking will be explained in the next sections. A pair of twin manipulators mounted on a common frame (Figure 4-6 (b), bottom) is required to manipulate gully loading and unloading operations in one cultivation layer. For concurrent operation in two cultivation layers, a total of four twin manipulators (eight linear actuators) mounted on two common frames have been employed in the AV.

Considering the developed 4-layer growing unit, the manipulators mounted on the upper common frame (see Figure 4-6 (c)) are allowed to operate in top three cultivation layers 2, 3 and 4, while the manipulators on the lower frame cover the operation in bottom three layers 1, 2 and 3. In order to move these two frames to the target cultivation layers, two sets of ball screw driven vertical lifts, shown in the same Figure, are developed and installed in the AV. Using these vertical lifts, the symmetric left and right manipulators fixed on a common frame are moved and stopped in a certain vertical position for being locked with lower and upper bars of the respective cultivation layer.

Gully supplier

The gully supplier sub-system displayed in Figure 4-7 is a low profile conveying line which is used for horizontal conveying of NFT gullies on the floor level. The defined functions of this sub-system are to deliver the gullies containing the new plants coming from the nursery to the MGU at the first cultivation day and to receive the fully grown plants from the MGU at the harvesting day. Two belt conveyors and two specially designed free roller conveyors are employed in this conveying line. The area in which a roller conveyor is located is called the “pick/drop zone”, that is the location where the gully exchange between the chain elevator of the AV and the gully supplier takes place.

Figure 4-7. A view of horizontal conveying line

Figure 4-8 displays a full view of automated gully convey-spacing system after the final development. As can be observed in this Figure, the AV and MGUs are connected to each other through an overhead rail. This is mainly adopted to provide more stability of AV and MGUS during loading and unloading of the gullies through mass integration of individual bodies. Final dimensions (length×width×height) of the AV and MGUs are (160×72×225) and (300×110×230) cm, respectively. A summary of system components and their specifications is presented in Table 4-1.

Figure 4-8. Connection of AV and 4-layer growing units for operation in experimental plant factory

Table 4-1.Specifications of the sub-systems, working units and mechanisms developed for automated gully convey-spacing system

Sub-system	Working unit/ mechanism	Number	Main operation	Function
Autonomous vehicle (AV)	Locomotion	1	AV motion	Provides linear motion for AV to support operation in multiple MGUs
	Twin manipulator[1]	4	Gully load/unloading & row spacing	Supplies the power for loading and unloading of gullies into/from MGU layers manipulates row spacing operation through controlled back and forth motion of linear actuators
	Chain elevator	1	Vertical gully conveying	Moves the gullies vertically upward and downward between different cultivation layers and also the pick/drop zone
	Manipulators vertical lift	2	Layer targeting	Each vertical lift moves a pair of manipulators mounted on a common frame to the target cultivation layer
MGU	Gully load/ unloading mechanism[2]	8 [3]	Gully load/unloading & row spacing	A couple of this mechanism, powered by two AV manipulators, loads and unloads the gullies into/from a cultivation layer. Adjustable row spacing is the result of controlled gully loading
Gully supplier	Belt conveyor	2	Horizontal gully conveying	Convey the gullies containing new or fully grown plants on the floor level
	Roller conveyor	2	Horizontal gully conveying	Provide a pick/drop zone in front of each MGU to exchange the gully between horizontal gully conveying line and AV chain elevator

[1] Each twin manipulator contains two linear actuators; [2] Each set includes one upper and one lower sliding bar and two roll-lift devices;

[3] Reported number is for one MGU

4.2.2.2. PLC, special modules and controller circuits

A programmable logic controller (PLC) is a special form of microprocessor-based controller that uses programmable memory to store instructions and to implement functions such as logic, sequencing, timing, counting and, arithmetic in order to control machines and processes (Bolton, 2009). PLC as popular and widely used controller in automation applications is also employed to control the different functions and operations of the developed automated convey-spacing system.

The controller unit selected for automated convey-spacing system consists of a PLC main unit (XGB series, XBC DN-64H, LSIS Korea) with 32 digital input and 32 digital output terminals, as well as a number of special or extended modules (products of LSIS, Korea) that are connected to the main unit from its side. Each of these modules enables the controller unit to find a special ability which may not be present or sufficient in the PLC main unit, e.g., receiving and sending of analog signals. Figures 4-9 and 4-10 display several images of the complete controller unit used in the automated system. A list of available components in the controller unit is also presented in Table 4-2.

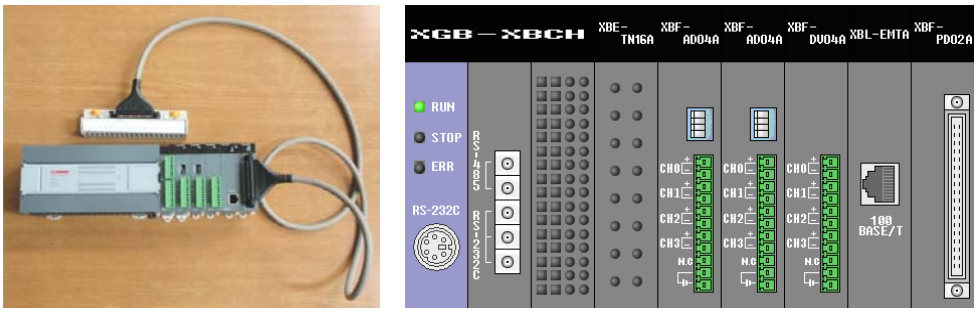

Figure 4-9. System controller including PLC main unit and special modules

Table 4-2. Components of the controller unit used for automated convey-spacing system and their specification

Type	Model	Function
PLC main unit	XGB, XBC-DN64H	CPU of the controller
Digital output module	XBE-TN16A	Adding 16 extra digital output terminals to the PLC
Analog input module[1]	XBF-AD04A	Converting the signals received from the analog sensors to numerical values usable for the PLC
Analog output module	XBF-DV04A	Providing analog control signal (output) for DC motor driver in the locomotion unit of AV
External positioning module	XBF-PD02A	Stepper motor control of the chain elevator
Communication module[2]	XBL-EMTA	Establishing wireless data transfer between the PLC and external master controller

[1] Two modules in the controller unit

[2] Used for an activity not related to this study

The controller unit is installed inside the autonomous vehicle (Figure 4-10). As shown in the left picture, access to the controller unit and other elements such as some of switch mode power supplies (SMPS), stepper motor drivers, solid state relays, etc., is possible through a hinged door on the back side of the AV.

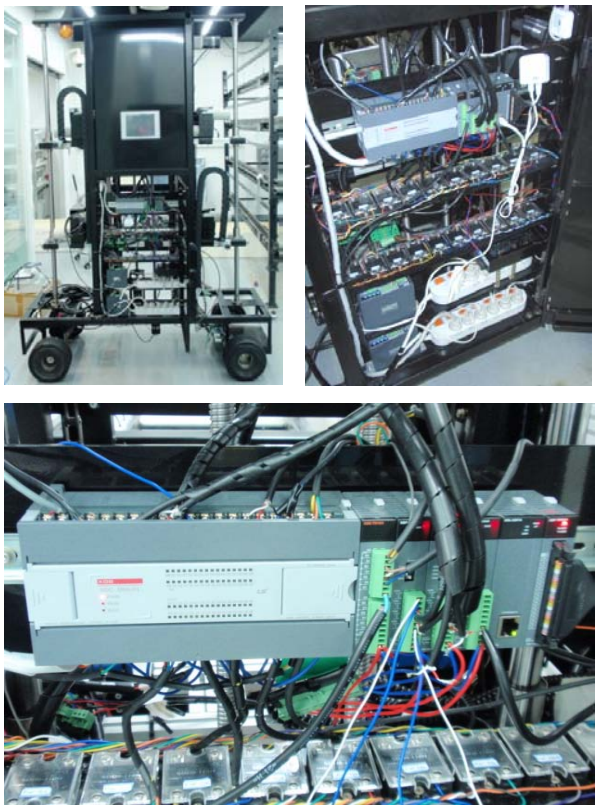

Figure 4-10. PLC and other accessories installed on the autonomous vehicle

Existence of a considerable number of input and output terminals and channels for receiving and sending digital and analog signals allows the controller unit to be connected to numerous sensors, motor and actuator drivers and the other instruments of the system and control the automated operation based on the developed control scheme and programs.

The terms sourcing and sinking applied to DC input and output circuits, are used to describe the way in which DC instruments are connected to a PLC (Bolton, 2009). The inputs of the PLC employed in the automated convey-spacing system, can be either sinking or sourcing, while the only available mode for connecting the PLC output terminals to the loads is sinking. In case of sinking input (Figure 4-11 (a)), the instrument connected to a PLC input, e.g., a digital sensor or switch, supplies current

to the controller and thus, the PLC input is the sink for the electrical current. In this case the common terminal of the PLC would be wired to negative pole of the power supply. With sourcing input on the other hand, using the conventional current flow direction from positive to negative, the instrument connected to PLC input receives current from it (Figure 4-11 (b)). Finally, if the current flows from a load in the circuit to the PLC output terminal, it would be called a sinking output (Figure 4-11 (c)). The voltage of operating signals in the PLC used in this study is 24 volts.

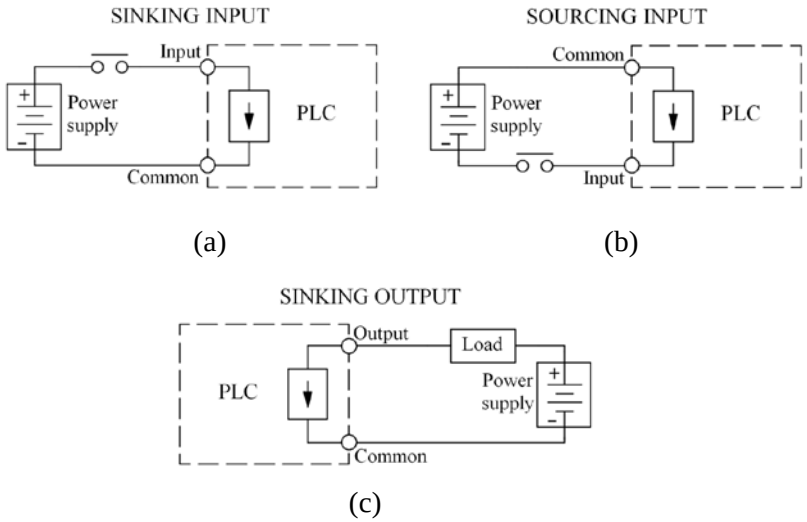

Figure 4-11. Concept of sinking and sourcing input-output in PLC circuits

According to the concepts mentioned above, the controller circuits and full wiring diagrams of the system are individually presented for input, output and also the special modules of the PLC in Figures 4-12 to 4-14, respectively.

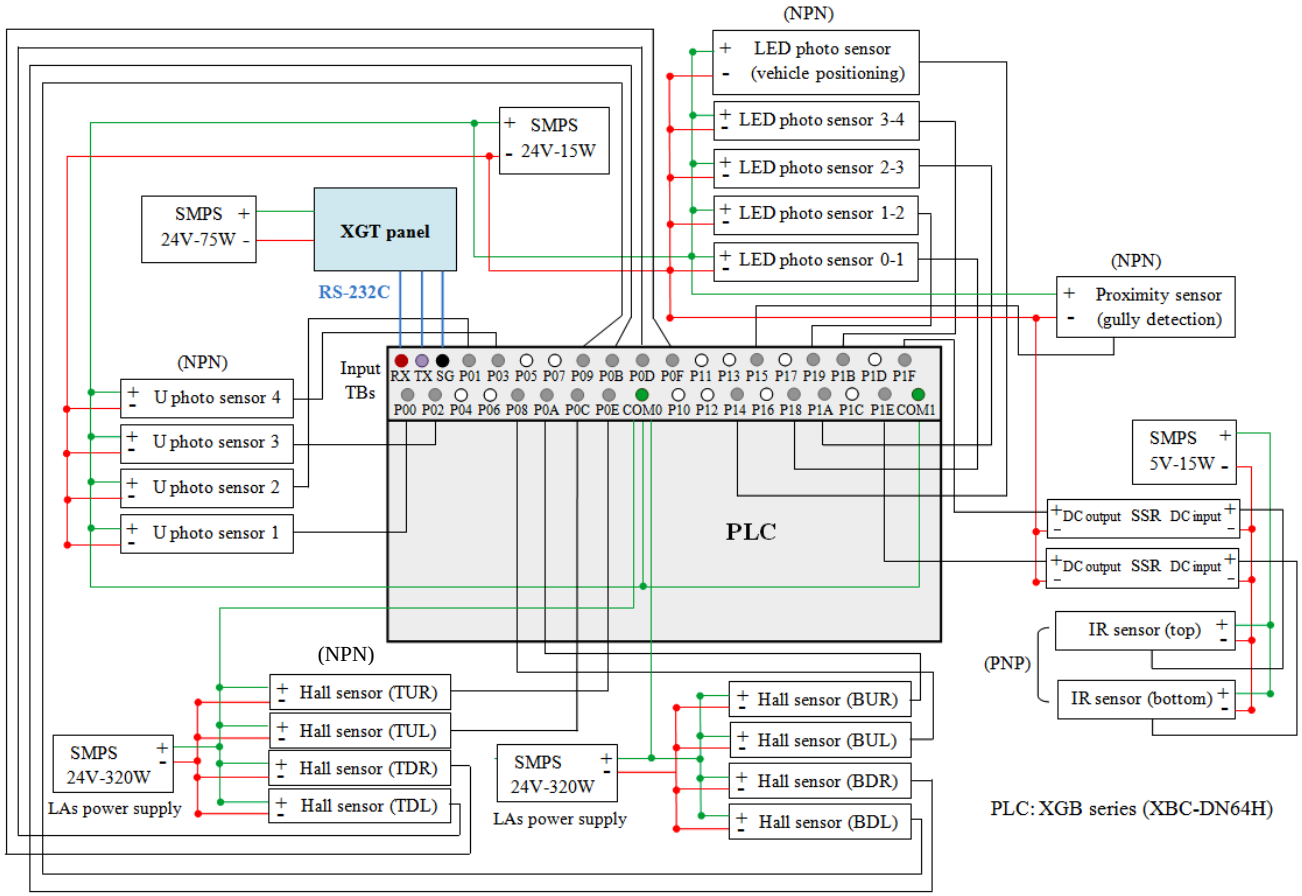

Figure 4-12. Control circuit and wiring diagram of PLC main unit inputs

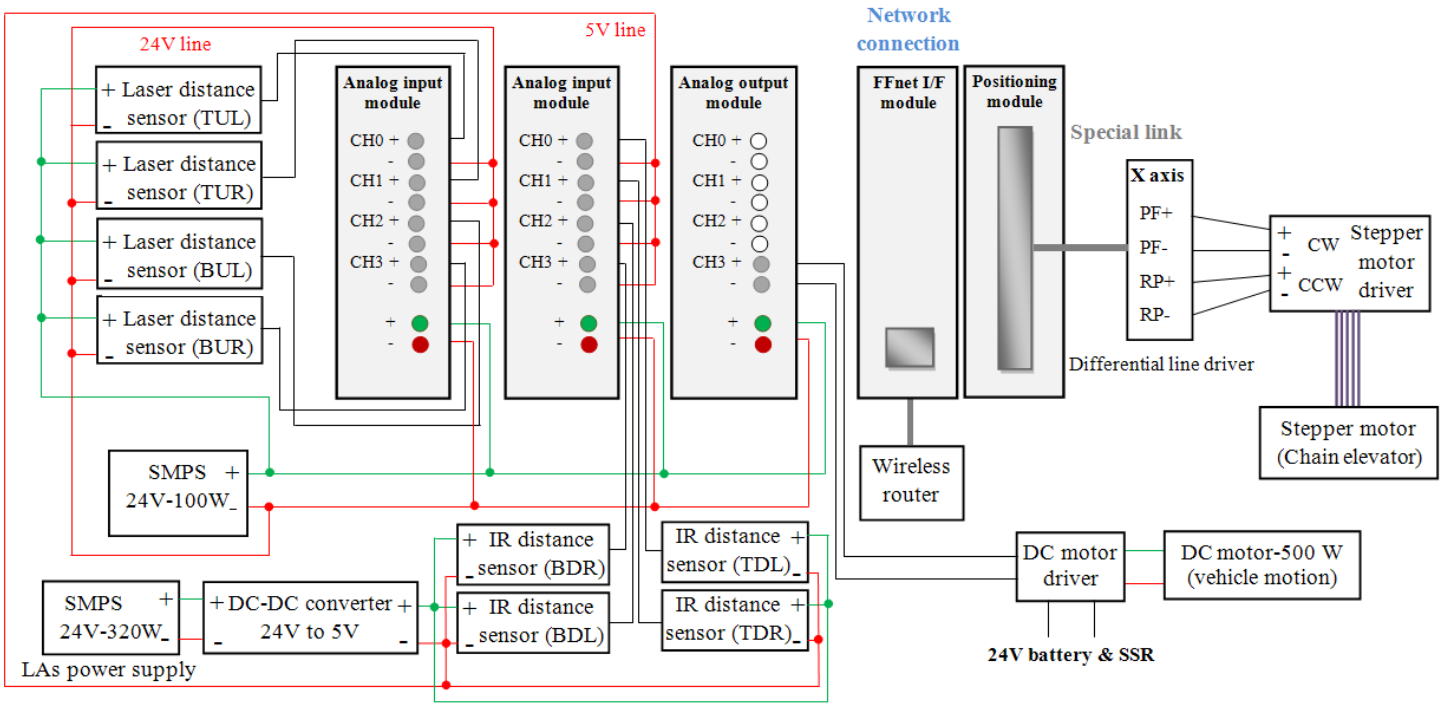

Figure 4-13. Control circuit and wiring diagram of PLC special modules

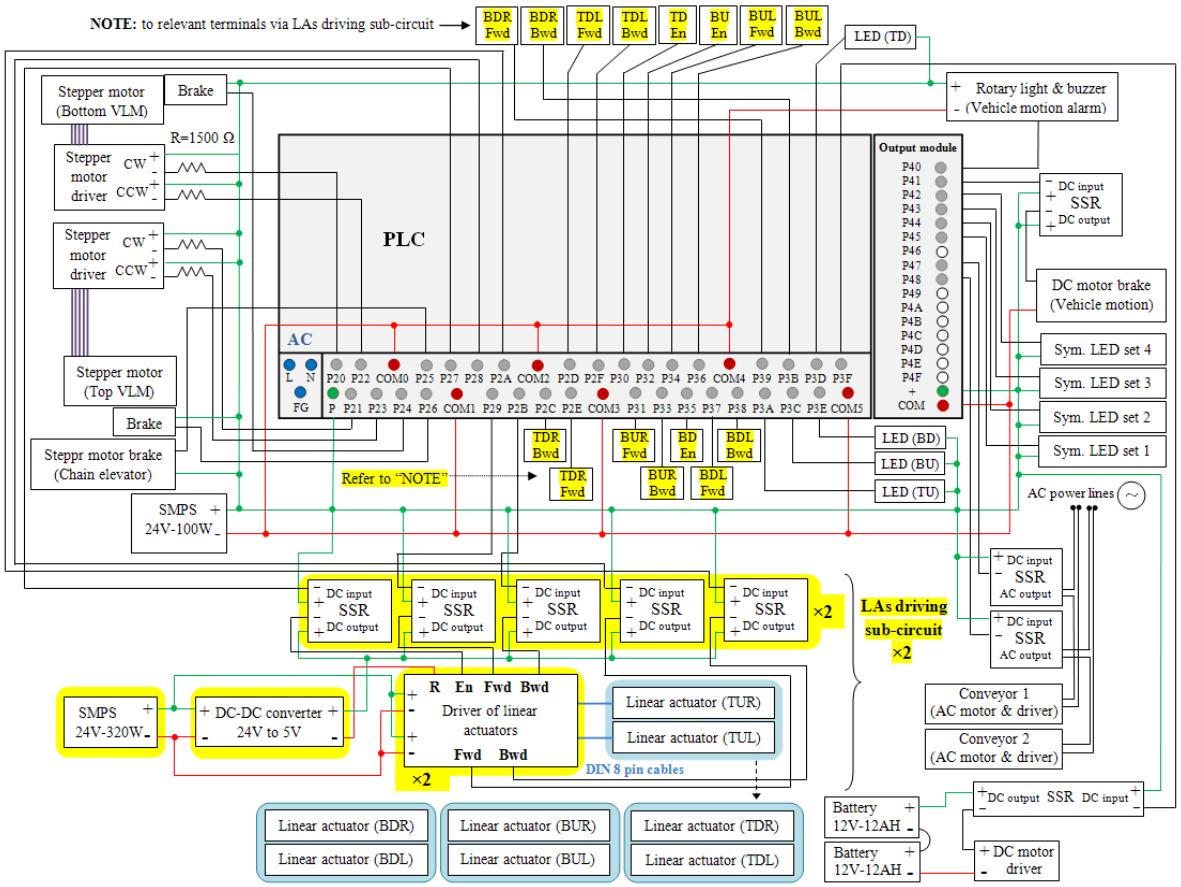

Figure 4-14. Control circuit and wiring diagram of PLC main unit outputs and additional output module

4.2.2.3. Sensors and actuators of the system

The list of the sensors (digital and analog) and actuators (motors and linear actuators) used in different working units of the automated convey-spacing system and a brief description of their function in the system is presented in Table 4-3.

Table 4-3. List of sensors and actuators in the system

Type	Item	Related unit	Number	Function
Actuator	Stepper motor	Chain elevator, vertical lifts	3	Provide precise vertical motion for gully carriers and twin manipulators
	Linear actuator	Manipulator	8	Pull and push lower and upper bars of load/unloading mechanism sets
	DC motor	Locomotion	1	Moves the autonomous vehicle
	AC motor	Gully supplier	2	Actuate horizontal belt conveyors
Sensor	LED photoelectric sensor	Locomotion, chain elevator	5	Detecting stopping positions of AV- Monitoring the vertical motion of gullies carried by the gully carriers
	U-shaped photo sensor	Manipulators vertical lift	4	Detecting the heights in which the manipulators operate
	IR sensor	Chain elevator	2	Making floating origin to control the stepper motor of chain elevator
	Proximity sensor	Gully supplier	1	Detecting the presence of gullies in pick-drop zone
	Hall sensor	Manipulator	8	Stopping the linear actuators in the locking positions
	Laser distance sensor*	Manipulator	4	Measuring the travel distance of the upper bars
	IR distance sensor*	Manipulator	4	Measuring the travel distance of the lower bars

*Analog output type

Actuators

Due to the necessity of providing precise position and speed control for chain elevator and manipulators vertical lifts, stepper motor was selected as the power source to actuate these working units. Stepper motors are designed to rotate in small angular increments, making them so effective for precise applications such as vertical positioning of gully carriers and manipulators in automated convey-spacing system. Three 5-phased stepper motors with electro-magnetic brake including one for driving the chain elevator (A200K-M599-GB10, Autonics, Korea) and two other motors (A16K-M569-B, Autonics, Korea) for moving manipulators vertical lifts are employed in the system. Shaft rotation per pulse for the stepper motors of chain elevator and vertical lifts are 0.072° and 0.72°, respectively. The selected motor driver for all three motors was MD5-HF14 (Autonics, Korea). Figure 4-15 displays a motor driver and the stepper motors used for chain elevator and one of the vertical lifts.

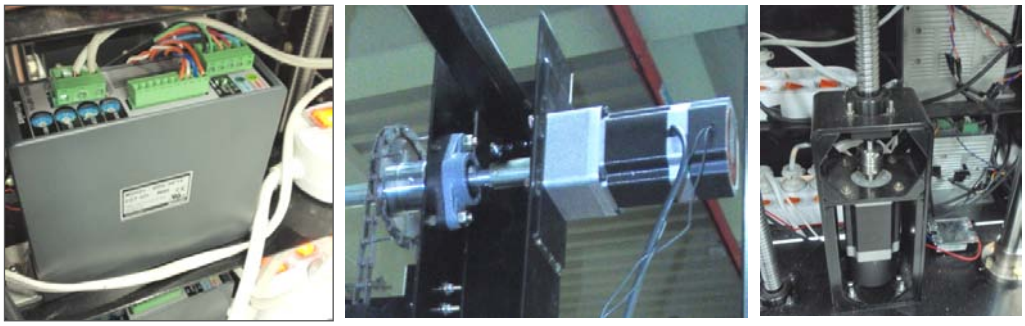

Figure 4-15. A motor driver and the stepper motors used for chain elevator, and for a vertical lift

Eight linear actuators (Megamat MBZ, Dewert, Germany) installed and arranged in four sets of twin manipulators are used to pull and push lower and bars of load/unloading mechanism sets in different layers of the MGU. The stroke length of these 24V linear actuators is 300 mm and they use internal hall sensors to provide the positioning feedback for the controller. The driver used for linear actuators is not a commercial product and has been independently developed in the lab. Figure 4-16 shows a pair of linear actuators arranged and installed in a twin manipulator and the

developed driver that can support four linear actuators at the same time. The control signals applicable to the driver for moving a linear actuator are 5V. To move each linear actuator, three input terminals on the driver have been assigned to receive the control signals related to “enabling the motion”, “forward motion” and, “backward motion” of the linear actuator.

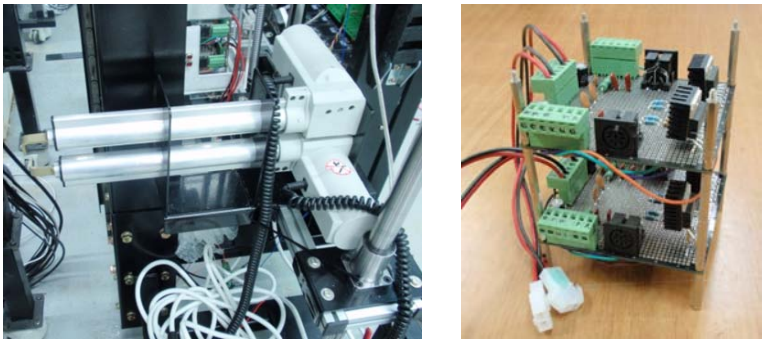

Figure 4-16. Two linear actuators in a twin manipulator and the driver supporting four linear actuators

Sensors

Successful operation of developed automated system greatly depends on the signals generated by different types of sensors installed in the system. Monitoring the upward-downward motion of the gullies (when carried by the gully carriers) for detecting their presence at certain heights of the system is the function defined for four of the diffuse reflective type LED photoelectric sensors (BJ300-DDT, Autonics, Korea) installed in the front side of the AV (Figure 4-17 (a)). The selected vertical positions for fixing these sensors include i) between gully conveying line and layer 1, ii) between layers 1 and 2, iii) between layers 2 and 3, and iv) between layers 3 and 4. The sensors would send signals to the PLC each time a vertically moving gully passes from these points. The other LED photoelectric sensor installed at the top of the AV (Figure 4-17 (b)) is employed to generate a signal to stop the vehicle when the certain working position in front of each MGU is detected.

The U-shaped sensor (BUP-30, Autonics, Korea) shown in Figure 4-17 (c) is a through-beam type photo sensor which would dispatch a digital signal to the PLC

when an object passes through its two extended wings and breaks the light beam between emitter and receiver. Four sensors of this model are installed in the interior space of the AV, close to vertical moving path of manipulators common frame such that the sensing object attached to the moving frame can pass through the sensor wings. The vertical positions these sensors are installed, are the heights in which AV manipulators operate for gully loading and unloading in cultivation layers 1, 2, 3, and 4. The application of these sensors is to detect these heights and send signals for controlling the motion of the manipulators vertical lifts in “layer targeting” and “manipulators locking” automated operations.

The infra-red (IR) sensors installed near one of the chain strands of the chain elevator are low cost digital sensors which provide signals when a marked gully carrier is detected. Since the sensor merely responds to the light colors, the output signal of the sensor is released only when the gully carrier with white spot on its body is detected (Figure 4-17 (d)). The generated signal is used to make floating origins for motion control of chain elevator stepper motor. The terms bottom and top are used for these sensors to distinguish the two IR sensors installed close to bottom and top sprockets of the chain elevator, respectively.

The proximity sensor (PR30-15DN, Autonics, Korea) displayed in Figure 4-17 (e) makes an output signal when the distance between its head and the metal-made gullies becomes less than 15 mm. This property is utilized to detect the presence of the gullies in the pick-drop zone, required in some compound automated operations such as the one by which the new gullies are moved from the starting point of gully conveying line and are finally loaded into a certain cultivation layer with adjusted row spacing values. The proximity sensor is installed in the front side of the vehicle and would be located beside the end of gully conveying line during the operation.

The signals generated by the hall sensors are employed to stop the linear actuators of the AV in secure positions for manipulators locking operation. As can be observed in Figure 4-17(f), due to the very small size of the hall sensors, it is possible to install them on the hook-like connectors located in the tip of linear actuators rods. In order to generate the required signals, small magnets are also embedded in appropriate positions inside the MGU, near the places where the hook-like connectors enter a layer for being locked with the brackets of lower and upper bars. A signal is released when the hall sensor reaches to the vicinity of a magnet.

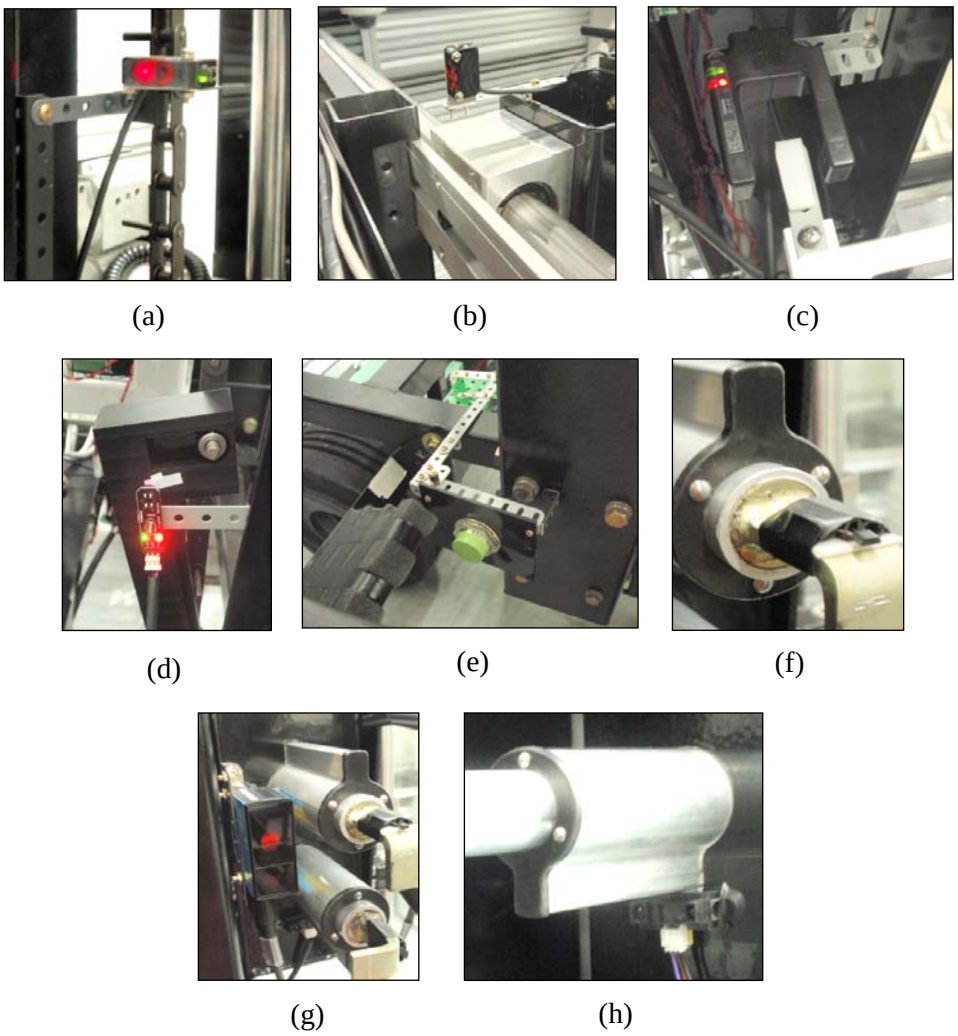

Figure 4-17. Different types of the sensors employed in automated gully convey-spacing system: (a) and (b) LED photo sensor, (c) U shaped photo sensor, (d) IR sensor, (e) proximity sensor, (f) hall sensor, (g) laser distance sensor with analog output, and (h) IR distance sensor with analog output

The sensors presented in the last two rows of Table 4-3 are the sensors with analog outputs which are used to measure the travel distance of MGU lower and

upper bars during gully loading and unloading operations. The sensor measuring the value of upper bar back and forth motions (Figure 4-17 (g)) is a high resolution laser distance sensor (DT20-N214B Sick, Germany) with current output (4-20 mA) and nominal measuring range of 100 to 600 mm. The sensors introduced for the similar purpose in the lower bars are inexpensive IR type distance measuring sensors (GP2Y0A21YK0F, Sharp, Japan) with voltage output, which enables the distance measurements ranging from 100 to 800 mm. An image of this sensor is shown in Figure 4-17 (h). Both sensors are installed in the front part of the twin manipulator.

All digital sensors introduced above, except of two IR sensors used in the chain elevator, are NPN type sensors with a sinking output which allow the current to flow into them when a signal is triggered by the sensor. A PNP sensor with sourcing output generates the signal by allowing the current to flow out of the sensor. Noticing the NPN or PNP type of the sensors is so critical when wiring to PLC inputs is made. 5V power supplies are used to provide the required power of IR digital and analog sensors, while all remaining sensors can use 24V power line for operation. Details about applications of the signals generated by the introduced sensors are presented in section 4.2.4.

4.2.2.4. Design of human-machine interface (HMI)

The hardware part of the human-machine interface (HMI) utilized in automated gully convey-spacing system is a special touch panel (XP-50 XGT panel, LSIS Korea) which enables the operator to observe, monitor and control entire operations and elements of the system through a number of interconnected control screens loaded on the panel. The software used to design and construct the different screens of the HMI is XP-Builder (LSIS, Korea). The XGT panel is connected to the PLC through an RS-232C link and its required power is independently supplied by a 24V DC 75 watts SMPS. The picture shown in the left of Figure 4-18 displays the position of HMI panel installed at the back side of the AV above the door through which the access to PLC is provided.

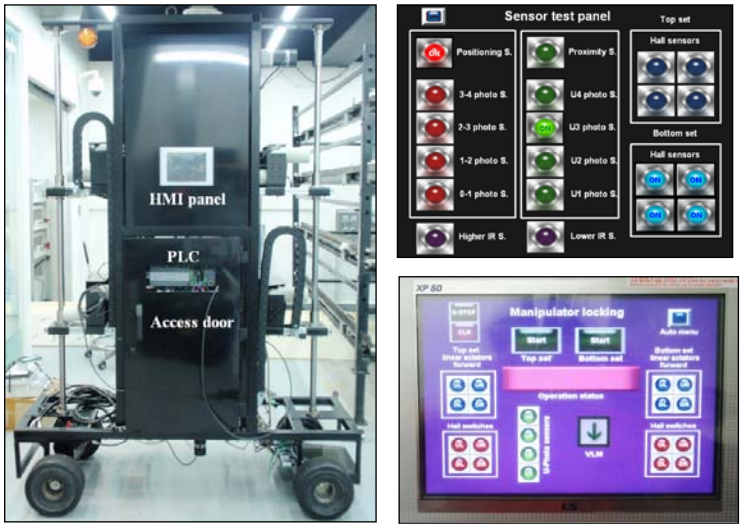

Figure 4-18. Position of HMI panel on the autonomous vehicle and examples of designed control screens

The images in the right of this Figure are two examples of the designed screens. In the upper image all digital sensors installed in different parts of the AV are indicated in a single screen such that a bit lamp is assigned to each sensor. This screen is used to monitor and test of digital sensors of the system before and during each automated operation and check if a disconnection or malfunction does exist in any of the sensors. The lower image shows the screen designed to monitor and control the manipulators locking experiment. Items such as start and emergency stop buttons, bit lamps of included sensors in this operation, working status of all eight linear actuators, etc., can be observed in this control screen.

4.2.2.5. Stepper motor control by PLC positioning modules

Precise motion control of the three stepper motors employed in the system is an essential factor for obtaining the demanded results from those automated operations in which the chain elevator and manipulators vertical lifts are involved. Stepper motor

control in the developed system is implemented by PLC built-in and special external positioning modules through adopting position and/or speed control methods. The PLC built-in positioning module supports a maximum of two motion axes which are used to control the two stepper motors driving the manipulators vertical lifts. The ability of controlling two more motion axes is added to the controller unit by using the special external positioning module (Table 4-2), one of which is used to control the stepper motor of the chain elevator.

The control programs of the PLC used for automated gully convey-spacing system are developed by XG5000 programming software (LSIS, Korea). Using a number of instructions specifically defined for positioning applications, the control programs a part of which is controlling the stepper motors, are developed in XG5000. However, before running such programs, the basic parameters applied by PLC positioning modules must be determined by the user in the setting window partly shown in Figure 4-19. The X axis in this Figure represents the stepper motor of chain elevator controlled by the special external positioning module, while the other axis is not in use. In this study, the “pulse/direction” (PLS/DIR) control signal is selected for driving the motors, although the “clockwise/counter-clockwise” (CW/CCW) control signal is also supported by PLC positioning modules and stepper motor driver.

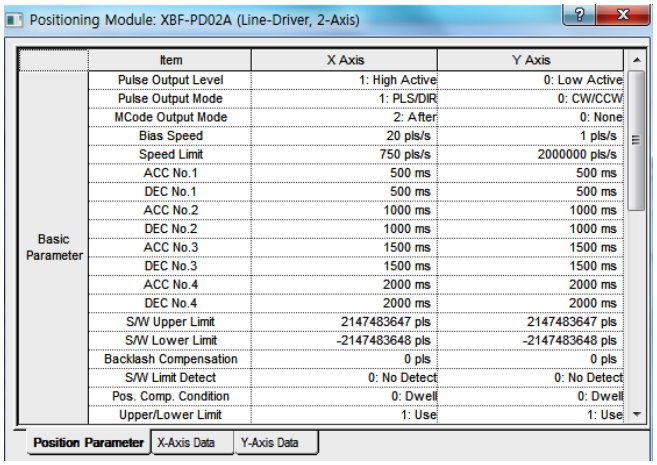

Figure 4-19. Adjustment of basic parameters for stepper motor control of the chain elevator in XG5000

In order to start the controlled motor rotation by the PLC, either of XG5000's direct or indirect starting instructions (DST& IST) can be used in the related programs. For indirect starting used in this study, the user must determine and adjust the type and value of different motion parameters such as coordinate type (absolute, incremental), control method (speed, position), operation pattern (end, keep, continuous), applied pulse rate, rotational direction, etc., for individual steps of multistep motion scenarios employed in more complicated control programs. Figure 4-20 shows the setting window in which the parameters of several steps are adjusted to control multistep motion of the chain elevator during one of automated operations of the system. The item "M code" observed in recent two windows is an optional auxiliary signal which can be generated based on the user demand during or after each step, and used for programming purposes.

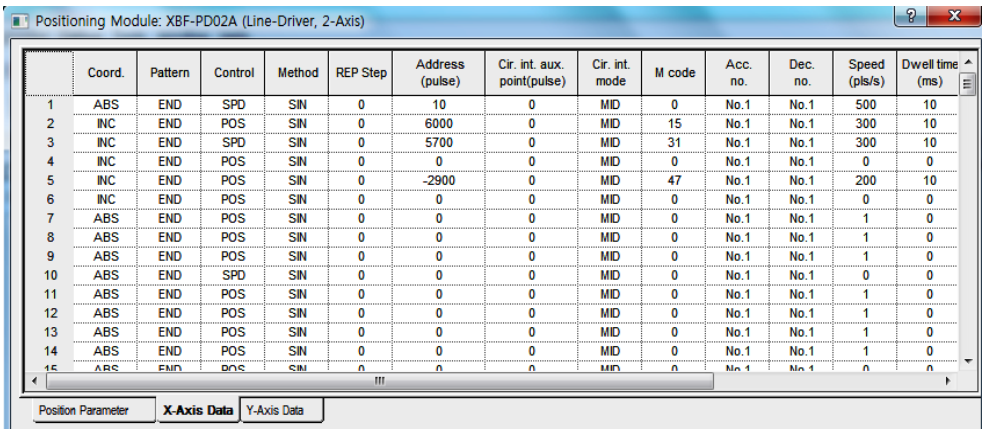

	Coord.	Pattern	Control	Method	REP Step	Address (pulse)	Cir. int. aux. point(pulse)	Cir. int. mode	M code	Acc. no.	Dec. no.	Speed (pls/s)	Dwell time (ms)
1	ABS	END	SPD	SIN	0	10	0	MID	0	No.1	No.1	500	10
2	INC	END	POS	SIN	0	6000	0	MID	15	No.1	No.1	300	10
3	INC	END	SPD	SIN	0	5700	0	MID	31	No.1	No.1	300	10
4	INC	END	POS	SIN	0	0	0	MID	0	No.1	No.1	0	0
5	INC	END	POS	SIN	0	-2900	0	MID	47	No.1	No.1	200	10
6	INC	END	POS	SIN	0	0	0	MID	0	No.1	No.1	0	0
7	ABS	END	POS	SIN	0	0	0	MID	0	No.1	No.1	1	0
8	ABS	END	POS	SIN	0	0	0	MID	0	No.1	No.1	1	0
9	ABS	END	POS	SIN	0	0	0	MID	0	No.1	No.1	1	0
10	ABS	END	SPD	SIN	0	0	0	MID	0	No.1	No.1	0	0
11	ABS	END	POS	SIN	0	0	0	MID	0	No.1	No.1	1	0
12	ABS	END	POS	SIN	0	0	0	MID	0	No.1	No.1	1	0
13	ABS	END	POS	SIN	0	0	0	MID	0	No.1	No.1	1	0
14	ABS	END	POS	SIN	0	0	0	MID	0	No.1	No.1	1	0

Figure 4-20. Adjustment of motion parameters for stepper motor control of the chain elevator by indirect starting in XG5000

An essential point to include in motion control programs is the necessity of applying a floating origin signal before starting a new step. A motion step which may use either of speed or position control methods would not be executed unless a manual or sensor made signal activates the FLT instruction in the program. Once the signal is applied, the current position of the stepper motor, in terms of pulses, becomes zero and this point is determined as the floating origin of the stepper motor.

4.2.2.6. Selection of control method for positioning of linear actuators

Controlling the travel distance of the linear actuators operating in the automated system is the most important part of the control schemes developed for gully loading-unloading and, more specifically row spacing operation. Preliminary experiments were conducted to find and select the reliable method for positioning control of linear actuators.

4.2.2.6.1. Position control using internal hall sensors

At first series of preliminary experiments, the performance of positioning control of linear actuators using the feedback signals generated by their internal hall sensors was examined and evaluated. In this method, the revolution of actuator motor shaft is sensed by two hall sensors embedded inside it. As a result, a series of output signals are generated and sent to the controller when the linear actuator works. The controller would stop the linear actuator when a certain number of signals are generated. Since the displacement of actuator rod, in terms of mm/signal, is a given item in the data sheet of the linear actuator, it is expected that a desired displacement can be achieved when its proportional number of signals are obtained. In order to examine the accuracy and reliability of this method, a pilot scale cultivation layer containing two sets of load/unloading mechanism was established and four fixed linear actuators were connected to lower and upper bars to move them back and forth. Figure 4-21 indicates details of this pilot experiment.

Two laser distance sensors (DT50-N1114, Sick, Germany) were installed at the two sides of the frame (just for reading the measured distances) and rectangular plates made from hard foam, used as sensing targets, were attached to the moving rod of each linear actuator. The distance between a sensor and the corresponding plate could be accurately measured and shown in mm by the sensor. The control program developed with Labview enabled the user to stop the actuator through determining the allowed number of hall signals. Based on this, the employed laptop was adopted as the controller.

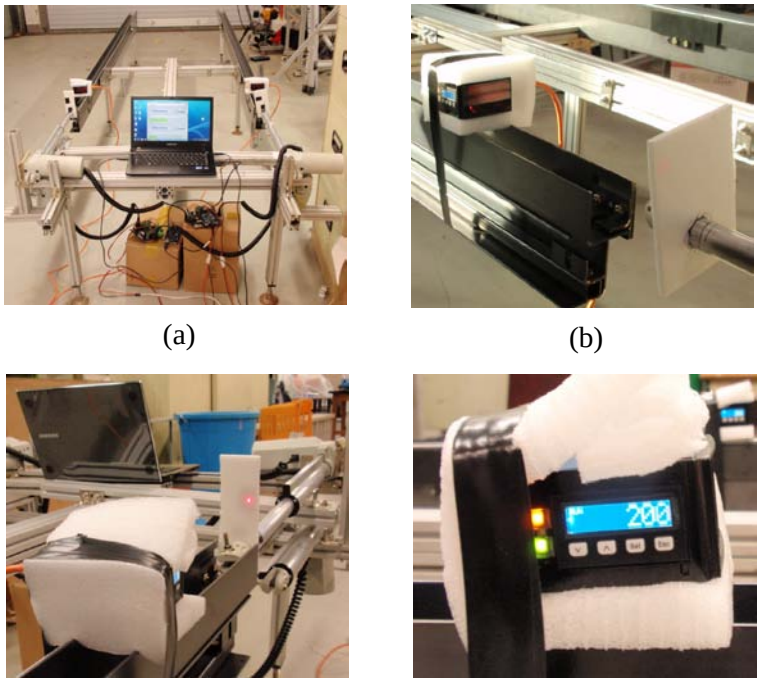

(a) (b)

(c) (d)

Figure 4-21. Experiments for positioning of linear actuators using internal hall signals: (a) front view of the experiment, (b) laser sensor for measuring the displacement of sensing target, (c) laser point on the sensing target and, (d) sensor panel indicating the measured distance

Based on Figure 4-22(a), the state in which the distance between the sensor and the sensing target is 300 mm, was selected as the initial position and starting point of the experiment. Using the term “run” for one back and forth motion of linear actuators (toward the frame and back to the initial position), each actuator was moved for 50 runs while the distance indicated by the sensor was observed and stored after each 5 runs. The experiment was repeated three times for all four linear actuators (two lower and two upper LAs). Number of signals applied by the user in the control program was 250 for back and forth travels each. The final positioning error after a certain number of runs is the difference between the distance shown by the sensor at the end of that run and the value 300 mm fixed in the initial position. Based on

Figures 4-22 (b) and (c), positive and negative errors occur when the final position of the sensing target at the end of runs is closer and further to the sensor compare to its initial position, respectively.

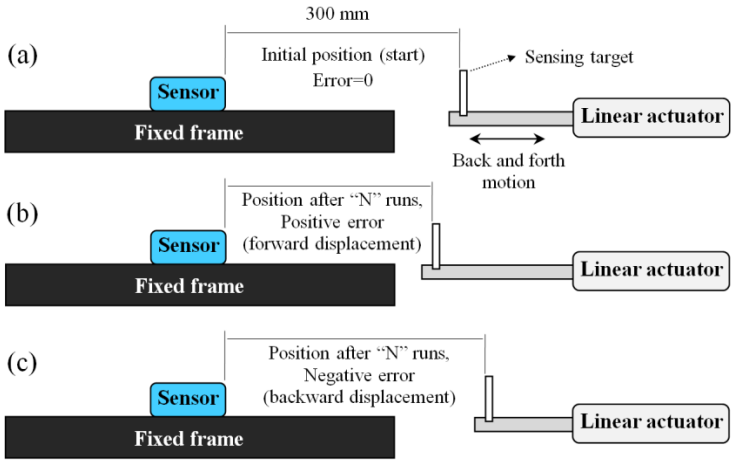

Figure 4-22. Schematic layout of positioning control experiment by internal hall sensors

4. 2.2.6.2. Position control using analog distance sensors

Figure 4-23 displays several images from the preliminary experiment conducted for positioning of two linear actuators using IR distance sensors. Adopting the similar sensing targets as in the experiments of the last section, the travel distance of the actuators fixed on a table were controlled using the signals of a couple of IR distance sensors. It was attempted to attain a number of travel distances ranging from 30 to 150 mm through the control program in both travel directions. Using a steel ruler, actual displacement of linear actuators was directly measured after each backward or forward stroke. The difference between the desired value inserted in the control program and the measured value indicating the actual displacement of the linear actuator was considered as the positioning error caused by the sensors. The starting point of each travel was the same (but different for forward and backward motions) and actuators were not under the load during the test. Each attempt of the experiment was repeated for three times.

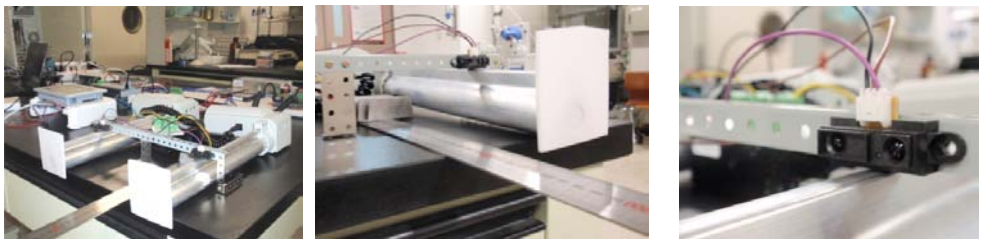

Figure 4-23. Experimenting the performance of IR distance sensors for positioning of linear actuators

The analog output signal (voltage type) of the sensors, that varies when the measured distance changes, is sent to PLC analog input module where it is converted to a proportional numerical value (digital output value) interpretable by the PLC main unit for the use in control programs. Using the “voltage-distance” chart of the sensor as well as the “analog input value (voltage)-digital output value” conversion chart of analog input module, different traveling distances for a single backward or forward stroke of the linear actuators were applied in the control program. Linear actuators were moved under controlled positioning to achieve the different distances selected for the experiment and the deviation between the distance value applied by the control program and the actual displacement of the linear actuator was adopted as the positioning error. In addition to this experiment, the performance of IR distance sensors in the real automated system, in which the conditions of ambient light and sensing targets were different, was also examined. Evaluation of laser distance sensors was also conducted when the sensors were installed on autonomous vehicle.

Reducing the noise or sudden changes of the analog signals generated by the distance sensors is feasible by activating the filter processing function in XG5000 PLC programming software. Filter processing is used to obtain stable digital output values from PLC analog input module (XBF-AD04A) through reducing or removing the existing noise in analog signals. Without filter processing, real-time exposure of the analog signal is executed such that the present analog to digital (A/D) converted value would be directly taken as the output of the module, while the activity of filter processing function modifies the output value of the module by including the effect of previous A/D converted value into the present one.

According to LS XGB analog manual, Equation 4-1 is employed to execute the filter processing in the analog input module.

$$F(n)=(1-C_F)\times A(n)+ C_F \times F(n-1) \qquad (4\text{-}1)$$

where A(n) is present A/D converted value, C_F is the filter constant selectable by the user from 1 to 99 and finally, F(n) and F(n-1) are present and previous filter output values, respectively. Applying a larger filter constant is more effective if the analog output signal of the sensor is severely unstable and fluctuates too much. Figure 4-24 demonstrates the setting window of analog input module in XG5000 software, in which the adjustment of filter processing for channels 0 and 3 of the module connected to laser distance sensors with current type analog output signals, can be observed.

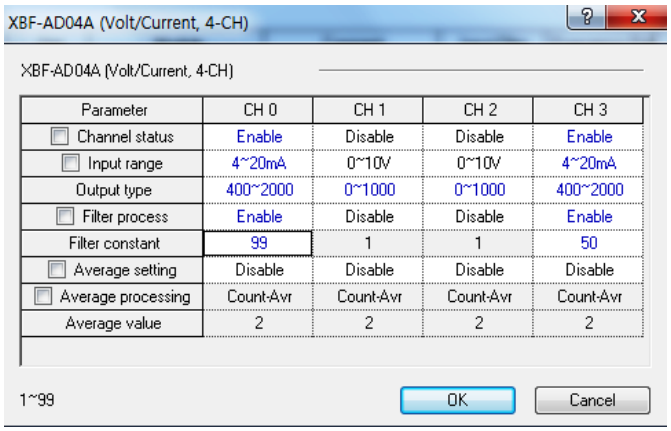

Figure 4-24. Adjustment of filter processing in XG5000 for noise reduction of laser sensor output signals

4.2.3. Motion analysis of automated row spacing operation by virtual prototyping

The main objective of developing the automated gully conveying-spacing system is to execute an adjustable row spacing operation such that any desired value of row spacing can be created and applied between the NFT gullies in either of the cultivation layers. The ability of adjusting different row spacing values in MGU layers can be utilized in static, dynamic and hybrid cultivations methods. Adjustment of row spacing in the static method is limited to the spacing value applied in the first day in which the gullies are loaded into the MGU layers. In multistage dynamic method, on the other hand, more than one time of row spacing adjustment is needed.

Adjusting the row spacing value by the system is a direct result of controlled loading of the gullies. In this section, it will be shown that obtaining a certain value of row spacing by the developed automated system is achieved when a serial of loading cycles with controlled sequential motions are executed. To examine the validity of the working steps employed for row spacing between the gullies in different situations and analyze the results, simulating the row spacing operation using the virtual prototype of the system was implemented. Virtual prototyping is a computer-based technique used for design, analysis and optimization of a system before its physical prototype is developed. According to McHugh and Zhang, 2011, this type of prototyping is the integration of computer-aided design (CAD), embedded software programming and simulation software to visualize and manipulate a mechatronic device in computer environment without the need for building its physical version. To construct the virtual prototype required for simulating and analyzing the row spacing operation, CAD models of AV and the 4-layer growing unit developed by CATIA V5R20 (Dassault systems, France) were used. The required data for motion analysis of system moving parts were obtained by Recurdyn V7R5 CAE (computer-aided engineering) simulation software (FunctionBay, Korea).

4.2.3.1. Configuration of automated row spacing operation and relevant motions

Figure 4-25 displays a side view from front section of a cultivation layer in the MGU and those parts of the AV which participate in loading the gullies into the MGU and thus, the row spacing operation. All components, dimensions and the relevant motions involved in gully loading and spacing are shown in this picture.

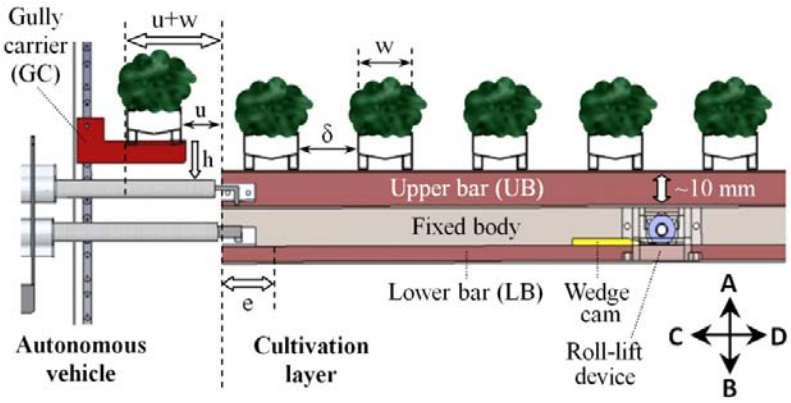

Figure 4-25. Side view from front section of a single set of gully load/unloading mechanism, a twin manipulator and gully carrier at the start of a loading cycle

According to the state shown in Figure 4-25, the cultivation layer is ready to receive a new gully from the gully carriers and put it onto the fixed body of the MGU such that the same row spacing value (δ) applied between the previously loaded gullies is created. As a result of gully loading, the vertically conveyed gullies stopped in the front of the layer (loading position) are transferred from the gully carriers into the cultivation layer. The relative position of a newly transferred gully to that of its preceding loaded gully determines the row spacing value between them.

Operation motions

In Figure 4-25, the linear actuators of twin manipulator have been locked into the brackets of lower and upper bars and are the power sources for indicated load/unloading mechanism. The allowed ranges for back and forth motion of lower and upper bars are shown by the white double arrows.

The 10 mm upward displacement of the upper bar is generated by the lifting action of the roll-lift device described in section 4.2.2.1 and happens when the lower bar is moved forward in the CD direction. The upward motion of the upper bars causes the gullies previously loaded in the layer to be lifted from the fixed body and allows them to be carried by the upper bars when they are horizontally moved. Downward motion of the upper bar and placing back the gullies on the fixed body in the new positions happens when the lower bar is pulled back to its initial moving point.

Another participating motion in loading and row spacing of the gullies is the small downward motion of the gully carriers made by the chain elevator. This downward vertical motion would let the gully on the gully carriers be placed on the upper bars when the bars are beneath the gully carriers after their move toward the vehicle in the DC direction.

4.2.3.2. Loading cycles and spacing modes

Continuous loading of gullies into a cultivation layer is possible through applying a number of multistep loading cycles. Each loading cycle consists of several motions described in section 4.2.3.1, which are implemented based on a specified sequential order. In this study, different types of loading cycles with 4, 5 or 6 working steps (motions) are determined whose details are shown in Table 4-4. The information presented in this table includes the travel direction and distance of the moving parts of the automated system as well as the sequence of the working steps executed in each type of the loading cycles.

Table 4-4. Travel direction and distance of system moving parts (based on Figure 4-25), and sequence of working steps in different loading cycles

Loading cycle	Moving parts	Step 1	Step 2	Step 3	Step 4	Step 5	Step 6
4-step	Upper bars	DC (ψ)[1]	BA[2] (10)	CD (ψ)	AB[2] (10)	-	-
	Lower bars	-	CD (e)	-	DC (e)	-	-
5-step	Upper bars	DC (u+w)	BA[2] (10)	-	CD (u+w)	AB[2] (10)	-
	Lower bars	-	CD (e)	-	-	DC (e)	-
	Gully carriers	-	-	AB (h)	-	-	-
6-step	Upper bars	DC ($w+\varepsilon$[3])	BA[2] (10)	DC (u-ε)	-	CD (u+w)	AB[2] (10)
	Lower bars	-	CD (e)	-	-	-	DC (e)
	Gully carriers	-	-	-	AB (h)	-	-

[1] $0<\psi<u+w$; [2] Operated by roll-lift device (in mm); [3] $0<\varepsilon<u$

To realize the travel directions presented in Table 4-4, referring to direction guide diagram indicated in the bottom right of Figure 4-25 is necessary. The parameters and numeric value 10 (in mm) shown in parentheses are the travel distances of system moving parts during each step of the loading cycles.

According to Figure 4-25, parameter “u” is the horizontal distance between the front edge of the cultivation layer and the right wall of the gully kept by the gully carriers. Parameters “e”, “h”, and “w” are maximum allowed back and forth stroke of the lower bar, downward travel distance of the gully carriers during a loading cycle, and width of a gully, respectively. The parameters “ε” and “ψ” represent distances smaller than “u” and u+w, respectively. These two parameters are individually used to express the applied row spacing values in different spacing modes explained below.

According to the definition of row spacing operation in the automated system, the purpose of executing serial loading cycles is to fill an empty cultivation layer with the

gullies such that any required spacing between the loaded gullies can be created. Since based on the system design the horizontal distance “u” (Figure 4-25) is fixed, it is used as a comparative reference for classifying different row spacing values created by the system. Accordingly, three spacing modes including those in which the target row spacing value is equal to, or larger and smaller than the fixed distance “u” were distinguished. The diagram in Figure 4-26 shows the execution order of the loading cycles required for filling an empty cultivation layer with gullies in each of these three spacing modes. As can be seen, the parameters “ψ” and “ε” indicated in Table 4-4 have been used to express the target row spacing values in spacing modes 2 and 3, respectively. Each box in the diagram represents a loading cycle and the number indicated in each box is the number of steps in that loading cycle. A red dashed line in Figure 4-26 indicates that a gully kept by the gully carriers is ready to be loaded into the layer (Figure 4-25), and a blue solid line represent the moment in which the transferring of a gully into the layer is completed.

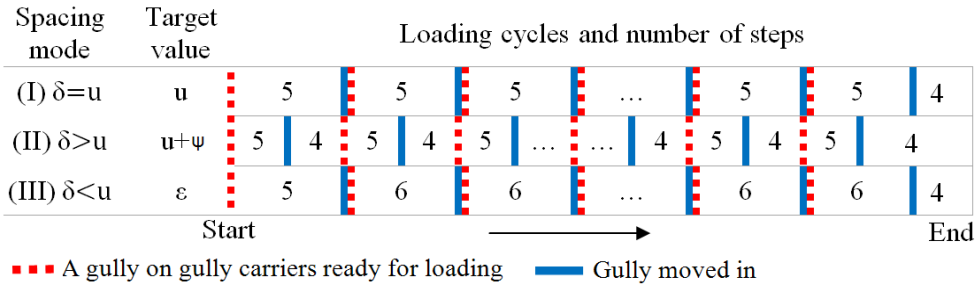

Figure 4-26. Diagram of serial loading cycles for filling an empty cultivation layer with gullies in different spacing modes

The procedure and result of transferring a gully from the gully carriers into the layer is the same in both 5-step and 6-step loading cycles. However, the purpose of using one additional step in the 6-step cycle is to move the previously loaded gullies in the layer a few centimeters to the left (DC direction) for obtaining a smaller row spacing value in spacing mode 3. As can be observed in the diagram of Figure 4-26, no gully is available for loading when 4-step loading cycles are started. This implies that this type of loading cycle is not used for transferring the gullies into the layer.

The function of a 4-step loading cycle is to move the previously loaded gullies deeper into the cultivation layer which would cause greater row spacing values in spacing mode 2. In this way, "ψ" would be the displacement of loaded gullies inside the cultivation layer by a 4-step loading cycle. The final loading cycle in all three spacing modes is also a 4-step cycle which is employed to make a distance between the left wall of the last loaded gully and the front edge of the layer. Figure 4-27 displays a flowchart in which the steps employed for filling an empty cultivation layer with a certain number of gullies (N_i) has been presented for all spacing modes. In this flowchart, N_i is the maximum number of the gullies which can be maintained in the layer. $N_{LC.5}$ and $N_{LC.6}$ are number of 5 and 6-step loading cycles which have been executed during gully loading operation in a layer, respectively. The diagram shown in Figure 4-26 is a sample result of executing this flowchart.

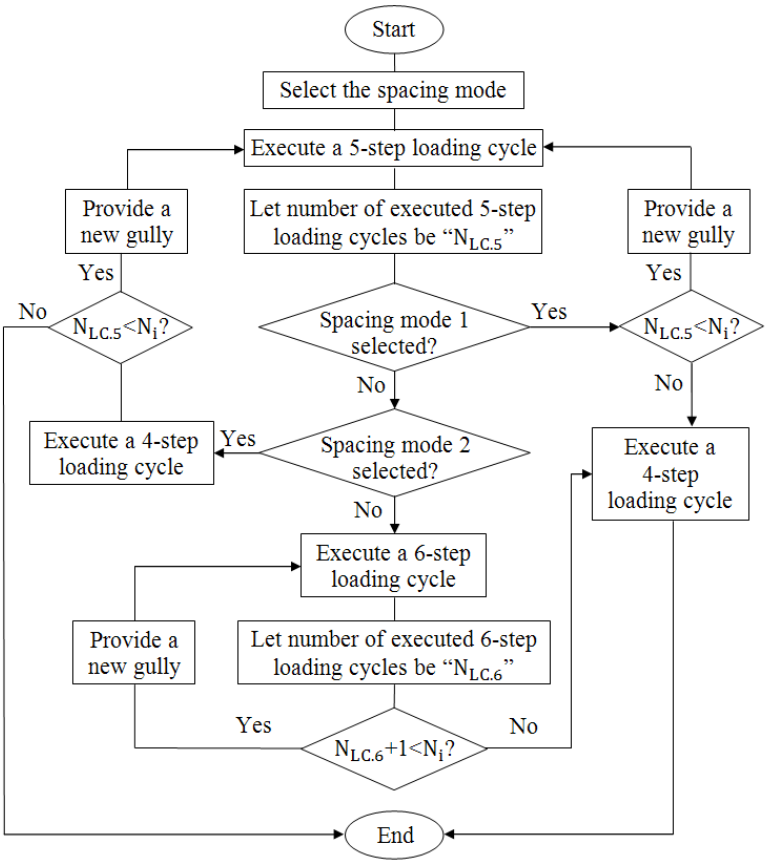

Figure 4-27. Flowchart indicating the steps of filling an empty cultivation layer with N_i gullies in different spacing modes

A similar definition to loading cycle can be presented for an unloading cycle, if a reverse gully transfer from the MGU layers onto the gully carriers is implemented. However, simulation of gully unloading operation and its motion analysis are not presented in this study.

4.2.3.3. CAE simulation and motion analysis

In order to observe the output of row spacing operation in different spacing modes, horizontal displacements of selected moving components such as lower and upper bars and the NFT gullies were monitored and investigated using the motion analysis. To this end, the CAD models of one cultivation layer equipped with two sets of gully loading-unloading mechanism, gully carries of chain elevator, a pair of twin manipulators for moving lower and upper bars and a number of gullies were all imported into Recurdyn simulation software. Motion analysis of the moving components was individually performed for each spacing mode by means of the virtual prototype shown in Figure 4-28.

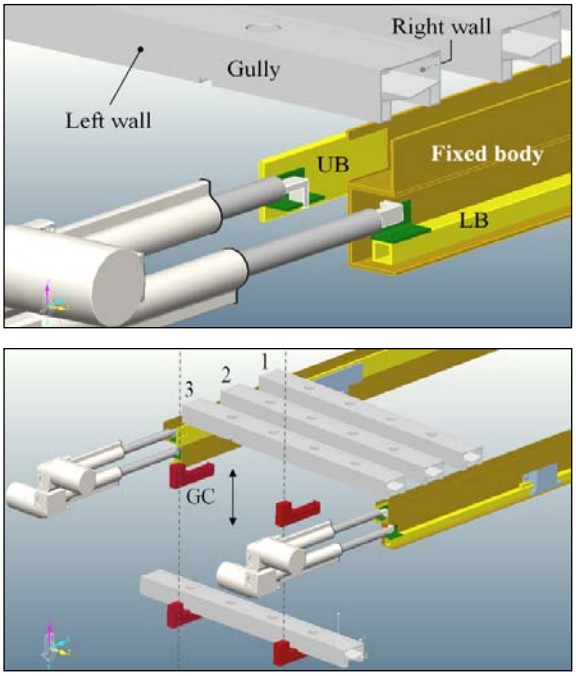

Figure 4-28. Simulation details of row spacing operation in automated system by virtual prototyping

Simulating the row spacing operation in different spacing modes is such that the first gully loaded into the empty layer is nominated as gully number 1. To depict the image of simulation condition at its starting moment, consider the status shown in Figure 4-25 when there is no gully in the cultivation layer. Table 4-5 shows the effective parameters used in simulations and the values selected for each parameter. One second delays are also applied between all serial working steps in all simulations. In order to trace the horizontal displacement of NFT gullies, position markers were added to the left and right walls of the gullies in CAE simulation environment. In case of lower and upper bars, markers were placed on the front edge of the bars, where the brackets are installed. Based on the values selected for "u" and "ε", the target row spacing values in modes 1, 2, and 3 are 50, 70, and 20 mm, respectively.

Table 4-5. Parameters and values used in simulation of row spacing operation

Parameter	Value in simulation
Horizontal distance between layer front edge and right wall of the gully kept by the GCs (u)	50 mm
Gully width (w)	80 mm
Maximum allowed back & forth stroke of the LBs (e)	50 mm
Displacement of a loaded gully inside the cultivation layer by 4-step loading cycle (ψ)	20 mm
Target row spacing value in spacing mode 3	20 mm
Travel speed of linear actuators moving LBs and UBs	10 mm/s
Time to provide a new gully by GCs for next loading	10 s
Time duration of GCs small downward motion (h mm)	2 s

4.2.4. Methods and control logics in the experiments of automated operation

In order to evaluate the working performance of automated gully convey-spacing system and examine the final automated schemes and control programs used to execute different operations in the system, several series of experiments including i) layer targeting, ii) manipulator locking, iii) controlled loading (row spacing operation) and unloading of gullies, iv) displacement of gullies from the conveying line into a cultivation layer and, v) displacement of gullies from a layer to another layer were conducted and carried out in the developed automated system. The employed control programs were developed by PLC ladder programming provided in XG5000 software. To verify and confirm the of the control programs in the experiments, the included signals in relevant automated operations were obtained and monitored using PLC trend monitoring toolkit available in XG5000. Major developed control programs (ladder diagrams) for executing the experiments of automated operation are individually presented in different sections of appendix C.

4.2.4.1. Layer targeting

Layer targeting is the first automated operation in the system which must be successfully accomplished to allow the linear actuators of manipulators to be connected to MGU lower and upper bars used for gully loading-unloading. By this operation, each of manipulators vertical lifts moves their respective manipulators from an unknown initial vertical position to the height of the desired cultivation layer and stops it in an exact vertical position determined for manipulators locking operation.

Based on the automated scheme defined for layer targeting, the only role of system operator is to select the target cultivation layer and start the operation by touching the corresponding buttons in the control screen designed for layer targeting in the HMI panel. The operator would also be able to observe and monitor different operational data such as speed, direction and position of the stepper motor, signal status of U-shaped photo sensors, controller error codes, etc., in the control screen. Layout of layer targeting operation from side view of the AV is shown Figure 4-29.

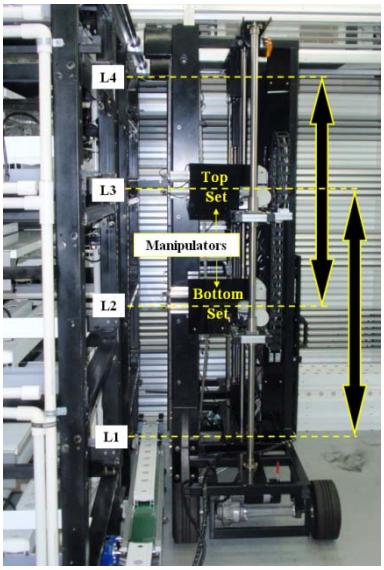

Figure 4-29. Layout of layer targeting in the autonomous vehicle

As can be seen in above figure, the vertical moving range of top set manipulators is between layers 2 and 4, while the manipulators of the bottom set are allowed to have a vertical movement between layers 1 and 3. Each attempt of layer targeting consists of a multistep motion scenario in which a combination of speed and position controls are used to move the stepper motors of the vertical lifts, while the output signals of four U-shaped photo sensors installed in the same working heights of MGU cultivation layers are used to determine the floating origin of these motion steps (see section 4.2.2.5).

According to Table 4-6 which indicates the principles adopted in making the control program of layer targeting, the direction of first vertical motion of bottom and top set manipulators would depend on the layer selected as the target, and the initial vertical position of manipulators which is indicated by the layers a set of manipulators locates between them at the starting point of the operation. During the first motion, the stepper motor of a vertical lift works under the speed control, by which the motor running speed is accurately controlled by the applied pulse rate.

Table 4-6. The principles used in control program of layer targeting

	Bottom set manipulators						Top set manipulators					
Target layer	1		2		3		2		3		4	
Initial vertical position[1]	1-2	2-3	1-2	2-3	1-2	2-3	2-3	3-4	2-3	3-4	2-3	3-4
Direction of first motion	▼	▼	▼	▼	▲	▲	▼	▼	▼	▼	▲	▲
U-photo sensors[2]	1	1,2	1,2	2	2,3	3	2	2,3	2,3	3	3,4	4
Ignored sensor	-	2	-	-	2	-	-	3	-	-	3	-

[1] Represented by the layers a set of manipulators locates between them

[2] Indicated by corresponding layer of each sensor

Based on the system design, maximum two U-shaped photo sensors can meet a common frame of manipulators along its vertical path during the first motion. If the first meeting sensor is the one corresponding to the target layer, the sensor output signal would be used for making the floating origin of a new motion step under position control which is used to reach the final target (locking position), located a few millimeters above the installing position of the sensors. Therefore, the direction of this terminator step is always upward. In cases that the first meeting sensor is not the one corresponding to the target layer, but the sensor located beneath that in a lower height represents the target layer, the signal made by the first sensor is ignored and the vertical motion of manipulators would be continued under the speed control toward the second sensor whose signal is employed to initiate the final step of operation including the small upward motion to the locking position under the position control. Finally, if the first meeting sensor does not represent the target layer and the sensor located above that in a higher height is the one relevant to the target layer, the stepper motor would be stopped for an extra short instant by the sensor signal which also makes the floating origin of a new upward motion under the speed

control. This upward motion, immediately started after the motor stop, is continued until the common frame of manipulators is detected by the sensor installed in the target layer. In this point, a change in method of motion control (from speed to position control) occurs by VTP (velocity to position) instruction used in the PLC program. Similar to previous cases described above, the small final motion made under the position control after this change, leads the manipulators to locking position.

Bottom set manipulators were used for layer targeting experiments. The initial vertical position of manipulators in the first type experiment was a height between layers 2 and 3, while this point was changed to a height between layers 1 and 2 in the second type experiment. In both types, layer 2 was selected as the target layer and each experiment type was repeated five times. To check the functionality of the control program during the experiments, the output signals of U-shaped photo sensors installed in layers 1 and 2, bit type signals indicating the travel direction of the stepper motor and the double word type analog signal showing the current position of the stepper motor, in terms of pulses, were obtained by PLC trend monitoring.

4.2.4.2 Manipulator locking

Connecting the linear actuators of a manipulator to MGU load/unloading mechanism for transmitting the required power to relevant lower and upper bars is the last operational stage prior to the automated gully handling operations. Automated manipulator locking is the operation used to establish this connection that is executed after the layer targeting. During this operation the hook-like connectors of twin manipulator's linear actuators (Figure 4-6) and the brackets of lower and upper bars (Figure 4-3) are engaged into each other. An error-free and easy locking operation can be expected only if the manipulators belonging to a certain set have been accurately stopped in the determined locking positions by the preceding layer targeting operation. Any vertical deviation from the right locking position resulted from an inaccurate layer targeting would cause physical damages serious due to the clashes between MGU parts and linear actuators during the locking operation.

The automated scheme defined for manipulator locking has two stages. The first stage includes extending the rods of the linear actuators of a twin manipulator and stopping them in appropriate horizontal positions for the final locking. The horizontal position of the rods after the actuators are stopped must be such that the hook-like connectors attached to the rod tips can pass through the openings made on the brackets of lower and upper bars without any collision, if the actuators move downward. The signal which stops a linear actuator in such a position is generated when the tiny hall sensor installed on the hook-like connector of the actuator (Figure 4-17(f)) reaches near the small magnets stuck to the interior surface of the space from which the actuator connector moves into the MGU. The second stage in manipulator locking operation is the small downward motion of manipulator (linear actuators) implemented by the respective vertical lift. This downward motion is provided through a single step speed-controlled motion and is terminated when the common frame of manipulators is detected by the first U-shaped photo sensor closely beneath the starting point of the motion. Figures 4-30 (a) and (b) demonstrate the relative position of a hook-like connector and the bracket of an upper bar before and after the downward locker motion. Figure 4-30 (c) also shows the connector of a linear actuator and the bracket of a lower bar when they are successfully interlocked.

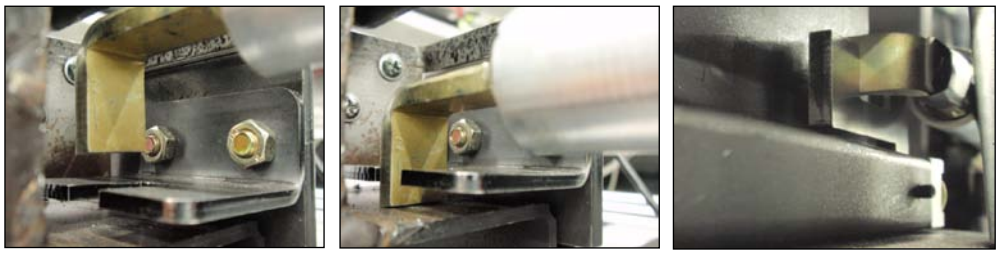

(a) (b) (c)

Figure 4-30. Views from locking the connectors of linear actuators into the brackets of lower and upper bars

The experiment for manipulator locking contained testing the timeliness of hall sensors responses and the adequacy of their performance for a sound and flawless locking. Since the locking of left and right manipulators mounted on a common frame

is simultaneously executed, four linear actuators in top set manipulators were selected for the experiment and the automated scheme defined for manipulator locking was examined during ten replications. To monitor the operation through the control program, output signals of the four hall sensors installed on the actuators as well as the forward motion operating signals of all four actuators were acquired through PLC trend monitoring.

4.2.4.3. Loading-unloading of gullies and row spacing operation

Automated loading and unloading of gullies are the most significant gully handling operations in the system. As the names reveal, by means of gully loading operation a certain number of gullies, coming from another layer or the horizontal gully conveying line, are regularly loaded into a cultivation layer in a controlled manner. Unloading the gullies does the contrast action of gully loading by which the gullies arranged inside a layer are moved out from there for being displaced to another cultivation layer or to the gully conveying line directed to the harvesting unit. Linear actuators, all sets of load/unloading mechanism and the gully carriers of the chain elevator, are the parts participating in these operations. The method used to measure and control the travel distance of MGU lower and upper bars are the key points to be noticed in the automated schemes and control programs of gully loading and unloading operations. Here, it is reminded that the row spacing operation, as a result of which a certain distance between the gullies in a layer is created, is the consequence of controlled gully loading operation. Details of the working steps of loading (row spacing) and unloading operations are explained in section 4.2.3.

Three series of experiments were conducted to evaluate the ability of the system in executing automated row spacing operation for different row spacing values and observe the obtained precision. Each experiment was repeated for three times and six gullies were used in each experiment. Similar experiments were also carried out to examine the performance of automated unloading operation in different conditions. Top set manipulators were used to execute all experiments which were implemented in layer 3 of one of the growing units. In order to measure the travel distances of the two upper bars of layer 3 by laser distance sensors fixed on the front wall of manipulators (Figure 4-17 (g)), two sensing targets one of which is shown in Figure

4-31 (a), were attached to the inner free side of the upper bars. Based on the system design, the maximum allowed distance between a laser sensor and the sensing target is about 230 mm that is the same situation shown in Figure 4-31 (b). Since the moving direction of the upper bars from this situation is always toward the sensors (Figure 4-31 (c)), the lowest possible distance between a sensing target and the sensor during the experiments can be 100 mm which is the minimum measurable distance by the employed laser sensor. Based on this, the approximate working stroke of the upper bars during the experiments that is provided by upper linear actuators of top set manipulators would be 130 mm. Figure 4-31 (d) demonstrates the sensor panel when the sensing target attached to an upper bar is in minimum and maximum distances determined for the experiments.

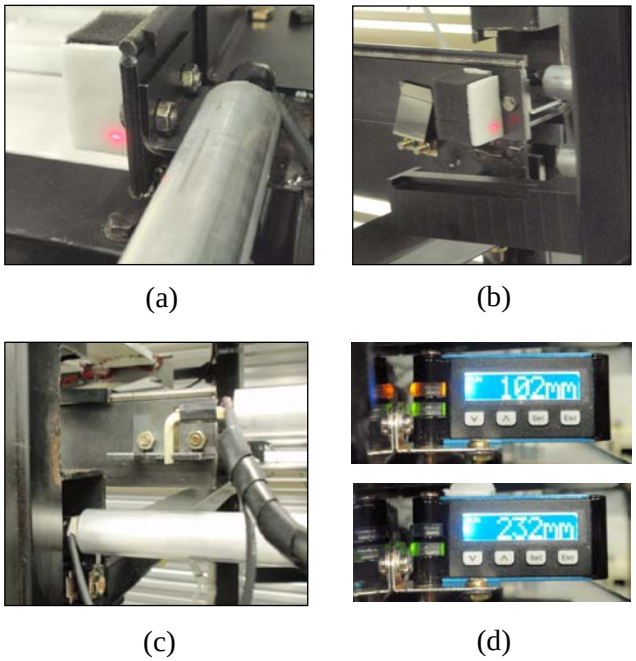

(a) (b)

(c) (d)

Figure 4-31. (a) Sensing target attached to the inner side of the upper bar, (b) situation of the sensing target at its maximum distance from the sensor, (c) traveling of the upper bar toward the vehicle, and (d) minimum and maximum measured distances during one travel of the upper bar indicated on the sensor panel

4.2.4.4. Displacement of gullies from horizontal conveying line into a layer

The experiment plan of this compound automated operation is to transfer five gullies from the horizontal gully conveying line to the height of layer 3 and load them into this layer such that the user-desired row spacing value is applied between them. The only task of operator in the experiment is to put the gullies on the starting conveyor belt one by one in certain time intervals. Horizontal conveying of gullies from the starting point to pick-drop zone, their vertical conveying to layer 3 and controlled loading of the gullies into layer 3 with desired row spacing are automatically executed based on the control program. Chain elevator, top set manipulators, load/unloading mechanism sets of layer 3 and gully conveyors are the included working parts in this experiment. Bottom IR sensor in the chain elevator, proximity sensor, the LED photo sensor installed between layer 2 and 3 and the sensors used for loading operation in layer 3 are the required items for executing the automated scheme of the experiment. Figure 4-32 illustrates a schematic layout of the experiment from the side view.

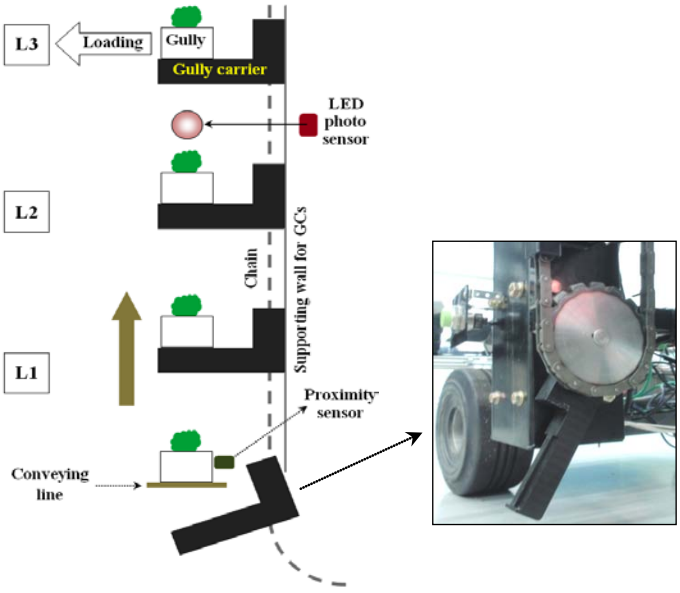

Figure 4-32. Schematic layout of the experiment conducted for automated transfer of gullies from the horizontal conveying line into layer 3

By touching the start button in the HMI panel, the stepper motor of the chain elevator starts running under speed control such that the gully carriers move upward. As previously stated in section 4.2.2.3 and also shown in Figure 4-17 (d), one of the gully carriers has been marked with a white spot for being detected by the IR sensors of the chain elevator. The chain elevator stops when the marked carrier is detected by the bottom IR sensor. The generated signal of the IR sensor is also used as the floating origin of the next motion step of the chain elevator. Immediately after the chain elevator is stopped, the belt conveyors start working. In this moment the first gully should be placed on the conveyors. The gully is conveyed toward the pick-drop zone where its further progress is prevented by a soft obstacle. When the presence of the first gully in the pick-drop zone is detected by the proximity sensor located at the end of conveying line (Figures 4-33 (a) and (b)), the chain elevator starts moving upward under the position control (second motion of the stepper motor), as a result of which the first gully is lifted from the conveying line and moved upward by the first coming gully carriers. The chain elevator stops again after the position determined for the second motion is achieved. In this time the belt conveyors start working again and a cycle similar to that implemented for the first gully is repeated for the second gully. The upward motion of the chain elevator for picking the third gully from the conveying line is governed under the speed control which is converted into a position control when the first gully is detected during its upward motion by the LED photo sensor installed in a height between layers 2 and 3 (Figures 4-33 (c) and 4-17 (a)). The recent released signal determines the floating origin of the next motion step running under a position control. The latter motion accurately stops the first gully in a height appropriate for loading it into the layer 3. The belt conveyors start working again after the first gully is stopped in loading position. Loading of the first gully is started after the fourth gully is present in the pick-drop zone. This cyclic trend is continued until all five gullies used for the experiment enter layer 3.

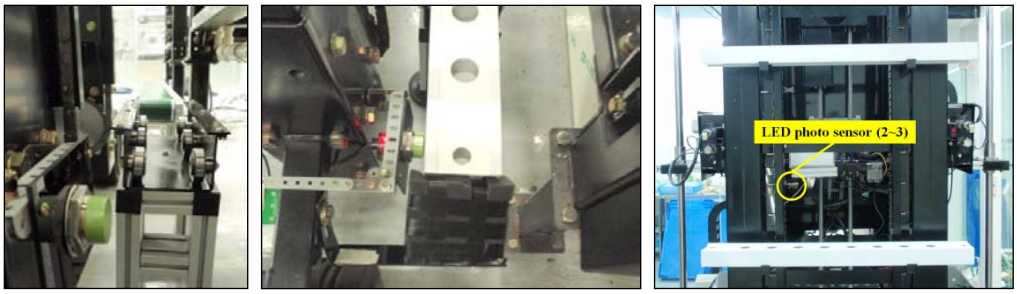

(a) (b) (c)

Figure 4-33. (a) Position of proximity sensor at the end of horizontal conveying line, (b) detection of gully in pick-drop zone by the proximity sensor, and (c) position of LED photo sensor in a front view of the AV

4.2.4.5. Layer to layer displacement of gullies

Application of automated layer to layer displacement of gullies is merely limited to multistage dynamic cultivation. The automated scheme specified for layer to layer gully displacement compound operation comprises unloading a certain number of gullies from a layer and redistribute them into a new empty layer through controlled gully loading operation such that the row spacing between the gullies in the new layer is larger than what it was in the initial layer. The working units participating in the experiment automated gully transfer from layer 3 to layer 2 are the chain elevator, top and bottom set manipulators and, load/unloading mechanism sets embedded in layers 2 and 3. Signals generated by the IR sensor located at the top of the chain elevator, the LED photo sensor installed between layer 2 and 3 as well as the sensors employed in loading and unloading of gullies are employed in different parts of the control program executing the automated scheme. In order to figure out the layout of displacing the gullies from layer 3 to layer 2, consider the upper half part of the layout shown in Figure 4-32 when the main travel direction of the chain elevator is downward and, loading and unloading of gullies occur in layers 3 and 2, respectively. Application of top IR sensor and LED photo sensor are the same as it was in the experiment described in the last section. A combination of the motion steps running under speed and position controls are used for stepper motor control of chain elevator.

4.2.4.6. Device allocation in control programs and signal trend monitoring graphs

In PLC programming with ladder diagrams, a series of elements such as normally open and close contacts and different types of the coils as well as a wide range of instructions (functions) such as timers, counters, logic operations, data transfer are used to configure a program. To import the output signals of system sensors into the control programs and exploit their effects in the determined moments, a special “code name” including a letter (data area) followed by a number (in hexadecimal) must be allocated to the signals of each sensor. Using these code names, the status (bit type, digital), or the value (word type, analog) of the signals generated by different sensors can be recognized by the program. In LS XG5000 PLC programming software, each of these code names are called a “device”. In addition to sensors, allocating a permissible device name to the control and monitoring signals related to different motors and linear actuators of the system is necessary. Since each device represents a specific input or output signal during an automated operation, interpreting the details of an operation and examining the executive performance of its program would be possible if respective trend monitoring graphs involving the activities of considered devices are provided. Table 4-7 presents the full list of the devices included in the trend monitoring graphs obtained for different experiments of this study.

Table 4-7. Characteristics of the devices indicated in PLC trend monitoring graphs during different experiments

Device	Type	I/O	Experiment	Related hardware- position	Interpretation of signal
P0000C	Bit	Input	Manipulator locking	Hall sensor- TUL linear actuator	ON: LA forward motion is stopped
P0000D	Bit	Input	Manipulator locking	Hall sensor- TDL linear actuator	ON: LA forward motion is stopped
P0000E	Bit	Input	Manipulator locking	Hall sensor- TUR linear actuator	ON: LA forward motion is stopped
P0000F	Bit	Input	Manipulator locking	Hall sensor- TDR linear actuator	ON: LA forward motion is stopped
P00028	Bit	Output	Manipulator locking	TUL linear actuator	ON: LA is moving forward
P00029	Bit	Output	Manipulator locking	TDL linear actuator	ON: LA is moving forward
P0002D	Bit	Output	Manipulator locking	TUR linear actuator	ON: LA is moving forward
P0002E	Bit	Output	Manipulator locking	TDR linear actuator	ON: LA is moving forward
P00000	Bit	Input	Layer targeting	U-photo sensor- Beside the moving path of bottom set manipulators vertical lift	ON: Bottom set manipulators are in the working height of layer 1
P00001	Bit	Input	Layer targeting	U-photo sensor- Beside the moving path of bottom set manipulators vertical lift	ON: Bottom set manipulators are in the working height of layer 2
P0420A	Bit	Output	Layer targeting	Stepper motor- vertical lift of bottom set manipulators	ON: Common frame of bottom set manipulators is moving upward
P0420B	Bit	Output	Layer targeting	Stepper motor- vertical lift of bottom set manipulators	ON: Common frame of bottom set manipulators is moving downward

Continue on the next page

Continue of Table 4-7

Device	Type	I/O	Experiment	Related hardware- position	Interpretation of signal
K0422	Double word	Output	Layer targeting	Stepper motor- vertical lift of bottom set manipulators	Shows current position of the stepper motor in terms of number of applied pulses
P00015	Bit	Input	Conveyors to layer 3	Proximity sensor- end of gully conveying line on vehicle body	ON: A gully has been detected in the pick-drop zone
P0001A	Bit	Input	Conveyors to layer 3- Layer 3 to layer 2	LED photo sensor- front side of vehicle	ON: A gully moving by chain elevator between layers 2-3 is detected
P0001E	Bit	Input	Conveyors to layer 3	Bottom IR sensor-chain elevator, right loop, bottom of the rear part	ON: Marked gully carrier is detected
P00049	Bit	Output	Conveyors to layer 3	AC motor- Belt conveyors	ON: Belt conveyors are working
M00100	Bit	Output	Conveyors to layer 3- Layer 3 to layer 2	Top set manipulators (linear actuators)	ON: Gully loading in operation
P0450A	Bit	Output	Conveyors to layer 3- layer 3 to layer 2	Stepper motor- chain elevator	ON: Gully carriers are moving upward
P0450B	Bit	Output	Conveyors to layer 3- layer 3 to layer 2	Stepper motor- chain elevator	ON: Gully carriers are moving downward
M01900	Bit	Output	Loading/ unloading	TUL and TUR linear actuators	ON: Linear actuators in operation
M01901	Bit	Output	Loading/ unloading	TDL and TDR linear actuators	ON: Linear actuators in operation

Continue on the next page

Continue of Table 4-7

Device	Type	I/O	Experiment	Related hardware- position	Interpretation of signal
D00030.0	Bit	Output	Loading/ unloading	Stepper motor- chain elevator	ON: Gully carriers are moving during gully loading and unloading
U02.02	Word	Input	Loading/ unloading	Laser distance sensor-Top left manipulator	Indicates horizontal position of left upper bars in layer 3
U02.05	Word	Input	Loading/ unloading	Laser distance sensor-Top right manipulator	Indicates horizontal position of right upper bars in layer 3
P0001F	Bit	Input	Layer 3 to layer 2	Top IR sensor- chain elevator, right loop, top of the rear part	ON: Marked gully carrier is detected
D00031.0	Bit	Output	Layer 3 to layer 2	Stepper motor- chain elevator	ON: Stepper motor in “position control”
D00031.1	Bit	Output	Layer 3 to layer 2	Stepper motor- chain elevator	ON: Stepper motor in “speed control”
M00000	Bit	Output	Layer 3 to layer 2	TUL and TUR linear actuators	ON: Linear actuators in operation
M00020	Bit	Output	Layer 3 to layer 2	BUL and BUR linear actuators	ON: Linear actuators in operation

The code diagram shown in Figure 4-34 helps to clarify the meaning of some abbreviated terms shown in Table 4-7. Considering a back view to the autonomous vehicle (as in Figure 4-18, left), the code diagram presented in this Figure distinguishes the eight linear actuators arranged on different manipulators of the autonomous vehicle based on their relative positions.

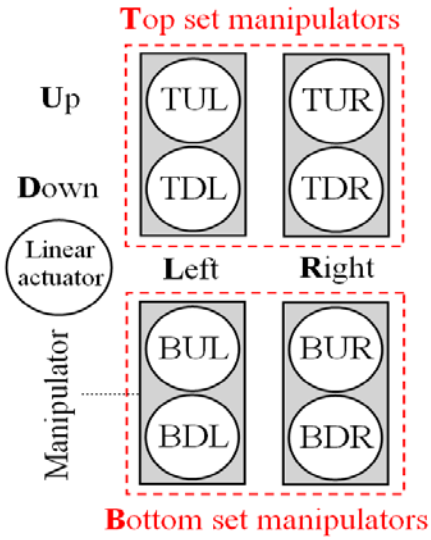

Figure 4-34. Code diagram of the linear actuators installed on top and bottom set manipulators (Back view to the vehicle)

4.2.5. Analysis of integrated operation of the automated system

The extreme goal of developing the automated system of this study is to employ it for full scale automated gully handling operation in a continuous plant production process based on the information presented by the respective cultivation schema. To achieve this, proper collaboration and integrated operation of all sub-systems, working units and the automation schemes, tested through individual experiments, would be necessary. In this way, determining the best order of executing the individual components of system automated operation which results in shortest total operation time for completing a certain cultivation plan is a significant issue in management and implementation of integrated automated operation. In this section, executing the optimal multilayer cultivation plan of the Korean lettuce (Table 3-19) by means of automated gully convey-spacing system has been considered as a case study for investigating this issue. Analyzing the executive manner and operation time of the individual working components involved in integrated automated operation required for executing the cultivation plan of the case study and thus, estimating the performance of the automated system according to operation time are discussed through this case study.

Referring to Table 3-19, the cultivation plan selected for this case study is a 2-stage dynamic cultivation implemented in total eight cultivation layers. However, as also stated in section 4.2.1, due to limited height inside the plant factory room, the 8-layer cultivation plan must be implemented in a couple of 4-layer growing units. According to 3-5 clustering determined for the case study cultivation plan, three and five cultivation layers are assigned to maintain the gullies of a growing crop batch in growth stages 1 and 2, respectively. Furthermore, because the under-utilization of the growing area in cluster 1 of the pure dynamic plan has been optimized, one of the three layers in this cluster is a hybrid static-dynamic layer. It is reminded that the growth period of Korean lettuce in the plant factory is 28 days. The information acquired from the related cultivation schema shows that, i) this period can be divided into two growth stages with equal number of 14 days without any problem, and ii) the number of gullies per crop batch (N_{CB}) is 70 gullies, in which 280 Korean lettuce heads are contained. Thus, based on the explanations in the previous chapter, 280

lettuce heads are produced every 14 days by the dynamic plan, while 20 extra heads are also supplied by the static plan supported by the hybrid layer every 28 days.

4.2.5.1. Crop circulation and order of automated operations in different working days

Numerical distribution of gullies in different layers, the row spacing which should be applied between the gullies in each layer, and the time schedule of displacing the crop batch gullies are the data given by the cultivation schema and used for implementing the automated operation of the system. According to the displacement schedule of the crop batches in the case study, the working days of the automated system would be repeated every 14 days and thus, the system would not operate in the other days. Figure 4-35 illustrates the diagram of crop batch circulation in the experimental plant factory. The digits in parentheses are the number of gullies which are loaded into or unloaded from a layer.

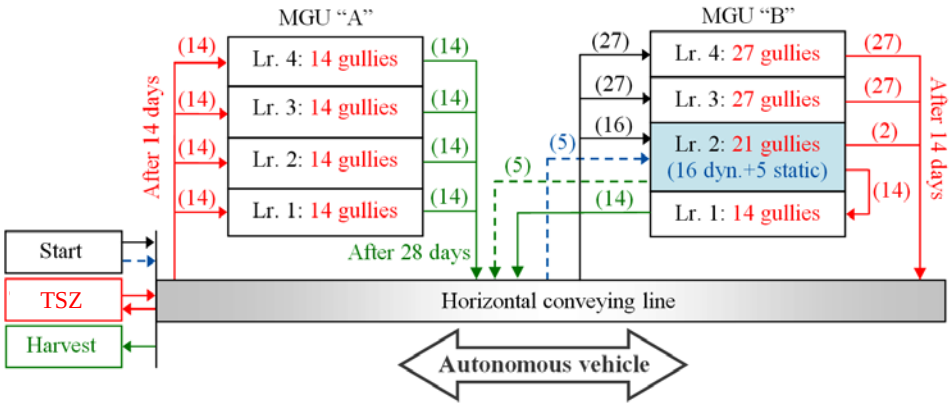

Figure 4-35. Diagram of crop batch circulation in the plant factory with two 4-layer growing units based on the cultivation plan of the case study

In this diagram, layers 2, 3 and 4 of the growing unit B form the cluster 1 which is assigned to maintain the gullies in growth stage 1. Layer 1 in unit B as well as all layers of unit A are considered as cluster 2 and used for growing the plants during the

second grow stage. Layer 2 in unit B is a hybrid static-dynamic layer divided into two sections. 16 (out of 70) gullies belonging to the crop batch of the dynamic cultivation are held in this layer, while 5 other gullies are also grown under static cultivation in this layer. The retention time of the latter gullies in the hybrid layer is 28 days.

In the first day of the cultivation process, all 70 gullies of a crop batch (dynamic plan), and the 5 gullies of the static plan (maintained in the hybrid layer) are one by one conveyed from the "start" point to the growing unit B using the horizontal conveying line of the system. Using the chain elevator and twin manipulators, the autonomous vehicle standing in the front of unit B moves and loads the gullies to layers 2B, 3B, and 4B (displacement of gullies from horizontal conveying line to a layer). This is the end of the first working day of the automated system.

The second working day of the system would be two weeks later in day 14. In this day, entire 70 gullies stored in layers 2B, 3B, and 4B that are growing under the dynamic plan (crop batch 1) must be displaced to layers 1B, 1A, 2A, 3A, 4A, and arranged there under a wider row spacing. To this end, 14 gullies of this crop batch are unloaded from layer 2B and reloaded into layer 1B (displacement of gullies between layers). The remaining 56 gullies are unloaded, moved downward to the horizontal conveying line, and finally, transferred to a temporary storage zone (TSZ) within the plant factory area. The reason for keeping these gullies in the TSZ is due to unavailability of the autonomous vehicle in unit A. Note that the 5 gullies in hybrid layer 2B that are grown under the static cultivation plan are not displaced in this day. Once layers 2B, 3B, and 4B are emptied from the gullies of crop batch 1, the 70 gullies of new crop batch 2 would be moved from the start point to these layers by the automated system. This is similar to the described process done in the first day. After this, the autonomous vehicle moves to growing unit A. The 56 gullies of crop batch 1 kept in TSZ are then moved and loaded into the four layers of unit A by the automated system which would be the end of system's second working day.

The third working day of the automated system during the continuous cultivation process would happen after spending another couple of weeks. This time spent for automated operation in this working day would be the longest because it includes i) unloading and moving 70 gullies of crop batch 1 from layers 1A, 2A, 3A, 4A, and 1B to the harvester, ii) unloading and moving 5 gullies grown under static plan from the hybrid layer 2B to the harvester, iii) displacing the 70 gullies of crop batch 2 from

layers 2B, 3B, and 4B to layer 1B and TSZ, and move them (56 gullies) again from TSZ to layers 1A, 2A, 3A, 4A, and finally, iv) moving 75 gullies including 70 gullies belonging to crop batch 3 of the dynamic plan, and 5 new gullies which would be grown under the static plan in the hybrid layer from the start point to layers 2B, 3B and 4B. Two times of moving the autonomous vehicle between units A and B would also be necessary in this working day. In this working day, the gully handling operation including controlled loading and unloading, as well as horizontal and vertical conveying are for a total of 220 gullies. The operations in next working days which are repeated every two weeks during the process are the same with the third working day. However, the number of gullies handled by automated operation in the working days with an even number, e.g., 4, 6, 8, etc. is 210 gullies because handling of the gullies grown by static cultivation is not involved in such working days. It is reminded that the working days 1, 2, and 3 of the automated gully convey-spacing system occur in the days 1, 14 and 28 of the continuous cultivation process. In order to summarize the above explanations, displacement routes of the first three cop batches as well as the movement of autonomous vehicle in working days 1, 2, and 3 of the automated system are shown in Table 4-8. The order of crop batch displacements and vehicle movements in each working day is also indicated in this table. The presented lists in Tables 4-9 to 4-11 are the best order of automated operations of the system in working day 1, 2 and 3 of the system, respectively. The resultant of employing these orders and combinations is the minimum amount of the operational movements and thus, the shortest total operation time for completing a given plan. As can be observed, both types of system automated operations including those directly dealing with gully handling, e.g., controlled loading and unloading of gullies, horizontal and vertical conveying of gullies, and also those related to supportive operation provided by the autonomous vehicle such as layer targeting, manipulators locking and unlocking and motion of autonomous vehicle between the growing units, are involved in these lists.

Table 4-8. Details of displacing the first three crop batches and movement of the autonomous vehicle for executing the optimal cultivation plan of Korean lettuce in two 4-layer growing units

Working day	Displacement of crop batch gullies (origin to destination)						Movement	
	Order	Crop batch 1	Order	Crop batch 2	Order	Crop batch 3	Order	Auto. vehicle
1	1	"Start" to 2B (dyn./st.)		-		-		-
	2	"Start" to 4B, 3B						
2	1	4B, 3B to "TSZ"	2	"Start" to 4B, 3B		-	5	Unit B to unit A
	3	2B (dyn.) to 1B and "TSZ"	4	"Start" to 2B (dyn.)				
	6	"TSZ" to 1A, 2A, 3A, 4A						
3	1	4A, 3A, 2A, 1A to harvest	4	2B (dyn.) to "TSZ" and 1B	6	"Start" to 2B (dyn./ st.)	2	Unit A to unit B
	3	1B to harvest	7	4B, 3B to "TSZ"	8	"Start" to 4B, 3B	9	Unit B to unit A
	5	2B (st.) to harvest	10	"TSZ" to 1A, 2A, 3A, 4A				

Table 4-9. Best order of automated operations of the system in working day 1

1. Fix the position of autonomous vehicle in front of unit B
2. Move and lock top set manipulators to layer 4B*
3. Move and lock bottom set manipulators to layer 2B*
4. Start point► Horizontal conveyors► Chain elevator► Layer 2B► Load 21 gullies (5 gullies: static plan+16 gullies: CB1, dynamic plan)
5. Unlock bottom set manipulators from layer 2B
6. Move and lock bottom set manipulators to layer 3B*
7. Start point► Horizontal conveyors ► Chain elevator► Layer 4B► Load 27 gullies (CB1)
8. Start point► Horizontal conveyors ► Chain elevator► Layer 3B► Load 27 gullies (CB1)

* Through layer targeting and manipulators locking

Table 4-10. Best order of automated operations of the system in working day 2

1. Unload 27 gullies (CB1) from layer 4B► Chain elevator ► Horizontal conveyors ► TSZ
2. Unload 27 gullies (CB1) from layer 3B► Chain elevator ► Horizontal conveyors ► TSZ
3. Start point► Horizontal conveyors ► Chain elevator► Layer 4B► Load 27 gullies (CB2)
4. Start point► Horizontal conveyors ► Chain elevator► Layer 3B► Load 27 gullies (CB2)
5. Unlock bottom set manipulators from layer 3B
6. Move and lock bottom set manipulators to layer 1B*
7. Unlock top set manipulators from layer 4B
8. Move and lock top set manipulators to layer 2B*
9. Unload 14 gullies (CB1) from layer 2B► Chain elevator ► Layer 1B► Load 14 gullies
10. Unload 2 gullies (CB1) from layer 2B► Chain elevator ► Horizontal conveyors ► TSZ
11. Start point► Horizontal conveyors ► Chain elevator► Layer 2B► Load 16 gullies (16 gullies: CB2, dynamic plan)
12. Unlock bottom set manipulators from layer 1B
13. Unlock top set manipulators from layer 2B
14. Move autonomous vehicle to unit A
15. Move and lock top set manipulators to layer 2A*

* Through layer targeting and manipulators locking

(Continue on the next page)

Continue of Table 4-10

16. Move and lock bottom set manipulators to layer 1A*
17. TSZ ► Horizontal conveyors ► Chain elevator► Layer 1A► Load 14 gullies (CB1)
18. TSZ ► Horizontal conveyors ► Chain elevator► Layer 2A► Load 14 gullies (CB1)
19. Unlock top set manipulators from layer 2A
20. Move and lock top set manipulators to layer 4A*
21. Unlock bottom set manipulators from layer 1A
22. Move and lock bottom set manipulators to layer 3A*
23. TSZ ► Horizontal conveyors ► Chain elevator► Layer 4A► Load 14 gullies (CB1)
24. TSZ ► Horizontal conveyors ► Chain elevator► Layer 3A► Load 14 gullies (CB1)

* Through layer targeting and manipulators locking

Table 4-11. Best order of automated operations of the system in working day 3

1. Unload 14 gullies (CB1) from layer 4A► Chain elevator ► Horizontal conveyors ► Harvest
2. Unload 14 gullies (CB1) from layer 3A► Chain elevator ► Horizontal conveyors ► Harvest
3. Unlock bottom set manipulators from layer 3A
4. Move and lock bottom set manipulators to layer 1A*
5. Unlock top set manipulators from layer 4A
6. Move and lock top set manipulators to layer 2A*
7. Unload 14 gullies (CB1) from layer 2A► Chain elevator ► Horizontal conveyors ► Harvest
8. Unload 14 gullies (CB1) from layer 1A► Chain elevator ► Horizontal conveyors ► Harvest
9. Unlock top set manipulators from layer 2A
10. Unlock bottom set manipulators from layer 1A
11. Move autonomous vehicle to unit B
12. Move and lock bottom set manipulators to layer 1B*
13. Unload 14 gullies (CB1) from layer 1B► Chain elevator ► Horizontal conveyors ► Harvest
14. Move and lock top set manipulators to layer 2B*
15. Unload 14 gullies (CB2) from layer 2B► Chain elevator ► Layer 1B► Load 14 gullies
16. Unload 2 gullies (CB2) from layer 2B► Chain elevator ► Horizontal conveyors ► TSZ

* Through layer targeting and manipulators locking

(Continue on the next page)

Continue of Table 4-11

17. Unload 5 gullies (Static plan) from layer 2B► Chain elevator ► Horizontal conveyors ► Harvest
18. Start point► Horizontal conveyors ► Chain elevator► Layer 2B► Load 21 gullies (5 gullies: static plan+16 gullies: CB2, dynamic plan)
19. Unlock top set manipulators from layer 2B
20. Move and lock top set manipulators to layer 4B*
21. Unlock bottom set manipulators from layer 1B
22. Move and lock bottom set manipulators to layer 3B*
23. Unload 27 gullies (CB2) from layer 4B► Chain elevator ► Horizontal conveyors ► TSZ
24. Unload 27 gullies (CB2) from layer 3B► Chain elevator ► Horizontal conveyors ► TSZ
25. Start point► Horizontal conveyors ► Chain elevator► Layer 4B► Load 27 gullies (CB3)
26. Start point► Horizontal conveyors ► Chain elevator► Layer 3B► Load 27 gullies (CB3)
27. Unlock bottom set manipulators from layer 3B
28. Unlock top set manipulators from layer 4B
29. Move autonomous vehicle to unit A
30. Move and lock top set manipulators to layer 4A*
31. Move and lock bottom set manipulators to layer 3A*

* Through layer targeting and manipulators locking

(Continue on the next page)

Continue of Table 4-11

28. Unlock top set manipulators from layer 4B
29. Move autonomous vehicle to unit A
30. Move and lock top set manipulators to layer 4A*
31. Move and lock bottom set manipulators to layer 3A*
32. TSZ ► Horizontal conveyors ► Chain elevator► Layer 4A► Load 14 gullies (CB2)
33. TSZ ► Horizontal conveyors ► Chain elevator► Layer 3A► Load 14 gullies (CB2)
34. Unlock bottom set manipulators from layer 3A
35. Move and lock bottom set manipulators to layer 1A*
36. Unlock top set manipulators from layer 4A
37. Move and lock top set manipulators to layer 2A*
38. TSZ ► Horizontal conveyors ► Chain elevator► Layer 2A► Load 14 gullies (CB2)
39. TSZ ► Horizontal conveyors ► Chain elevator► Layer 1A► Load 14 gullies (CB2)

* Through layer targeting and manipulators locking

4.2.5.2. Analysis of automated row spacing operation

As described in the previous sections of this chapter, adjustment of the distance between the adjacent gullies when they are serially being loaded into a cultivation layer is a task which is performed through automated row spacing operation. The detailed procedure used for creating different values of row spacing through executing a series of multi-step loading cycles by controlled motions of linear actuators and the chain elevator installed on the autonomous vehicle has been already described in section 4.2.3. Based on the data obtained from relevant cultivation schema of the case study, the row spacing values of about 29 and 133 mm are needed to be applied in growth stages 1 (layers 3B,4B) and 2 (layers 1A, 2A, 3A, 4A, 1B), respectively. The value of row spacing in the dynamic part of the hybrid static-dynamic layer (2B) would be almost the same with that of growth stage 1 (30 mm), while a 140 mm row spacing value should be adopted for the 5 gullies growing under the static plan. Figure 4-36 displays schematic illustrations of different cultivation layers of the growing units when the cultivation plan of the case study is executed.

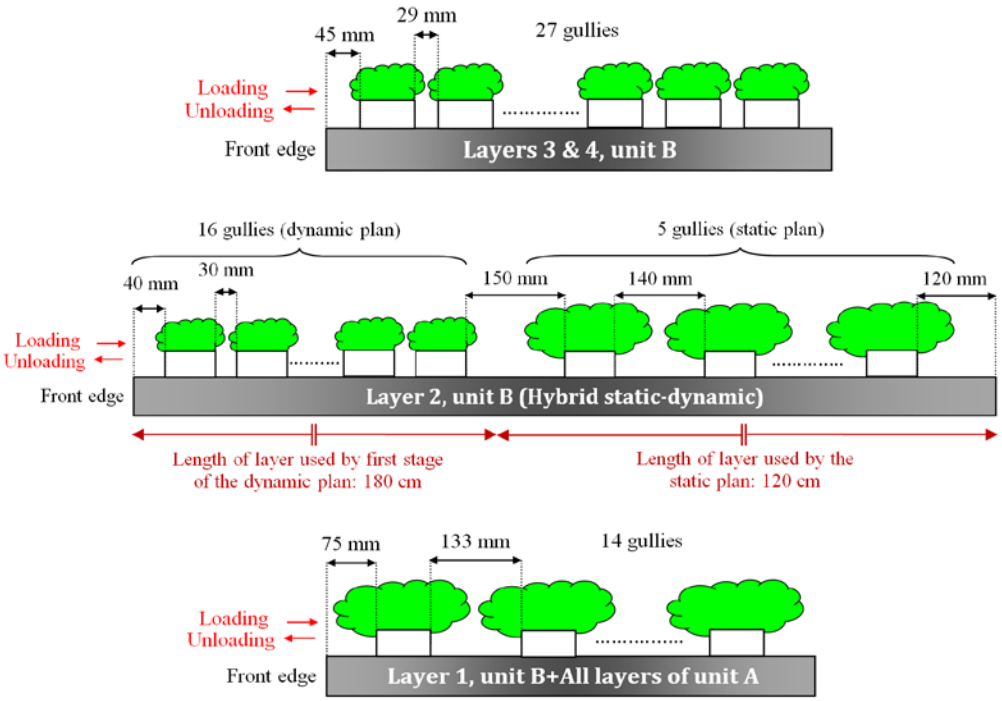

Figure 4-36. Detailed schematic illustrations of different layers of growing units A and B based on the cultivation plan of the case study

The status shown in different images of Figure 4-36 are based on the dimensions existing in the real system in which the length of cultivation layers and the width of gullies are 300 and 8 cm, respectively. Table 4-12 indicates the general characteristics used to execute the automated row spacing operation for optimal cultivation plan of the Korean lettuce in two 4-layer growing units which provides the conditions shown in Figure 4-36. As can be observed in this table, the working units involved in automated row spacing operation, (twin manipulators and chain elevator) must follow the automated scheme defined for spacing mode 3 with 6-step loading cycles in growth stage 1. This is because the target row spacing value of 29 mm is smaller than the parameter u (50 mm). On the other hand, the row spacing mode 2 with a combination of sequential 4 and 5-step loading cycles must be adopted by the automated system for row spacing operation in growth stage 2 (layers 1A, 2A, 3A, 4A, and 1B) because 133 mm is larger than 50 mm. The role of parameters "ε" and "ψ" shown in Table 4-12 were previously explained in section 4.2.3.2 and Table 4-4.

The three diagrams shown in Figure 4-37 demonstrate the sequence, number, and characteristics of the loading cycles that are required for filling different cultivation layers with gullies and making the determined row spacing values in each of them. The physical outcome of these diagrams is the status shown in Figure 4-36. These diagrams are a complete form of the diagram shown in Figure 4-26 which have been developed and specialized based on the specific requirements of the cultivation plan adopted in the case study. The time durations (in seconds) indicated for executing of the loading cycles in Figure 4-37 are presented according to direct measurements of the time spent for executing real loading cycles in the experiments conducted for automated loading of gullies (section 4.2.4.3). The gully loading and unloading cycles are always used in combination with other sub-operations of the automated system such as vertical conveying of gullies operated by the chain elevator. The outputs of this cooperation are integrated automated operations such as displacement of gullies between the different layers, or between the layers and the horizontal gully conveying line which need more complicated control algorithms. As an example in the case study, Figure 4-38 displays the sensor-based control algorithm developed for displacement and controlled loading and spacing of 27 gullies from the "start point" in Figure 4-35 to layers 3 and 4 in growing unit B. A related experiment of this case with more limited conditions has been described in section 4.2.4.4.

Table 4-12. General characteristics for executing the automated row spacing operation based on the optimal cultivation plan of the Korean lettuce in two 4-layer growing units

Row spacing[1] (mm)		Number of gullies								Row spacing mode		Main loading cycles for loading and spacing adjustment of one gully				
		Layers of unit A				Layers of unit B						GS_1		GS_2		
GS_1	GS_2	1	2	3	4	1	2[2]	3	4	GS_1	GS_2	Type	ε (mm)	Type	Ψ (mm)	u (mm)
29	133	14	14	14	14	14	21 (5+16)[3]	27	27	3	2	6-step	29	5-step 4-step	- 83	50

[1] Row spacing values in the hybrid layer are 30 and 140 mm in static and dynamic parts, respectively

[2] Hybrid static-dynamic layer

[3] 5 and 16 gullies grown by static and dynamic plans, respectively

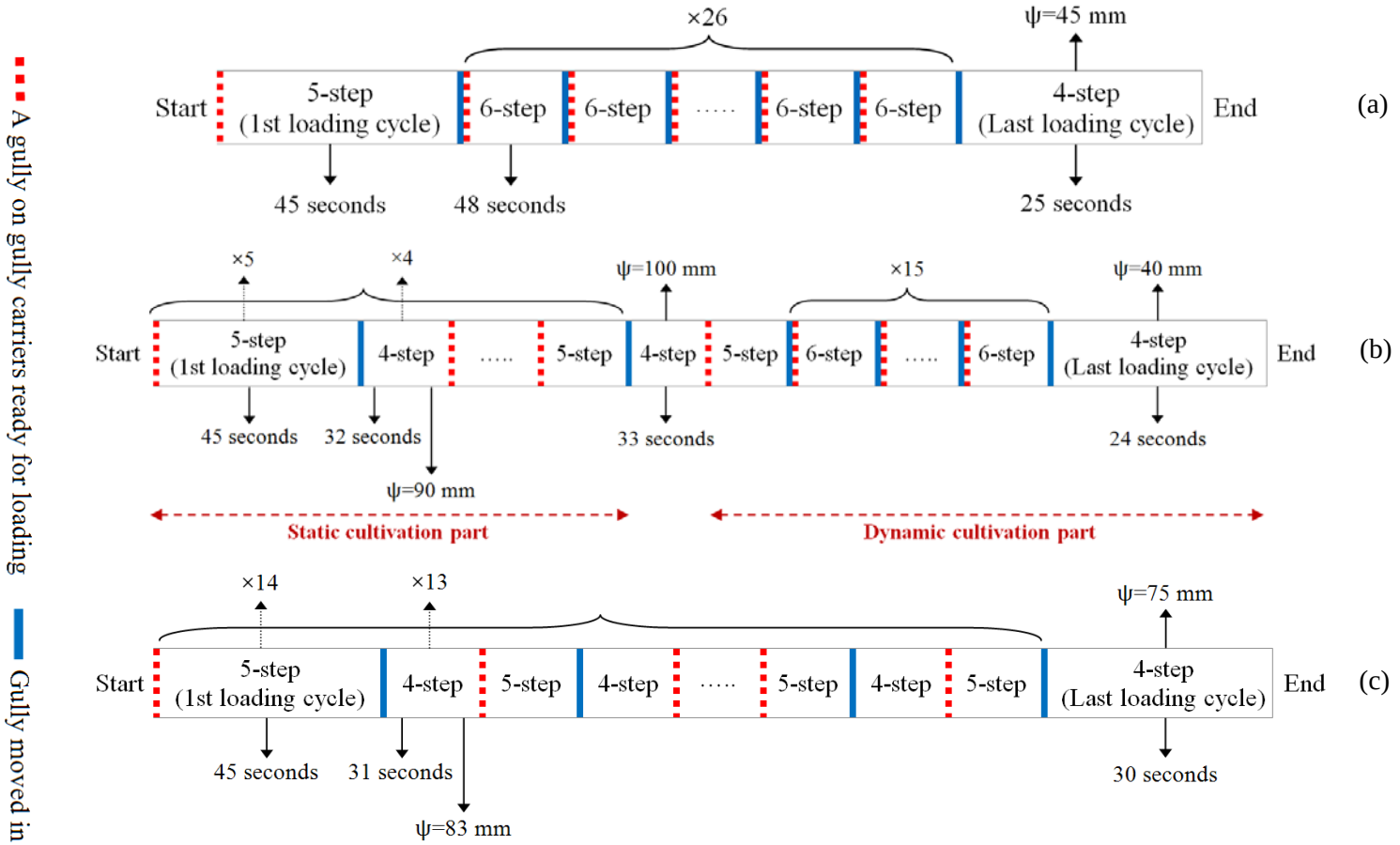

Figure 4-37. Sequence, number and characteristics of the loading cycles required for filling different cultivation layers and making the determined row spacing inside them, (a) 3B, 4B, (b) hybrid layer-2B, and (c) 1A, 2A, 3A, 4A, 1B

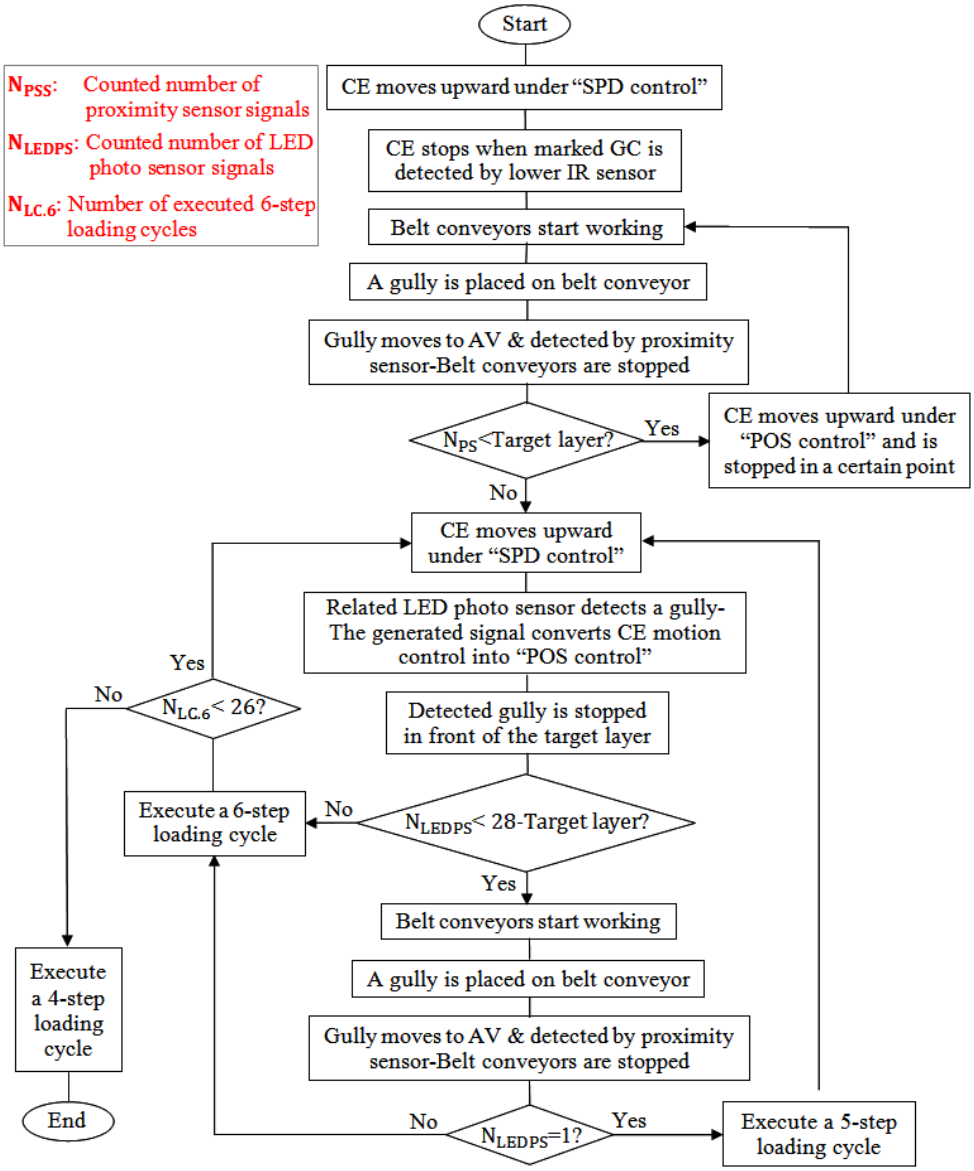

Figure 4-38. Sensor-based control algorithm for displacement and row spacing of 27 gullies from the start point to layers 3 and 4 in growing unit B

4.3. Results and discussion

4.3.1. Motion analysis of lower and upper bars during serial loading cycles in simulated row spacing operation

Resulted motion profiles related to horizontal displacement of lower and upper bars during the first two loading cycles executed to fill an empty layer are individually shown for different spacing modes in Figures 4-39 (a) to (c).

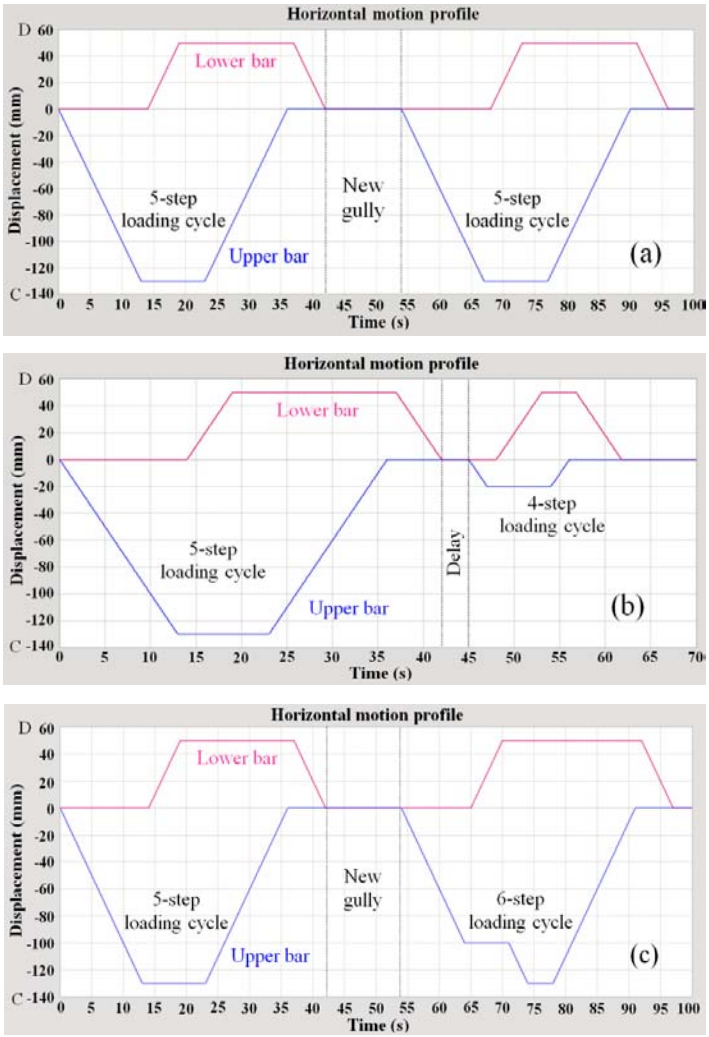

Figure 4-39. Motion profiles of horizontal displacement of lower and upper bars during first two loading cycles executed in an empty layer; (a) mode 1, (b) mode 2, and (c) mode 3

Vertical and horizontal axes in Figure 4-39 represent the horizontal displacement of the bars along the dual direction CD-DC (Figure 4-25) and the simulation time, respectively. Since the markers used to trace the horizontal position of the bars are placed on the front edge of each bar, the zero point on the vertical axis is the horizontal position of the longest vertical dashed line shown in Figure 4-25. Moving to the right and left of this line is indicated by positive and negative displacement values, respectively. Accordingly, because the lower bar is not allowed to move to the left of this line (see Figure 4-25), its motion profile is always standing within the positive range of the vertical axis, while opposite of this is true about the upper bar.

The vertical working motions such as those found in gully carriers can't be directly observed in the motion profiles of Figure 4-39, although the times spent for each of these motions (see Table 4-5) have been included in the graphs. For better understanding of the graphs shown in Figure 4-39, the time diagram of Figure 4-40, containing the details of simulation timing in all three modes has been presented. The singular time spent for each step of loading cycles as well as the time used to convey a new gully to the loading position after the end of cycle 1 are shown in the upper row assigned to the timing of each mode. The time values reported below the singular time values are the accumulated simulation time at the end of each working step. The units in the diagram are in seconds and each gray column represents a one second applied delay between every two working steps in the simulation which must be added to the accumulated time indicated in the previous step.

Mode & timing		Steps of loading cycle 1						New gully	Steps of loading cycle 2					
		1	1 (s) delay	2	3	4	5		1	2	3	4	5	6
Mode 1	Sing. time	13		5	2	13	5	10	13	5	2	13	5	-
	Acc. time	13		19	22	36	42	53	67	73	76	90	96	-
Mode 2	Sing. time	13		5	2	13	5	-*	2	5	2	5	-	-
	Acc. time	13		19	22	36	42	-	47	53	56	62	-	-
Mode 3	Sing. time	13		5	2	13	5	10	10	5	3	2	13	5
	Acc. time	13		19	22	36	42	53	64	70	74	78	91	97

*Consider an extra one second delay here.

Figure 4-40. Time diagram of simulation in different spacing modes in accordance with the motion profiles of Figure 4-39 (a) to (c)

The first loading cycle in all motion profiles is a 5-step cycle by which the gully 1 is received from the gully carriers, moved 130 mm to the right, and put on the fixed body of the layer. However, the second loading cycles shown in different motion profiles may contain 4, 5 or 6 steps based on the applied spacing mode. Conveying a new gully to the loading position by the gully carriers after the completion of first loading cycle followed by another similar 5-step cycle, builds the motion profile of mode 1 with a total duration of 96 seconds. Executing a 6-step loading cycle after providing a new gully is the procedure applied in mode 3. Based on this simulation, the total time required for executing two loading cycles in mode 3 is 97 seconds that is almost equal to the time spent for mode 1.

Using a partly different procedure for mode 2, no new gully would be conveyed by the gully carriers to the loading position after the first cycle is accomplished and instead, a 4-step loading cycle with 20 mm back and forth stroke in the upper bar is executed shortly after the end of the first cycle. Due to the lack of any gully for loading into the layer, the only function of this 4-step cycle is to move the previously loaded gully 20 mm to the right in the layer which causes a larger row spacing in this mode. The total simulation time of mode 2 is 62 seconds that is considerably shorter than those in modes 1 and 3. However, it is reminded that the output resulted from motion profiles of modes 1 and 3 in Figures 4-39 (a) and (c) is transferring two gullies into the layer, while by executing the loading cycles shown for mode 2 only one gully would be loaded into the layer. Based on the operational timing in the current simulations, the required time for loading two gullies with 70 mm row spacing between them would be 116 seconds which additionally contains the times needed for providing a new gully by the gully carriers and executing another 5-step loading cycle.

4.3.2. Motion analysis of gully displacement in different spacing modes of simulated row spacing operation

The motion profiles shown in Figure 4-41 (a) to (c) represent the horizontal displacement of NFT gullies in different spacing modes when three of them are loaded into an empty layer based on the loading cycles of Figures 4-39 (a) to (c). The indicated zero point on the vertical axis is the horizontal position of the shorter vertical dashed line shown in Figure 4-25, which is tangent to the left wall of the gully held on the gully carriers. The point to be mentioned here is that the first three steps in loading cycle 1, in which gully 1 has no horizontal motion have not been included in the motion profiles of Figure 4-41. Therefore, the zero time point located on the horizontal axis of these graphs implies the starting moment of step 4 in loading cycle 1 that is equivalent to second 23 in the motion profiles shown in Figure 4-39. The working situation in this point is such that gully 1 has been just placed on the upper bars for being moved into the cultivation layer and gullies 2 and 3 are on two separate pairs of gully carriers standing in different elevations of the chain elevator. It is reminded that the positioning markers used to generate different motion profiles of Figure 4-41 are located on left and right walls of these three gullies.

The first horizontal displacement of gully 1 in all three modes is a 130 mm movement to the right by the upper bars (step 4 in 5-step loading cycle 1). At the end of this motion, the horizontal positions of left wall of gully 1 and front edge of the cultivation layer would be the same. Execution of final step 5 causing the upper bars to move 10 mm downward results in settling of gully 1 on the fixed body of the cultivation layer. As illustrated in Figures 4-41 (a) to (c), condition of second horizontal displacement of gully 1 is different in each of the three spacing modes. In mode 1, the value and direction of the second displacement is exactly the same with the first displacement. The 41 seconds time interval between the end of first displacement and the start of second displacement is the total time spent for conveying gully 2 to the loading position by chain elevator, and executing the steps 1, 2 and 3 of loading cycle 2. During the second displacement in mode 1, both gullies 1 and 2 are simultaneously moved 130 mm to the right by the upper bars. As a result of this displacement, gully 2 occupies the previous position of gully 1 on the layer. The horizontal distance between left wall of gully 1 and the front edge of the layer would

also be increased from zero to 130 mm. Considering the gully width of 80 mm, the distance between the left wall of gully 1 and the right wall of newly loaded gully 2 would be 50 mm that is equal to the target row spacing value in mode 1.

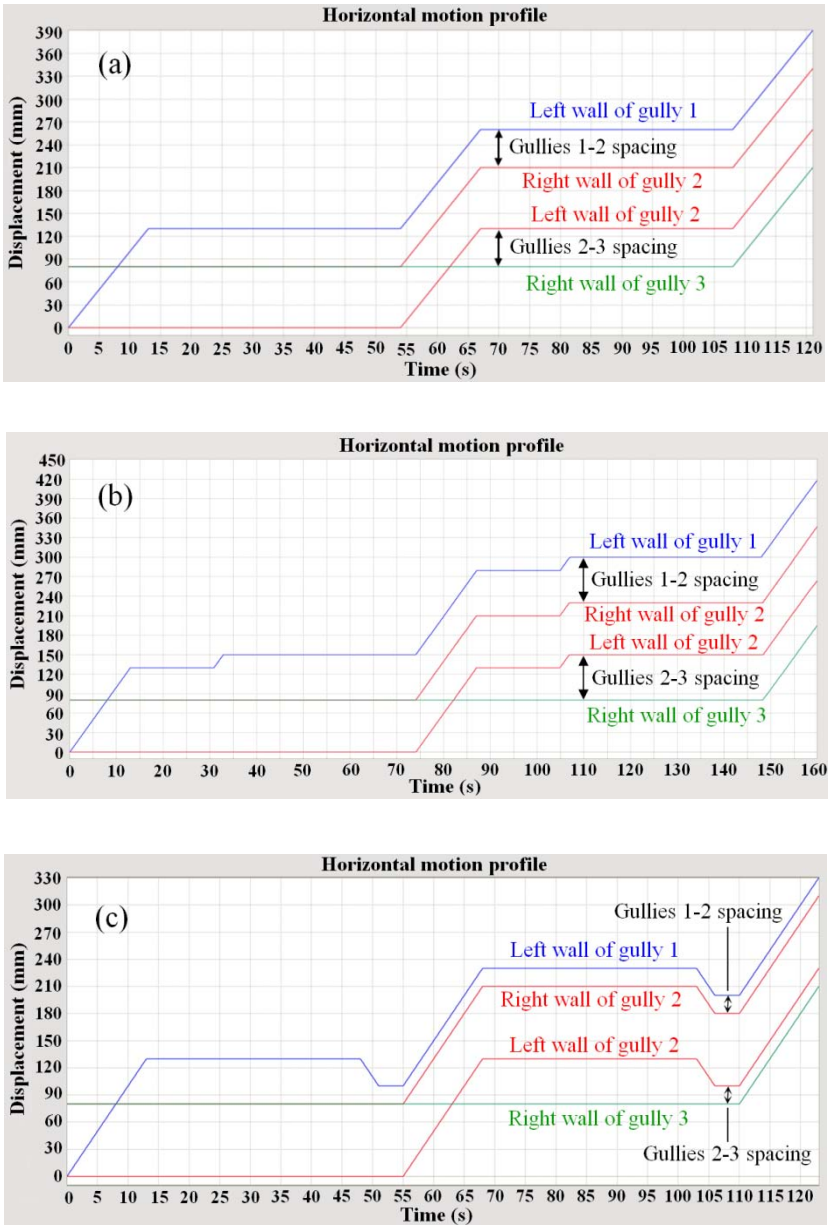

Figure 4-41. Motion profiles of horizontal displacement of three gullies when loading into an empty cultivation layer; (a) mode 1, (b) mode 2, and (c) mode 3

In mode 2, the second horizontal displacement of gully 1 is a 20 mm rightward movement. Since gully 2 is not conveyed to the loading position after the end of loading cycle 1, the time gap between the end of first displacement and the start of second displacement is reduced to 18 seconds. By the second displacement in mode 2, gully 1 is moved deeper into the cultivation layer such that the horizontal distance between the left wall of gully 1 and the front edge of the cultivation layer would be 20 mm after the second displacement is terminated. The third displacement in mode 2 is completed when vertical conveying of gully 2 to the loading position is followed by another 5-step loading cycle. During this displacement, both gullies 1 and 2 are moved 130 mm to the right. After this movement, the distance between the front edge of the cultivation layer and each of the two points “right wall of gully 2” and “left wall of gully 1”, would be 80 and 150 mm, respectively. The 70 mm difference between these two created distances is the target row spacing value in mode 2 which is successfully obtained in the simulation.

The second displacement of gully 1 in mode 3 is a negative 30 mm displacement, resulted from executing step 3 in the 6-step loading cycle. This means that gully 1 is partly pulled out from the interior space of the cultivation layer by leftward motion of the upper bars such that the left wall of this gully would be located 30 mm in the left of the layer edge, after the end of this negative displacement. As a result, a 20 mm horizontal distance remains between the left wall of gully 1 and the right wall of gully 2, which has been conveyed to the loading position by the gully carriers after the end of previous loading cycle. Establishment of 20 mm distance between these two gullies implies that the target value considered for row spacing in mode 3 has been attained in this simulation as well. The third displacement is the 130 mm rightward movement of gullies 1 and 2 into the layer that occurs when step 5 is executed.

As can be observed in the motion profiles of all modes, the resulted horizontal distance between the walls of gully 2 is always 80 mm that is equal to the selected gully width for the use in simulation. This equality also confirms the soundness of obtained simulation results.

4.3.3. Positioning of linear actuators

The data presented in Table 4-13 are the results obtained from three replications of the experiment described in section 4.2.2.6.1 which was conducted to examine the performance of positioning control of four linear actuators using their internal hall sensors. Reminding the concept of “run” in this experiment, i.e., one back and forth motion of a linear actuator, the indicated values in this table are the accumulated positioning errors of tested linear actuators used in the experiment after executing a certain number of runs.

Referring to the concept of positive and negative positioning errors in this experiment (Figure 4-22), the trend of positioning errors is negative in three linear actuators. The existence of negative errors in these actuators implies that the horizontal position of their attached sensing targets, when stopped at the end of a run, is gradually shifting backward as more runs are executed. The reason for such phenomena is because the distance traveled by the linear actuator rod during the first half of its run (forward stroke) is smaller than of that in the second half (backward stroke), although the number of feedback hall signals causing both strokes to be stopped by the controller is equally 250 pulses. The opposite of this fact is true about the positive errors of the fourth actuator which travels more during the forward stroke compared to its backward stroke mate. Higher number of missing feedback signals, i.e., no signal is received by the controller in some moments even when the linear actuator is working, during the longer stroke can be a probable reason of the inequality between the travel distances of forward and backward strokes in the experiment. This is mainly due to incapability of internal hall sensors in proper counting of motor revolution in some moments.

As can be seen in Table 4-13, the mean accumulated errors found at the end of run 50 vary from about 22 mm to 41 mm in different tested linear actuators which are all far beyond the precision needed in controlled gully loading and unloading operations. Another noticeable point in the obtained data is dissimilar and variable positioning behaviors in different linear actuators and replications which make it impossible to rely on this control method. As a general result, large values of the accumulated errors shown in this table and unpredictability in their occurrence confirm that the positioning control of working linear actuators by internal hall

sensors is not a reliable method for automated gully conveying-spacing system. Therefore, employment of external distance sensors such as infra-red and laser types is needed for this purpose.

Table 4-13. Accumulated errors (mm) in different replications of the experiment of linear actuators positioning by internal hall sensors

	Number of executed runs[1]	Error in lower LAs		Error in upper LAs	
		Left	Right	Left	Right
Replication 1	5	0	-3	-1	+4
	10	-1	-7	-2	+5
	15	-3	-10	-8	+11
	20	-4	-14	-10	+16
	25	-4	-18	-11	+19
	30	-6	-23	-10	+20
	35	-9	-29	-14	+22
	40	-11	-34	-14	+26
	45	-12	-39	-18	+31
	50	-15	-44	-20	+35
Replication 2	5	0	-6	-4	+5
	10	0	-8	-8	+9
	15	-2	-14	-12	+11
	20	-7	-18	-14	+18
	25	-11	-24	-17	+20
	30	-14	-32	-21	+22
	35	-15	-38	-21	+21
	40	-18	-40	-22	+27
	45	-22	-44	-20	+27
	50	-23	-44	-22	+30
Replication 3	5	-2	-8	-6	+3
	10	-2	-11	-12	0
	15	-4	-13	-13	+1
	20	-9	-14	-15	+4
	25	-13	-14	-20	+9
	30	-17	-17	-24	+12
	35	-19	-19	-30	+17
	40	-20	-23	-34	+20
	45	-22	-27	-33	+23
	50	-29	-34	-35	+29
	Mean[2]	-22.3	-40.7	-25.7	+31.3

[1] One back and forth motion=one run

[2] Calculated for the accumulated errors of all 3 experiments after 50 runs

Tables 4-14 and 4-15 contain the numerical results of the experiments done to evaluate the employment of IR distance sensors for positioning of two linear actuators (section 4.2.2.6.2). Based on the experiment plan, the resulted positioning errors during backward and forward strokes of the linear actuators have been separately calculated. The five travel distances shown in the first column of these tables are the target values which should be achieved in different trials by means of analog output signals of tested IR distance sensors. The values displayed in next six columns are the actual distances a linear actuator could travel during three replications of each trial. The mean absolute errors presented in last two columns are derived based on the results of all three replications, while the defined error is the deviation between target and actual travel distances.

Table 4-14. Resulted errors during controlled positioning of left linear actuator by analog signals of IR distance sensor in preliminary tests

Target travel distance (mm)	Actual travel distance (mm)						Mean absolute error (mm)	
	Rep. 1		Rep. 2		Rep. 3			
	Fwd	Bwd	Fwd	Bwd	Fwd	Bwd	Fwd	Bwd
50	53	52	48	52	53	49	2.7	1.7
100	104	98	106	103	104	104	4.7	3
150	156	154	159	153	158	156	7.7	4.3
200	212	207	210	213	209	205	10.3	8.3
250	268	259	271	264	263	261	17.3	11.3

Table 4-15. Resulted errors during controlled positioning of right linear actuator by analog signals of IR distance sensor in preliminary tests

Target travel distance (mm)	Actual travel distance (mm)						Mean absolute error (mm)	
	Rep. 1		Rep. 2		Rep. 3			
	Fwd	Bwd	Fwd	Bwd	Fwd	Bwd	Fwd	Bwd
50	56	53	54	50	54	46	4.7	2.3
100	94	103	107	109	110	103	7.7	5
150	162	158	160	156	157	154	9.7	6
200	214	208	217	209	208	212	13	9.7
250	264	261	274	262	270	266	19.3	13

According to last two columns, a general non-linear increase is observed in the value of mean absolute error in both traveling directions, when positioning control in longer distances is tried. As can be seen in Tables 4-14 and 4-15, although the filter processing was activated and used to stabilize the output signals of tested sensors, the final error values are still high for precise motion control of linear actuators specially in longer strokes. Based on this, IR distance sensors were not adopted as the final distance measurement device for positioning control of MGU upper bars during controlled gully loading and unloading operations. However, to find out the suitability of IR distance sensors for controlled positions of the lower bars, which have a larger tolerance to positiong errors, two sensors were installed on the top set manipulators, and similar trials were carried out under real working conditions. Results of latter trials showed that employment of IR distance sensors for controlled positioning of lower bars is reasonable for a finite number of loading-unloading cycles, while failures such as “no stop” of linear actuators at the end of determined strokes were also observed in limited cases. Relatively unstable performance of cheap IR distance sensors in the real system may be due to the factors such as increased level of electrical noise inside the autonomous vehicle caused by numerous AC and DC wirings and devices, decresaed level of ambient light in the real working environment, and difficulty in consistent finding of the sensing targets located on the tip of the lower bars. Since the travel speed of linear actuators rods is constant during the back and forth motions, controlling the travel time of the lower bars, when being pulled and pushed by linear actuators, was alternatively employed for accomplishment of gully loading and unloading experiments in layer 3. These forward and backward travel times were controlled by the timer functions used in the PLC program.

4.3.4. Noise reduction in distance sensors by filter processing

According to the results obtained from the motion analysis of automated row spacing operation (sections 4.3.1 and 4.3.2), accurate positioning of the upper bars is the most critical factor which ensures the establishment of a desired row spacing value between the gullies entering a cultivation layer. Since utilization of internal hall sensors of linear actuators and IR distance sensors do not meet the required demands

of sensitive positioning of the upper bars, high resolution laser distance sensors were selected to be used for this purpose. To attain the best possible performance of the laser distance sensors installed in electrically noisy environment of the autonomous vehicle, filter processing was applied to the output analog signals of the laser sensors. Figures 4-42 (a) and (b) demonstrate the output signals of the two laser distance sensors installed on top set manipulators when the sensing target is immobilized. For better vision of the graph, scale of the vertical axis (A/D converted value) has been intentionally decreased. The sensor connected to channel 0 (CH0) of PLC analog input module is used to control the positioning of the left upper bar through TUL linear actuator, while the one connected to channel 3 (CH3) has the same duty for the right side. In both Figures, the maximum possible value of filter constant (99) is used to stabilize the output signal of the right sensor (CH3). However, in Figure 4-42 (a) and (b), the filter constants applied to the output signal of the left sensor (CH0) are zero (no filter processing) and 50 (moderate filter processing), respectively.

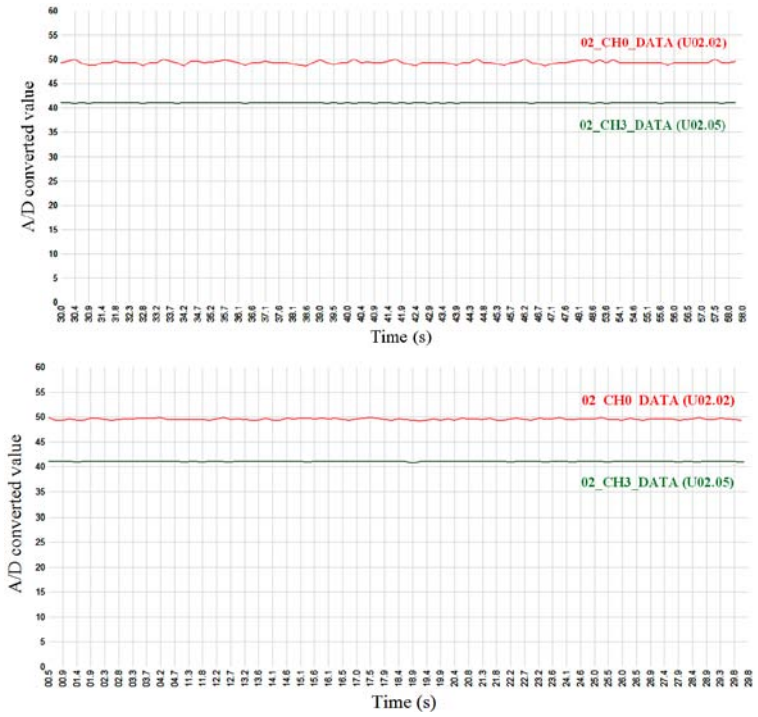

Figure 4-42. Effect of different filter constants on the outputs of left and right laser sensors (fixed sensing targets)

Effect of applying different filter constants on the output signals of left and right laser distance sensors, when the sensing targets were moving by manually controlled operation for about 130 mm, is shown in Figures 4-43 (a) and (b). Original scale of the vertical axes is kept in these figures. The sensing targets were attached to the upper bars of layer 3. At the starting point, the distance between the sensor and target is adjusted to be 100 mm. Based on the selected option in the settings window of PLC analog input module (Figure 4-24), the equivalent A/D converted value for this distance is 400. The forward stroke of the linear actuators pushing the upper bars was stopped when the distance between sensors and the sensing targets increased to about 230 mm. The trend observed in the graphs shows that the generated current in the output of the laser distance sensors (in mA) increases linearly when the sensing target gets further from the sensor.

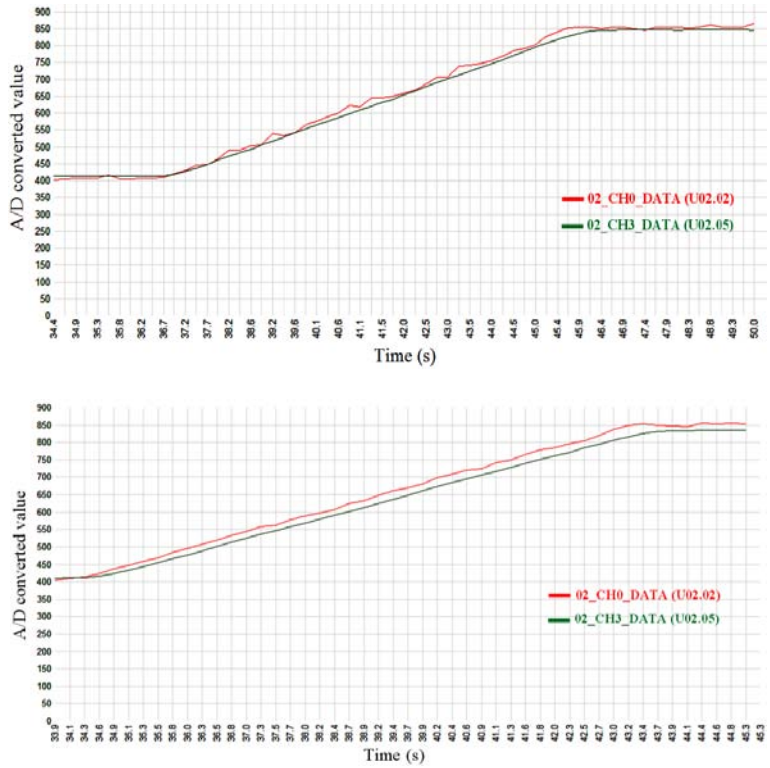

Figure 4-43. Effect of different filter constants on the outputs of left and right laser sensors (moving sensing targets)

Similar to the previous case, a filter constant of 99 has been applied to the output signal of the right sensor (CH3) in both Figures, while the output signal of the left sensor (CH0) shown in Figure 4-43 (a) has not been processed with filtering. The filter constant used to reduce the electrical noise in the output signal of the left sensor is 50 in Figure 4-43 (b). In general, using the highest degree of filter processing for laser distance sensors, maximum value of observed positioning errors was not more than 1 mm during all strokes of related automated operations.

4.3.5. Evaluation tests of automated operation

4.3.5.1. Layer targeting of bottom set manipulators

As stated in section 4.2.4.1, two types of layer targeting experiments, each containing five replications, have been conducted to examine the automated scheme and the control program by which the common frame of bottom set manipulators is accurately transferred to the manipulator locking height of layer 2 through a fully automated operation. The accuracy of vertical positioning of the common frame and its adequacy was successfully confirmed for all five replications of each experiment type by executing manual locking of linear actuators into lower and upper bars brackets after the frame was stopped at the end of each replication. No failure or serious deviation from the determined locking height was observed in total ten trials.

Figures 4-44 and 4-45 show the trend monitoring graphs of some selected digital and analog signals, during one of the trials of first and second experiment, respectively. In these figures, P00000 and P00001 represent the output signals of U-shaped photo sensors installed in working height of layers 1 and 2, respectively. “ON” status of P0420A and P0420B monitoring signals declares that manipulators vertical lift is moving upward and downward, respectively, and finally, the analog signal K0422 indicated in the bottom part is also used to monitor the current position of vertical lift’s stepper motor in terms of number of applied pulses to the motor.

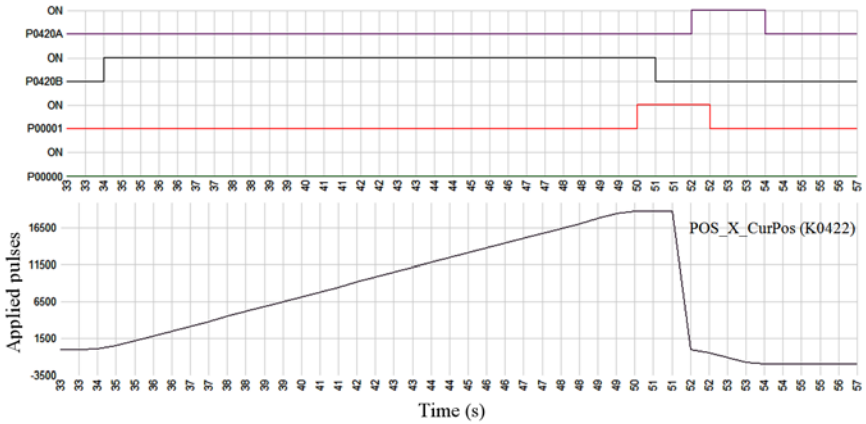

Figure 4-44. Trend monitoring of control signals in first type layer targeting experiment

In the sample trial of the first type experiment (Figure 4-44), in which the initial vertical position of manipulators common frame is selected to be a point between layers 2 and 3, the first motion of the vertical lift is downward (P0420B: ON) and under speed control. About 16 seconds after the downward motion is started, the manipulators common frame is detected by the U-photo sensor installed in the working height of layer 2 (P00001: ON). This causes the vertical lift to be stopped in less than a second (P0420B & P0420A: OFF). Note that P00001 is still on during these seconds because the common frame has been stopped in the sensing zone of the relevant U-photo sensor. Since the target layer selected for the experiment is layer 2, the second or final motion of the vertical lift is a slow and short upward motion (P0420A: ON) under position control which is automatically stopped after a certain number of pulses, determined in the control program, is applied to the stepper motor. The overall length of this experiment was approximately 20 seconds. However, due to choosing different initial vertical positions in other four replications of this experiment, the overall duration was not the same in all replications.

As can be observed in the trend graph of analog signal K0422, the value of signal is zero at the starting points of both first and second motions of the vertical lift, right when the status of P0420A and P0420B are changed to ON. This is because these two points are the floating origins of first and second motions of the operation in which the current position of the stepper motor is reset. The analog K0422 signal can be used to monitor the amount and direction of vertical lift motion during the experiment. According to the analog graph, increasing in the signal value means that the vertical lift is moving downward, while decreasing this value, e.g., the second motion starting from second 52, represent the upward motion of the vertical lift and manipulators common frame. As stated in section 4.2.2.3, shaft rotation per pulse for the stepper motors of vertical lifts is 0.72°. Since the lead of the ball screw (progress of nut per shaft rotation) utilized in the vertical lift is 4 mm, the vertical distance traveled by the vertical lift can be approximated by the values shown by the analog signal. As an example in Figure 4-44, an approximate of 19000 pulses has been applied to complete the first downward motion of the vertical lift. Applying this number of pulses to the stepper motor would cause 38 full shaft rotations. By translating this amount of

rotation into the linear motion through ball screw mechanism, a distance of 15.2 cm is found for the first downward motion of the vertical lift.

The trend monitoring graph of one sample trial conducted under second type experiment is shown in Figure 4-45. In second type of layer targeting experiment, the initial vertical position of manipulators common frame is an unknown height between layers 1 and 2.

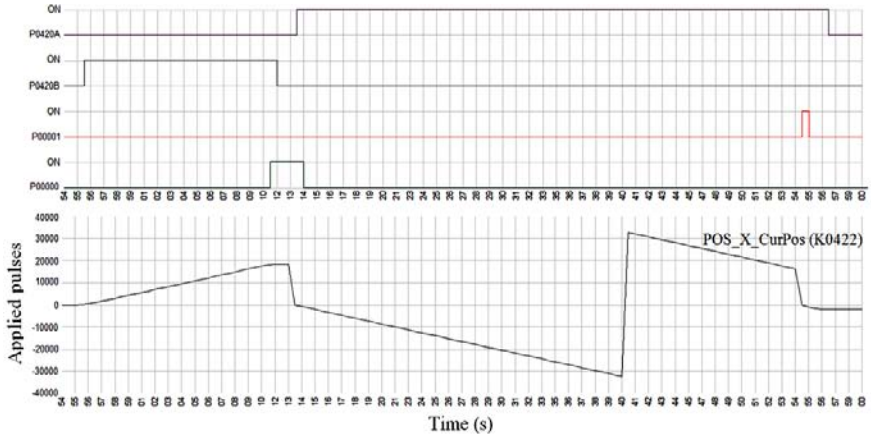

Figure 4-45. Trend monitoring of control signals in second type layer targeting experiment

Referring to Table 4-6, the second experiment also starts with a downward motion (P0420B: ON) under speed control. This motion is stopped when the U-photo sensor installed in working height of layer 1 finds the common frame (P00000: ON). Since the target layer 2 is far above the sensing zone of this sensor, the second motion of the vertical lift is a long upward motion under speed control (P0420A: ON). Resetting the value of analog signal K0422 also happens at the start of the second motion (floating origin of the second motion). The upward motion of the vertical lift is controlled by speed control method until the signal of the U-photo sensor installed in layer 2 is generated (P00001: ON). In this point, the control method of motor motion is changed to position control. Note that in this point, P0420A signal is still on which implies that the vertical lift is not stopped during this change. Since the motion made after the change in the control method (speed to position) is considered as a new motion step, signal of the U-photo sensor of layer 2 creates a new floating origin and the value of analog signal K0422 in this point becomes zero again. This can be

clearly found between seconds 54 and 55 of the trend graph. The sudden increase of analog signal value during the second motion occurred in second 40 is due to software limitation in demonstrating the values larger than 32767.5 at high and low extremes. This jump in analog signal graph has no effect on the running motion and as can be seen, it is immediately continued from the top.

4.3.5.2. Locking of top set manipulators

Obtaining timely responses of the four hall sensors employed in automated locking of top set manipulators is a requisite for successful execution of this operation which was evaluated through an experiment with ten replications. A total of 40 responses belonging to four hall sensors were investigated among which 3 failed responses (found in 2 replications) were observed. Two out of three failed cases were because of delay in sensor responses, and only one of failures was due to the lack of signal generation by the sensor. In case of delayed signals, the linear actuators stopped in a place after the locking zone and the respective linear actuator in the third failure (no signal generation) continued moving forward without any stop. One probable reason of these failures can be insufficient power of the magnetic filed within the locking zone due to inappropriate position of embedded magnets. The signal trend monitoring graphs displayed in Figure 4-46 are related to one of replications of the automated manipulator locking experiment (first stage) executed for top set manipulators.

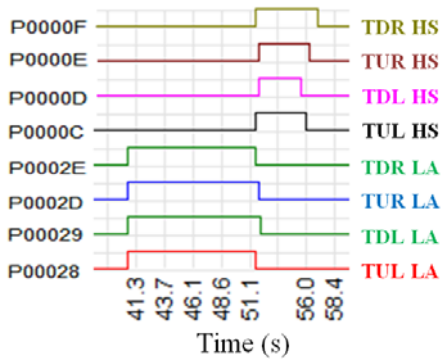

Figure 4-46. Trend monitoring of signals in the first stage of automated locking of top set manipulators

In Figure 4-46, abbreviations HS and LA stand for “hall sensor” and “linear actuator”, respectively, and the other abbreviations are related to positions of linear actuators in the autonomous vehicle (see Figure 4-34). Top four graphs (P0000C to P0000D) shown in Figure 4-46 represent the status of the signals generated by different hall sensors, while the ON status of the remaining signals indicated at the bottom part of the figure denotes that respective linear actuators are moving forward. Although all four linear actuators start moving forward together, small time differences between the moments they are stopped can be observed which is because of asynchronous responses of different hall sensors. Hall sensors signals go off when the second stage of manipulator locking operation including small downward motion of linear actuators starts.

4.3.5.3. Controlled loading-unloading of gullies in different spacing modes

Table 4-16 contains the results of three experiments (each with three replications) conducted to evaluate the ability of the system in controlled loading of gullies (automated row spacing operation) in layer 3. Each experiment is identified based on the spacing mode it executes (section 4.2.3.2). The indicated values in this table are the measured distances between six gullies consecutively loaded into the layer through fully automated operation. In the first column of the table, the two consecutive gullies the distance between which is measured are presented. For example, G1~G2 implies the measured distance between first and second gullies loaded into the layer. The second column separates the resulted data of three replications for each experiment. The distances between serial gullies have been measured at both left and right ends of the gullies and are individually shown in the table. Based on the dimension of real constructed system, the values of “u” and “w” (see Figure 4-25) are the same as applied in the simulations of row spacing operation using the virtual prototype of the system (50 and 80 mm). Accordingly, the target row spacing values in the experiments conducted for modes 1, 2 and 3 are 50, 70 and 20 mm, respectively.

Table 4-16. Measured row spacing values in left and right ends of the gullies serially loaded into layer 3 based on three spacing modes

Included gullies	Rep.	Distance in the left side (mm)			Distance in the right side (mm)		
		Mode I	Mode II	Mode III	Mode I	Mode II	Mode III
G1~G2	1	54	74	23	53	74	21
	2	53	70	20	53	74	23
	3	50	70	21	53	75	21
G2~G3	1	52	73	22	53	75	22
	2	50	73	21	54	75	20
	3	52	71	23	53	74	20
G3~G4	1	50	74	22	53	74	22
	2	53	74	22	53	74	22
	3	53	74	23	55	75	23
G4~G5	1	53	72	22	53	75	23
	2	53	71	20	54	75	22
	3	52	73	20	52	75	23
G5~G6	1	52	73	24	52	74	22
	2	52	71	23	53	75	21
	3	52	73	20	55	75	21

In most cases, different values of row spacing were observed in left and right sides of the same gullies which is because of the operation and conditions of independent left and right parts of the system participated in automated row spacing operation (load/unloading mechanisms, manipulators, sensors, etc.). However, the differences between left and right measured values were negligible and parallel rows of gullies were distinguished at the end of experiments. Investigating the numerical results obtained from different replications of all experiments reveal that the largest deviation from target spacing values is 5 mm, which is mostly found in the experiment replications of mode 2 in the right side. Since the target spacing value in mode 2 is 70 mm, the maximum positioning error of gullies caused by this deviation is about 7%. Discussing based on the mean errors, the average deviation from the target spacing values found in the experiments related to modes 1, 2, and 3 were 2.7, 3.5, and 1.7 mm, respectively. These average values are equivalent to 5.4, 5 and 8.5% positioning errors in modes 1, 2, and 3, respectively. In section 4.3.4, it was stated that the maximum observed positioning error of the upper bars controlled by laser

distance sensors is 1 mm in highest degree of filter processing. Referring to this statement, it can be concluded that the probable measurement error of the laser distance sensor is not the only source of the observed errors in the experiments of automated row spacing operation. Mechanical factors such as slipping the bottom surface of gullies on the moving upper bars can also seriously affect the amount of these deviations. Since all distance measurements have been made at the end of each experiment, the errors from different loading cycles of an experiment with both control and mechanical origins are accumulated in the values indicated in the table. The pictures shown in Figure 4-47 illustrate some views from the row spacing created between consecutive gullies at the end of experiments.

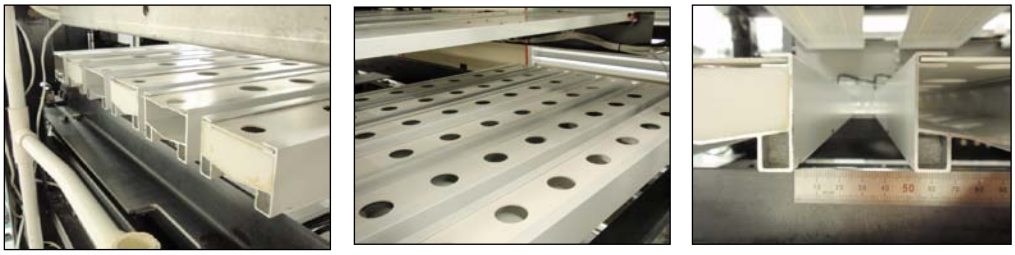

Figure 4-47. Views from created row spacing between consecutive gullies at the end of the experiments

Figures 4-48 (a) to (c) demonstrate the signal trend monitoring graphs related to controlled gully loading or automated row spacing experiments conducted for different spacing modes, obtained through online tracing of operating signals in developed PLC control programs. The ON status of the three digital signals shown in the top part denotes that the linear actuators and chain elevator participating in the experiment are in operation. In this regard, M1900 and M1901 represent motion activating signals of two upper (TUL & TUR) and two lower (TDL & TDR) linear actuators of top set manipulators, respectively, and the monitoring signal D00030.0 indicates the motion of the gully carriers moved by the chain elevator. Note that the existence of each ON signal in these three figures represents a single step of a loading cycle. As can be observed in the graphs, four possible directions of these motions are tagged near each ON signal using abbreviations FWD, BWD, DWD and UPD. The

analog signal (U02.02) shown in the bottom graph is the output signal of the laser distance sensor (based on A/D converted value) used for positioning control of TUL linear actuator.

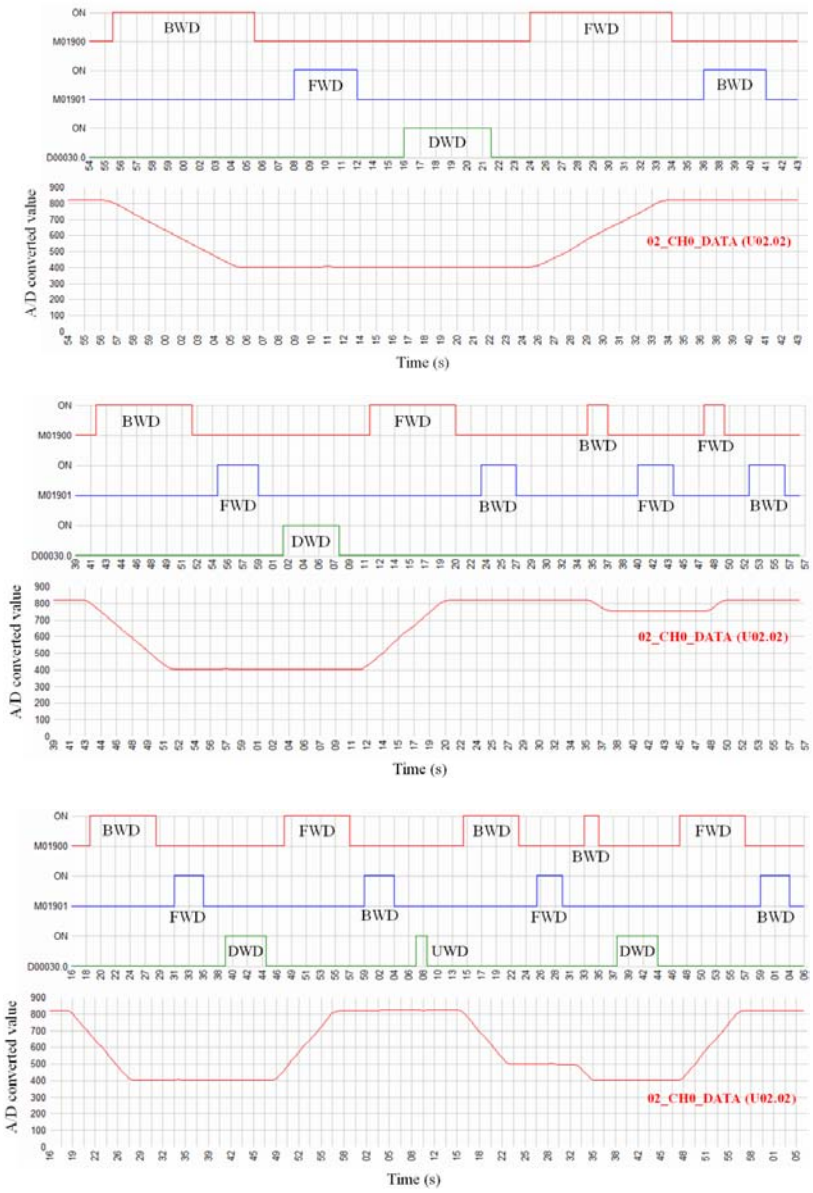

Figure 4-48. Signal trend monitoring graphs obtained from the experiments related to controlled loading (automated row spacing) of gullies: (a) a single 5-step loading cycle in mode 1, (b) 5 and 4-step loading cycles in mode 2, and (c) 5 and 6-step loading cycles in mode 3

The signal trend monitoring graphs shown in Figure 4-48 (a) contains the status of motion signals obtained from executing a single 5-step loading cycle in the experiment done for row spacing operation in mode 1. The details of such step have been previously described in Table 4-4. The total duration of executing this single loading cycle in the real system is about 46 seconds which is 4 seconds longer than its simulated version in the virtual system. As can be seen, the value of analog signal decreases from 830 to 400 when the backward motion of upper two linear actuators TUL and TUR pulls back the upper bars during the first step of the loading cycle. Note that A/D converted values 830 and 400 are equal to 230 and 100 mm distances between the sensing target attached to the upper bars and the laser distance sensors fixed on the autonomous vehicle. In step 4 of the loading cycle during which the TUL and TUR linear actuators moves forward to their initial horizontal positions, an opposite increasing trend can be observed in the value of the analog signal (400 to 830).

The trend monitoring graphs of Figure 4-48 (b) have been acquired from controlled gully loading experiment in mode 2 when the first two loading cycles (5-step and 4-step) were executed to load the first gully in empty layer 3. The first 5-step loading cycle is the same with Figure 4-48 (a), while the step related to motion of the chain elevator can't be found in the second executed loading cycle containing 4 steps. As explained in previous sections, the 4-step loading cycle is implemented just to increase the row spacing value between the gullies and no new gully is transferred into the layer after its completion. The variation in the numerical value of analog signal during forward and backward motions of TUL and TUR linear actuators in mode 2 (830 to 765 and *vice versa*) is equivalent to a displacement of 20 mm. The total length of executing these two cycles in the real experiment was about 74 seconds which was 12 seconds longer than similar simulated attempt.

Figure 4-48 (c) illustrates the signal trend monitoring of controlled loading of gullies in mode 3. These graphs have been obtained during the execution of first two loading cycles (5-step and 6-step) by which loading of two gullies with target row spacing of 20 mm into empty layer 3 is accomplished. The upward motion of gully carries observed between two loading cycles, where the signal D00030.0 has become ON for the second time, is an additional motion in this experiment used to provide the second gully for 6-step loading cycle. The signal of this upward motion is not

considered as a step of loading cycles. Status of TUL and TUR linear actuators running signal (M1900) and variations in the value of analog output signal of laser distance sensor (U02.02) during steps 1 and 3 of the second loading cycle shows that the 130 mm backward motion of the upper bars in 6-step loading cycle has been completed in two stages. The first stage includes a 100 mm backward motion during which the lower bars are not pushed forward and thus, the previously loaded gully is not moved outward by the upper bars. In this stage the value of analog signal has been decreased from 830 (230 mm) to 500 (130 mm). As can be seen in the figure, the remaining 30 mm backward motion has been continued after the forward motion of the lower bars and actuating roll-lift device were done. As a result of this, the previous gully loaded into the layer was carried outward on the upper bars to decrease the row spacing determined for mode 3. The total duration spent to execute the two cycles in the real experiment was around 106 seconds that was 9 seconds longer than the duration of the same trial in simulation.

The performance of the automated system in controlled unloading of gullies was also examined through similar experiments done for loading operation. To assimilate the initial conditions based on three spacing modes explained above, six gullies with adjusted row spacing 50, 70 and 20 mm were manually placed into the layer 3. One experiment for each row spacing value (with one replication only) was carried out to move out all six gullies from the layer and put them onto the gully carriers. No serious problem or failure was observed during these three experiments as well. Figures 4-49 (a) to (c) present the signal trend monitoring graphs which have been obtained from the PLC during three conducted unloading experiments. The trend monitoring graphs of In Figure 4-49 (c) only contain the signals obtained from a single 6-step unloading cycle. The different execution order of the working steps in loading and unloading operations can be clearly observed by comparing the existing order of the digital signals presented in Figures 4-48 and 4-49.

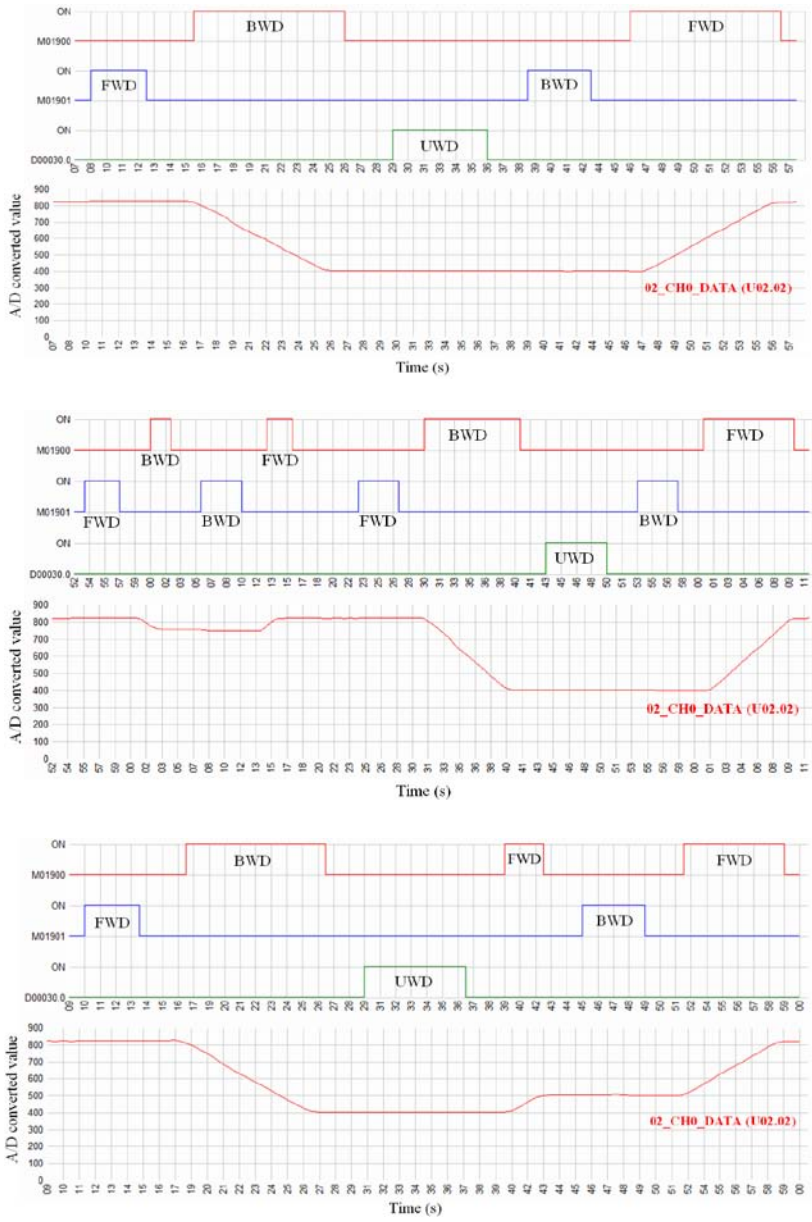

Figure 4-49. Signal trend monitoring graphs obtained from the experiments related to controlled unloading of gullies: (a) a single 5-step unloading cycle in mode 1, (b) 5 and 4-step unloading cycles in mode 2 and, (c) a single 6-step unloading cycle in mode 3

4.3.5.4. Displacement of gullies from horizontal conveying line into layer 3

The trend monitoring graphs of the signals acquired from the experiment carried out for displacing five gullies from the surface of horizontal conveying line into layer 3 are shown in Figure 4-50 (section 4.2.4.4). Gullies were loaded into layer 3 under spacing mode 1 with 50 mm target spacing value. In this figure, the ON status of M0100 signal means that a loading cycle of mode 1 has been executed to move the gully transferred to the front of layer 3 into that. The M0100 signal remained ON during all 5 steps of executed loading cycles. Similar to the trend monitoring graphs shown earlier, P0450A and P0450B were on when chain elevator (gully carriers) had upward and downward motions, respectively. The five downward motions of the gully carriers within the graph (P0450B: ON) represent step 3 of the five loading cycles executed during the experiment. The signal P00049 was on when the belt conveyors were in operation. The remaining signals P0001E, P0001A and P00015 are feedback signals generated by bottom IR sensor, LED photo sensor installed between layers 2 and 3 and, proximity sensor, respectively.

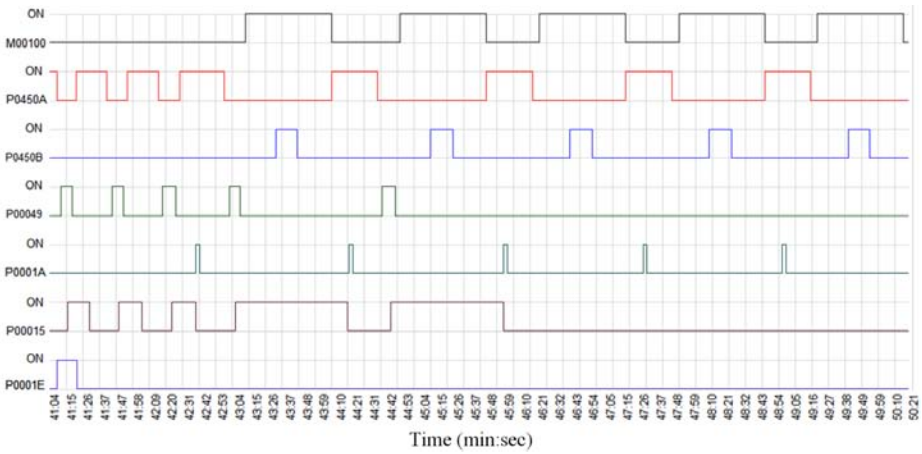

Figure 4-50. Signal trend monitoring graphs of the experiment conducted for displacing five gullies from the horizontal conveying line into layer 3

Based on the graphs observed in Figure 4-50, initial upward motion of the chain elevator was stopped when the marked gully carrier was detected by the bottom IR sensor (P0001E: ON). This signal has been used to start the belt conveyors (P00049: ON) and also adopted as the floating origin for the next motion of the chain elevator. The ON status of P00015 was achieved when the first gully moved by horizontal gully line was detected by the proximity sensor. This signal turned the belt conveyors off after 3 seconds and provided the starting pulse for the second upward motion of the chain elevator under position control. Since some seconds were needed for lifting the first gully from the surface of the conveying line, the P00015 signal remained on a few seconds after starting of the chain elevator. Thus, an overlap can be observed between on status of P000015 and P0450A. The cycle including the start-stop of belt conveyors and chain elevator was repeated until the third gully was also lifted up by upward motion of gully carriers under speed control. Some seconds after the start of this motion, the first gully vertically carried by the gully carriers was detected by the LED photo sensor (P0001A: ON). This signal was adopted as a new floating origin for the upward motion of the gully carriers. Based on the control program, the speed control of the chain elevator was converted into the position control by this signal and gully carriers were accurately stopped in the loading height in front of layer 3. However, loading of gully 1 was started after the fourth signal of the proximity sensor was made due to presence of gully 4 in pick-drop zone. After completion of the loading cycle used to transfer gully 1 into the layer, another upward motion of the chain elevator under speed control was started. From this point on, similar steps have been executed until the last gully (fifth one) was likewise loaded into layer 3. Direct observation and monitoring of the experiment indicated that all operational steps were successfully executed based on the control program developed according to automated scheme and no problem related to process control was observed. As can be perceived from the trend monitoring graphs, the total time spent for the experiment was 9 minutes and 15 seconds.

Although in the described experiment above, values designated to number of gullies, layer the gullies were loaded in, and target row spacing were 5, 3 and 50 mm, displacement of any number of gullies to a desired layer and applying any required row spacing value is possible by minor modifications and changing the related settings in the control program.

4.3.5.5. Displacement of gullies between layers 2 and 3

In this experiment, five gullies with adjusted row spacing of 20 mm were unloaded from layer 3 and successfully reloaded again into the lower layer 2, while the row spacing in the new layer was adjusted to be 50 mm. No major problem or malfunction was observed during loading and unloading of the gullies or operation and control of the chain elevator which confirms the validity of the control program developed for this automated scheme. The graphs in Figure 4-51 demonstrate the trend of different signals generated when the first gully was displaced between the layers. The ON status of the signal M0000 means that TUL and TUR linear actuators are moving to unload the gullies from layer 3. Similarly, M00020 is ON when BUL and BUR linear actuators are in operation for loading the gullies into layer 2. P000F1 represent the output signal of top IR sensor and finally, the monitoring signals D00031.0 and D00031.1 were on when the stepper motor of the chain elevator was running under “position” and “speed” controls, respectively. Other signals have been introduced and employed in earlier trend monitoring graphs.

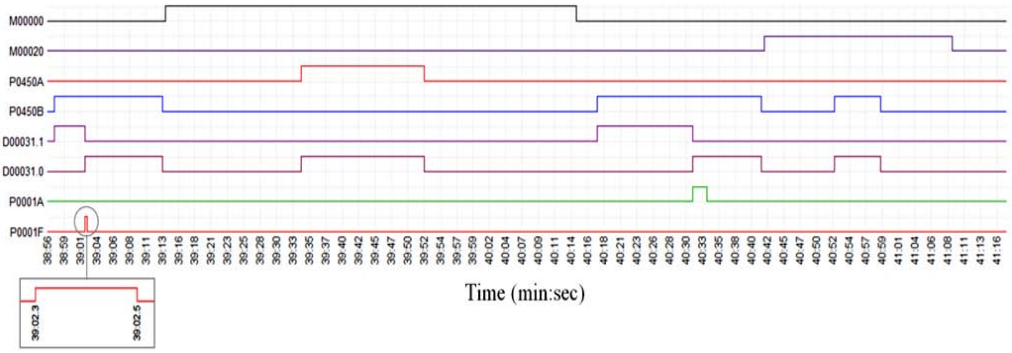

Figure 4-51. Signal trend monitoring graphs during the experiment conducted for displacement of a gully from layer 3 to layer 2

Based on the monitored signals shown in Figure 4-51, the starting motion of the chain elevator was downward (P0450B: ON) and running under speed control (D00031.1: ON). The stepper motor control has been converted into position control (D00031.0: ON) when the marked gully carrier causes the top IR sensor to generate a signal (P0001F: ON). As shown in the magnified view, the duration of this signal is

only 0.2 seconds. The downward motion of the gully carriers was stopped when certain number of pulses assigned to the position controlled motion step was achieved. Since the vertical position in which the carriers were stopped was the respective height determined for unloading the gullies from layer 3, an unloading cycle is executed to move out the gully from the layer and place it on the gully carriers (M00000: ON). The upward motion of the chain elevator during the unloading cycle is under position control (D00031.0: ON). In order to convey the unloaded gully to the loading height of layer 2, second downward motion of the gully carriers was started under speed control after the gully unloading from layer 3 was accomplished. The speed control of stepper motor during the second downward motion was swapped into position control by the output signal of the LED photo sensor installed between layers 2 and 3. This caused the conveying gully to be stopped in the exact vertical position specified for loading the gullies into layer 2. The trend monitoring was stopped after the completion of loading cycle in layer 2.

4.3.5.6. Functional problems in the operation of the automated system

Despite the generally satisfactory results obtained from different conducted experiments of the automated gully convey-spacing system, a number of technical problems and malfunctions were also observed during the tests and continuous operation of the system which have to be removed in the modified version. Following items are some of the most highlighted problems found during the system operation:

1- Employment of linear actuators with a low “duty cycle” (10%) causes temporary pauses in the working of linear actuators in some cases. This interrupts the trend of automated gully loading or unloading operations and makes undesired delays that elongates the active time of operation. This was observed when a faster series of gully loading cycles with shorter breaks between them were executed. The low travel speed of linear actuators (1-1.5 cm/s) is another technical drawback which makes the duration of gully loading and unloading operations unnecessarily long. This would waste a considerable amount of time in integrated automated operation when a great number of gullies have to be displaced and handled.

2- Failure of linear actuators driver (Figure 4-16) due to excessive heat generation when frequent loading/unloading cycles were executed. This was observed several times during high working rates and stopped the system operation.

3- Inaccuracy in final positioning of the autonomous vehicle when moving from one growing unit to another. Results of several examinations showed that the response of positioning sensor (LED photo sensor at the top of the vehicle) and the generating time of the signal used for stopping the vehicle through turning off the DC motor driver and brake the motor is appropriate. However, it was found that the reason of this inaccuracy is the existing backlash in the locomotion DC motor and big mass of the vehicle.

4- Instability of gullies on the gully carriers during vertical conveying in the higher heights of the chain elevator due to gradual deviation of the gully carriers to their sides. This was mainly because of the problems caused by improper installing of vertical chain strands as well as misalignment in the positions of lower and higher pairs of sprockets in the manufacturing stage.

5- Malfunctioning in a number of gully loading/unloading mechanisms embedded in the body of 4-layer growing units was observed as follows:

i) In some cases, the 10 mm lift of the upper bars was successfully provided; however, this amount of rise could not lift the gullies from the fixed body of the cultivation layer. This prevented the proper execution of gully loading/unloading, and row spacing operation due to no movement of gullies inside the layer. This problem started to appear when the PVC troughs of the nutrient solution system, used to pass and distribute the nutrient solution in each cultivation layer, were physically added to multilayer growing units. The failure happened because the side walls of these PVC troughs were sometimes higher than the value considered in automated system design.

ii) In some other cases, the upper bars and gullies on them could not return down after they were lifted upwards for 10 mm. This problem was related to excessive thickness of PVC troughs walls which made a disturbing friction between the side of the upper bars and the PVC walls. This friction imposed extra loads on the working movements of linear actuators as well. Modification in general dimensions of the PVC troughs used in nutrient solution system can simply solve the two observed problems mentioned above.

4.3.6. Estimated performance of system operation by time analysis

According to the principles presented in section 4.2.5, estimating the total operation time of the automated system in different working days, and considering it as the performance of the system is possible through breaking the integrated automated operation into its smaller forming components (Table 4-9 to 4-11), and analyzing the operational details and finding the working time in each of them.

In this section, the resulted operation time estimated in each of the first three working days of the systems for executing the dynamic cultivation plan of the case study, has been distinguished and divided into two major parts including the automated operations done for gully handling operation, e.g., executing gully loading and unloading cycles, horizontal and vertical conveying of gullies, and those which do not deal with the mobility of gullies, but prepare the system for initiation of gully handling operation, e.g., layer targeting, manipulator locking and unlocking, and motion of autonomous vehicle between the growing units.

Table 4-17 indicates the number and total operation time of the loading cycles required to fill the different empty layers of 4-layer growing units A and B by the automated row spacing operation, according to the optimal cultivation plan of the Korean lettuce adopted as the case study. Referring to diagrams of Figure 4-27 can be a helping guide to understand the details of this table. The time values indicated in Table 4-17 include the active time spent by the motions of linear actuators and chain elevator during a loading cycle as well as the short delays between the multiple steps of each cycle. Thus, the time related to required delays between the consecutive loading cycles and providing the new gullies for the next loading through horizontal and vertical conveying of gullies are not included in this table. As can be observed, the time of executing the loading cycles required for loading 27 gullies in layers 3B and 4 B, and making the row spacing 29 mm between them is the longest among all with near 22 minutes. The reported time for executing the loading cycles in the hybrid layer involves the total time needed for loading 16 gullies under the dynamic plan with 30 mm row spacing, as well as the 5 gullies grown by the static plan, spaced in 140 mm distances.

Table 4-17. Number and operation time of the loading cycles required to fill the empty layers of growing units A and B by automated row spacing operation based on the optimal cultivation plan of Korean lettuce

Layer-unit	Number of applied loading cycles			Time used by loading cycles (s)			Total operation time*
	4-step	5-step	6-step	4-step	5-step	6-step	
Layers 3,4-B	1	1	26	25	45	1248	21 min-58 sec
Layer 1,2,3,4-A Layers 1-B	14	14	-	433	630	0	17 min-43 sec
layer 2-B (hybrid)	6	6	15	185	270	720	19 min-35 sec

* The time related to delays between the consecutive cycles and providing new gullies are not included

The total time required for accomplishing the gully handling operation in different working days of automated gully convey-spacing system also contains the other time elements such as the time spent for providing new gullies for next loading cycles by horizontal and vertical conveying of gullies, and the applied delays between the consecutive loading cycles (5 seconds). Table 4-18 shows the details of the time required for gully handling operation in working day 1 which includes the time spent for moving 75 from the start point of the system to layers 2B, 3B and 4B and load them into the layers based on the plan adopted for the case study (Figure 4-35 and Table 4-12). The sum of the three individual operation times indicated in the last row of Table 4-18 is about 123 minutes. Table 4-19 presents the estimated operation time of all automated system in working day 1 in which the total time spent for executing the other automated operations of the system such as locking, unlocking and layer targeting of autonomous vehicle manipulators is also shown along with the estimated time of gully handling operation. As a result, the automated system needs to continuously work for about 126 minutes in its first working day for conveying and row spacing of 75 gullies or 300 young plants based on the case study plan. The time durations used to estimate different parts of the automated operation are obtained based on direct measurements in the real experiments of the automated system. As an example, the average time used for manipulators locking/unlocking and layer targeting acquired from Figures 4-45 and 4-46 are about 20 and 40 seconds, respectively. Based on a similar estimating procedure, the total time required for executing all automated operations of the system in working days 2 and 3 are also obtained and presented in Tables 4-20 and 4-21. In all cases, the combination and order of the automated operation based on which the estimation of total operation time has been made are the same with the lists presented in Tables 4-9 to 4-11. Therefore, the values shown as the total operation time in Tables 4-19 to 4-21 are the shortest possible active working times of the automated system.

Table 4-18. Time spent for gully handling operation in working day 1

Item	Required time for filling the layers		
	Layer 2B[1]	Layer 3B	Layer 4B
Executing loading cycles & delays[2]	20 min-5 sec	22 min-3 sec	22 min-3 sec
Providing new gullies for next loading[3]	16 min-5 sec	21 min-10 sec	21 min-50 sec
Total operation time	36 min-10 sec	43 min-13 sec	43 min-53 sec

[1] Time for filling the hybrid layer with gullies grown under both static and dynamic plans
[2] Delays between the consecutive loading cycles
[3] Operation begins from the "start" point

Table 4-19. Summary of the estimated time for executing all automated operations of the system in working day 1

Gully handling operation	Operation time	Other operations	Operation time	Total
"Start" to layers 2B,3B,4B	123 min	Lock, unlock and layer targeting of manipulators	3 min	126 min

Table 4-20. Summary of the estimated time for executing all automated operations of the system in working day 2

Gully handling operations[1]	Operation time	Other operations	Operation time
Layers 3B,4B to TSZ	87 min	Lock, unlock, layer targeting of manipulators[2]	11 min
"Start" to layers 3B,4B	87 min	Motion of autonomous vehicle	1 min
Layer 2B[3] to layer 1B	38 min		
Layer 2B[3] to TSZ	3 min		
"Start" to layer 2B[3]	25min		
TSZ to layers 1A,2A,3A,4A	115 min		
Total	5 hr-55 min		12 min

[1] Including loading, unloading and conveying of gullies between different locations

[2] Top and bottom set manipulators

[3] Applicable to gullies grown under dynamic plan only

Table 4-21. Summary of the estimated time for executing all automated operations of the system in working day 3

Gully handling operations[1]	Operation time	Other operations	Operation time
Layers 1A,2A,3A,4A to harvest	115 min	Lock, unlock, layer targeting of manipulators[2]	17 min
Layer 1B to harvest	31 min		
Layer 2B[3] to layer 1B	38 min		
Layer 2B[3] to TSZ	3 min		
Layer 2B[4] to harvest	11 min		
"Start" to layer 2B[5]	36 min	Motion of autonomous vehicle	2 min
Layers 3B,4B to TSZ	87 min		
"Start" to layers 3B,4B	87 min		
TSZ to layers 1A,2A,3A,4A	115 min		
Total	8 hr-43 min		19 min

[1] Including loading, unloading and conveying of gullies between different locations
[2] Top and bottom set manipulators
[3] Applicable to gullies grown under dynamic plan
[4] Applicable to gullies grown under static plan
[5] Fills the hybrid layer with gullies grown under static and dynamic plans

Investigating the final data presented in Tables 4-19 to 4-21 indicate that more than 96% of the total time spent for executing the automated operation within an integrated plan is used by the gully handling operation. This means that any attempt and operational modification for shortening the total operation time of the system must be done in the automated tasks dealing with the gully handling operations.

As can be observed in the last row of Table 4-21, the total operation time of the automated system in working day 3, i.e., 28 days after the start of the continuous cultivation process, is estimated to be about 9 hours. In this day, a total of 220 gullies (880 lettuce heads) including 210 gullies belonging to three different crop batches of the dynamic plan plus 10 gullies growing under the static are displaced between different locations of the plant factory (e.g., start point, TSZ, different layers, harvester), and spaced within the cultivation layers based on the cultivation plan of the case study. Since due to stability in continuous plant production process, the full capacity of the both 4-layer growing units are effectively in use in working day 3, the total operation time obtained in this day can be considered as the maximum operation time of the automated system during a working day. However, assuming that no technical problem or failure in the system occurs during the automated operation, a continuous operation of 9 hours in one working day for this number of gullies seems to be rather lengthy. This would be a problem if more number of growing units and cultivation layers are employed for plant cultivation in the plant factory. As also stated in section 4.3.5.6, the major reason of such long total operation time is the low travel speed of the current linear actuators installed in the system which causes slow loading and unloading of gullies in the system. However, the total operation time can also be partly reduced by partial increase in vertical conveying speed of the gullies up to a possible value in which a stable and secure controlled conveying is ensured. With a more limited effect, avoiding the unnecessary delays between the consecutive operations and working steps is another factor which should be mentioned for decreasing the total operation time.

4.4. Conclusions

The major conclusions and remarkable points drawn from this chapter of the study which discussed about the development and evaluation of an automated gully-convey-spacing system with modular design for the use in multilayer NFT hydroponic cultivation are summarized and listed as follows:

1- The automated schemes for creating any desired row spacing value between the gullies in a cultivation layer were developed through sequential combination of 4, 5 and 6-step loading cycles and the chain elevator operation. Three row spacing modes were specified according to the range of desired row spacing and existing dimensions in the system. The automated scheme was simulate and examined through virtual prototyping of the system and motion analysis of the participating moving parts before running the real experiments. No deviation from target row spacing values was observed at the end of simulations and results of the motion analysis obtained by CAE simulation confirmed the effectiveness of the automated schemes proposed for row spacing operation in all spacing modes. Thus, the principles presented in these schemes were used in final control programs of the automated row spacing operation and executed by the developed system.

2- The least possible error in horizontal positioning of the upper bars of gully loading/unloading mechanisms, embedded in 4-layer growing units, was the most critical factor in creating a certain row spacing value by the system. Accordingly, precise control of back and forth motions of the linear actuators connected to the upper bars during the row spacing operation is the most important technical feature in this issue. Employment of laser distance sensors was found to be the best sensing approach for accurate positioning of the linear actuators after examining several methods through different experiments. Reducing the effect of electrical noise by extra filter processing could reduce the positioning error of these sensors to 1 mm during automated gully loading/ unloading operations.

3- Investigating the numerical results obtained from different replications of the experiments conducted to evaluate the system ability in executing automated row spacing operation revealed that the average deviation from the target row spacing values in specified spacing modes 1, 2, and 3 (50, 70, and 20 cm) were 2.7, 3.5 and 1.7 mm, respectively. These average values are equivalent to 5.4, 5 and 8.5 %

positioning errors in modes 1, 2 and 3, respectively. This implies that the measurement error of the laser distance sensor is not the only source of positioning error during the automated row spacing operation. Mechanical problems such as slipping the bottom surface of gullies on the moving upper bars are the factors which can seriously affect the row spacing accuracy and gully positioning errors.

4- Negligible differences were found between created row spacing values in left and right ends of the gullies after the completion of automated row spacing experiments. As a result, parallel rows of NFT gullies were observed at the end of these experiments.

5- All other automated schemes and their respective PLC control programs developed for evaluating the proper functionality of system working units were successfully tested through several independent experiments including the layer targeting of bottom set manipulators, locking of top set manipulators, controlled loading-unloading of gullies in different spacing modes, displacement of gullies from the conveyor belt to layer 3, and displacement of gullies between layers 2 and 3. The performance of each program was checked and analyzed using the signal trend monitoring graphs and no serious problem was observed in functionality of the control programs and related automation plans. However, a limited number of mechanical problems related to system hardware and manufacturing stage were detected during the experiments which should be considered and modified in probable future attempts.

6- To estimate the performance of automated gully convey-spacing system during an integrated cultivation plan, executing the optimal cultivation plan of the Korean lettuce in two 4-layer growing units was investigated. Best order of executing the required automated operations in different working days of this plan was determined. It was found that a total operation time of 9 hours per working day is required when full capacity of the 4-layer growing units is used. In such a case, displacement and row spacing of a total of 220 gullies are supported by relevant automated operations of the system. Low speed of the linear actuators employed in the manipulators of the autonomous vehicle was found to be the main source of such long operation. This duration can be partly reduced by using faster linear actuators with higher duty cycles, and increasing the vertical speed of gully conveying up to technically allowed levels.

5. SUMMARY AND FURTHER WORK

This study was a research conducted and organized in two interrelated parts both of which dealt with continuous production of plants in multilayer plant factories that support hydroponic cultivation in NFT gullies. The first part of the study is considered as the theory part of this research which was an attempt to develop an evaluation model and computer simulation module for obtaining the respective cultivation schema (plan and procedure) of continuous plant production process in multilayer plant factory. In the second part of this study, on the other hand, development details and control plans of an automated gully convey-spacing system designed for executing the multilayer cultivation plans explained and found in the first part of the study were described.

Going into more details, the first part of the current research presented in chapter 3 starts with introducing the characteristics and implementing approaches of two gully-based cultivation methods in the plant factories with multilayer growing units including the single-stage static cultivation with fixed row spacing, and multistage dynamic cultivation with variable row spacing. Employment of dynamic cultivation in multilayer units can further increase the plant production rate if an appropriate cultivation plan is adopted and executed during the continuous cultivation process. To this end, a model was developed for i) evaluating the performance of multilayer dynamic cultivation plans and comparing their performances with alternative static option, and ii) finding the details of the procedure used for executing the evaluated cultivation plan. In this model which operated based on a stepwise algorithm, indices such as plant production rate (PPR), turning point day (TPD), and total number of produced plants during a certain cultivation period were defined and used to measure the performance of different multilayer dynamic and static cultivation plans. The model was then converted into a simulation module with visual input-output panel by Labview programming. The displayed data in this panel after the end of each simulation represented a cultivation schema containing the characteristics and performance of the respective cultivation plan as well as the procedure to execute it. In this way, those data of the cultivation schema which indicated the numerical distribution of gullies in different cultivation layers, the row spacing values to be applied in each layer and the displacement schedule of the gullies belonging to

different crop batches build the detailed procedure to execute the examined cultivation plan.

The information provided by a cultivation schema can assist the crop grower to make an appropriate decision about selecting a certain cultivation plan and execute it in the most efficient way. In order to experience such application in this study and observe its outcomes, the developed panel was used to obtain the cultivation schemas of all dynamic and static cultivation plans applicable for continuous crop production of two lettuce cultivars (Romaine and Korean Cheong Chug Myeon lettuce cultivars) with different canopy growth behaviors in total eight cultivation layers during a maximum 180-day period. Various input conditions such as dissimilar clustering, different gully widths and layer lengths, zigzag and square planting arrangements, and different equations of canopy diameter growth were adopted and examined in several series of simulations and the optimal cultivation plan with best plant production performance was selected in each case at the final. Detailed conclusions and outcomes of these trials have been presented in section 3.4. Adoption of hybrid static-dynamic layers for optimizing the area utilization in multilayer dynamic cultivation was another highlighted point in this chapter.

A general comment for obtaining more dependable data from the simulation panel is to find more accurate growth equations for estimating the size of plant canopy diameter in different growing days and insert them into the panel input. This can considerably increase the reliability of the obtained results and build a highly reliable cultivation schema. This would be a more critical issue in the crops with faster horizontal canopy growth.

In this study, performance of dynamic cultivation plans with up to three growth stages and implemented in maximum eight cultivation layers were investigated by the simulation panel. The existence of such low number of growth stages and layers makes a limited number of clustering options and a reasonable amount of the output data. However, the advantage and helpfulness of the simulating tools, such as the panel developed in this study, in facilitating the analysis of different cultivation plans would be more highlighted when larger plant factories with significant number of cultivation layers and greater number of growth stages and thus, numerous clustering options are available for continuous cultivation process. Therefore, modification of

the simulation panel for obtaining the cultivation schemas of the plans with more complicated conditions and wider options is recommended as a future work.

Going into the details of the second part of this study presented in chapter 4, an automated gully convey-spacing system with modular design was developed with three sub-systems including i) a couple of 4-layer growing units equipped with gully load/unloading mechanisms, ii) an autonomous vehicle, and iii) gully supplier (horizontal conveying line). Each sub-system contains a number of working units for implementing the assigned specific operations.

To enable the execution of the multilayer cultivation plans based on the cultivation schemas obtained in the first part of the study, two major functional objectives were defined for the automated gully convey-spacing system which were i) providing controlled vertical conveying of gullies between different cultivation layers of a multilayer growing unit, and also between the horizontal conveying line and the layers, and ii) enabling an automated row spacing operation in all layers of the growing unit such that the adjustment and creation of any desired row spacing value between the gullies are provided with high precision. Different types of actuators, sensors with analog and digital outputs, and a PLC extended with special modules as the controller unit of the system were employed to execute the automated schemes developed for system operations. The automated operations supported by the system were divided into a couple of groups. The first group were those directly related with automated gully handling operation including the horizontal and vertical conveying of gullies, controlled loading of gullies (automated row spacing operation), and finally, unloading of gullies. The automated operations involved in the second group were moving and positioning of the autonomous vehicle, layer targeting, and manipulators locking and unlocking which although do not directly deal with the gullies, but they act as necessary prerequisites to prepare the system for initiation of the first group operations. Among all automated operations, adjustment of row spacing values between the gullies, i.e., automated row spacing operation was the most critical function of the automated system for executing multilayer cultivation plans. Therefore, the automated scheme and ability of the automated system to execute this operation was examined through both virtual prototyping of the system and conducting a series of real experiments. The results obtained in both cases were promising such that an automated row spacing operation with low error and

reasonably accurate positioning of gullies was provided. The automated schemes and control programs developed for evaluating the proper functionality of other working units of the system were also tested and successfully confirmed through several independent experiments. At the ending part of chapter 4, integrated employment of all automated operations of the system for executing the optimal cultivation plan of the Korean lettuce was investigated through a case study and the performance of system in terms of operation time was evaluated. The detailed conclusions of the second part of this study have been presented in section 4.4

An advantageous feature of the automated gully convey-spacing system introduced in this study, compared to other similar systems developed for multilayer cultivation is that all the power sources required and used for actuating the automated operation in all cultivation layers and growing units are centralized in a single autonomous vehicle. Based on this, less number of motors and actuators would be used for running the automated operation in all growing units. This can make a significant save in the number of actuators and motors and their purchase costs, if numerous multilayer growing units and layers are installed in a plant factory. Faster providing of the gullies in different working heights through continuous vertical conveying of gullies on several pairs of gully carriers of the chain elevator (versus the single gully carrier of the lead screw lift used in other systems), and the ability to create a wide range of row spacing values with a high accuracy at any cultivation layer of the growing unit, simply through tuning of related parameters in the control program, are some other new technical features and advantages of the described automated system.

Increasing the speed of automated loading and unloading operations through employing faster linear actuators, or appropriate application of pulse width modulation, i.e., technique for motor speed control (of linear actuators), can be a technical issue for the further work and investigation in the developed system. In addition, finding the threshold speed of the chain elevator operation in which the stability of gullies during the vertical conveying is also kept, and apply this speed to automated operation, considered as a decreasing factor of total operation time of the system should be considered in future attempts. Designing gully convey-spacing systems enable to execute other crop flow patterns such as first in- first out, and more complicated spacing methods such as two dimensional plant spacing can be the topic of future research activities in this area.

REFERENCES

Annevelink, E. 1992. Operational planning in horticulture: Optimal space allocation in pot-plant nurseries using heuristic techniques. Journal of Agricultural Engineering Research 51: 167-177.

Annevelink, E. 1999. Internal transport control in pot plant production. Doctoral thesis, P 259, Wageningen Agricultural University, The Netherlands.

Bolton, W. 2009. Programmable logic controllers. Fifth edition, Elsevier Science.

Chang, Y.S., H.G. Song and D.E. Kim. 2005. Development of a chain conveyor type row spacing system for plant factory. Journal of Bio-environment Control 14(1): 7-14 (In Korean with English abstract).

Chang, Y.S., D.E. Kim, H.H Kim, J.G. Kim and I.H. Yu. 2006. Utilization effect of sliding type crop row spacing system. Journal of Bio-environment Control 15(1): 63-69 (In Korean, with English abstract).

Despommier, D. 2010. The vertical farm- feeding the world in 21st century. 320 P, St. Martin's Press , New York, USA.

Drury, G. 1984. Apparatus and method for transporting growing plants. U.S. Patent No. 4476651 A.

Fang, W., K.C. Ting and G.A. Giacomelli. 1990. Animated simulation of greenhouse internal transport using SIMAN/CINEMA. Transactions of the ASABE. 33 (1): 336-340.

Garcia Victoria, N., B. Eveleens and H.J. Van Telgen. 2007. Development of a phase dependent growth strategy for mobile rose cultivation systems. Acta Horticulturae 751: 137-148.

Giacomelli, G.A. Movable row tomato production system for the greenhouse. 1987. Applied Engineering in Agriculture 3 (2): 228-232.

Giacomelli, G.A., N. Catilla, E. Van Henten, D. Mears and S. Sase. Innovation in greenhouse engineering. 2007. Acta Horticulturae 801: 75-88.

Goto, E., L.D. Albright, R.W. Langhans and A.R. Leed. Plant spacing management in hydroponic lettuce production. 1994. ASAE paper 94-4574.

Grift, T., Q. Zhang, N. Kondoh and K.C. Ting. 2008. A review of automation and robotics for the bio-industry. Journal of Biomechatronics Engineering 1(1): 37-54.

Hashimoto, Y. Plant factory in the 21st century. 2000. In: Proceedings of 3rd International Conference of Agricultural Machinery Engineering (ICME 2000), pp. 1-13, Seoul, Republic of Korea.

Haub, J.T., J.G. Krassas, S.C. Rustad and N. Davis. 1982. Method and apparatus for increasing the spacing between plants in accordance with their growth rate. U.S. Patent No. 4216618 A.

Hayashi, S., S. Saito, Y. Iwasaki, S, Yamamoto, T. Nagoya and K, Kano. 2011. Development of circulation-type movable bench system for strawberry cultivation. Japan Agricultural Research Quarterly 45 (3): 285-293.

Horibe K., K. Mori, K. Matsuo, K. Kondoh and T. Kameoka. 1993. Studies on the development of plant transfer equipment (part 2). Journal of Japanese Society of Agricultural Machinery 55(6): 49-57 (In Japanese with English abstract).

Hydroponic production lines. Available at: http://www.greenautomation.fi/content/en 11501/857/857.html (15 January 2015).

Ikeda, A., S. Nakayama., T. Ishii and I. Itakura. 1986. Apparatus for plant cultivation. U.S. Patent No. 4617755 A.

Ioslovich, I. and P.O. Gutman. 2000. Optimal control of crop spacing in plant factory. Automatica 36: 1665-1668.

Jansen, W.H.A. 2004. System with plant carriers that can be moved over rails. European Patent (EP) No. 1374666 A1.

Kim, D.O., J.O. Ho, J.B. Yoon and K.L. Choi. 2013. Automation in the plant factories with artificial lighting. In: The plant factory, pp. 79-95. Rural Development Administration (RDA), Republic of Korea (In Korean).

Kim, D.O., J.O. Ho, J.B. Yoon and K.L. Choi. 2013. Automation in the plant factories with natural lighting. In: The plant factory, pp. 173-189. Rural Development Administration (RDA), Republic of Korea (In Korean).

Kim, J.Y., S.H. Yang, C.G. Lee, A. Ashtiani-Araghi and J.Y. Rhee. 2011. Simulation of planted area index (PAI) for crop spacing methods in plant factory. Journal of Biosystems Engineering 36(5): 348-354 (In Korean, with English abstract).

Kim, Y.H. 2011. Studies on the automatic system for plant factory. In: Proceedings of 4th Urban-Type Plant Factory Symposium, pp. 125-140, Seoul, Republic of Korea.

Korea Rural Development Administration (RDA). 2005. Development of plant production factory system for fresh leaf vegetables production all the year round. Technical report (In Korean).

Korea Ministry for Food, Agriculture, Forestry and Fisheries (MFAFF). 2003. Development of plant factory system and production technology for rose. Project report, P. 404 (In Korean).

Kozai, T. 2006. Closed systems for high quality transplants using minimum resources. In: Plant tissue culture engineering, Ed. S. Dutta Gupta and Y. Ibaraki, pp. 275-311. Springer, The Netherlands.

Kozai, T. 2013. Resource use efficiency of closed plant production system with artificial light: concept, estimation and application to plant factory, In: Proceedings of the Japan Academy, Series B: Physical and Biological Sciences., pp. 447-461.

Kozai, T. 2013. Sustainable plant factory: closed plant production systems with artificial light for quality products. Acta Horticulturae 1004: 27-40.

Kurata, I. 1984. Studies on movable crop bed system in greenhouse (2). Journal of Japanese Society of Agricultural Machinery 46(2): 205-210 (In Japanese with English abstract).

Marshall, B. and J.A. Roberts. 2000. Leaf development and canopy growth. Blackwell Press, Taylor and Francis Group, UK.

McHugh, R. and H.H. Zhang. 2011. Virtual prototyping and Mechatronics for 21st century engineering. International Journal of Engineering Research and Innovation 3(2): 69-75.

Mobile gully system (MGS). Available at: http://www.hortiplan.com/site/index.php?menu=3 (15 January 2015).

Mori, K. 1991. Greenhouse automation technology. SHITA Report No. 2: 16-24 (In Japanese).

Mori K., K. Horibe, Y. Horino, A. Isomura, Y. Yonekawa, Y. Andoh, K. Matsuo and K. Kondoh. 1991. Studies on the development of plant transfer equipment (part 1). Journal of Japanese Society of Agricultural Machinery 55(1): 49-57 (In Japanese, with English abstract).

Murase, H. 2000. Microprecision irrigation system for transplant production. In: Transplant production in 21st century, Eds. C. Kubota and Chun. C., Springer Science, The Netherlands.

Edan, Y., S. Han and N. Kondo. 2009. Automation in agriculture. In: Springer Handbook of Automation, Ed. S. Y. Nof, pp. 1095-1128. Berlin, Heidelberg, Germany.

Pekkeriet, E.J. and E. Van Henten. 2011. Current developments of High-tech robotic and mechatronic systems in horticulture and challenges for the future. Acta Horticulturae 893: 85-94.

Prince, R.P. and J.W. Bartok. 1978. Plant spacing for controlled environment plant growth. Transaction of ASAE 21(2): 332-336.

Prince, R.P., J.W. Bartok and D.W. Prothere. 1981. Lettuce production in a controlled environment plant growth unit. Transaction of ASAE 24(3):725-730.

Rasin, B. 1998. Device for moving of growing troughs in a growing plant. European Patent (EP) No. 0663791 B1.

Raviv, M. and J.H. Lieth. 2008. Soilless culture: theory and practice. 587 P. Elsevier Science, Amsterdam, The Netherlands.

Roberts, D.S. 1990. Method and apparatus for hydroponic gardening. U.S. Patent No. 4932158 A.

Roodbergen, K.J. and I.F.A. Vis. 2009. A survey of literature on automated storage and retrieval systems. European Journal of Operational Research 194(2): 343-362.

Ruthner, A. 1966. Apparatus for the artificial cultivation of plants, bacteria, and similar organism. U.S. Patent No. 3254447 A.

Schueller, J.K. 2013. Agricultural automation: an introduction. In: Agricultural automation: fundamentals and practices, Eds. Q. Zhang and F.J. Pierce, pp. 1-12. CRC press, Taylor & Francis Group, USA.

Seginer, I. and I. Ioslovich. 1999. Optimal spacing and cultivation intensity for an industrialized crop production system. Agricultural systems 62: 143-157.

Space-O-Mat System. Available at: http://www.visser.eu/products/all-products/Space-O-Mat%20System/ (15 January 201 5).

Takakura, T. 1996. State of the art: Factory style plant production systems. In: Practical Plant Factories Toward the 21st Century, pp. 3-10, Seoul, Republic of Korea.

Takatsuji, M. 2008. The Plant factory. Korean edition published by Ohmu-sha Ltd. & World science Co. 129 P. Seoul, Republic of Korea (in Korean).

Ting, K.C., P.P. Ling and G.A. Giacomelli. 1996. Research on flexible automation and robotics for plant production at Rutgers university. Advances in Space Research 18 (1/2): 175-180.

Ting, K. C. 1997. Automation and systems analysis. In: Plant production in closed ecosystems, Eds. E. Goto, K. Kurata, M. Hayashi and S. Sase, pp. 171-187. Kluwer Academic Publishers, Amsterdam, The Nether lands.

Van Henten, E. 2006. Greenhouse mechanization: state of the art and future perspective. Acta Horticulturae 710: 55-69.

Van ’t ooster, A., J. Bontsema, E. Van Henten and S. Hemming. 2012. GWorkS-A discrete event simulation model on crop handling processes in a mobile rose cultivation system. Biosystems Engineering 112(2): 108-120.

Van ’t ooster, A., J. Bontsema, E. Van Henten and S. Hemming. 2014. Simulation of harvest operations in a static rose cultivation system. Biosystems Engineering 120: 34-46.

Yeh, Y.H.F., T.C. Lai, T.Y. Liu, C.C. Liu, W.C. Chung and T.T. Lin. 2014. An automated growth measurement system for leafy vegetables. Biosystems Engineering 117: 43-50.

Appendix A.1. Block diagram of the simulation VI for square planting

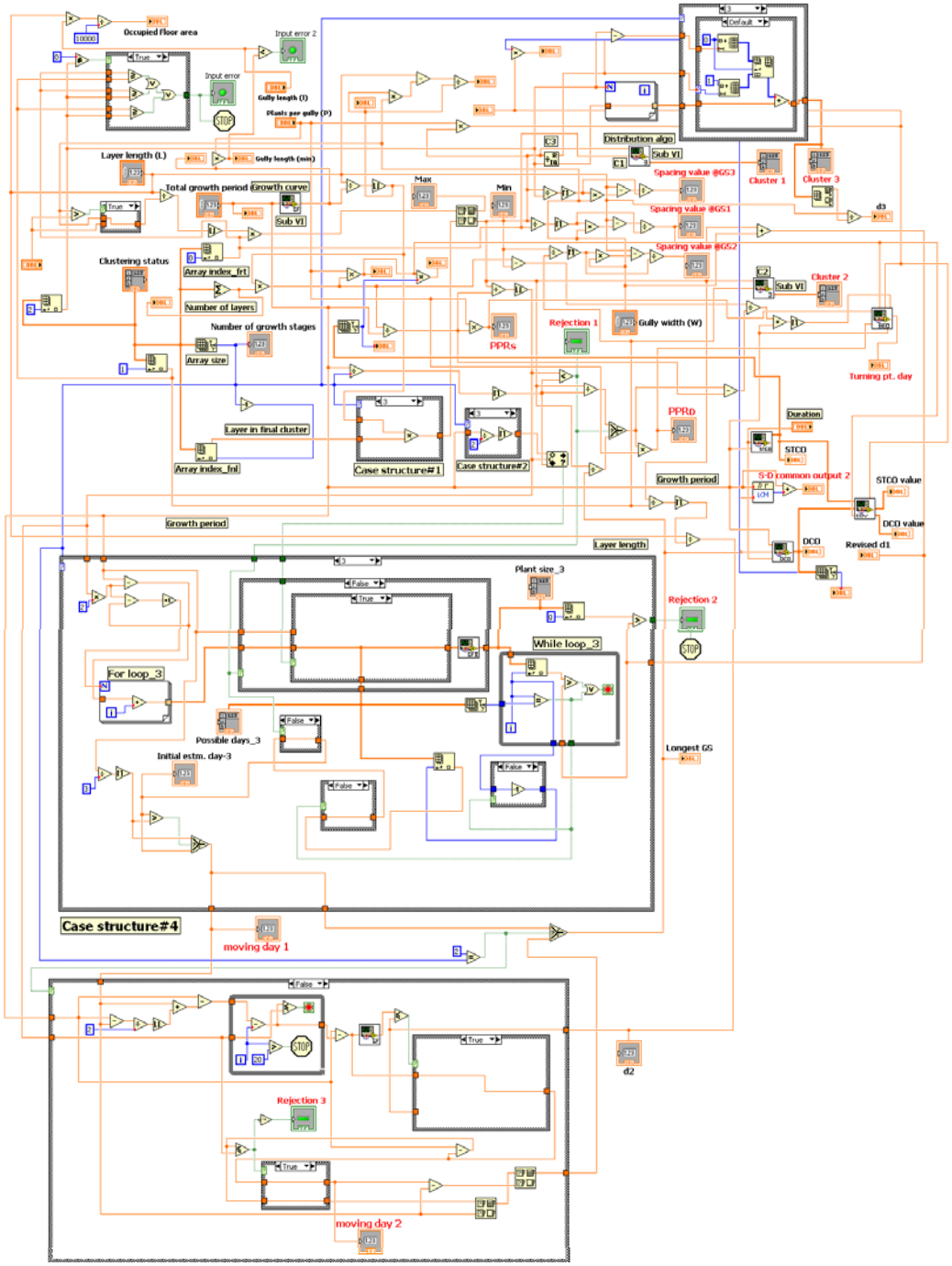

Appendix A.2. Block diagram of the simulation VI for zigzag planting

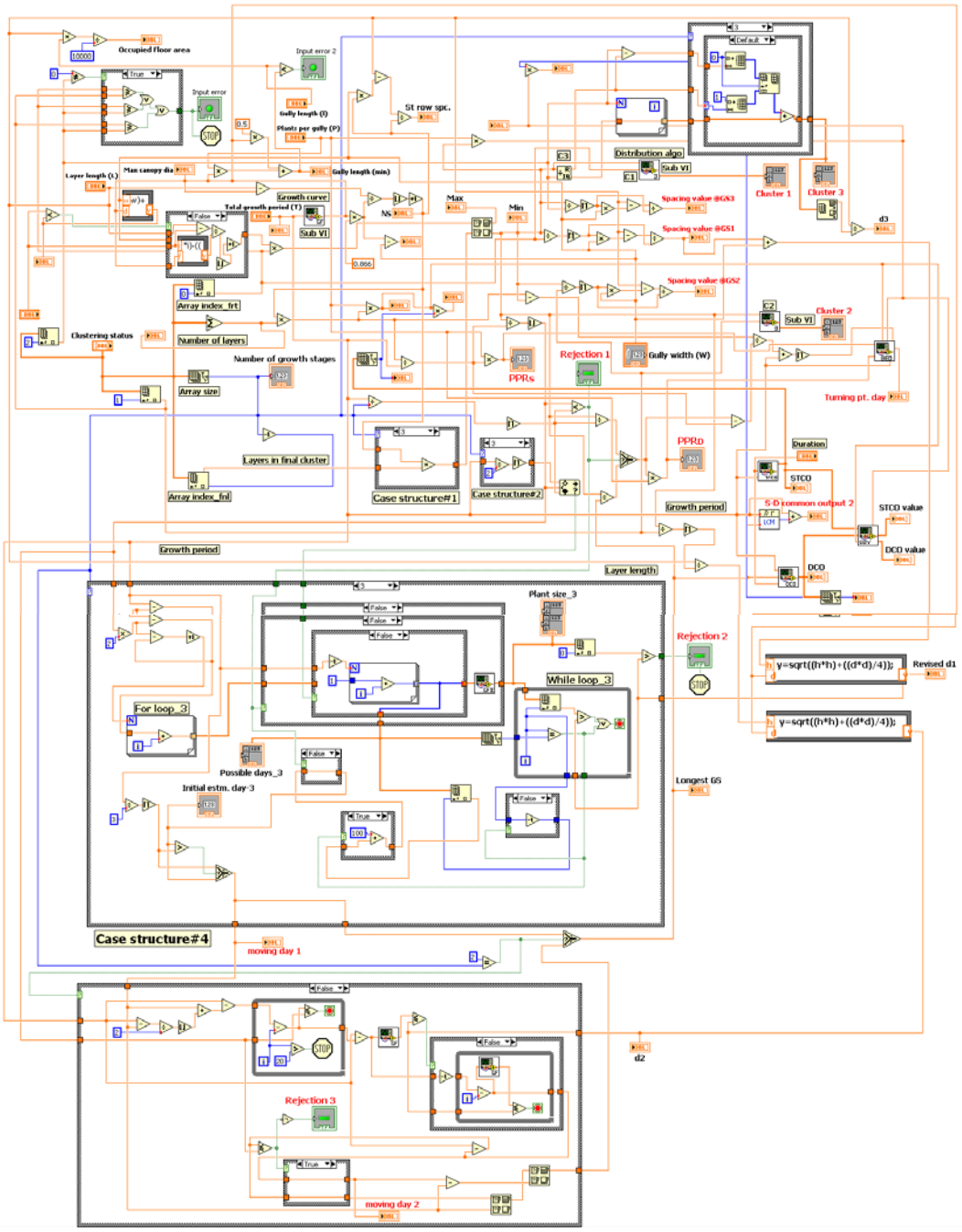

Appendix B.1. Details of regression analysis for different canopy growth models in Romaine lettuce

Note: In all following models, dependent and independent variables are "canopy diameter" and "plant growing day", respectively.

i) Linear

Table B.1.1. Summary of linear model

R	R^2	Adjusted R^2	Standard error of estimate
0.939	0.882	0.881	17.775

Table B.1.2. ANOVA results table for linear model

Source	Sum of squares	Degree of freedom	Mean square	F	Sig.
Regression	1837915.860	1	1837915.860	5817.348	0.000
Residual	247062.781	782	315.937		
Total	2084978.642	783			

Table B.1.3. Coefficients of linear model

Coefficient	Unstandardized coefficients		Standardized coefficients	t	Sig.
	Value	Standard error	Beta		
b_1	5.994	0.079	0.939	76.272	0.000
b_0 (constant)	73.767	1.304		56.552	0.000

ii) Quadratic

Table B.1.4. Summary of quadratic model

R	R^2	Adjusted R^2	Standard error of estimate
0.961	0.924	0.924	14.212

Table B.1.5. ANOVA results for quadratic model

Source	Sum of squares	Degree of freedom	Mean square	F	Sig.
Regression	1927233.464	2	963616.732	4770.889	0.000
Residual	157745.178	781	201.978		
Total	2084978.642	783			

Table B.1.6. Coefficients of quadratic model

Coefficient	Unstandardized coefficients		Standardized coefficients	t	Sig.
	Value	Standard error	Beta		
b_2	-0.183	0.009	-0.858	-21.029	0.000
b_1	11.308	0.260	1.771	43.426	0.000
b_0 (constant)	47.198	1.638		28.808	0.000

iii) Cubic

Table B.1.7. Summary of cubic model

R	R^2	Adjusted R^2	Standard error of estimate
0.97	0.941	0.941	12.522

Table B.1.8. ANOVA results for cubic model

Source	Sum of squares	Degree of freedom	Mean square	F	Sig.
Regression	1962683.341	3	654227.780	4172.668	0.000
Residual	122295.300	780	156.789		
Total	2084978.642	783			

Table B.1.9. Coefficients of cubic model

Coefficient	Unstandardized coefficients		Standardized coefficients	t	Sig.
	Value	Standard error	Beta		
b_3	-0.016	0.001	-2.082	-15.037	0.000
b_2	0.528	0.048	2.472	11.020	0.000
b_1	2.910	0. 604	0.456	4.819	0.000
b_0 (constant)	69.252	2.058		33.652	0.000

iv) Exponential

Table B.1.10. Summary of exponential model

R	R^2	Adjusted R^2	Standard error of estimate
0.929	0.863	0.863	0.135

Table B.1.11. ANOVA results for exponential model

Source	Sum of squares	Degree of freedom	Mean square	F	Sig.
Regression	90.004	1	90.004	4940.242	0.000
Residual	14.247	782	0.18		
Total	104.251	783			

Table B.1.12. Coefficients of exponential model

Coefficient	Unstandardized coefficients		Standardized coefficients	t	Sig.
	Value	Standard error	Beta		
b_1	0.042	0.001	0.929	70.287	0.000
b_0 (constant)	82.285	0.815		100.956	0.000

v) Power

Table B.1.13. Summary of power model

R	R^2	Adjusted R^2	Standard error of estimate
0.937	0.879	0.878	0.127

Table B.1.14. ANOVA results for power model

Source	Sum of squares	Degree of freedom	Mean square	F	Sig.
Regression	91.597	1	91.597	5660.589	0.000
Residual	12.654	782	0.16		
Total	104.251	783			

Table B.1.15. Coefficients of power model

Coefficient	Unstandardized coefficients		Standardized coefficients	t	Sig.
	Value	Standard error	Beta		
b_1	0.412	0.005	0.937	75.237	0.000
b_0 (constant)	55.645	0.781		71.231	0.000

vi) Sigmoidal Boltzmann

Table B.1.16. Iteration history for sigmoid model parameters (based on Boltzmann equation) for growth of canopy diameter in Romaine lettuce

Major iteration number*	Residual sum of squares	Parameter			
		b1	b2	b3	b4
0	306124.808	76.000	216.000	14.000	4.000
1	184231.794	86.722	229.847	13.982	3.995
2	106819.607	70.005	220.084	11.287	3.225
3	97071.501	72.696	214.512	10.917	3.119
4	95996.640	77.499	212.824	11.248	2.842
5	95899.614	77.610	212.310	11.206	2.768
6	95867.761	76.611	212.521	11.139	2.823
7	95855.772	76.989	212.526	11.156	2.816
8	95855.645	77.012	212.538	11.157	2.815
9	95855.644	77.011	212.538	11.157	2.815

*Optimal solution is found after 9 iterations.

Table B.1.17. ANOVA results for sigmoid model in Romaine lettuce

Source	Sum of squares	Degree of freedom	Mean squares
Regression	22230445.356	4	5557611.339
Residual	95855.644	780	122.892
Uncorrected total	22326301	784	
Corrected total	2084978.642	783	

*R^2 = 1-(Residual sum of squares/corrected sum of squares) = 0.954

Appendix B.2. Details of regression analysis for different canopy growth models in Korean lettuce (청축면 상추)

Note: In all following models, dependent and independent variables are "canopy diameter" and "plant growing day", respectively.

i) Linear

Table B.2.1. Summary of linear model

R	R^2	Adjusted R^2	Standard error of estimate
0.977	0.954	0.954	12.692

Table B.2.2. ANOVA results table for linear model

Source	Sum of squares	Degree of freedom	Mean square	F	Sig.
Regression	1119786.044	1	1119786.044	6951.765	0.000
Residual	53800.516	334	161.079		
Total	1173586.560	335			

Table B.2.3. Coefficients of linear model

Coefficient	Unstandardized coefficients		Standardized coefficients	t	Sig.
	Value	Standard error	Beta		
b_1	7.147	0.086	0.977	83.377	0.000
b_0 (constant)	52.557	1.423		36.941	0.000

ii) Quadratic

Table B.2.4. Summary of quadratic model

R	R^2	Adjusted R^2	Standard error of estimate
0.981	0.962	0.962	11.563

Table B.2.5. ANOVA results for quadratic model

Source	Sum of squares	Degree of freedom	Mean square	F	Sig.
Regression	1129062.543	2	564531.271	4222.191	0.000
Residual	44524.017	333	133.706		
Total	1173586.560	335			

Table B.2.6. Coefficients of quadratic model

Coefficient	Unstandardized coefficients		Standardized coefficients	t	Sig.
	Value	Standard error	Beta		
b_2	-0.090	0.011	-0.368	-8.329	0.000
b_1	9.763	0.324	1.334	30.167	0.000
b_0 (constant)	39.477	2.036		19.388	0.000

iii) Cubic

Table B.2.7. Summary of cubic model

R	R^2	Adjusted R^2	Standard error of estimate
0.983	0.967	0.966	10.868

Table B.2.8. ANOVA results for cubic model

Source	Sum of squares	Degree of freedom	Mean square	F	Sig.
Regression	1134373.359	3	378124.453	3201.405	0.000
Residual	39213.200	332	118.112		
Total	1173586.560	335			

Table B.2.9. Coefficients of cubic model

Coefficient	Unstandardized coefficients		Standardized coefficients	t	Sig.
	Value	Standard error	Beta		
b_3	-0.010	0.001	-1.074	-6.706	0.000
b_2	0.330	0.064	1.350	5. 200	0.000
b_1	4.797	0.801	0.656	5.993	0.000
b_0 (constant)	52.517	2.728		19.249	0.000

iv) Exponential

Table B.2.10. Summary of exponential model

R	R^2	Adjusted R^2	Standard error of estimate
0.956	0.914	0.914	0.129

Table B.2.11. ANOVA results for exponential model

Source	Sum of squares	Degree of freedom	Mean square	F	Sig.
Regression	59.140	1	59.140	3560.554	0.000
Residual	5.548	334	0.017		
Total	64.688	335			

Table B.2.12. Coefficients of exponential model

Coefficient	Unstandardized coefficients		Standardized coefficients	t	Sig.
	Value	Standard error	Beta		
b_1	0.052	0.001	0.956	59.670	0.000
b_0 (constant)	67.442	0.974		69.217	0.000

v) Power

Table B.2.13. Summary of power model

R	R^2	Adjusted R^2	Standard error of estimate
0.963	0.928	0.928	0.118

Table B.2.14. ANOVA results for power model

Source	Sum of squares	Degree of freedom	Mean square	F	Sig.
Regression	60.027	1	60.027	4301.462	0.000
Residual	4.661	334	0.014		
Total	64.688	335			

Table B.2.15. Coefficients of power model.

Coefficient	Unstandardized coefficients		Standardized coefficients	t	Sig.
	Value	Standard error	Beta		
b_1	0.510	0.008	0.963	65.586	0.000
b_0 (constant)	41.617	0.829		50.214	0.000

vi) Sigmoidal Boltzmann

Table B.2.16. Iteration history for sigmoid model parameters (based on Boltzmann equation) for growth of canopy diameter in Korean lettuce

Major iteration number*	Residual sum of squares	Parameter			
		b1	b2	b3	b4
0	62286.696	57.000	240.000	14.000	4.000
1	53681.170	57.073	240.019	14.000	4.798
2	45869.515	61.170	245.028	13.959	4.840
3	41577.705	57.350	238.567	13.088	4.621
4	39723.709	37.082	254.682	12.822	6.097
5	38314.777	34.688	247.487	12.016	5.720
6	38113.688	31.795	245.792	11.790	5.819
7	38047.478	30.626	247.399	11.813	5.905
8	38029.735	28.994	248.130	11.749	5.982
9	38023.003	27.340	248.785	11.685	6.067
10	38022.590	26.959	248.861	11.664	6.085
11	38022.584	26.930	248.864	11.662	6.086
12	38022.584	26.933	248.861	11.662	6.086

*Optimal solution is found after 12 iterations.

Table B.2.17. ANOVA results for sigmoid model in Korean lettuce.

Source	Sum of squares	Degree of freedom	Mean squares
Regression	9331815.416	4	2332953.854
Residual	38022.584	332	114.526
Uncorrected total	9369838	336	
Corrected total	1173586.560	335	

*R^2 = 1-(Residual sum of squares/corrected sum of squares) = 0.968

Appendix C.1. PLC program-ladder diagram for layer targeting

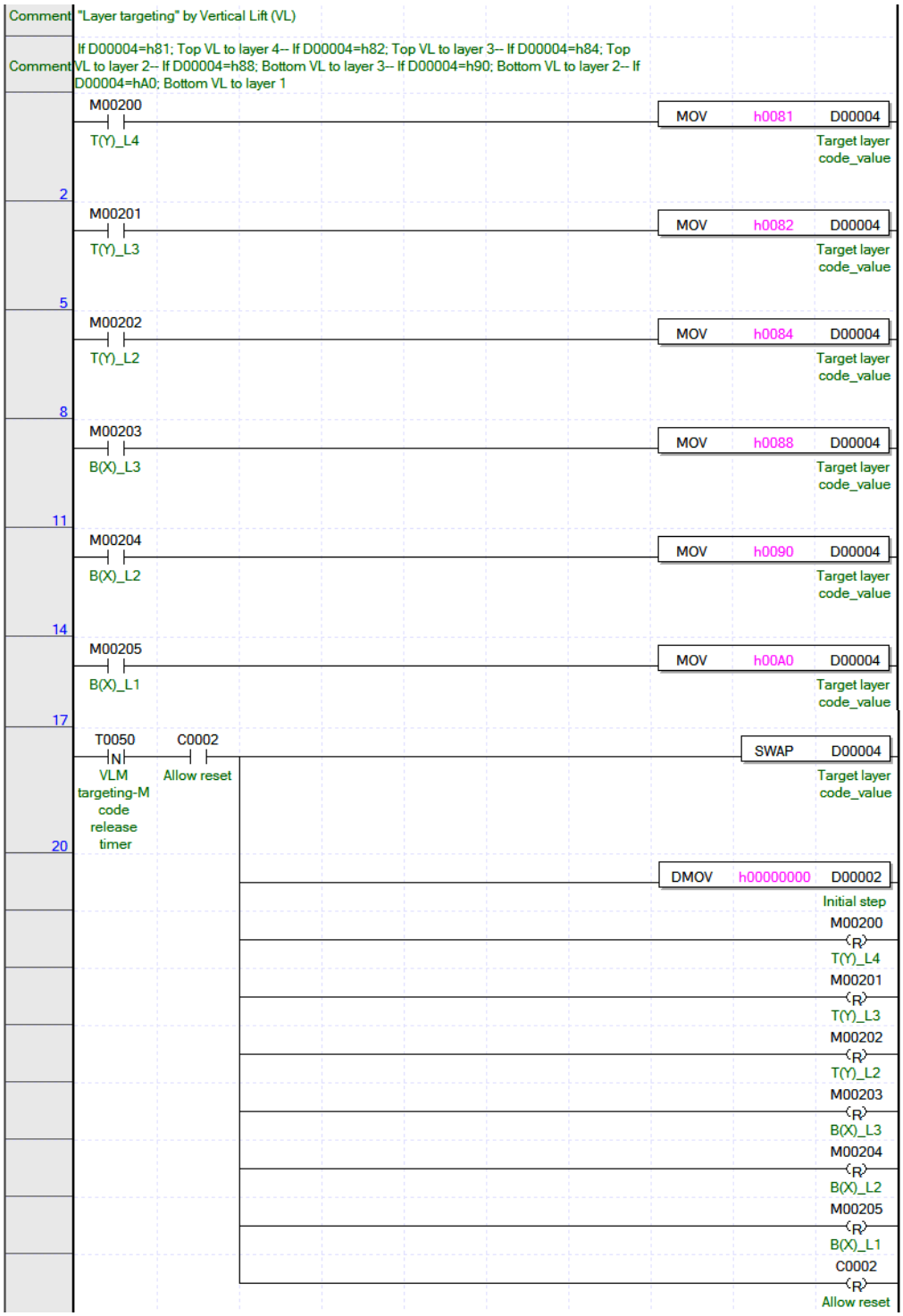

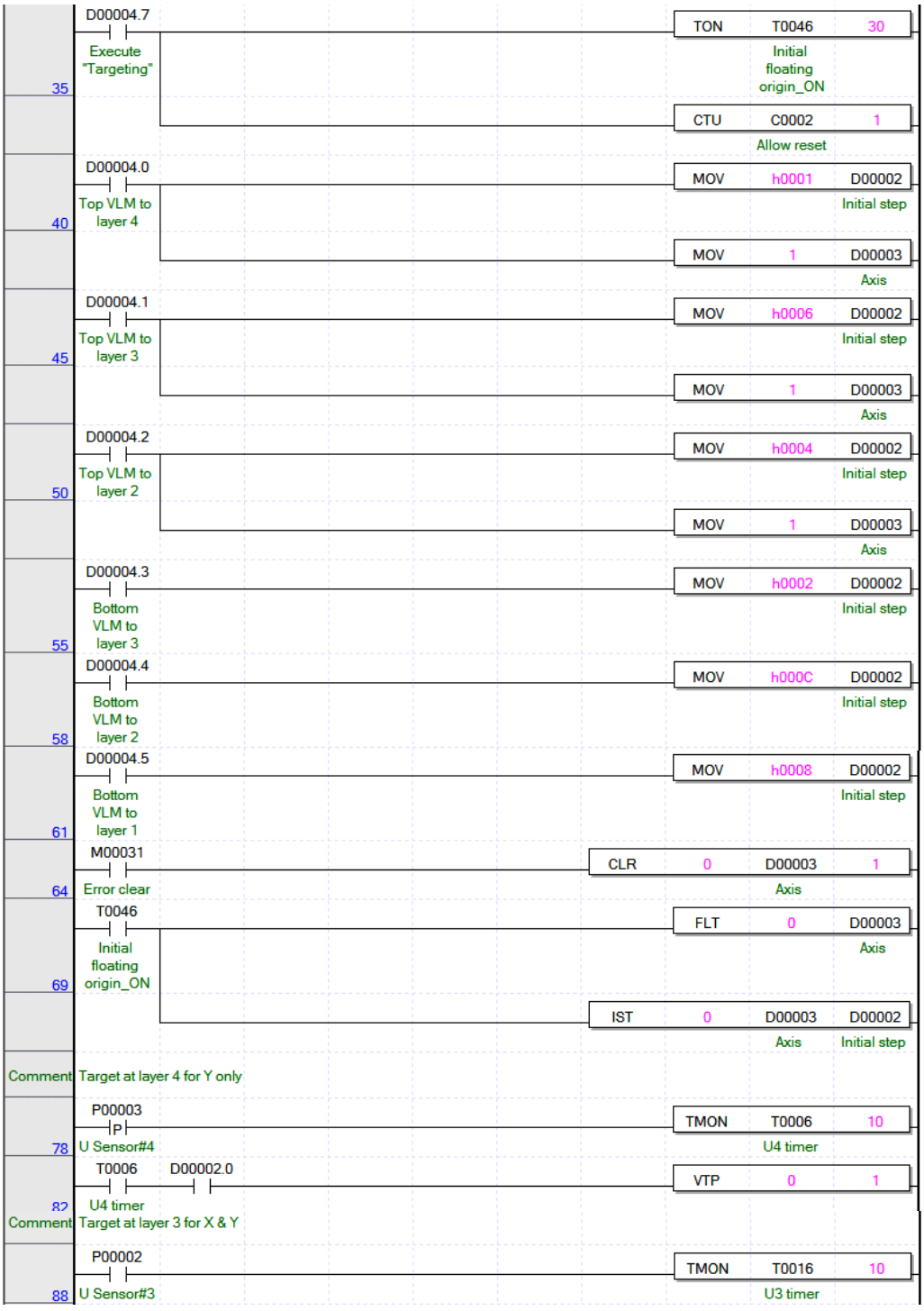
35
D00004.7
Execute "Targeting"
TON T0046 30
Initial floating origin_ON
CTU C0002 1
Allow reset
40
D00004.0
Top VLM to layer 4
MOV h0001 D00002
Initial step
MOV 1 D00003
Axis
45
D00004.1
Top VLM to layer 3
MOV h0006 D00002
Initial step
MOV 1 D00003
Axis
50
D00004.2
Top VLM to layer 2
MOV h0004 D00002
Initial step
MOV 1 D00003
Axis
55
D00004.3
Bottom VLM to layer 3
MOV h0002 D00002
Initial step
58
D00004.4
Bottom VLM to layer 2
MOV h000C D00002
Initial step
61
D00004.5
Bottom VLM to layer 1
MOV h0008 D00002
Initial step
64
M00031
Error clear
CLR 0 D00003 1
Axis
69
T0046
Initial floating origin_ON
FLT 0 D00003
Axis
IST 0 D00003 D00002
Axis Initial step
Comment
Target at layer 4 for Y only
78
P00003
U Sensor#4
TMON T0006 10
U4 timer
82
T0006 D00002.0
U4 timer
VTP 0 1
Comment
Target at layer 3 for X & Y
88
P00002
U Sensor#3
TMON T0016 10
U3 timer

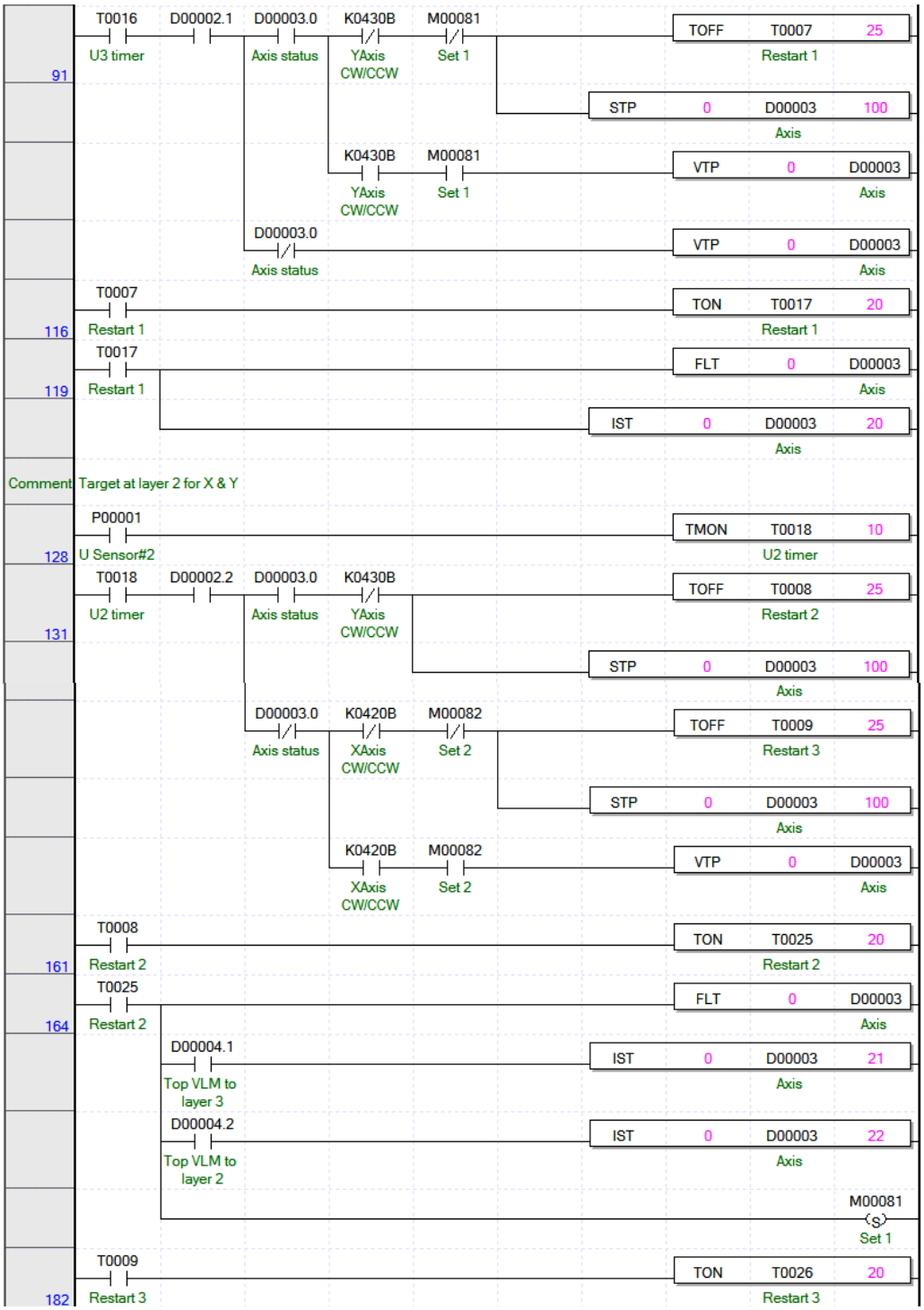
91
T0016
U3 timer
D00002.1
D00003.0
Axis status
K0430B
YAxis
CW/CCW
M00081
Set 1
TOFF T0007 25
Restart 1
STP 0 D00003 100
Axis
K0430B
YAxis
CW/CCW
M00081
Set 1
VTP 0 D00003
Axis
D00003.0
Axis status
VTP 0 D00003
Axis
116
T0007
Restart 1
TON T0017 20
Restart 1
119
T0017
Restart 1
FLT 0 D00003
Axis
IST 0 D00003 20
Axis
Comment
Target at layer 2 for X & Y
128
P00001
U Sensor#2
TMON T0018 10
U2 timer
131
T0018
U2 timer
D00002.2
D00003.0
Axis status
K0430B
YAxis
CW/CCW
TOFF T0008 25
Restart 2
STP 0 D00003 100
Axis
D00003.0
Axis status
K0420B
XAxis
CW/CCW
M00082
Set 2
TOFF T0009 25
Restart 3
STP 0 D00003 100
Axis
K0420B
XAxis
CW/CCW
M00082
Set 2
VTP 0 D00003
Axis
161
T0008
Restart 2
TON T0025 20
Restart 2
164
T0025
Restart 2
FLT 0 D00003
Axis
D00004.1
Top VLM to layer 3
IST 0 D00003 21
Axis
D00004.2
Top VLM to layer 2
IST 0 D00003 22
Axis
M00081
(S)
Set 1
182
T0009
Restart 3
TON T0026 20
Restart 3

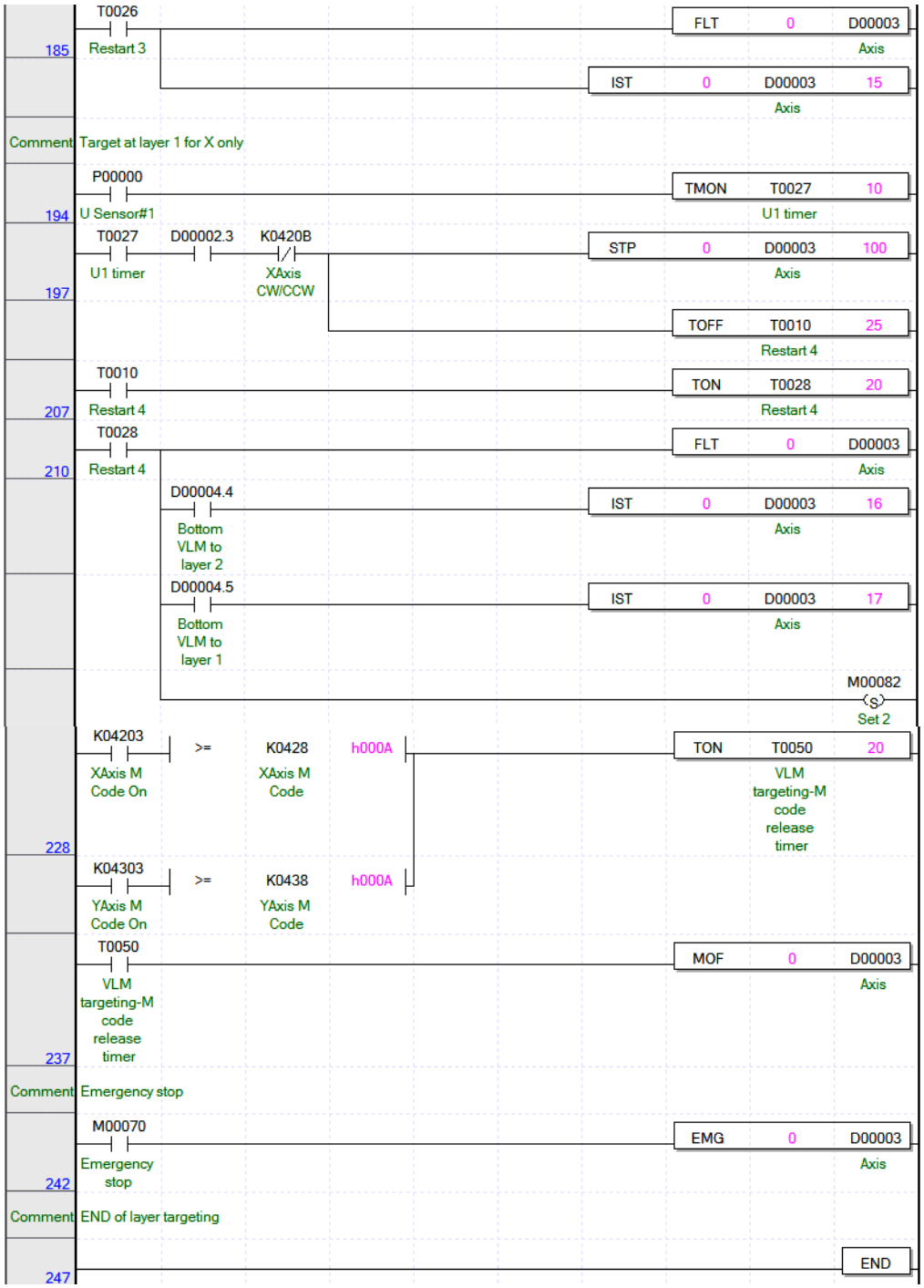
185
T0026
Restart 3
FLT 0 D00003
Axis
IST 0 D00003 15
Axis
Comment
Target at layer 1 for X only
194
P00000
U Sensor#1
TMON T0027 10
U1 timer
197
T0027
U1 timer
D00002.3
K0420B
XAxis CW/CCW
STP 0 D00003 100
Axis
TOFF T0010 25
Restart 4
207
T0010
Restart 4
TON T0028 20
Restart 4
210
T0028
Restart 4
FLT 0 D00003
Axis
D00004.4
Bottom VLM to layer 2
IST 0 D00003 16
Axis
D00004.5
Bottom VLM to layer 1
IST 0 D00003 17
Axis
M00082
S
Set 2
228
K04203
XAxis M Code On
>=
K0428
XAxis M Code
h000A
TON T0050 20
VLM targeting-M code release timer
K04303
YAxis M Code On
>=
K0438
YAxis M Code
h000A
237
T0050
VLM targeting-M code release timer
MOF 0 D00003
Axis
Comment
Emergency stop
242
M00070
Emergency stop
EMG 0 D00003
Axis
Comment
END of layer targeting
247
END

Appendix C.2. PLC program-ladder diagram for manipulator locking

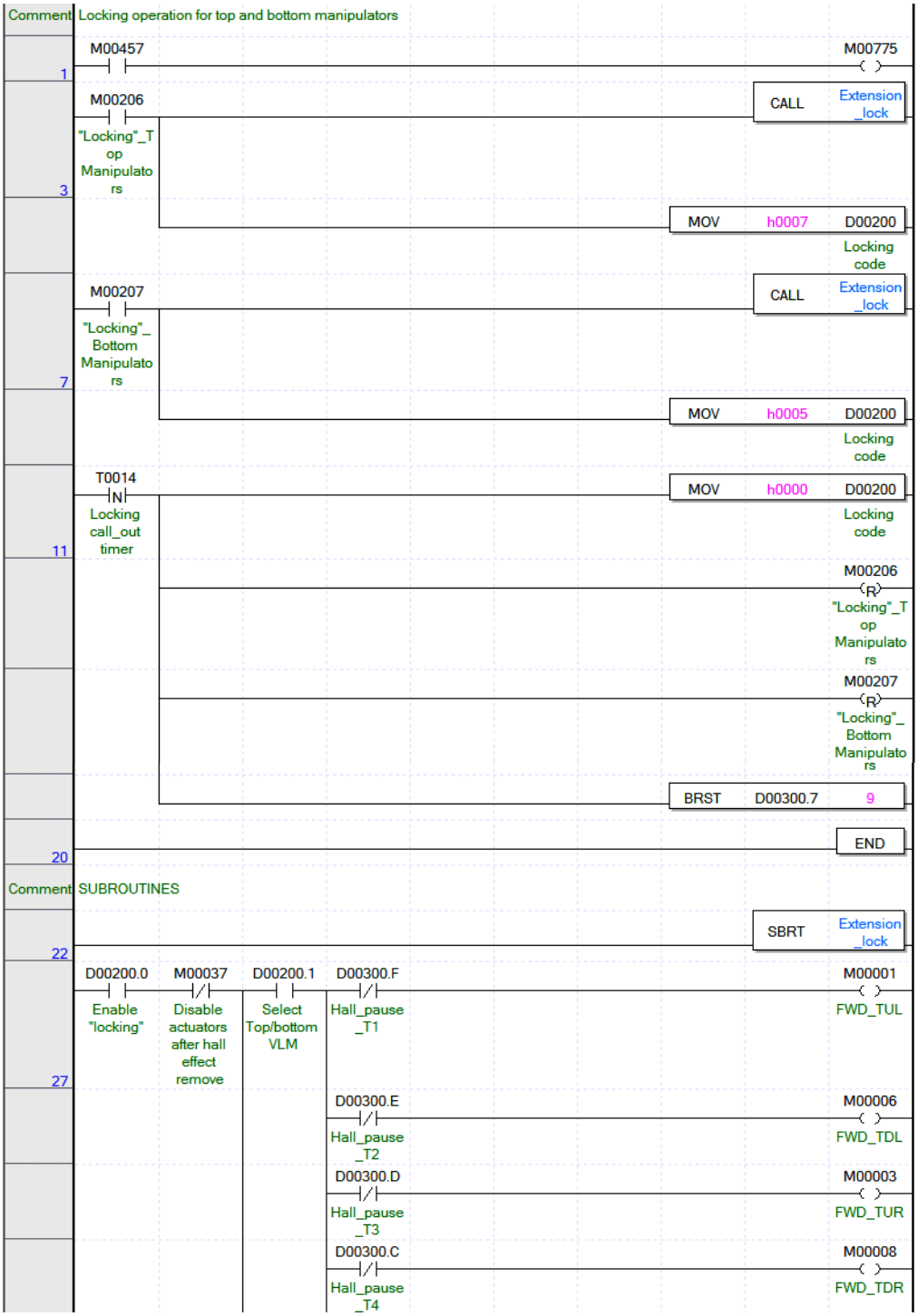

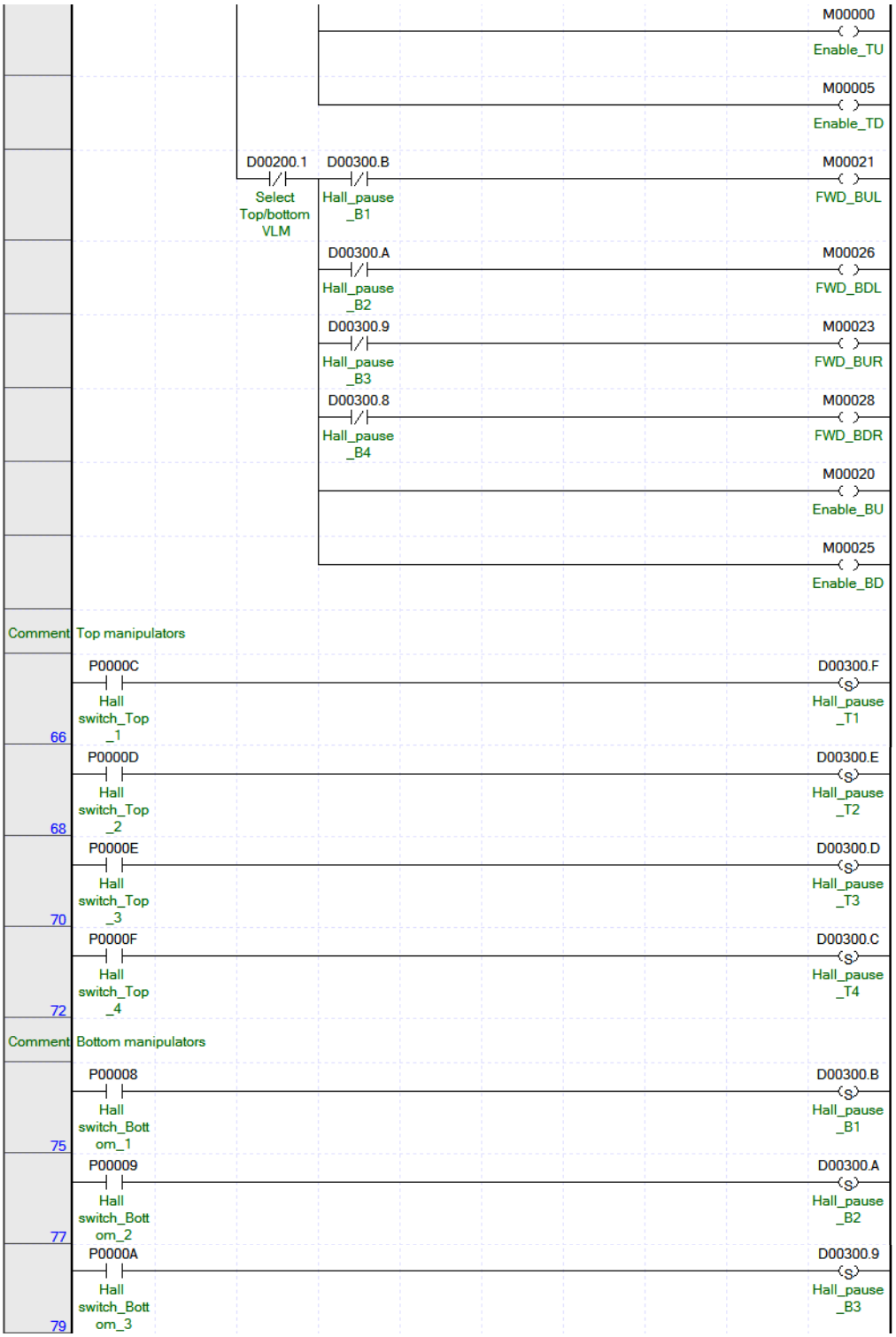
M00000
Enable_TU
M00005
Enable_TD
D00200.1
Select Top/bottom VLM
D00300.B
Hall_pause _B1
M00021
FWD_BUL
D00300.A
Hall_pause _B2
M00026
FWD_BDL
D00300.9
Hall_pause _B3
M00023
FWD_BUR
D00300.8
Hall_pause _B4
M00028
FWD_BDR
M00020
Enable_BU
M00025
Enable_BD
Comment
Top manipulators
66
P0000C
Hall switch_Top _1
D00300.F
Hall_pause _T1
68
P0000D
Hall switch_Top _2
D00300.E
Hall_pause _T2
70
P0000E
Hall switch_Top _3
D00300.D
Hall_pause _T3
72
P0000F
Hall switch_Top _4
D00300.C
Hall_pause _T4
Comment
Bottom manipulators
75
P00008
Hall switch_Bott om_1
D00300.B
Hall_pause _B1
77
P00009
Hall switch_Bott om_2
D00300.A
Hall_pause _B2
79
P0000A
Hall switch_Bott om_3
D00300.9
Hall_pause _B3

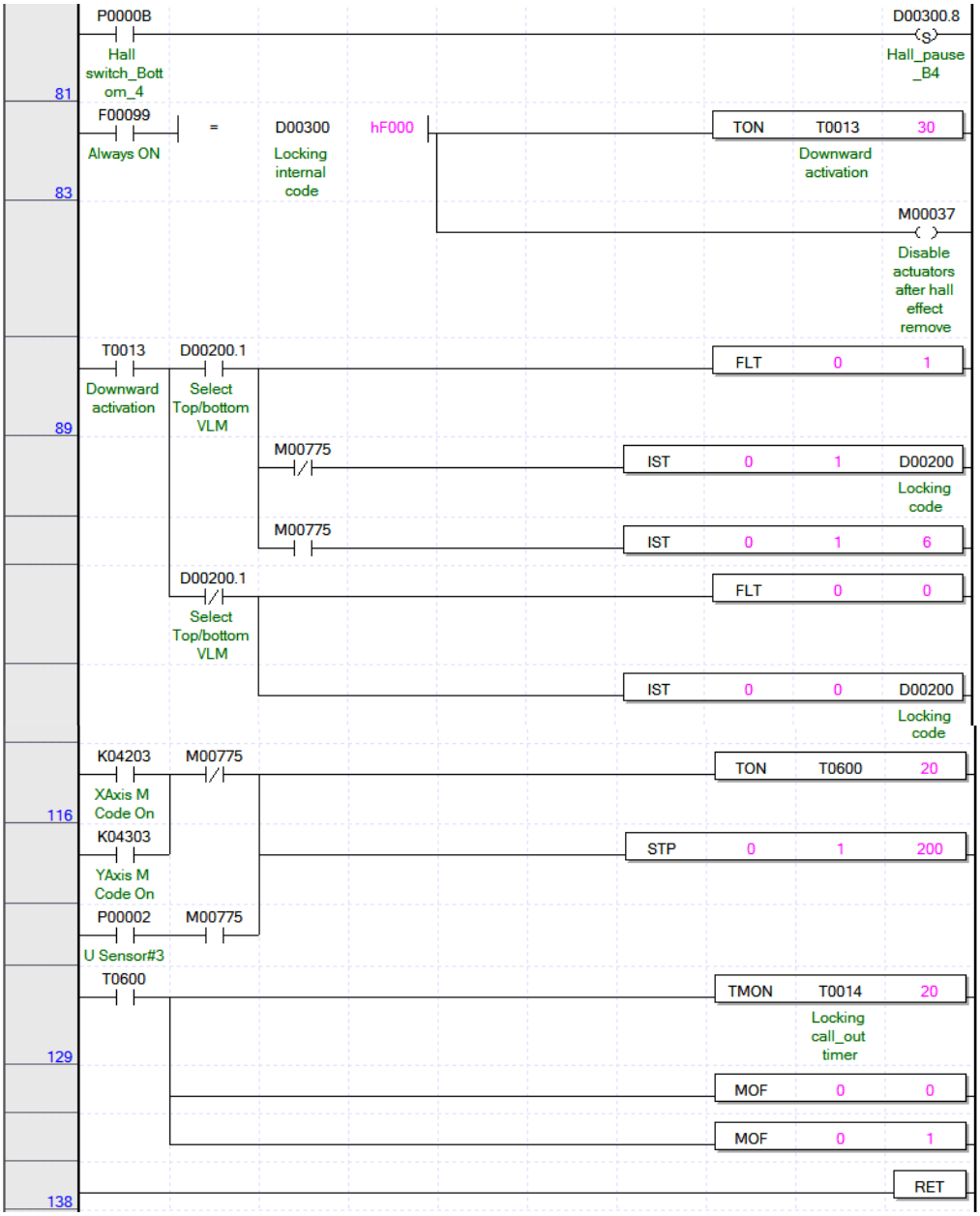
81
P0000B
Hall switch_Bottom_4
D00300.8
Hall_pause_B4
83
F00099
Always ON
=
D00300
Locking internal code
hF000
TON
T0013
30
Downward activation
M00037
Disable actuators after hall effect remove
89
T0013
Downward activation
D00200.1
Select Top/bottom VLM
FLT
0
1
M00775
IST
0
1
D00200
Locking code
M00775
IST
0
1
6
D00200.1
Select Top/bottom VLM
FLT
0
0
IST
0
0
D00200
Locking code
116
K04203
XAxis M Code On
M00775
TON
T0600
20
K04303
YAxis M Code On
STP
0
1
200
P00002
U Sensor#3
M00775
129
T0600
TMON
T0014
20
Locking call_out timer
MOF
0
0
MOF
0
1
138
RET

Appendix C.3. PLC program-ladder diagram for automated gully loading

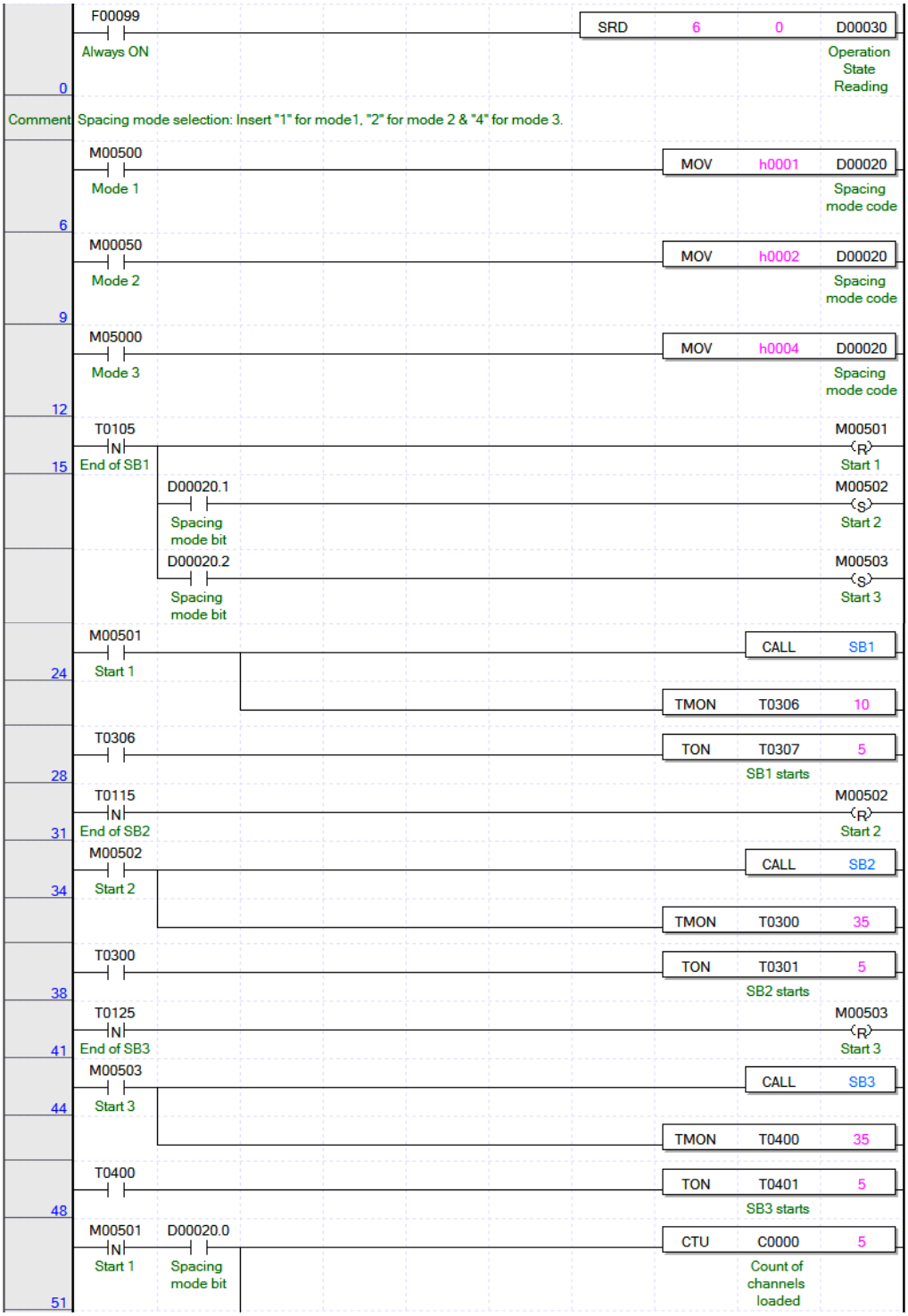

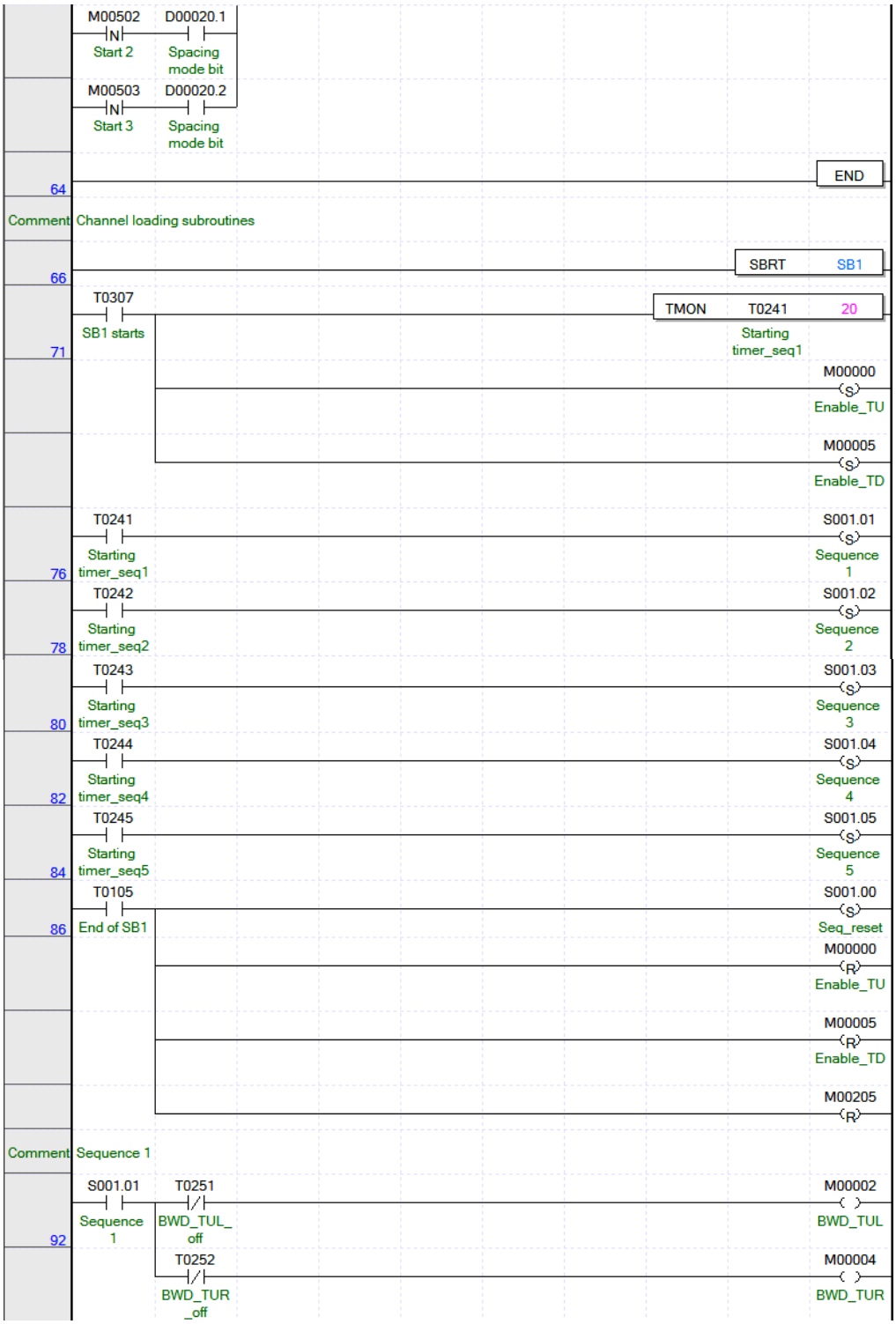
M00502
N
Start 2
D00020.1
Spacing mode bit
M00503
N
Start 3
D00020.2
Spacing mode bit
64
END
Comment
Channel loading subroutines
66
SBRT
SB1
T0307
SB1 starts
71
TMON
T0241
Starting timer_seq1
20
M00000
S
Enable_TU
M00005
S
Enable_TD
T0241
Starting timer_seq1
76
S001.01
S
Sequence 1
T0242
Starting timer_seq2
78
S001.02
S
Sequence 2
T0243
Starting timer_seq3
80
S001.03
S
Sequence 3
T0244
Starting timer_seq4
82
S001.04
S
Sequence 4
T0245
Starting timer_seq5
84
S001.05
S
Sequence 5
T0105
End of SB1
86
S001.00
S
Seq_reset
M00000
R
Enable_TU
M00005
R
Enable_TD
M00205
R
Comment
Sequence 1
S001.01
Sequence 1
T0251
BWD_TUL_ off
92
M00002
BWD_TUL
T0252
BWD_TUR _off
M00004
BWD_TUR

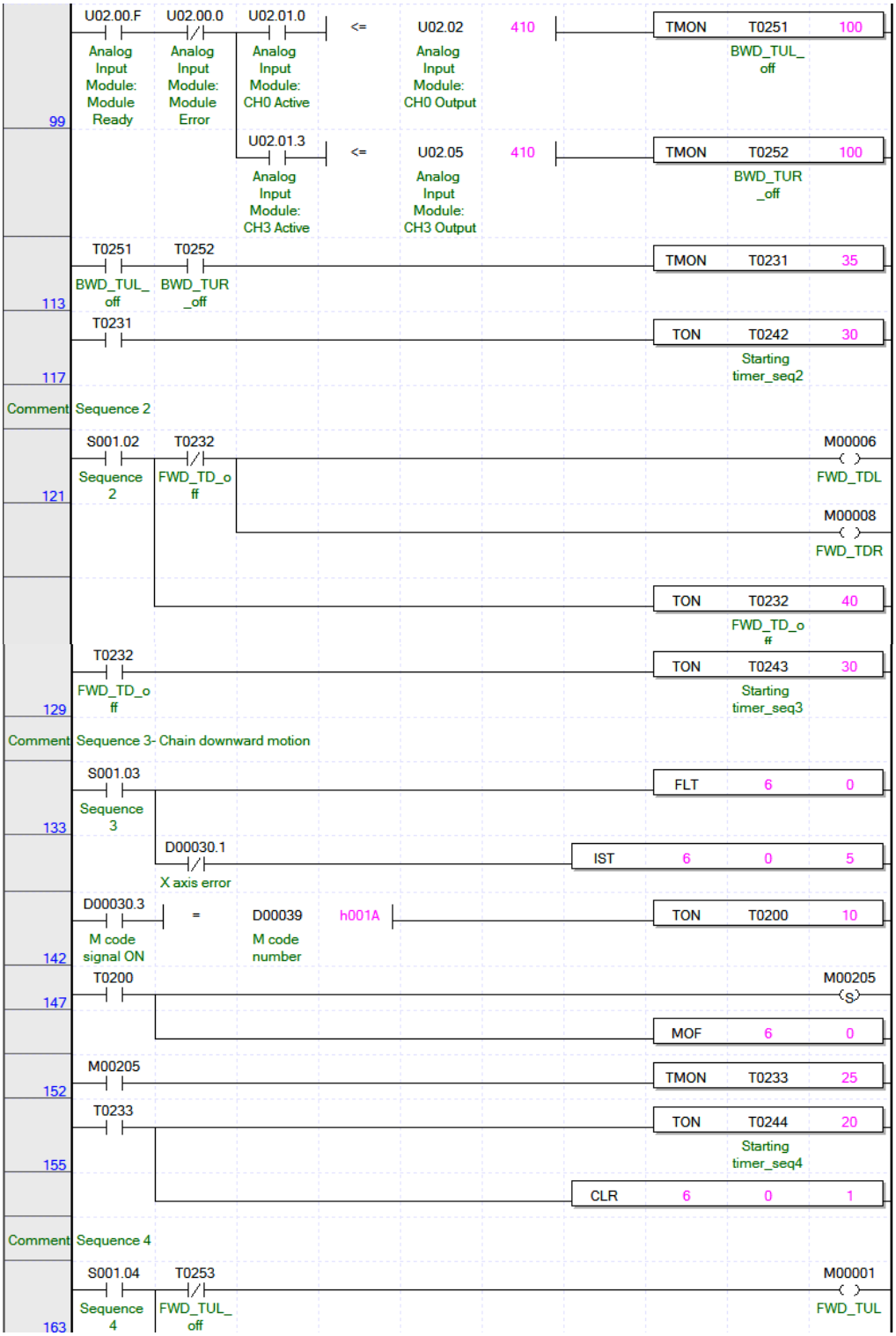
99
U02.00.F
Analog Input Module: Module Ready
U02.00.0
Analog Input Module: Module Error
U02.01.0
Analog Input Module: CH0 Active
<=
U02.02
Analog Input Module: CH0 Output
410
TMON T0251 100
BWD_TUL_ off
U02.01.3
Analog Input Module: CH3 Active
<=
U02.05
Analog Input Module: CH3 Output
410
TMON T0252 100
BWD_TUR _off
113
T0251
BWD_TUL_ off
T0252
BWD_TUR _off
TMON T0231 35
117
T0231
TON T0242 30
Starting timer_seq2
Comment Sequence 2
121
S001.02
Sequence 2
T0232
FWD_TD_o ff
M00006
FWD_TDL
M00008
FWD_TDR
TON T0232 40
FWD_TD_o ff
129
T0232
FWD_TD_o ff
TON T0243 30
Starting timer_seq3
Comment Sequence 3- Chain downward motion
133
S001.03
Sequence 3
FLT 6 0
D00030.1
X axis error
IST 6 0 5
142
D00030.3
M code signal ON
=
D00039
M code number
h001A
TON T0200 10
147
T0200
M00205
MOF 6 0
152
M00205
TMON T0233 25
155
T0233
TON T0244 20
Starting timer_seq4
CLR 6 0 1
Comment Sequence 4
163
S001.04
Sequence 4
T0253
FWD_TUL_ off
M00001
FWD_TUL

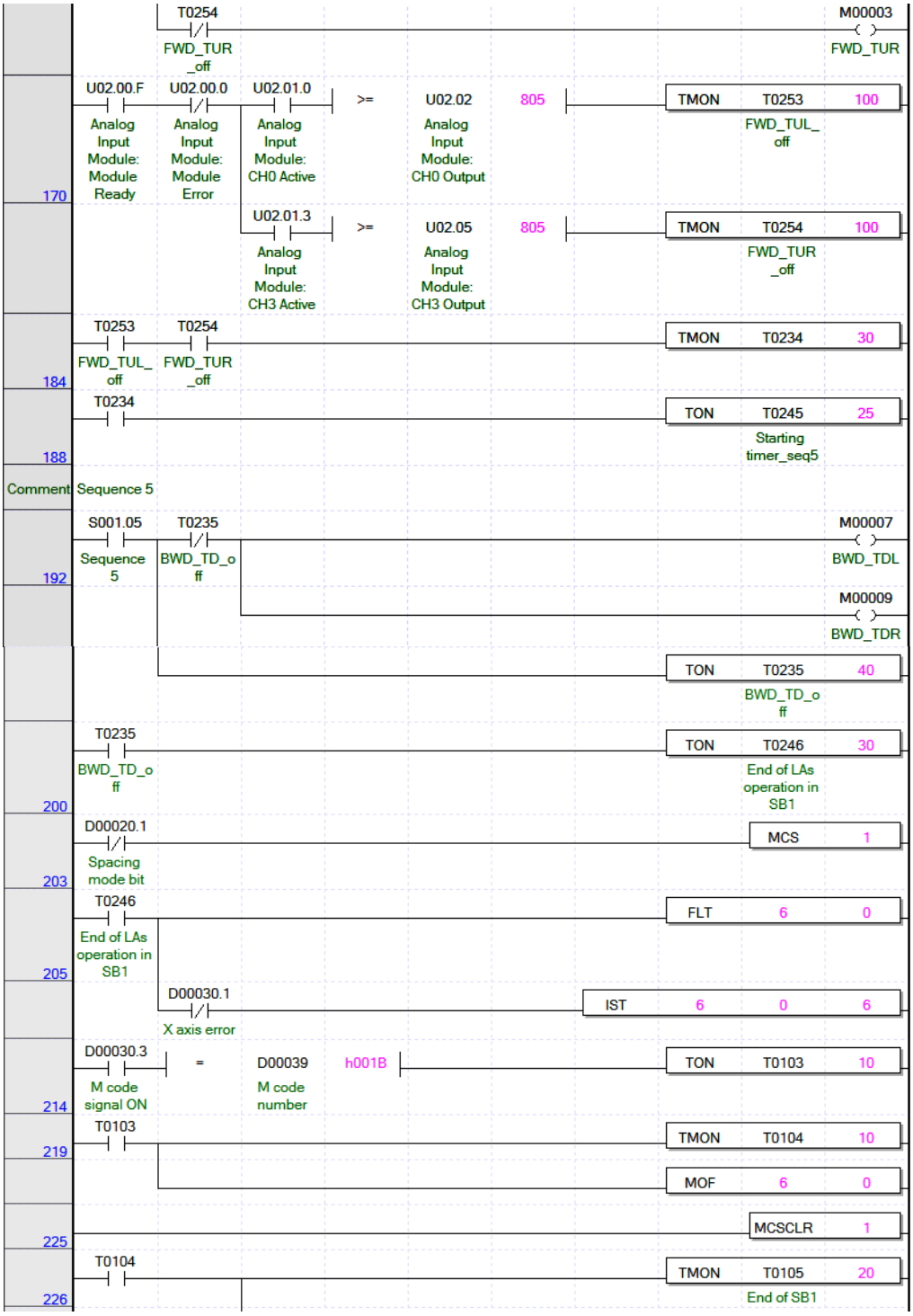
T0254
FWD_TUR_off
M00003
FWD_TUR
U02.00.F
Analog Input Module: Module Ready
U02.00.0
Analog Input Module: Module Error
U02.01.0
Analog Input Module: CH0 Active
>=
U02.02
Analog Input Module: CH0 Output
805
TMON T0253 100
FWD_TUL_off
170
U02.01.3
Analog Input Module: CH3 Active
>=
U02.05
Analog Input Module: CH3 Output
805
TMON T0254 100
FWD_TUR_off
T0253
FWD_TUL_off
T0254
FWD_TUR_off
TMON T0234 30
184
T0234
TON T0245 25
Starting timer_seq5
188
Comment Sequence 5
S001.05
Sequence 5
T0235
BWD_TD_off
M00007
BWD_TDL
192
M00009
BWD_TDR
TON T0235 40
BWD_TD_off
T0235
BWD_TD_off
TON T0246 30
End of LAs operation in SB1
200
D00020.1
Spacing mode bit
MCS 1
203
T0246
End of LAs operation in SB1
FLT 6 0
205
D00030.1
X axis error
IST 6 0 6
D00030.3
M code signal ON
=
D00039
M code number
h001B
TON T0103 10
214
T0103
TMON T0104 10
219
MOF 6 0
MCSCLR 1
225
T0104
TMON T0105 20
End of SB1
226

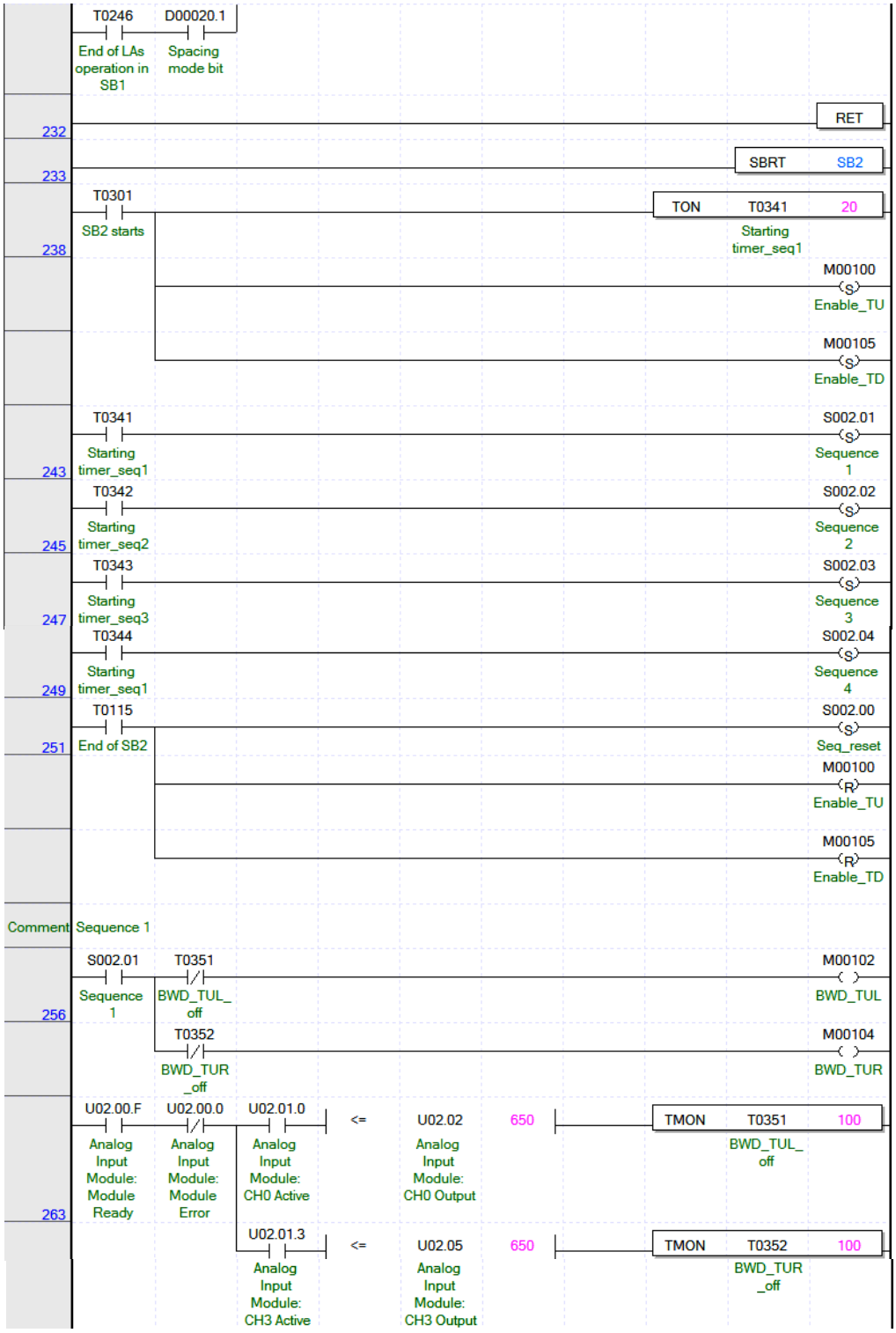
T0246
End of LAs operation in SB1
D00020.1
Spacing mode bit
232
RET
233
SBRT
SB2
T0301
SB2 starts
238
TON
T0341
Starting timer_seq1
20
M00100
Enable_TU
M00105
Enable_TD
T0341
Starting timer_seq1
243
S002.01
Sequence 1
T0342
Starting timer_seq2
245
S002.02
Sequence 2
T0343
Starting timer_seq3
247
S002.03
Sequence 3
T0344
Starting timer_seq1
249
S002.04
Sequence 4
T0115
End of SB2
251
S002.00
Seq_reset
M00100
Enable_TU
M00105
Enable_TD
Comment
Sequence 1
S002.01
Sequence 1
T0351
BWD_TUL_ off
256
M00102
BWD_TUL
T0352
BWD_TUR _off
M00104
BWD_TUR
U02.00.F
Analog Input Module: Module Ready
U02.00.0
Analog Input Module: Module Error
U02.01.0
Analog Input Module: CH0 Active
<=
U02.02
Analog Input Module: CH0 Output
650
TMON
T0351
BWD_TUL_ off
100
263
U02.01.3
Analog Input Module: CH3 Active
<=
U02.05
Analog Input Module: CH3 Output
650
TMON
T0352
BWD_TUR _off
100

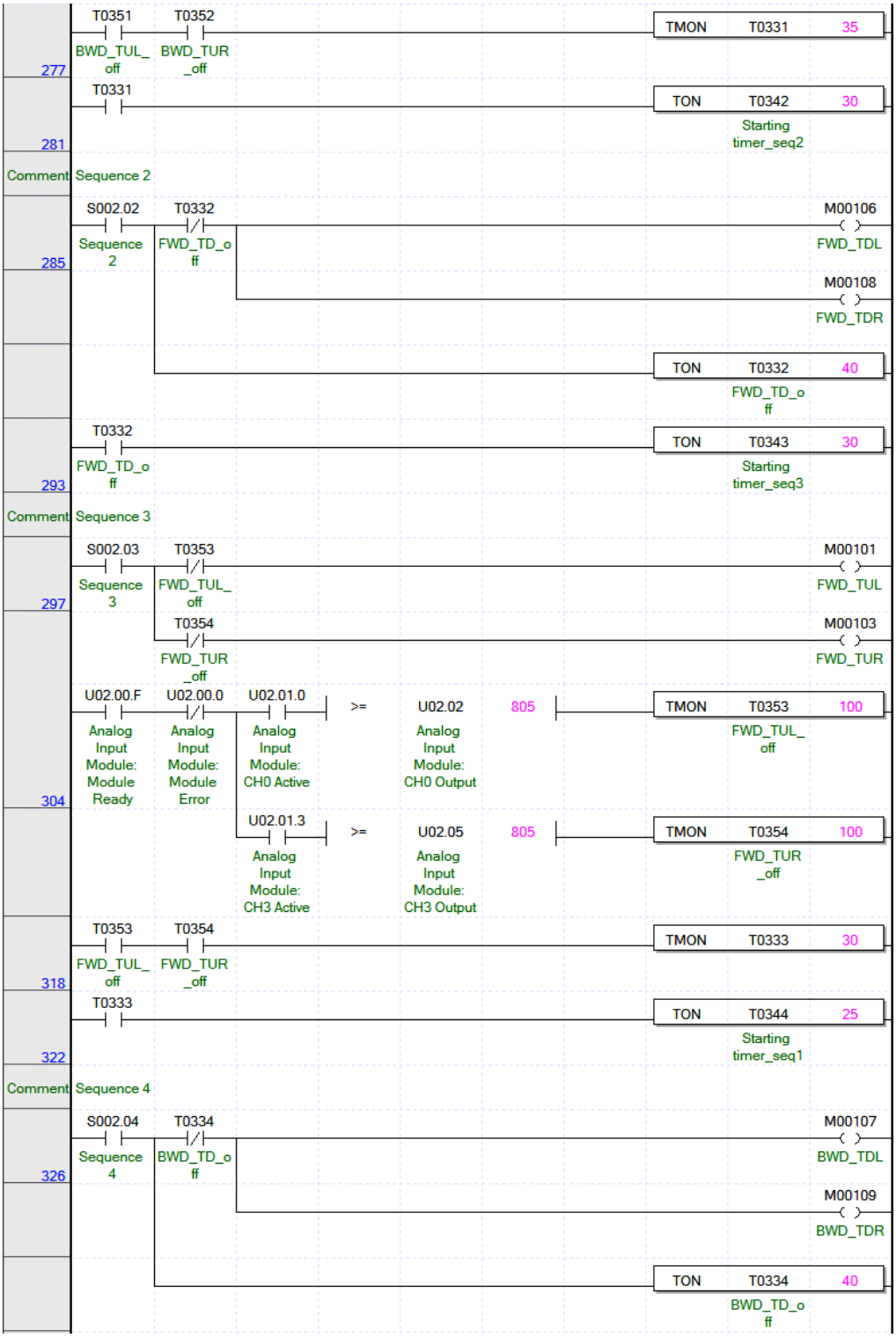
277
T0351
BWD_TUL_off
T0352
BWD_TUR_off
TMON T0331 35
281
T0331
TON T0342 30
Starting timer_seq2
Comment Sequence 2
285
S002.02
Sequence 2
T0332
FWD_TD_off
M00106
FWD_TDL
M00108
FWD_TDR
TON T0332 40
FWD_TD_off
293
T0332
FWD_TD_off
TON T0343 30
Starting timer_seq3
Comment Sequence 3
297
S002.03
Sequence 3
T0353
FWD_TUL_off
M00101
FWD_TUL
T0354
FWD_TUR_off
M00103
FWD_TUR
304
U02.00.F
Analog Input Module: Module Ready
U02.00.0
Analog Input Module: Module Error
U02.01.0
Analog Input Module: CH0 Active
>=
U02.02
Analog Input Module: CH0 Output
805
TMON T0353 100
FWD_TUL_off
U02.01.3
Analog Input Module: CH3 Active
>=
U02.05
Analog Input Module: CH3 Output
805
TMON T0354 100
FWD_TUR_off
318
T0353
FWD_TUL_off
T0354
FWD_TUR_off
TMON T0333 30
322
T0333
TON T0344 25
Starting timer_seq1
Comment Sequence 4
326
S002.04
Sequence 4
T0334
BWD_TD_off
M00107
BWD_TDL
M00109
BWD_TDR
TON T0334 40
BWD_TD_off

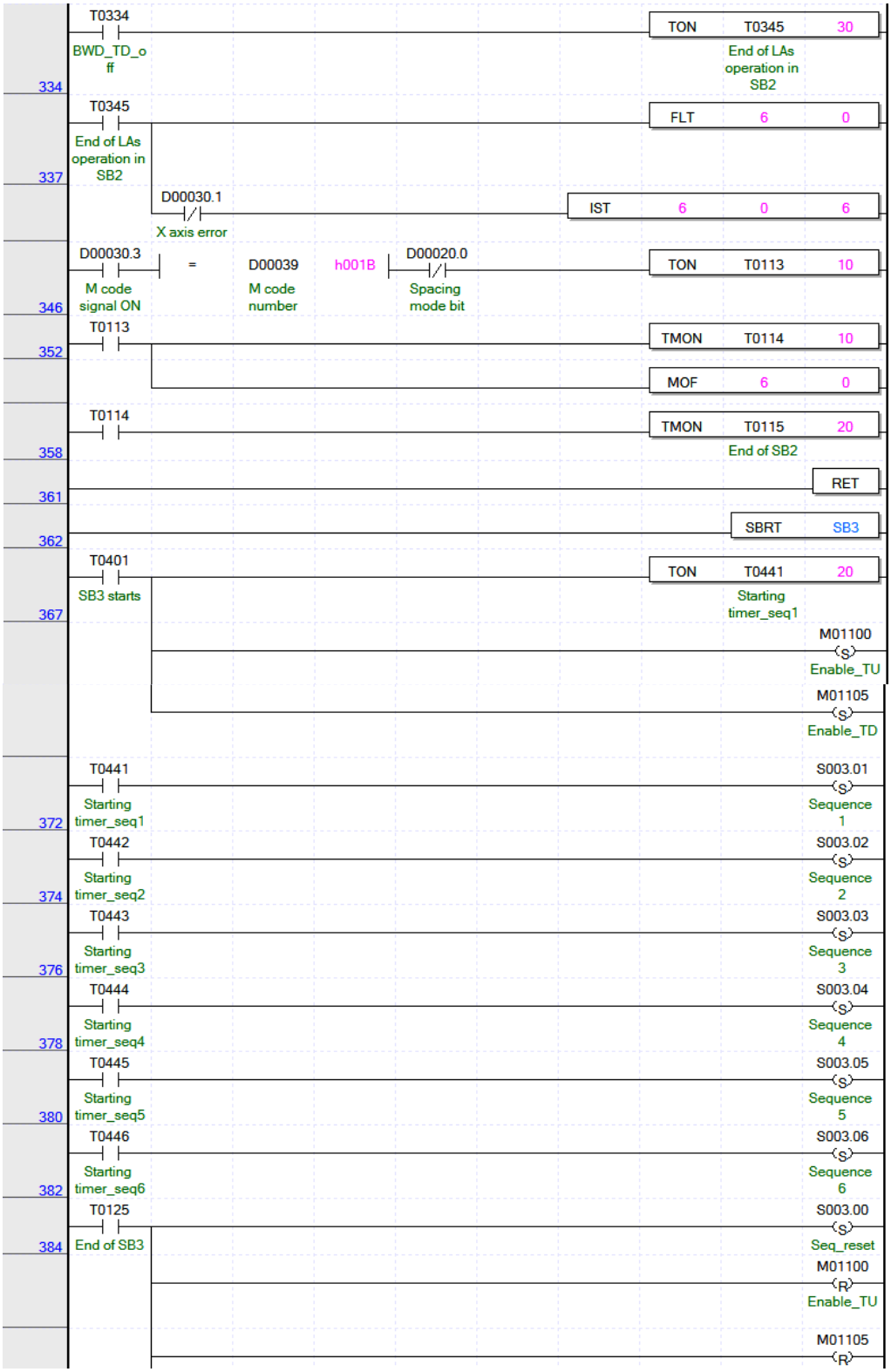
334
T0334
BWD_TD_off
TON T0345 30
End of LAs operation in SB2
337
T0345
End of LAs operation in SB2
FLT 6 0
D00030.1
X axis error
IST 6 0 6
346
D00030.3
M code signal ON
=
D00039
M code number
h001B
D00020.0
Spacing mode bit
TON T0113 10
352
T0113
TMON T0114 10
MOF 6 0
358
T0114
TMON T0115 20
End of SB2
361
RET
362
SBRT SB3
367
T0401
SB3 starts
TON T0441 20
Starting timer_seq1
M01100
Enable_TU
M01105
Enable_TD
372
T0441
Starting timer_seq1
S003.01
Sequence 1
374
T0442
Starting timer_seq2
S003.02
Sequence 2
376
T0443
Starting timer_seq3
S003.03
Sequence 3
378
T0444
Starting timer_seq4
S003.04
Sequence 4
380
T0445
Starting timer_seq5
S003.05
Sequence 5
382
T0446
Starting timer_seq6
S003.06
Sequence 6
384
T0125
End of SB3
S003.00
Seq_reset
M01100
Enable_TU
M01105

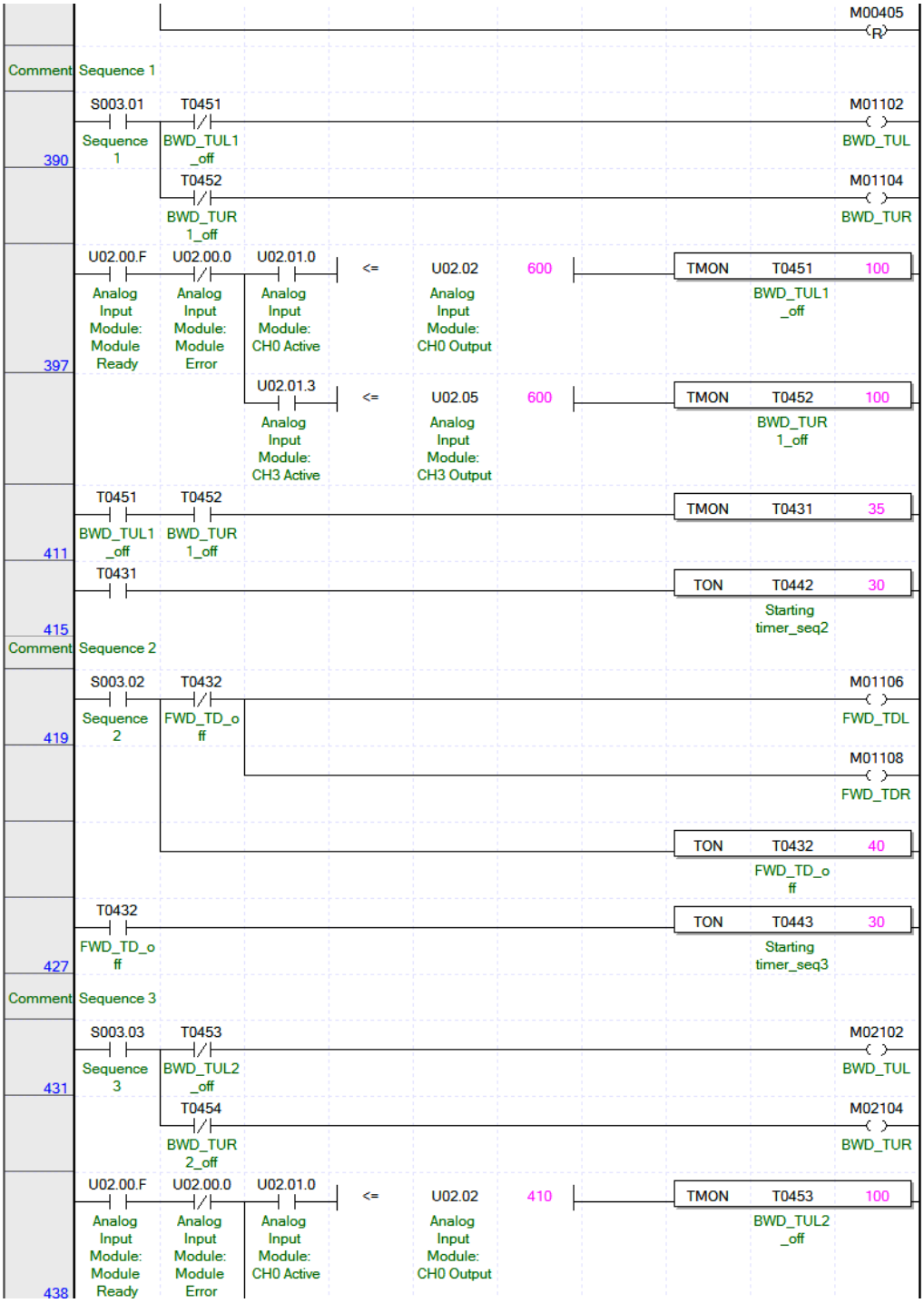
M00405
R
Comment
Sequence 1
S003.01
Sequence 1
T0451
BWD_TUL1_off
M01102
BWD_TUL
390
T0452
BWD_TUR1_off
M01104
BWD_TUR
U02.00.F
Analog Input Module: Module Ready
U02.00.0
Analog Input Module: Module Error
U02.01.0
Analog Input Module: CH0 Active
<=
U02.02
Analog Input Module: CH0 Output
600
TMON
T0451
100
BWD_TUL1_off
397
U02.01.3
Analog Input Module: CH3 Active
<=
U02.05
Analog Input Module: CH3 Output
600
TMON
T0452
100
BWD_TUR1_off
T0451
BWD_TUL1_off
T0452
BWD_TUR1_off
TMON
T0431
35
411
T0431
TON
T0442
30
Starting timer_seq2
415
Comment
Sequence 2
S003.02
Sequence 2
T0432
FWD_TD_off
M01106
FWD_TDL
419
M01108
FWD_TDR
TON
T0432
40
FWD_TD_off
T0432
FWD_TD_off
TON
T0443
30
Starting timer_seq3
427
Comment
Sequence 3
S003.03
Sequence 3
T0453
BWD_TUL2_off
M02102
BWD_TUL
431
T0454
BWD_TUR2_off
M02104
BWD_TUR
U02.00.F
Analog Input Module: Module Ready
U02.00.0
Analog Input Module: Module Error
U02.01.0
Analog Input Module: CH0 Active
<=
U02.02
Analog Input Module: CH0 Output
410
TMON
T0453
100
BWD_TUL2_off
438

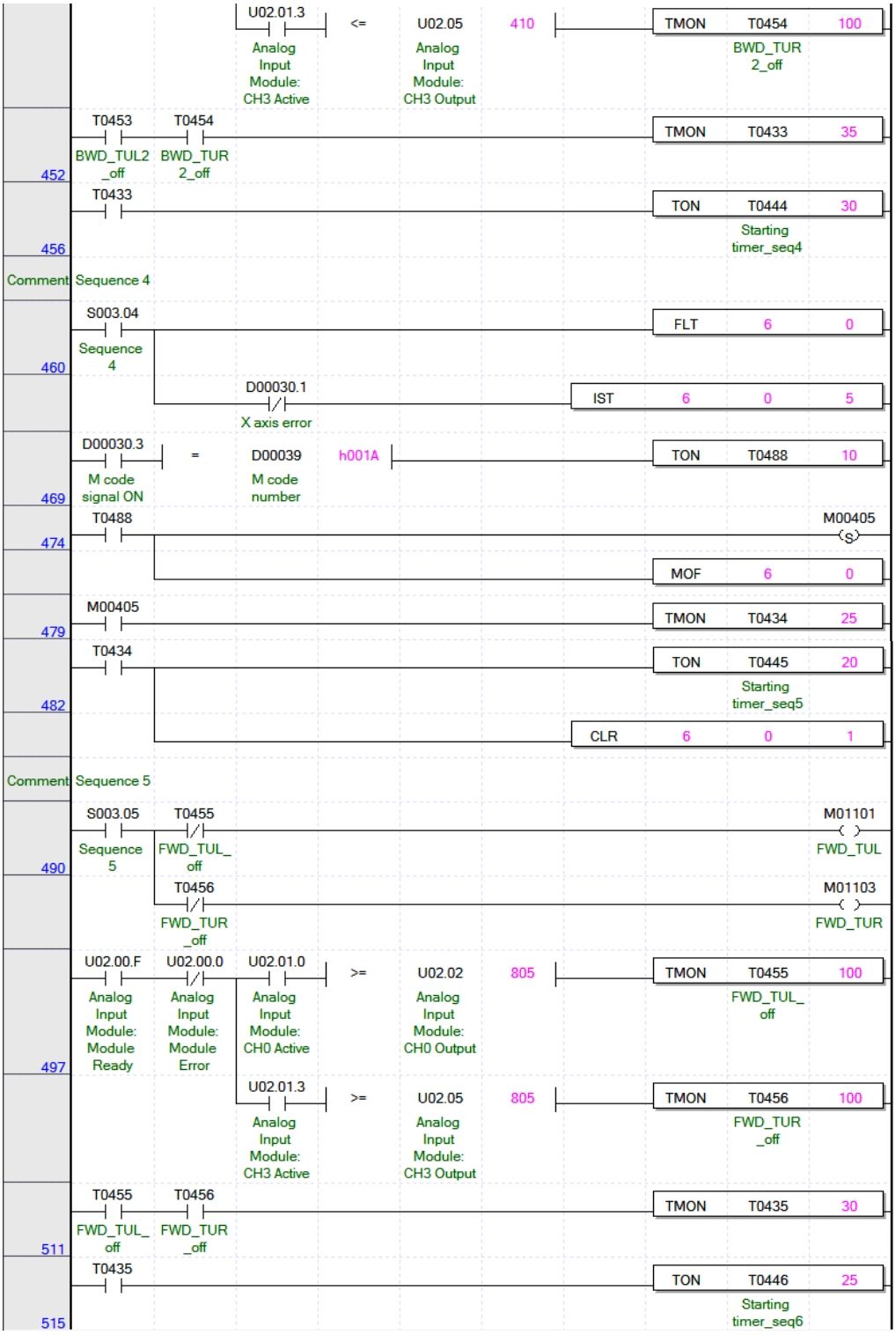
U02.01.3
<=
U02.05
410
TMON T0454 100
Analog Input Module: CH3 Active
Analog Input Module: CH3 Output
BWD_TUR 2_off
T0453
T0454
TMON T0433 35
BWD_TUL2 _off
BWD_TUR 2_off
452
T0433
TON T0444 30
Starting timer_seq4
456
Comment Sequence 4
S003.04
FLT 6 0
Sequence 4
460
D00030.1
IST 6 0 5
X axis error
D00030.3
=
D00039
h001A
TON T0488 10
M code signal ON
M code number
469
T0488
M00405
474
MOF 6 0
M00405
TMON T0434 25
479
T0434
TON T0445 20
Starting timer_seq5
482
CLR 6 0 1
Comment Sequence 5
S003.05
T0455
M01101
Sequence 5
FWD_TUL_ off
FWD_TUL
490
T0456
M01103
FWD_TUR _off
FWD_TUR
U02.00.F
U02.00.0
U02.01.0
>=
U02.02
805
TMON T0455 100
Analog Input Module: Module Ready
Analog Input Module: Module Error
Analog Input Module: CH0 Active
Analog Input Module: CH0 Output
FWD_TUL_ off
497
U02.01.3
>=
U02.05
805
TMON T0456 100
Analog Input Module: CH3 Active
Analog Input Module: CH3 Output
FWD_TUR _off
T0455
T0456
TMON T0435 30
FWD_TUL_ off
FWD_TUR _off
511
T0435
TON T0446 25
Starting timer_seq6
515

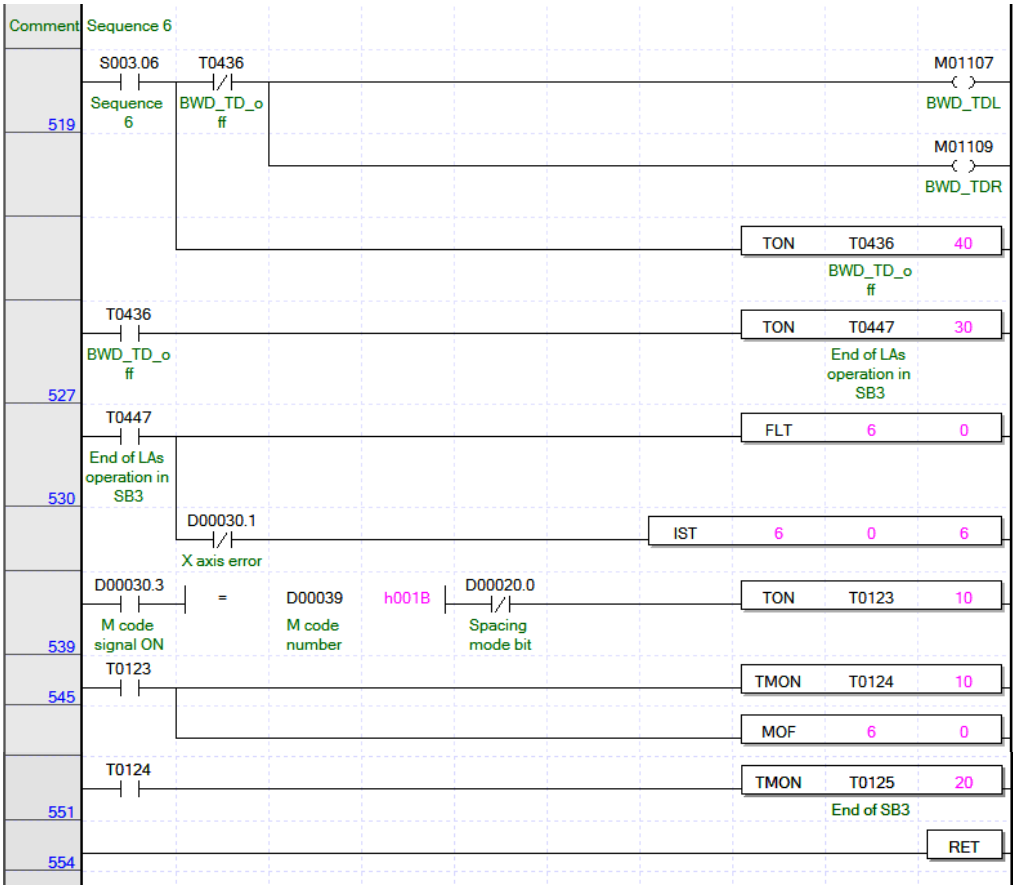
Comment
Sequence 6
519
S003.06
Sequence 6
T0436
BWD_TD_off
M01107
BWD_TDL
M01109
BWD_TDR
TON T0436 40
BWD_TD_off
527
T0436
BWD_TD_off
TON T0447 30
End of LAs operation in SB3
530
T0447
End of LAs operation in SB3
FLT 6 0
D00030.1
X axis error
IST 6 0 6
539
D00030.3
M code signal ON
=
D00039
M code number
h001B
D00020.0
Spacing mode bit
TON T0123 10
545
T0123
TMON T0124 10
MOF 6 0
551
T0124
TMON T0125 20
End of SB3
554
RET

Appendix C.4. PLC program-ladder diagram for automated displacement of gullies from horizontal conveying line to layer 3

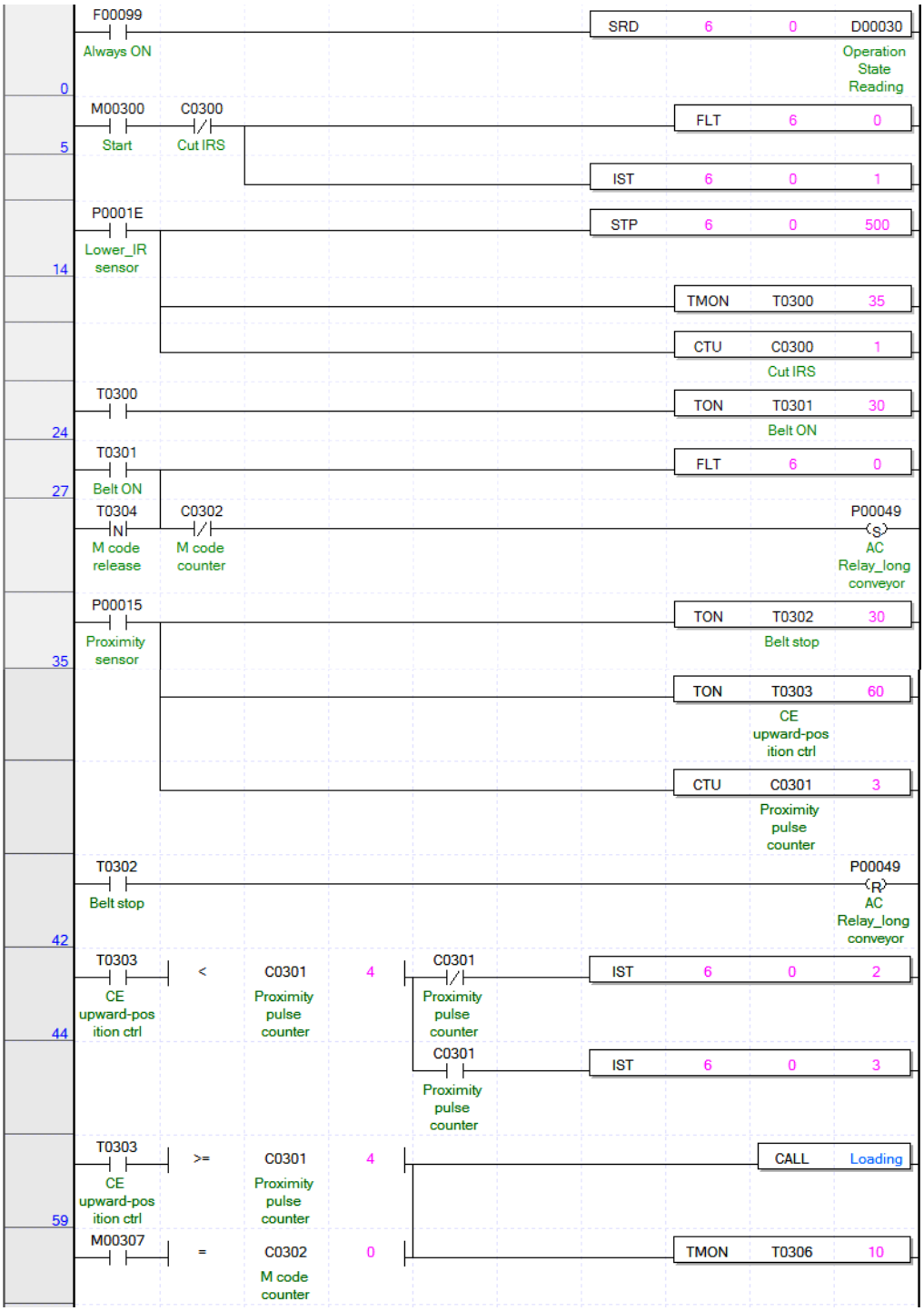

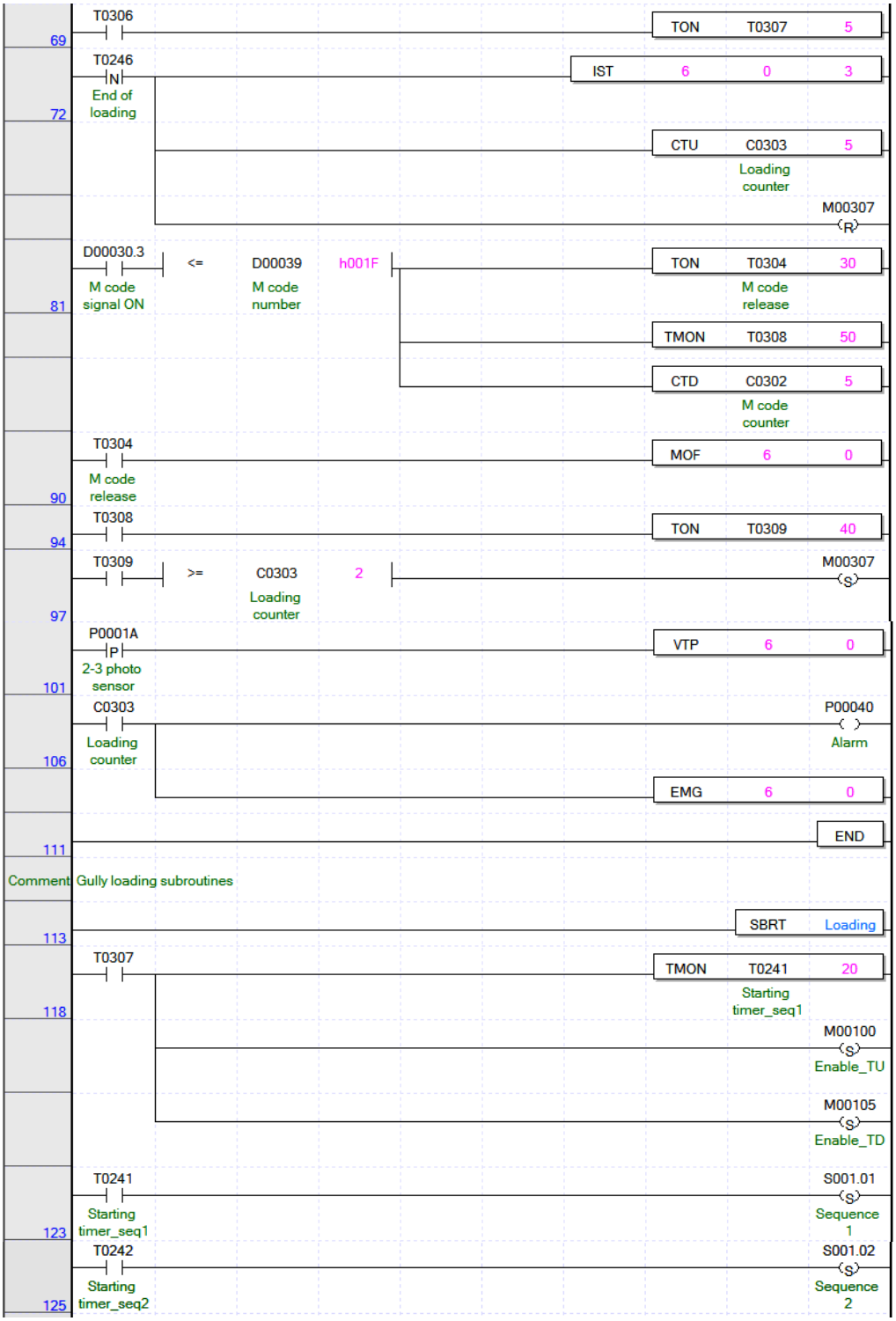
69
T0306
TON T0307 5
72
T0246
N
End of loading
IST 6 0 3
CTU C0303 5
Loading counter
M00307
R
81
D00030.3
M code signal ON
<=
D00039
M code number
h001F
TON T0304 30
M code release
TMON T0308 50
CTD C0302 5
M code counter
90
T0304
M code release
MOF 6 0
94
T0308
TON T0309 40
97
T0309
>=
C0303
Loading counter
2
M00307
S
101
P0001A
P
2-3 photo sensor
VTP 6 0
106
C0303
Loading counter
P00040
Alarm
EMG 6 0
111
END
Comment
Gully loading subroutines
113
SBRT Loading
118
T0307
TMON T0241 20
Starting timer_seq1
M00100
S
Enable_TU
M00105
S
Enable_TD
123
T0241
Starting timer_seq1
S001.01
S
Sequence 1
125
T0242
Starting timer_seq2
S001.02
S
Sequence 2

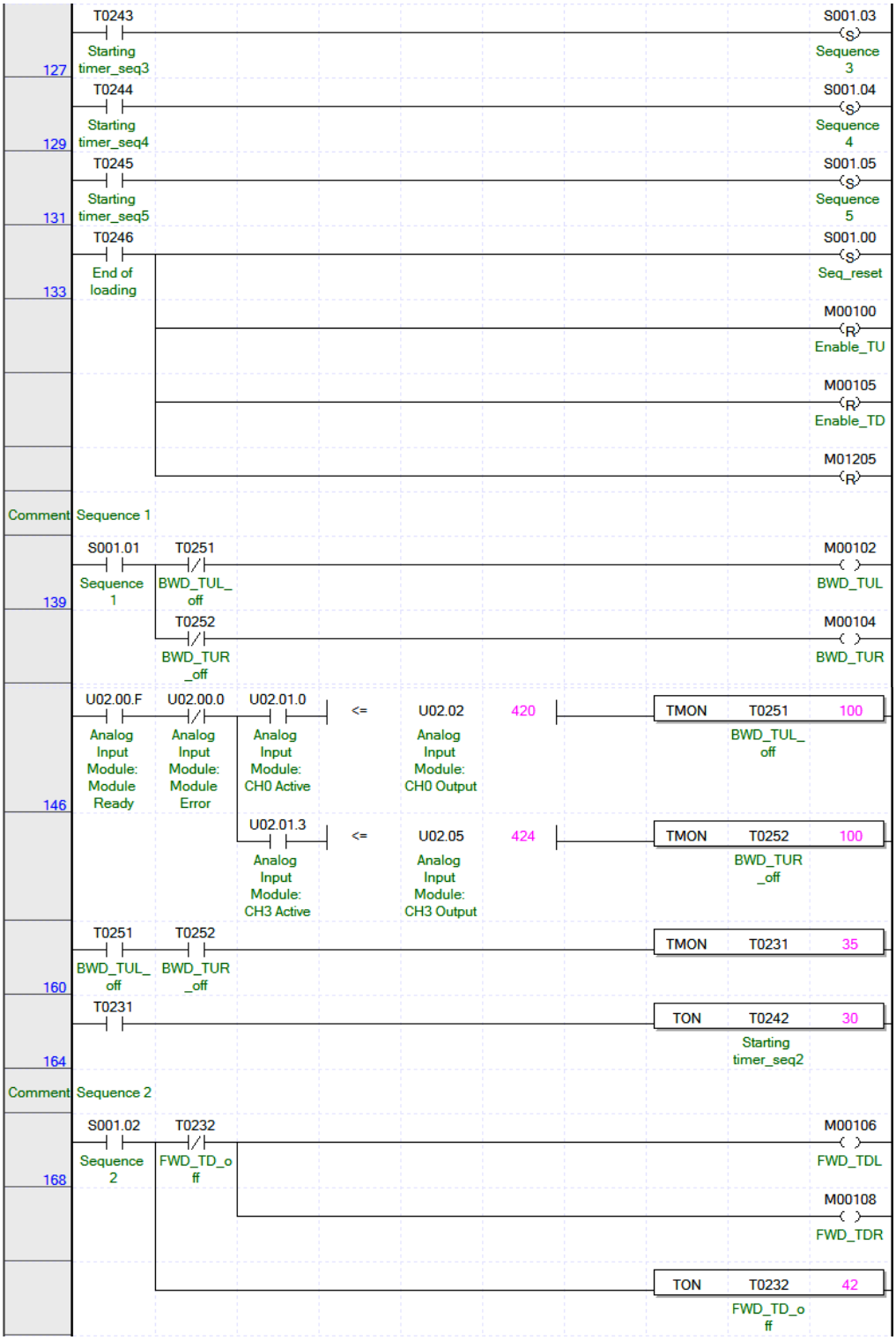
127
T0243
Starting timer_seq3
S001.03
Sequence 3
129
T0244
Starting timer_seq4
S001.04
Sequence 4
131
T0245
Starting timer_seq5
S001.05
Sequence 5
133
T0246
End of loading
S001.00
Seq_reset
M00100
Enable_TU
M00105
Enable_TD
M01205
Comment Sequence 1
139
S001.01
Sequence 1
T0251
BWD_TUL_ off
M00102
BWD_TUL
T0252
BWD_TUR _off
M00104
BWD_TUR
146
U02.00.F
Analog Input Module: Module Ready
U02.00.0
Analog Input Module: Module Error
U02.01.0
Analog Input Module: CH0 Active
<=
U02.02
Analog Input Module: CH0 Output
420
TMON T0251 100
BWD_TUL_ off
U02.01.3
Analog Input Module: CH3 Active
<=
U02.05
Analog Input Module: CH3 Output
424
TMON T0252 100
BWD_TUR _off
160
T0251
BWD_TUL_ off
T0252
BWD_TUR _off
TMON T0231 35
T0231
TON T0242 30
Starting timer_seq2
164
Comment Sequence 2
168
S001.02
Sequence 2
T0232
FWD_TD_o ff
M00106
FWD_TDL
M00108
FWD_TDR
TON T0232 42
FWD_TD_o ff

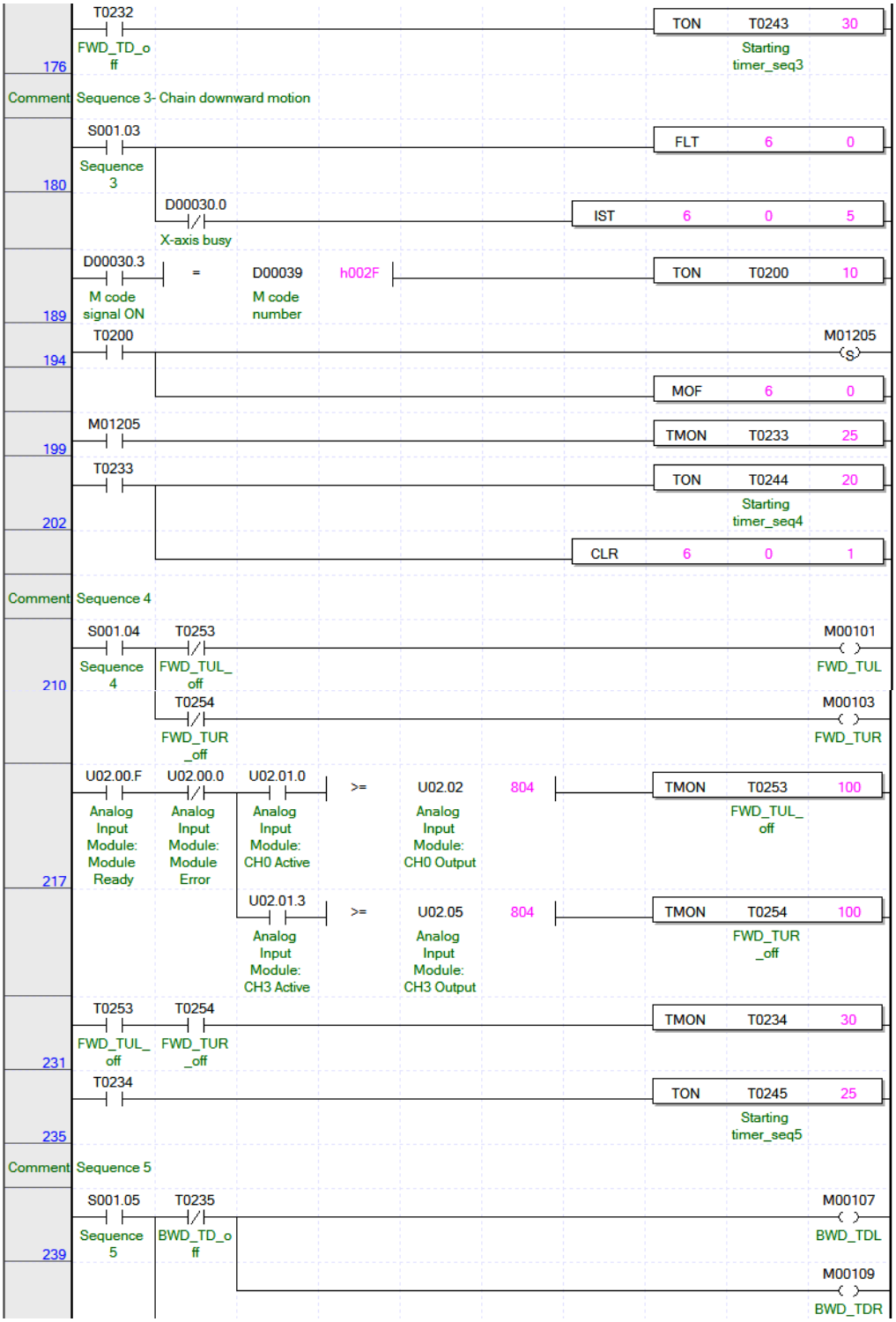
176
T0232
FWD_TD_off
TON T0243 30
Starting timer_seq3
Comment Sequence 3- Chain downward motion
180
S001.03
Sequence 3
FLT 6 0
D00030.0
X-axis busy
IST 6 0 5
189
D00030.3
M code signal ON
=
D00039
M code number
h002F
TON T0200 10
194
T0200
M01205
MOF 6 0
199
M01205
TMON T0233 25
202
T0233
TON T0244 20
Starting timer_seq4
CLR 6 0 1
Comment Sequence 4
210
S001.04
Sequence 4
T0253
FWD_TUL_off
M00101
FWD_TUL
T0254
FWD_TUR_off
M00103
FWD_TUR
217
U02.00.F
Analog Input Module: Module Ready
U02.00.0
Analog Input Module: Module Error
U02.01.0
Analog Input Module: CH0 Active
>=
U02.02
Analog Input Module: CH0 Output
804
TMON T0253 100
FWD_TUL_off
U02.01.3
Analog Input Module: CH3 Active
>=
U02.05
Analog Input Module: CH3 Output
804
TMON T0254 100
FWD_TUR_off
231
T0253
FWD_TUL_off
T0254
FWD_TUR_off
TMON T0234 30
235
T0234
TON T0245 25
Starting timer_seq5
Comment Sequence 5
239
S001.05
Sequence 5
T0235
BWD_TD_off
M00107
BWD_TDL
M00109
BWD_TDR

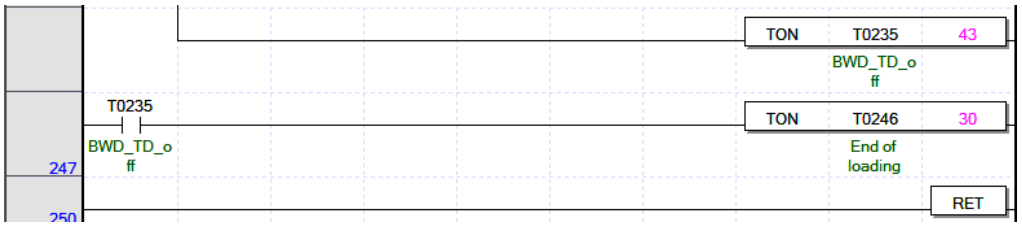
TON
T0235
43
BWD_TD_o
ff
T0235
BWD_TD_o
ff
TON
T0246
30
End of
loading
247
RET
250

Appendix C.5. PLC program-ladder diagram for automated displacement of gullies from layer 3 to layer 2

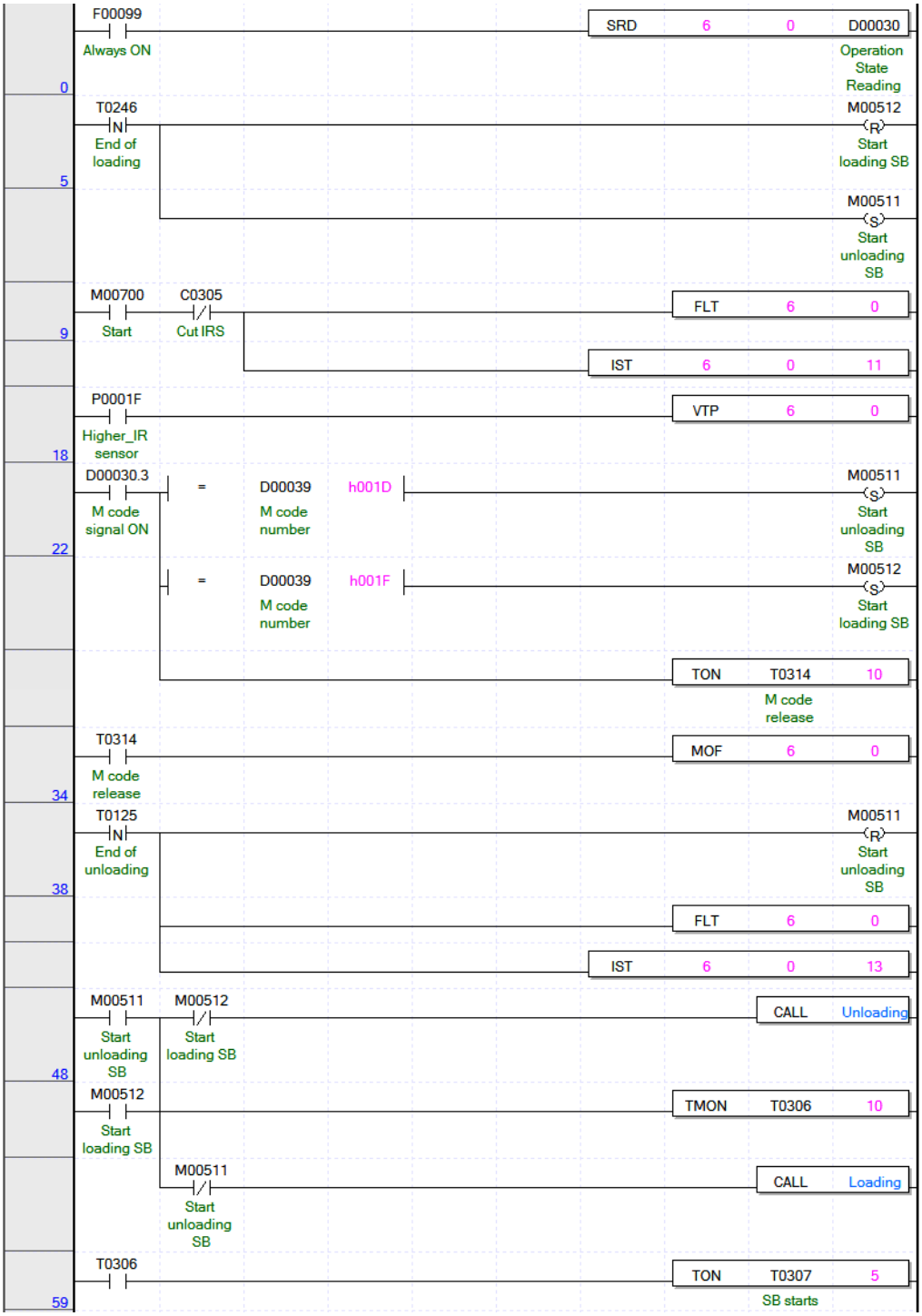

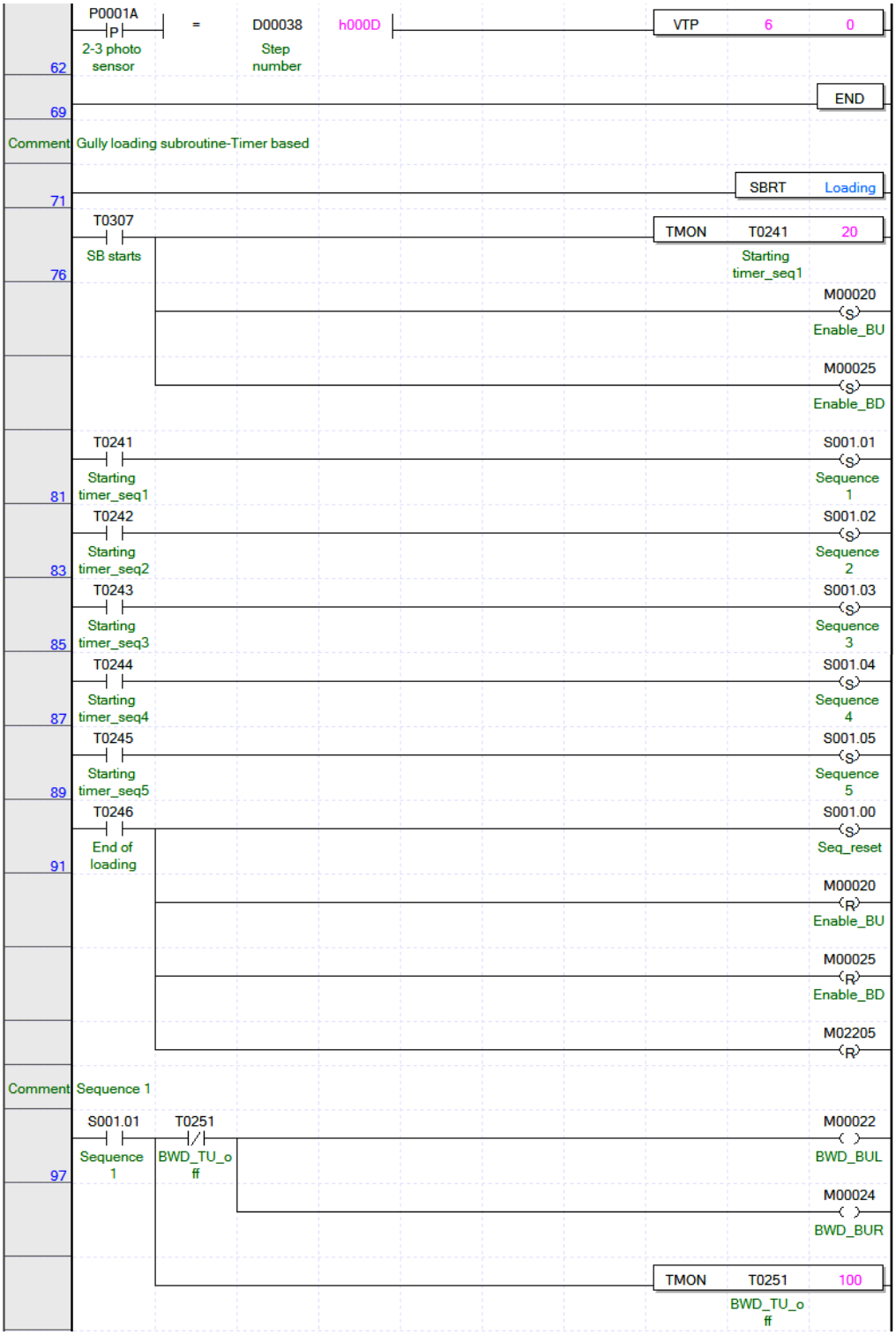
62
P0001A
P
2-3 photo sensor
=
D00038
Step number
h000D
VTP
6
0
69
END
Comment
Gully loading subroutine-Timer based
71
SBRT
Loading
76
T0307
SB starts
TMON
T0241
Starting timer_seq1
20
M00020
S
Enable_BU
M00025
S
Enable_BD
81
T0241
Starting timer_seq1
S001.01
S
Sequence 1
83
T0242
Starting timer_seq2
S001.02
S
Sequence 2
85
T0243
Starting timer_seq3
S001.03
S
Sequence 3
87
T0244
Starting timer_seq4
S001.04
S
Sequence 4
89
T0245
Starting timer_seq5
S001.05
S
Sequence 5
91
T0246
End of loading
S001.00
S
Seq_reset
M00020
R
Enable_BU
M00025
R
Enable_BD
M02205
R
Comment
Sequence 1
97
S001.01
Sequence 1
T0251
BWD_TU_off
M00022
BWD_BUL
M00024
BWD_BUR
TMON
T0251
BWD_TU_off
100

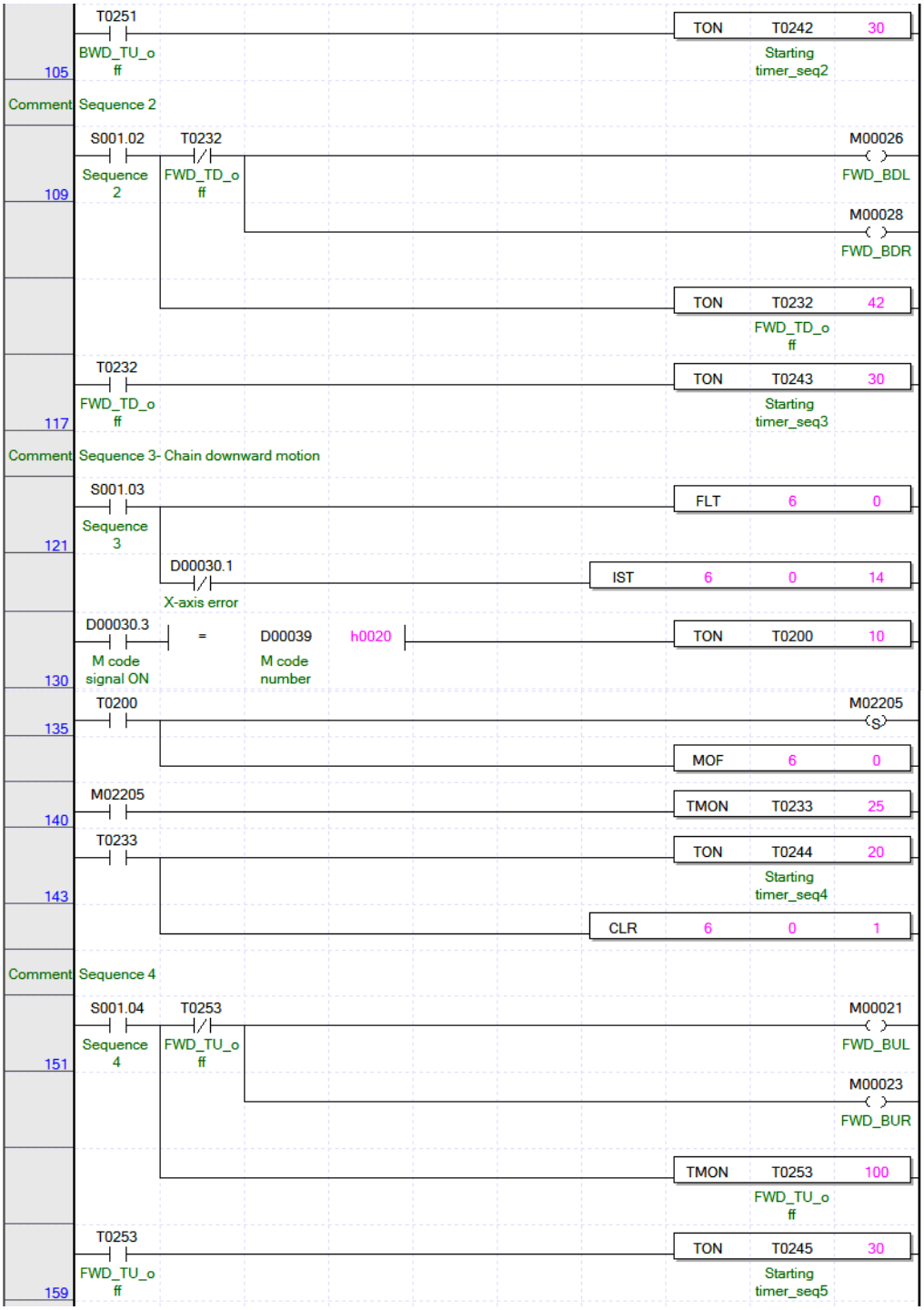
105
T0251
BWD_TU_off
TON T0242 30
Starting timer_seq2
Comment Sequence 2
109
S001.02
Sequence 2
T0232
FWD_TD_off
M00026
FWD_BDL
M00028
FWD_BDR
TON T0232 42
FWD_TD_off
117
T0232
FWD_TD_off
TON T0243 30
Starting timer_seq3
Comment Sequence 3- Chain downward motion
121
S001.03
Sequence 3
FLT 6 0
D00030.1
X-axis error
IST 6 0 14
130
D00030.3
M code signal ON
=
D00039
M code number
h0020
TON T0200 10
135
T0200
M02205
MOF 6 0
140
M02205
TMON T0233 25
143
T0233
TON T0244 20
Starting timer_seq4
CLR 6 0 1
Comment Sequence 4
151
S001.04
Sequence 4
T0253
FWD_TU_off
M00021
FWD_BUL
M00023
FWD_BUR
TMON T0253 100
FWD_TU_off
159
T0253
FWD_TU_off
TON T0245 30
Starting timer_seq5

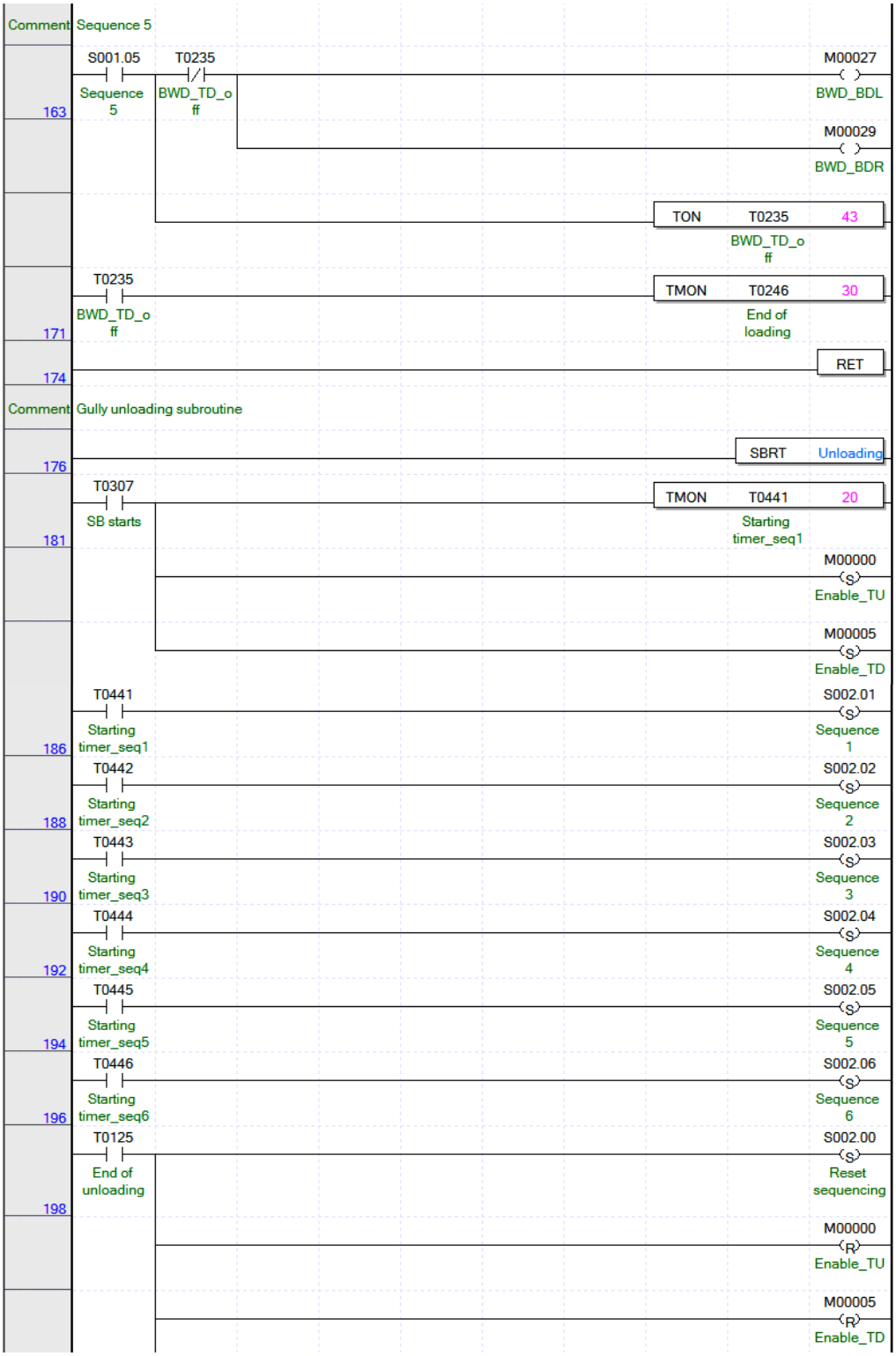
Comment
Sequence 5
S001.05
Sequence 5
T0235
BWD_TD_off
M00027
BWD_BDL
163
M00029
BWD_BDR
TON
T0235
43
BWD_TD_off
T0235
BWD_TD_off
TMON
T0246
30
End of loading
171
RET
174
Comment
Gully unloading subroutine
SBRT
Unloading
176
T0307
SB starts
TMON
T0441
20
Starting timer_seq1
181
M00000
Enable_TU
M00005
Enable_TD
T0441
Starting timer_seq1
S002.01
Sequence 1
186
T0442
Starting timer_seq2
S002.02
Sequence 2
188
T0443
Starting timer_seq3
S002.03
Sequence 3
190
T0444
Starting timer_seq4
S002.04
Sequence 4
192
T0445
Starting timer_seq5
S002.05
Sequence 5
194
T0446
Starting timer_seq6
S002.06
Sequence 6
196
T0125
End of unloading
S002.00
Reset sequencing
198
M00000
Enable_TU
M00005
Enable_TD

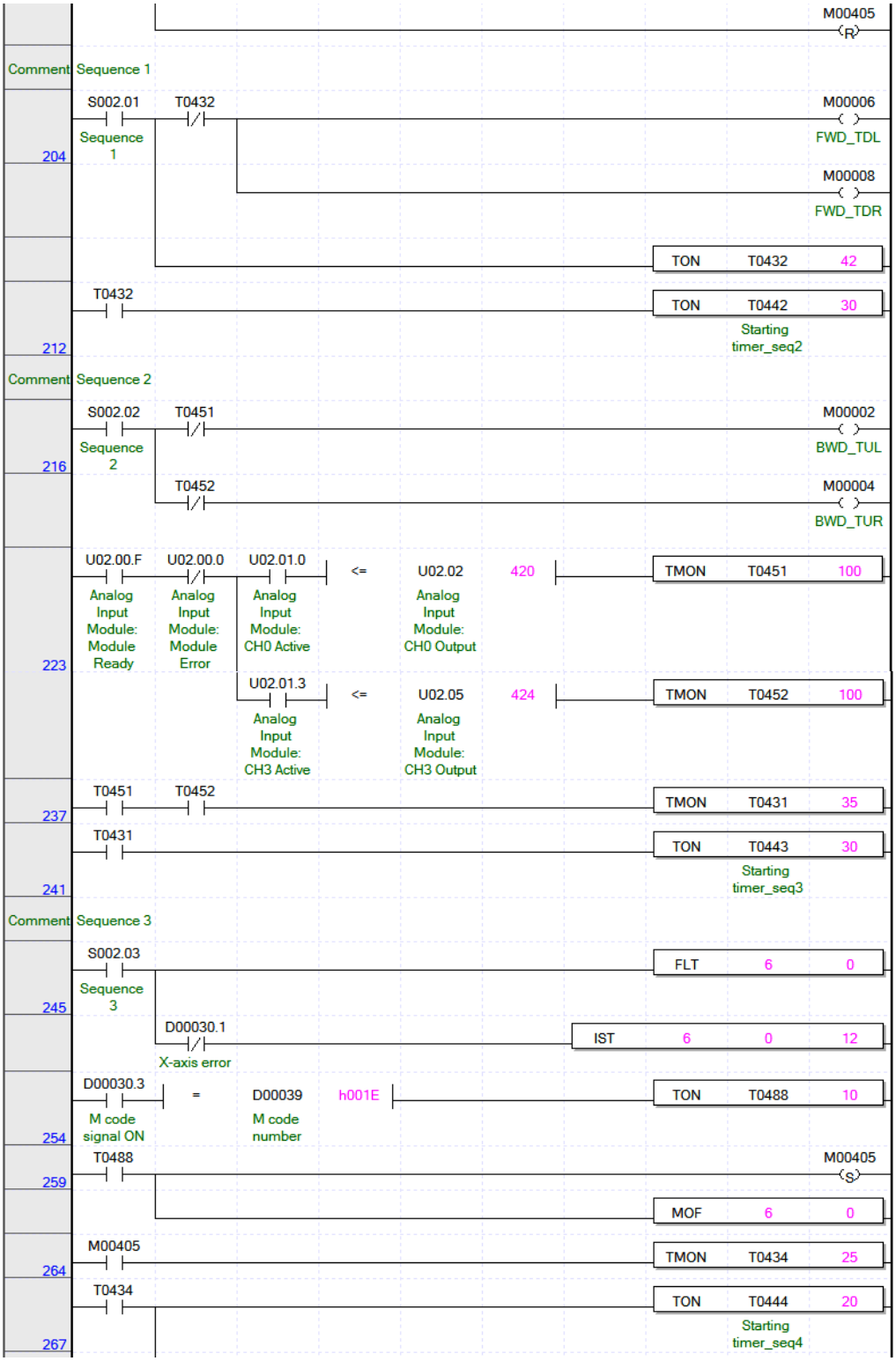
M00405
R
Comment
Sequence 1
S002.01
Sequence 1
T0432
M00006
FWD_TDL
204
M00008
FWD_TDR
TON T0432 42
T0432
TON T0442 30
Starting timer_seq2
212
Comment
Sequence 2
S002.02
Sequence 2
T0451
M00002
BWD_TUL
216
T0452
M00004
BWD_TUR
U02.00.F
Analog Input Module: Module Ready
U02.00.0
Analog Input Module: Module Error
U02.01.0
Analog Input Module: CH0 Active
<=
U02.02
Analog Input Module: CH0 Output
420
TMON T0451 100
223
U02.01.3
Analog Input Module: CH3 Active
<=
U02.05
Analog Input Module: CH3 Output
424
TMON T0452 100
T0451
T0452
TMON T0431 35
237
T0431
TON T0443 30
Starting timer_seq3
241
Comment
Sequence 3
S002.03
Sequence 3
FLT 6 0
245
D00030.1
X-axis error
IST 6 0 12
D00030.3
M code signal ON
=
D00039
M code number
h001E
TON T0488 10
254
T0488
M00405
S
259
MOF 6 0
M00405
TMON T0434 25
264
T0434
TON T0444 20
Starting timer_seq4
267

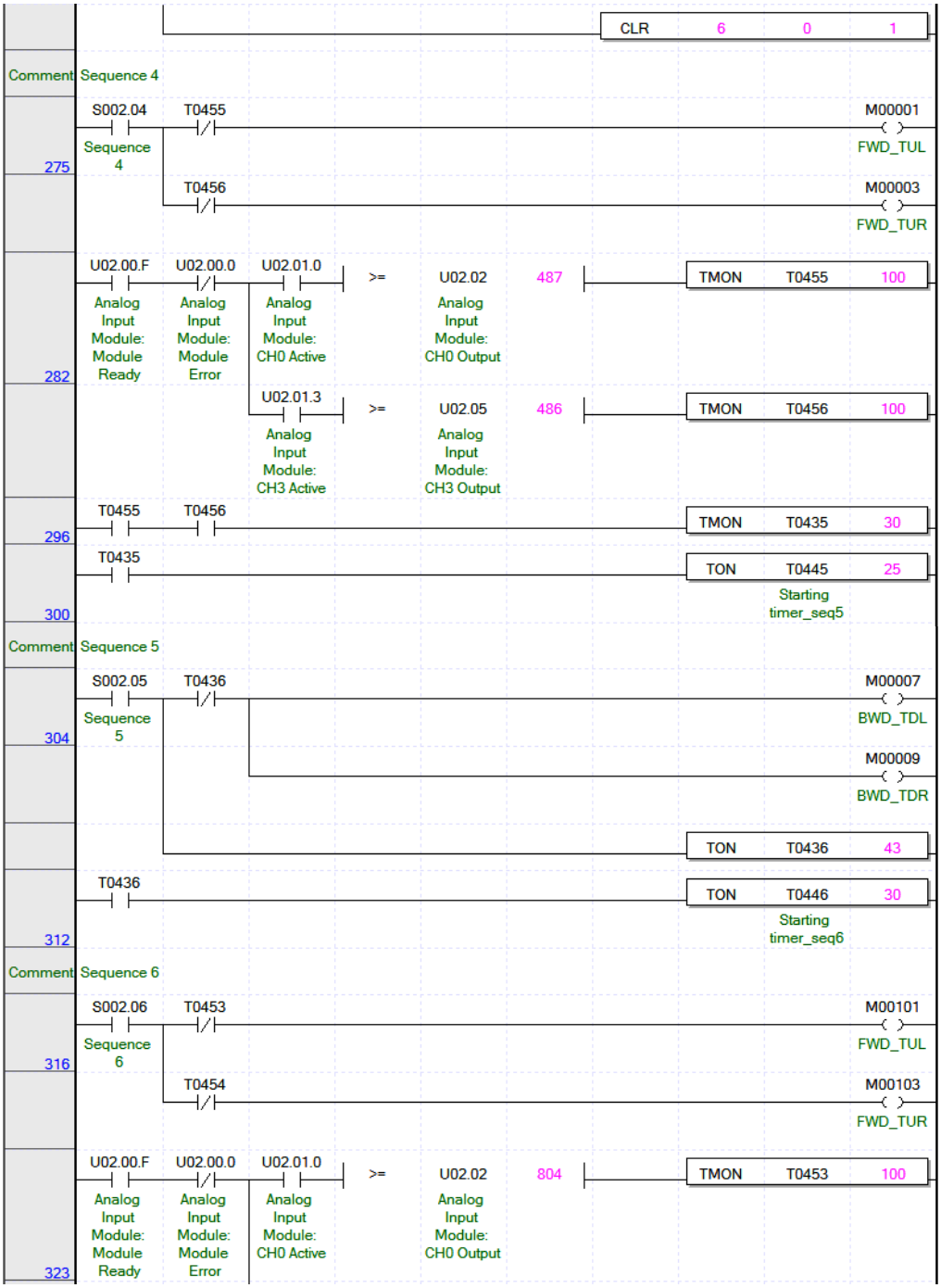
CLR 6 0 1
Comment Sequence 4
275
S002.04
Sequence 4
T0455
M00001
FWD_TUL
T0456
M00003
FWD_TUR
282
U02.00.F
Analog Input Module: Module Ready
U02.00.0
Analog Input Module: Module Error
U02.01.0
Analog Input Module: CH0 Active
>=
U02.02
Analog Input Module: CH0 Output
487
TMON T0455 100
U02.01.3
Analog Input Module: CH3 Active
>=
U02.05
Analog Input Module: CH3 Output
486
TMON T0456 100
296
T0455
T0456
TMON T0435 30
300
T0435
TON T0445 25
Starting timer_seq5
Comment Sequence 5
304
S002.05
Sequence 5
T0436
M00007
BWD_TDL
M00009
BWD_TDR
TON T0436 43
312
T0436
TON T0446 30
Starting timer_seq6
Comment Sequence 6
316
S002.06
Sequence 6
T0453
M00101
FWD_TUL
T0454
M00103
FWD_TUR
323
U02.00.F
Analog Input Module: Module Ready
U02.00.0
Analog Input Module: Module Error
U02.01.0
Analog Input Module: CH0 Active
>=
U02.02
Analog Input Module: CH0 Output
804
TMON T0453 100

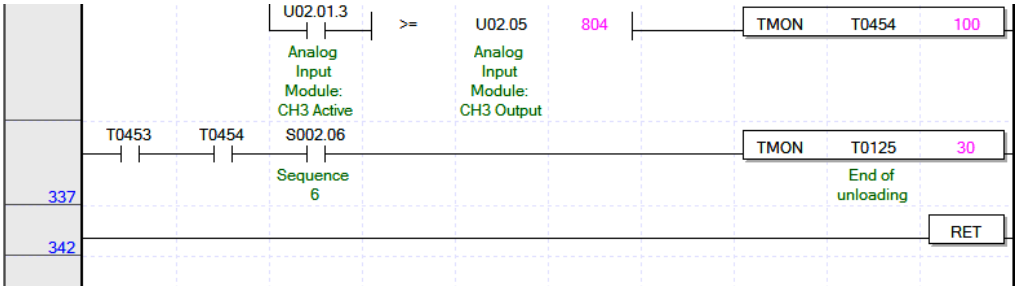
U02.01.3
Analog Input Module: CH3 Active
>=
U02.05
Analog Input Module: CH3 Output
804
TMON
T0454
100
T0453
T0454
S002.06
Sequence 6
TMON
T0125
30
End of unloading
337
342
RET

Development of Cultivation Schema and Automated Gully Convey-Spacing System for Multilayer Plant Factory

Alireza Ashtiani Araghi
알리레자 아쉬티아니 아라기

국문초록

본 연구는 식물공장의 한 형태인 NFT 방식의 식물공장에서 단위면적당 생산량을 높이고 NFT gully 의 운반과 배치를 자동으로 수행하는 시스템을 개발하는 것으로서, 초기비용이 높은 식물공장의 한계를 극복하는 방향에서 추진된 것으로서, 평면재배 방식이 아닌 다층(Multilayer)의 작물재배상에서 굴리의 간격을 식물의 재배단계에 따라 조정할 수 있되, 비용을 낮추기 위하여 작물재배상에 자동화설비를 배치하는 대신에 작물재배상을 옮겨 다니며 작업하는 자동화차량을 개발하여 이 차량에 모든 자동화작업을 수행할 수 있는 매니퓰레이터를 설치하는 것을 목적으로 하고 있다.

구체적인 연구목표는 제안하는 시스템을 개발하고 이 시스템의 성능을 평가하며, 개발된 시스템을 효율적으로 이용하기 위하여 작물의 생장모델을 고려하여 재배방식별 재배기간과 생산량을 추정할 수 있는 시뮬레이션 프로그램을 개발하는 것이다.

연구결과 재배방식에 대한 시뮬레이션은 다양한 조건에서 작물의 재배과정 중 재배상의 이용과 생산량을 쉽게 예측할 수 있었으며, 분석한 결과 굴리의 간격을 고정하는 고정 방식(Static cultivation method)과 작물의 재배 단계에 따라 간격을 변화시키는 동적 방식(Dynamic cultivation method)에 있어서 동적방식의 공간이용 효율 즉 단위면적당 생산량을 증가하는 효과는 식물공장을 1-2 개월 이상 장기적으로 운영하는 경우에 나타나는 것으로 분석되었다. 또한 식물의 생육특성이 반경방향보다 키가 커지는 경우에는 동적인 재배방식의 이점이 뚜렷하지 못하였다. 또한 동적재배 양식을 사용하는 경우에는 재배단계를 균등하게 하지 못하는

경우에는 재배상에 이용되지 못하는 공간이 발생하며 이를 극복하기 위해서는 동적인 재배양식과 정적인 재배양식을 같이 사용하는 하이브리드형 재배양식을 사용해야만 공간의 이용효율을 높일 수 있는 것으로 분석되었다.

개발된 시뮬레이션 프로그램은 NFT 다층재배양식 식물공장을 설계할 때, 주어진 공간에서 설계조건별로 결과를 예측하는데 사용할 수 있으나 최적화 설계를 직접 제시하지는 못하였다.

시스템 개발에 있어서 굴리의 간격을 소프트웨어상의 변수를 조정함으로써 다양한 간격을 구현할 수 있도록 작물재배상을 2 개 제작하고 굴리를 운반하고 위치시키는 자동화 차량을 개발하였으나 굴리의 운반과 위치시키는 작업을 단계별로 구현하는 것은 성공하였으나 연속으로 자동화하는 것은 구현하지 못하였다. 단위 작업별 시스템의 동작과 신호를 분석하여 작 세부동작별 사이클 시간을 측정하고 반복시험을 통해 매니퓰레이터의 에러가 증가하지 않음을 보였으나 동작간 작물재배상과 차량의 매니퓰레이터간 결합과 분리에 있어서 오차가 연속적인 작동을 불가능하게 하였다. CAD 와 Recurdyn 을 이용한 모션 시뮬레이션 결과로는 작동할 수 있음이 확인되었으나 제작과정에서 작물재배상의 치수오차와 개발한 시스템의 구동용량 부족 등 선정된 부품의 부적합성에 기인한 것으로 분석되었다. 개발된 시스템이 정상적으로 작동되는 경우를 가정하여 성능을 추정하는 작업을 수행하였으며 2 개의 4 단재배상의 연속작동시간은 9 시간으로 추정되어 이 시스템이 여러 재배상에서 구현된다면 경제적으로 저렴한 자동화된 식물공장이 가능함을 증명하였다. 그러나 제안된 식물공장의 자동화된 굴리 간격 조정시스템은 식물재배상을 정밀하게 재작해야 한다는 문제와 자동화차량의 굴리를 운반하고 배치하는 작동시간을 단축시켜야만 개발된 시스템이 실용적인 가치를 보일 것으로 판단되며, 식물공장의 자동화를 위한 새로운 자동화 재배장치를 제안하고 공간효율을 높이기 위한 작물재배기술에 대한 시뮬레이션 등은 공학박사로서 학술적 가치가 인정된다.

주요어: 오토메이션, 수경재배, 다층 재배상, 시뮬레이션, 식물공장

학번: 2008-31118